GRAN SASSO SCIENCE INSTITUTE
SCHOOL OF ADVANCED STUDIES
Scuola Universitaria Superiore

Probing the physics of γ-ray bursts through high-energy and multi-messenger observations

PhD defense

PhD candidate

Samuele Ronchini

Supervisors

Marica Branchesi
Gor Oganesyan

Outline

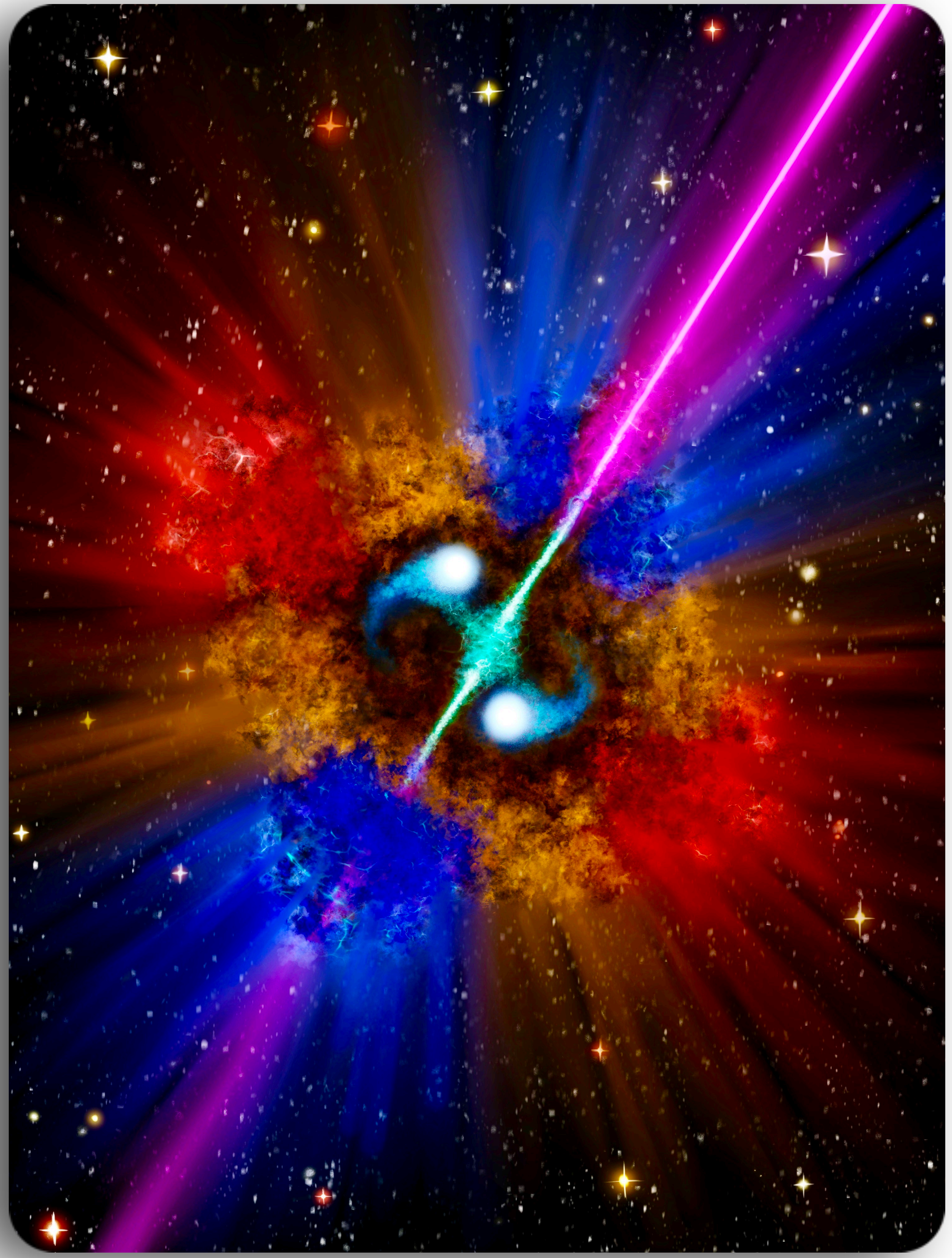

- Introduction
- Part I and II: understand the physics of GRBs with X-ray archival data
- Part III: GRBs in the multi-messenger context - future prospects with 3G gravitational wave detectors
- Conclusions

First GRB observations: the cornerstones

Temporal window explored by the instrument

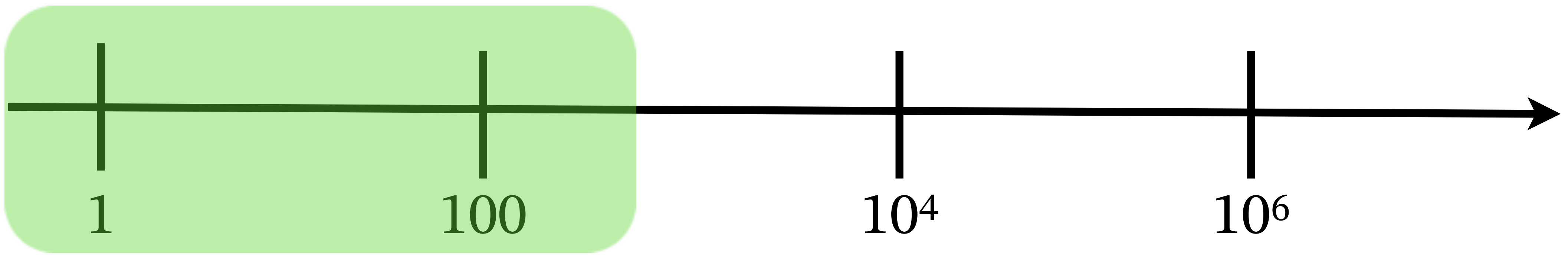

BATSE, 10 keV-20 MeV, '90s

Light curves

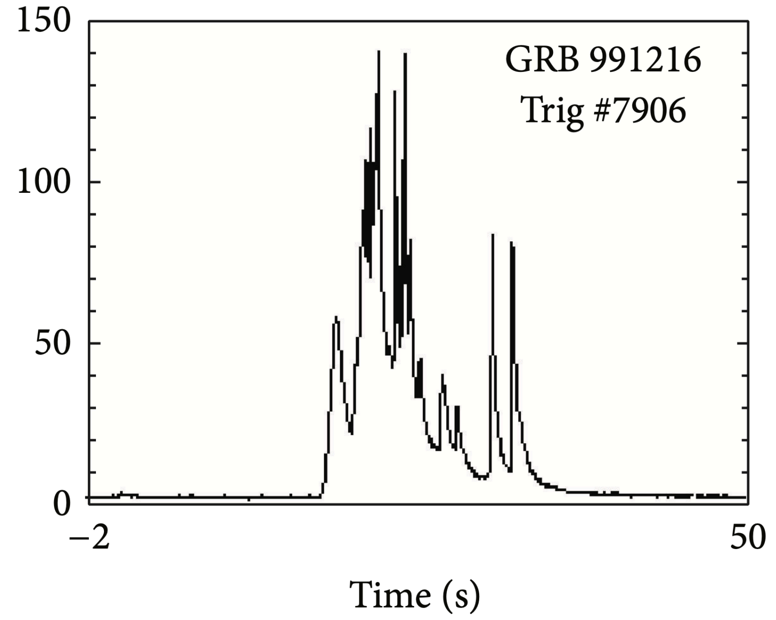

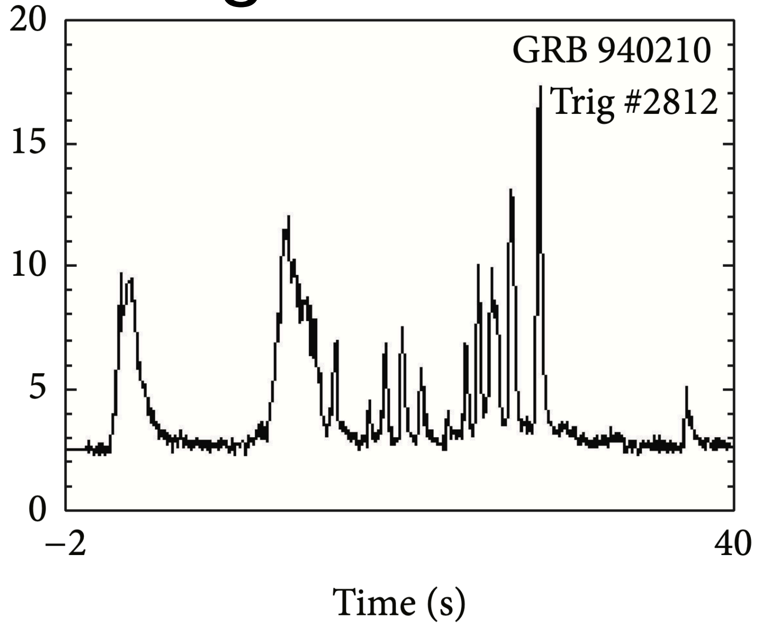

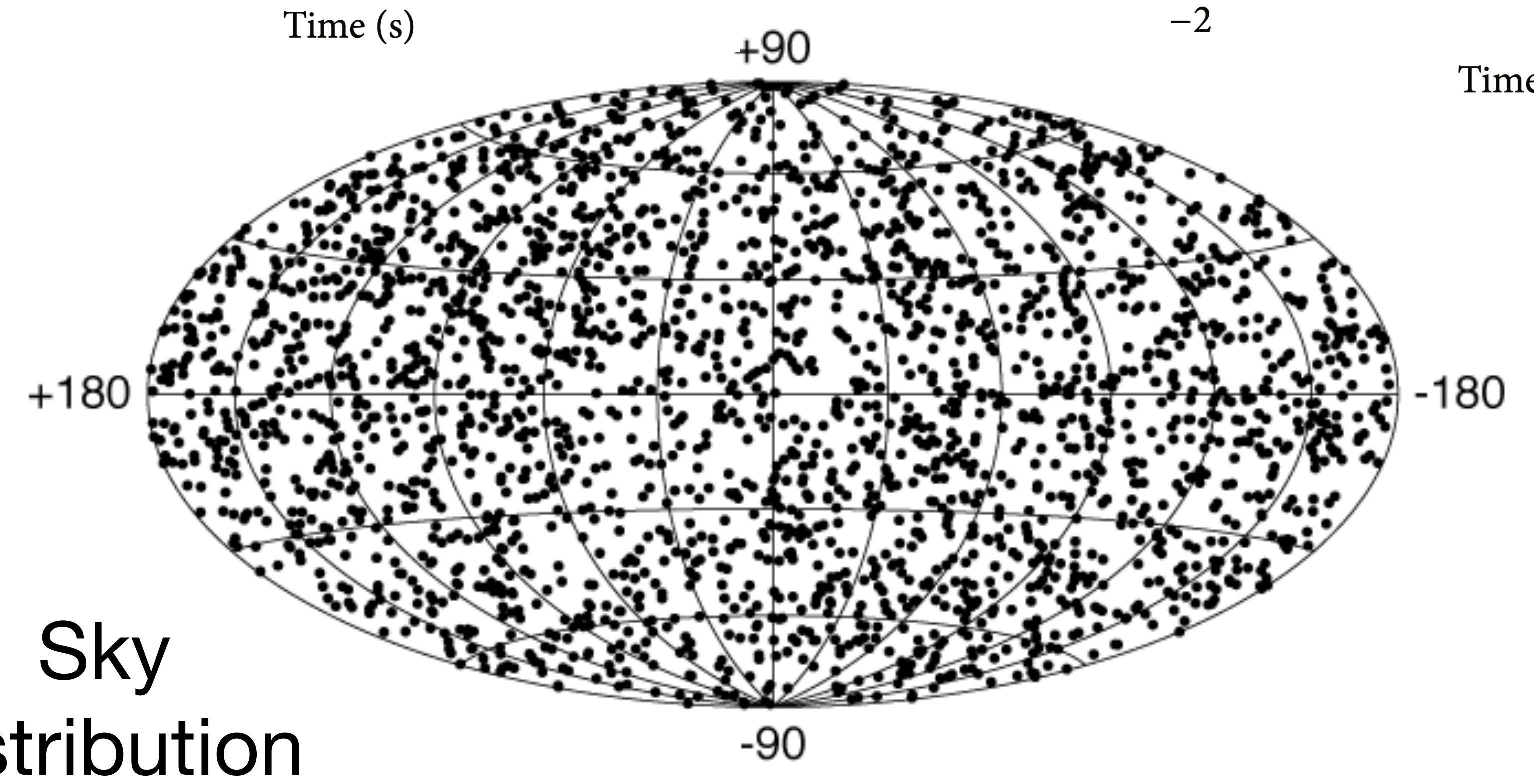

Sky distribution

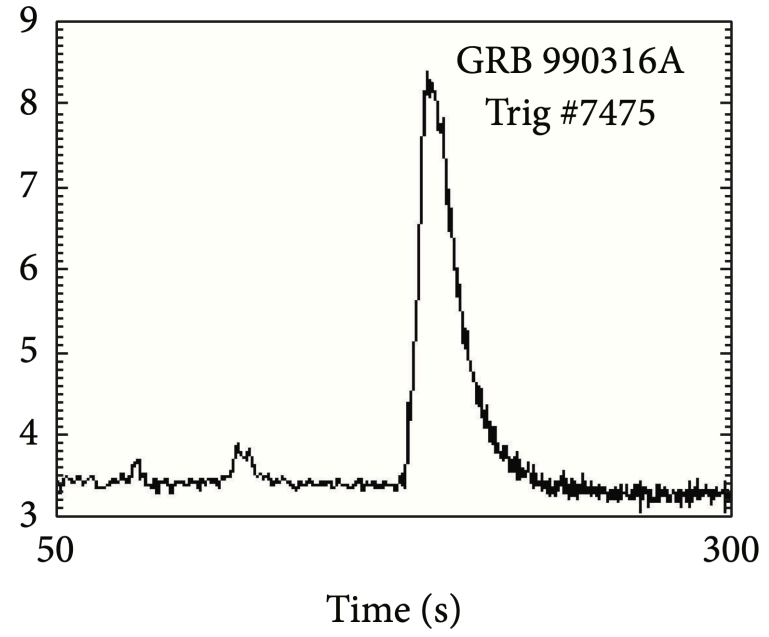

- First GRBs discovered by Vela satellite, late '60s
- Erratic and highly variable light curves
- Bi-modality in the duration-hardness plane (Kouveliotou 1993)—> **two classes of GRBs**
- Isotropic distribution in the sky

Distribution of GRB duration

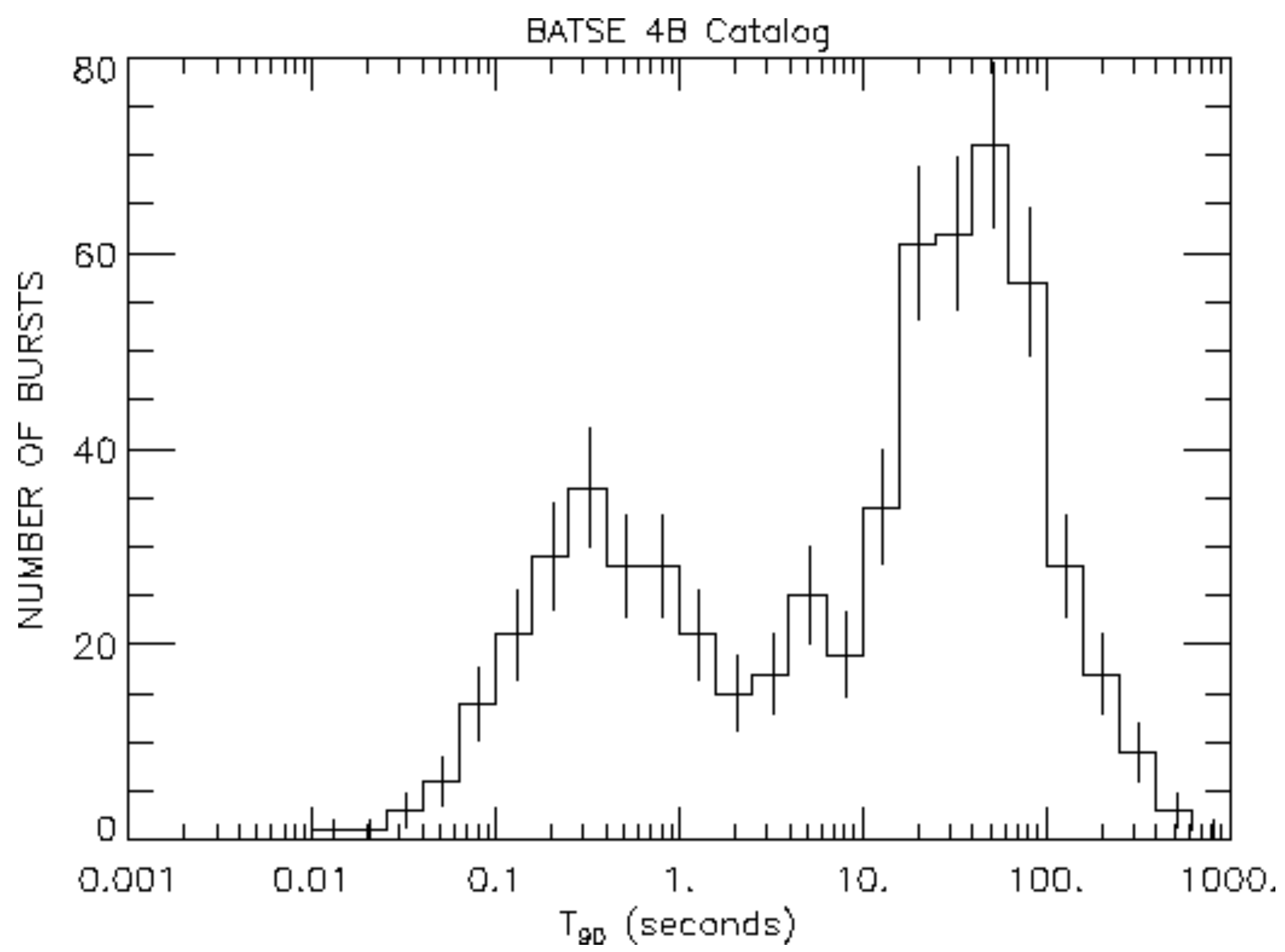

Meegan + 1996

First GRB observations: the cornerstones

Temporal window explored by the instrument

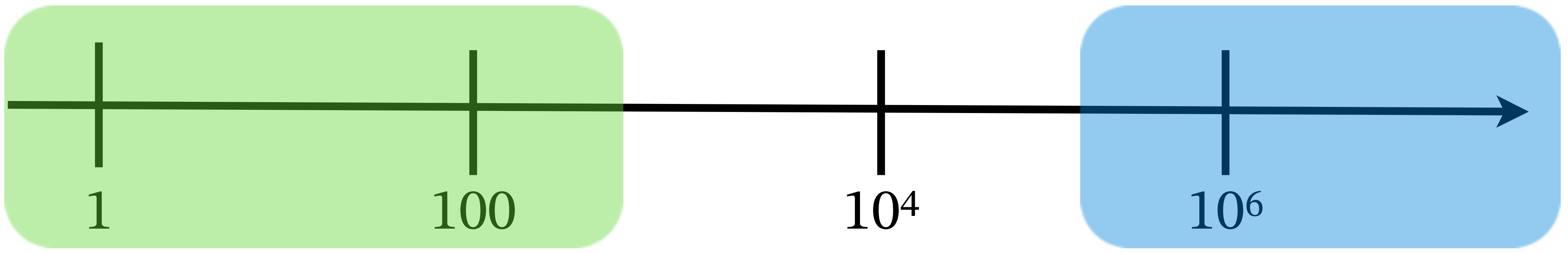

Time from trigger (s)

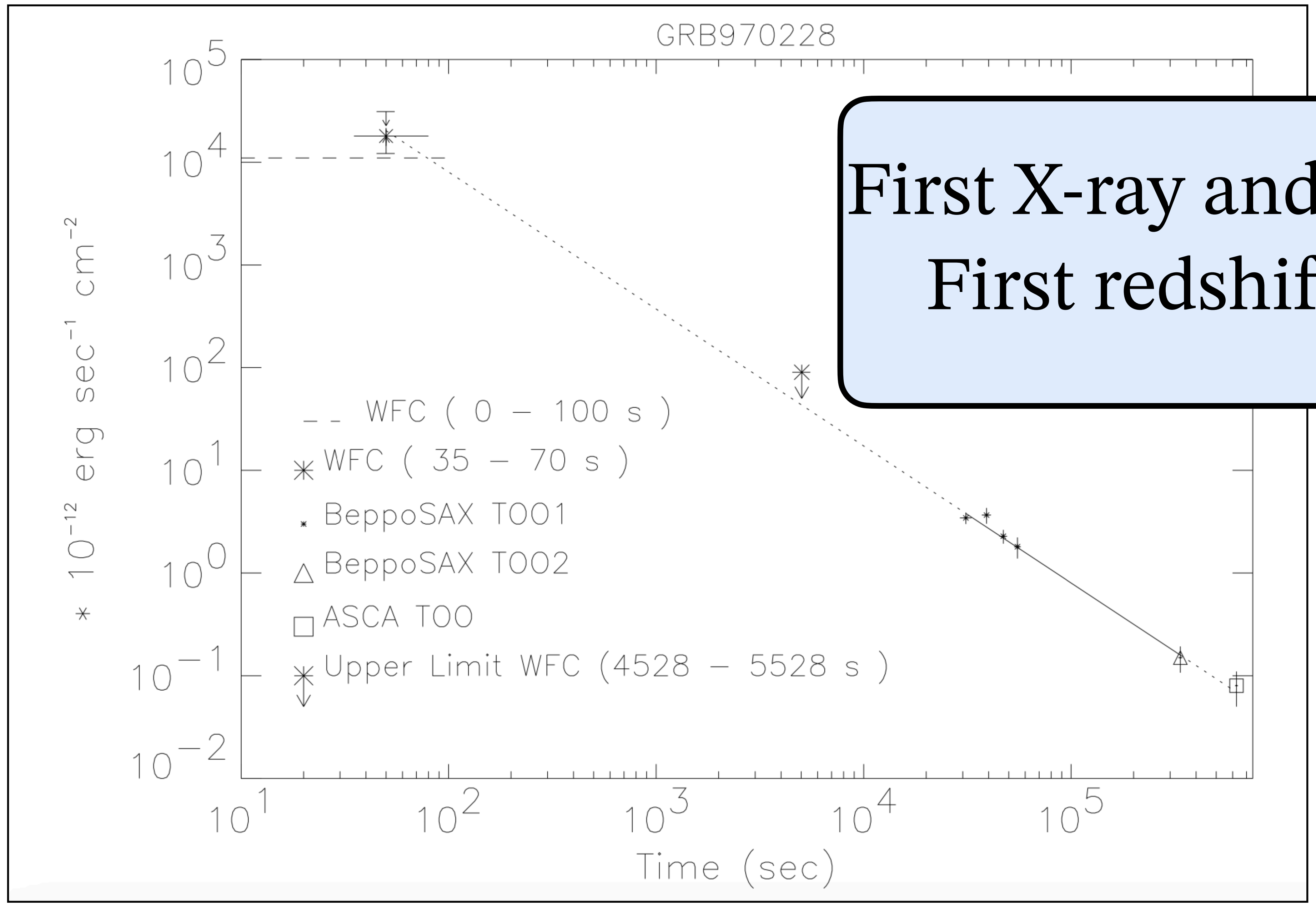

First X-ray and optical afterglow
First redshift measurement

Costa et al. 1997, Van Paradijs 1997

Beppo SAX:
GRB monitor + X-ray WFC (arcmin loc.)
+ focusing X-ray telescope for follow-up

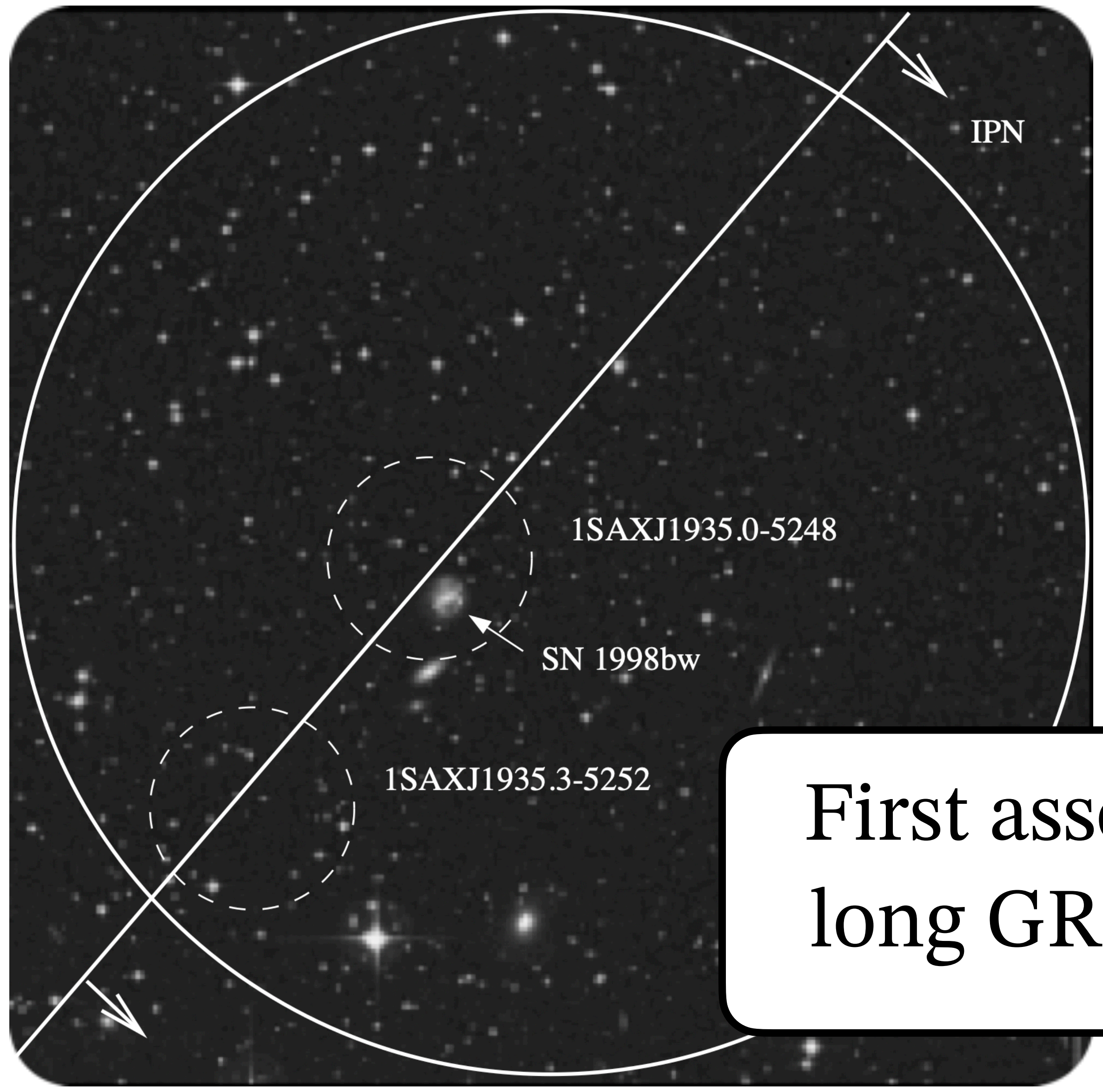

Kulkarni 1998,
Hjorth 2003,
Stanek 2003

First association between a long GRB and a supernova

From the observations of the afterglow and the association with SNae we found that:

- There is a **relativistic jet** launched by a central engine
- **Stellar explosions** can be able to produce a **long GRB**

First GRB observations: the cornerstones

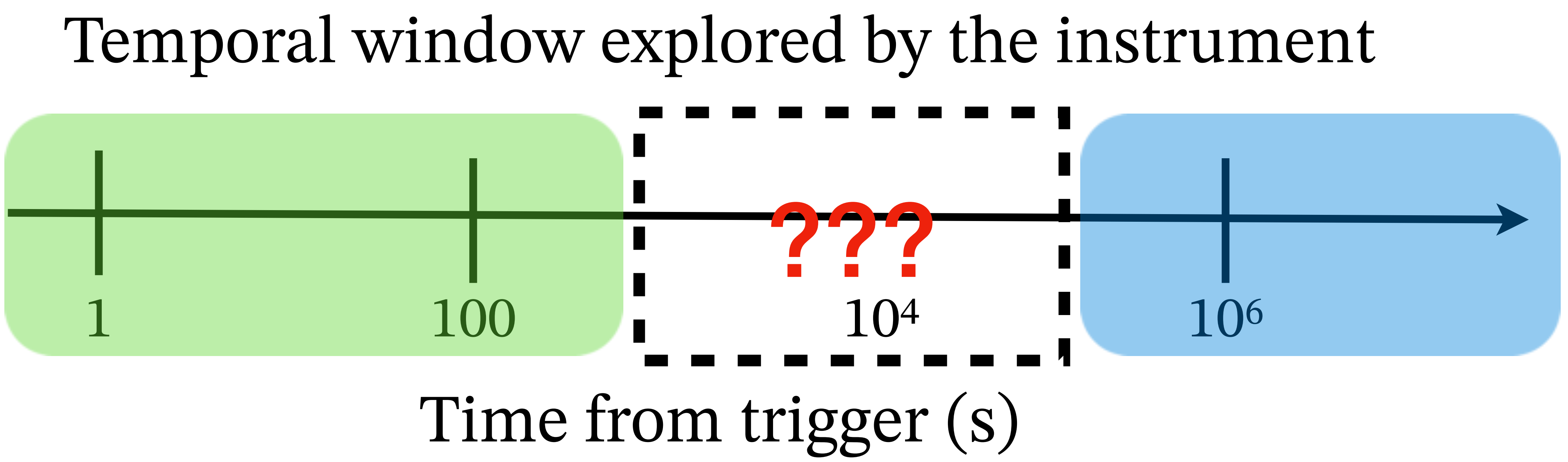

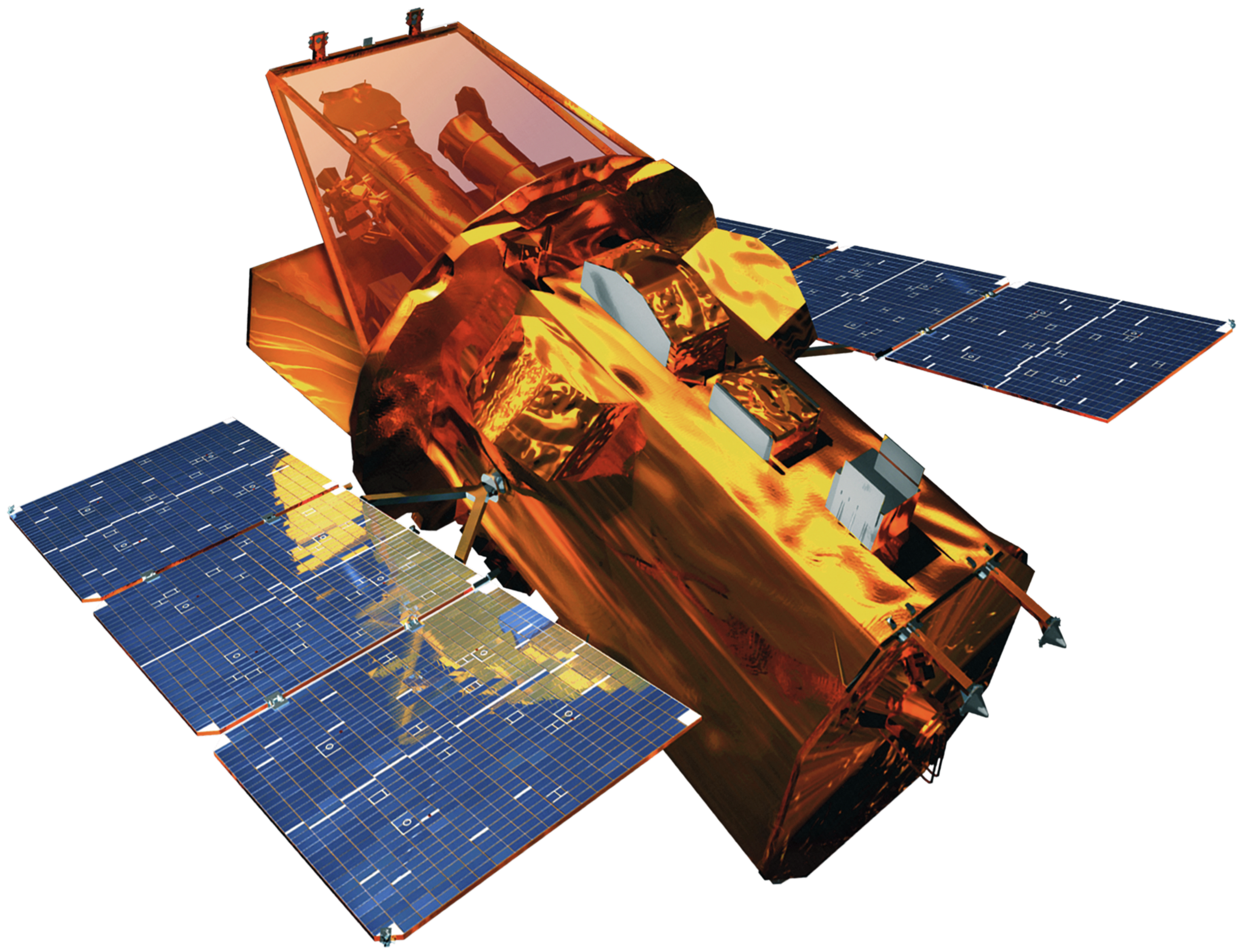

The Neil Gehrels *Swift* Observatory, 2004

Fully autonomous observatory devoted for the detection of GRBs, thanks to the interplay of three instruments on board:

- Burst Alert Telescope (BAT), 15-150 keV —> detects the prompt emission and localizes the burst with arcmin precision

- X-ray Telescope (XRT), 0.5-10 keV —> slews after ≲100 sec to the BAT position and characterizes the X-ray emission

- UV-Optical Telescope (UVOT), 170-650 nm —> characterizes the multi-band emission

Swift: main achievements

Radio afterglow

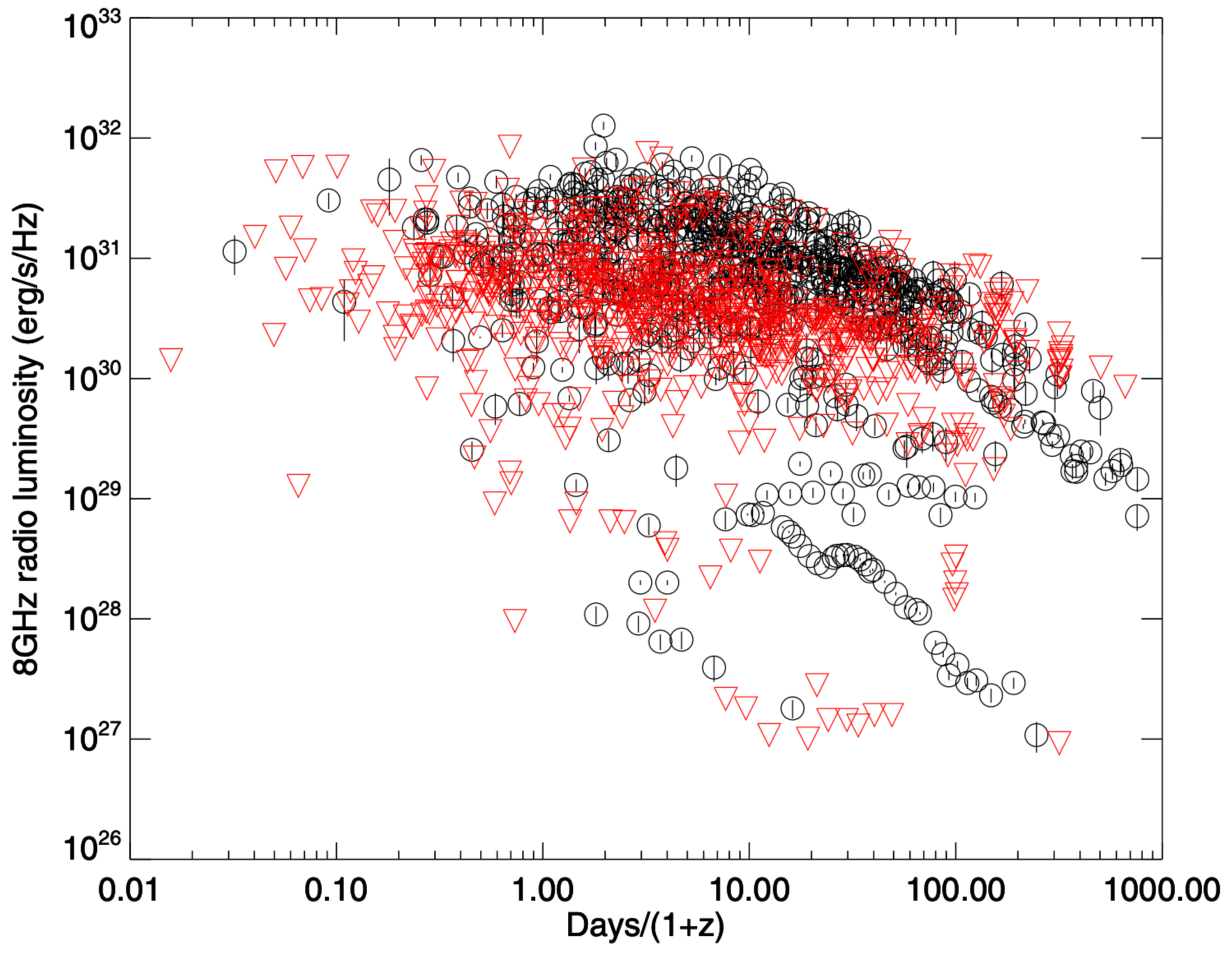

From Chandra & Frail 2012

Optical afterglow

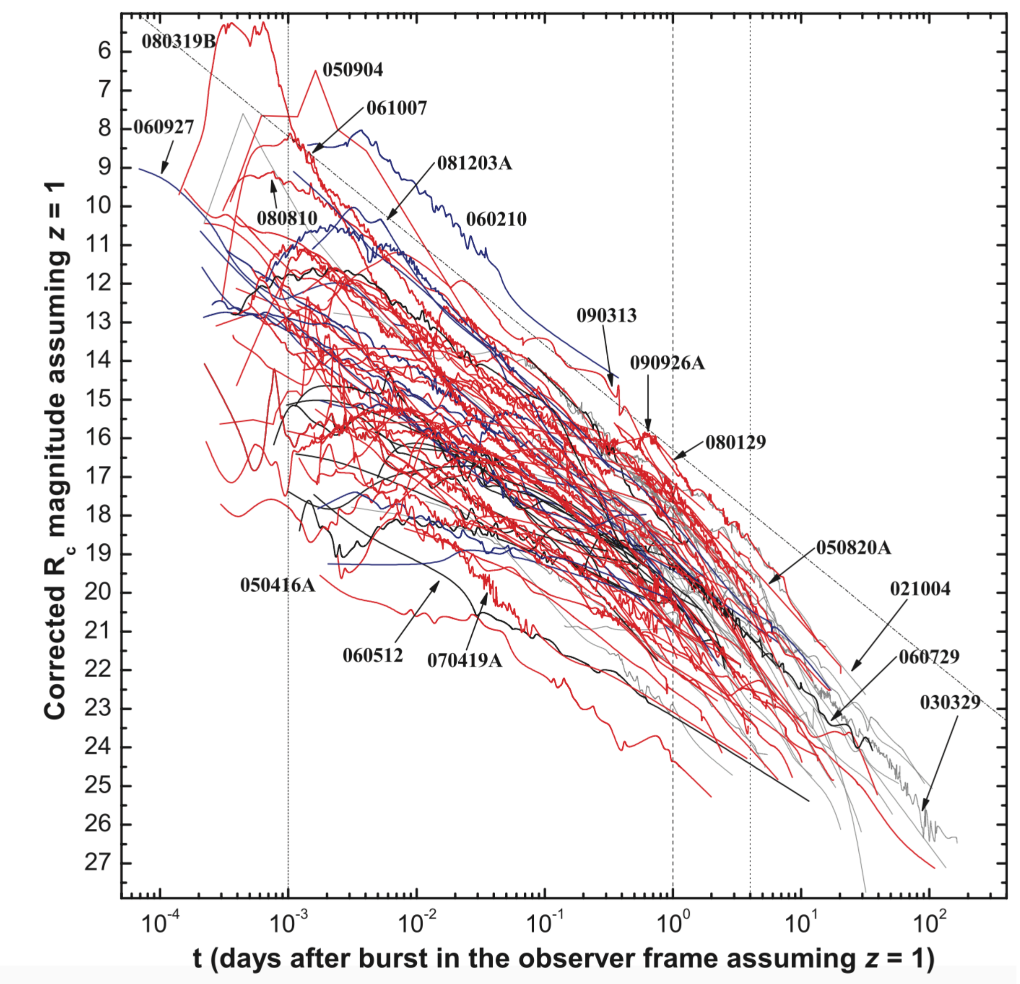

From Kann et al. 2010

Average spectrum during afterglow

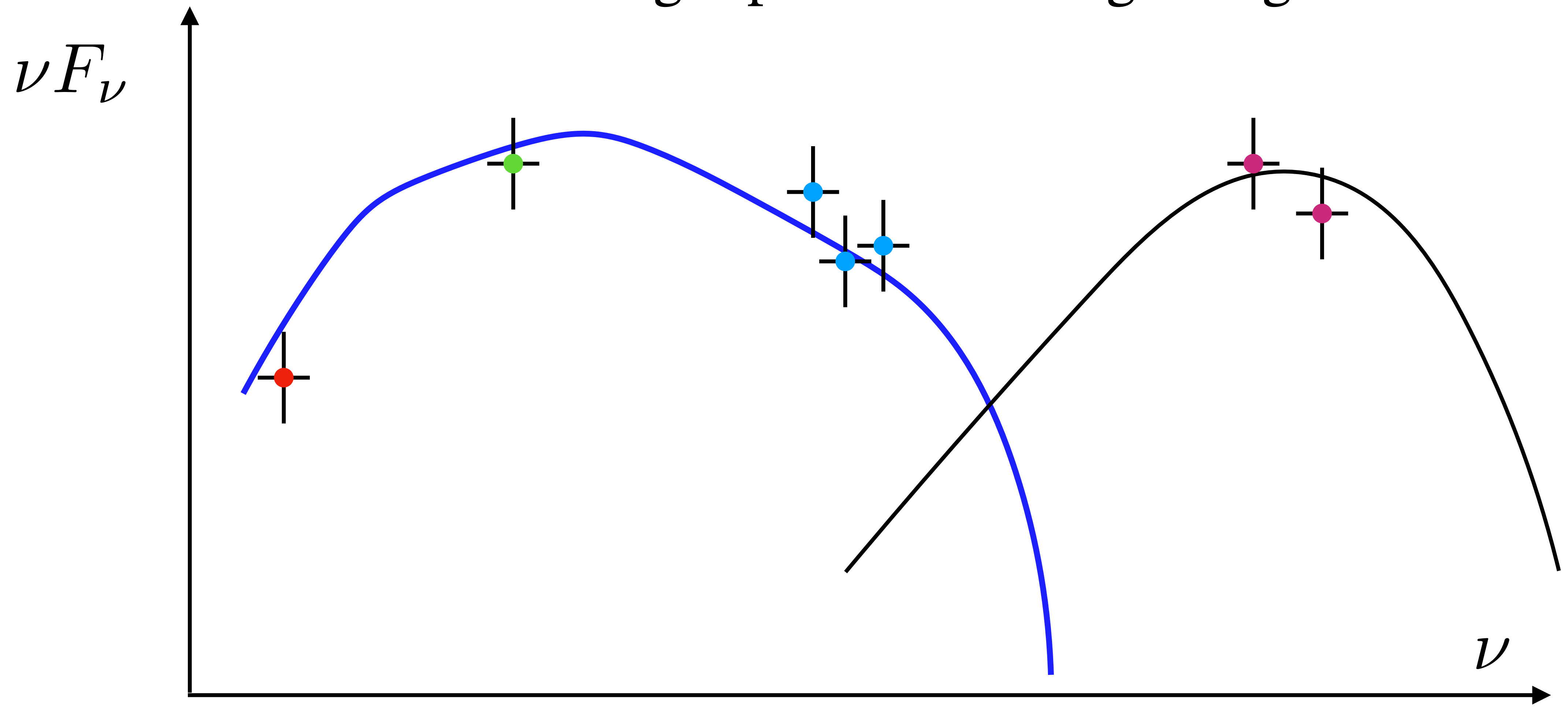

X-ray afterglow

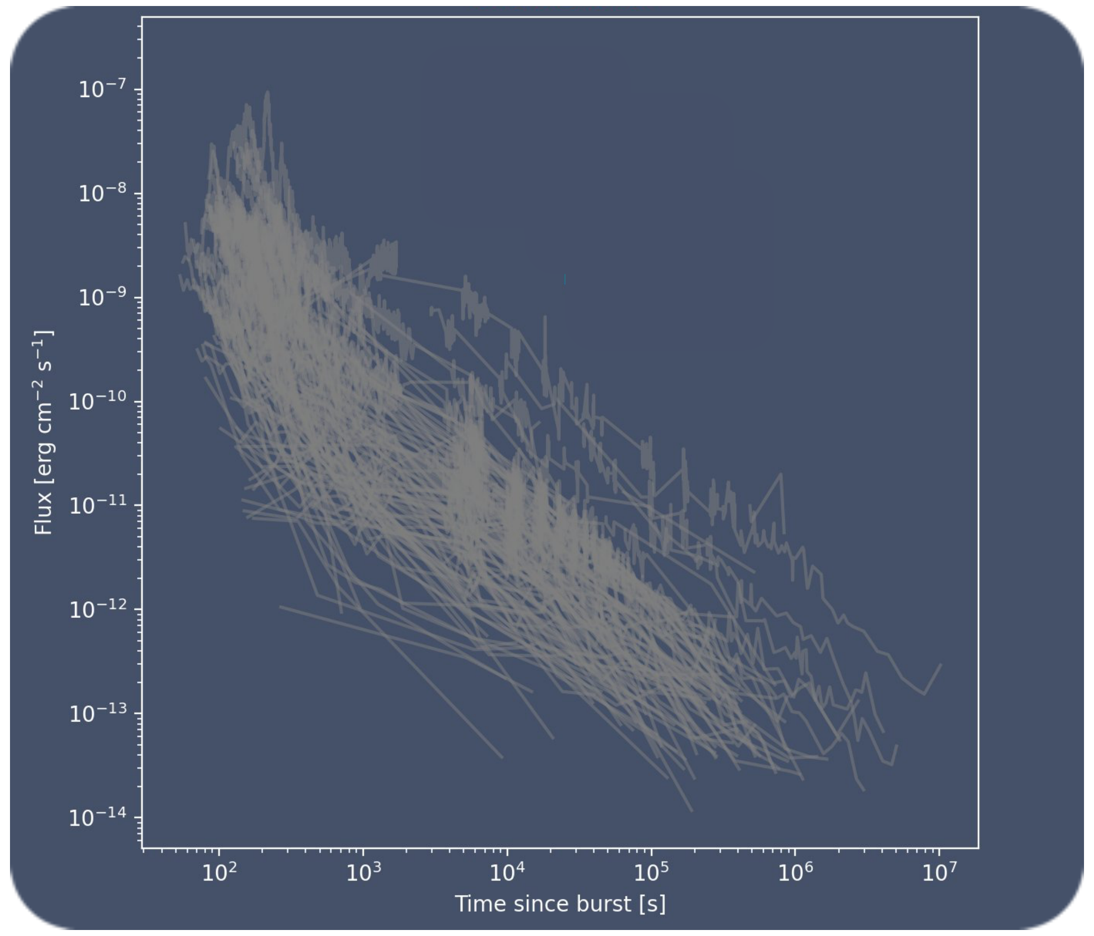

From astro-colibri.com

TeV afterglow

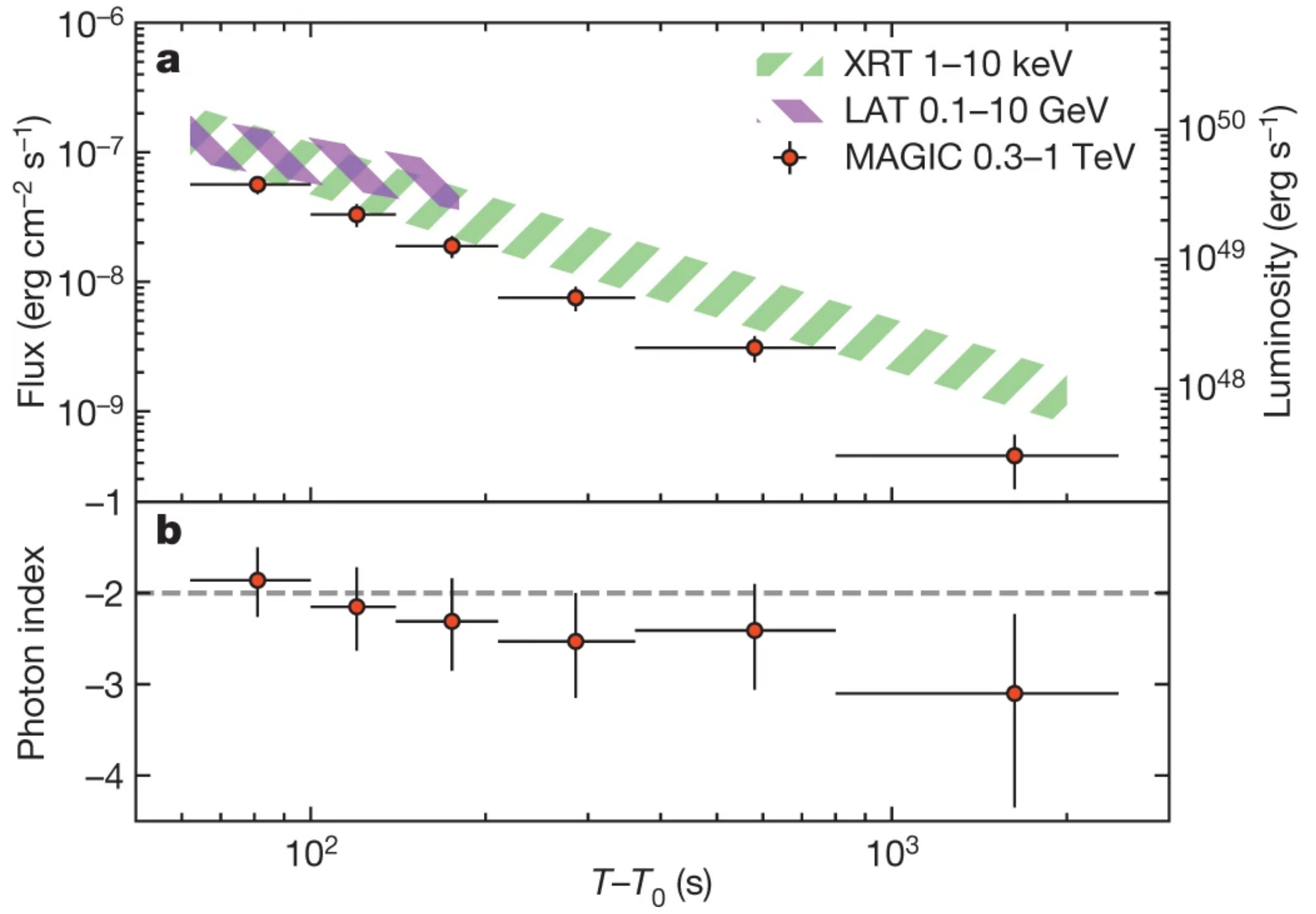

MAGIC collaboration, 2019

The systematic detection of the panchromatic afterglow

- The GRB is detected by BAT
- XRT slews to the sky location
- An accurate position of the burst is circulated to the astronomical community

Swift: main achievements

Discovery of a complex morphology of X-ray light curves

Standard decay (*)

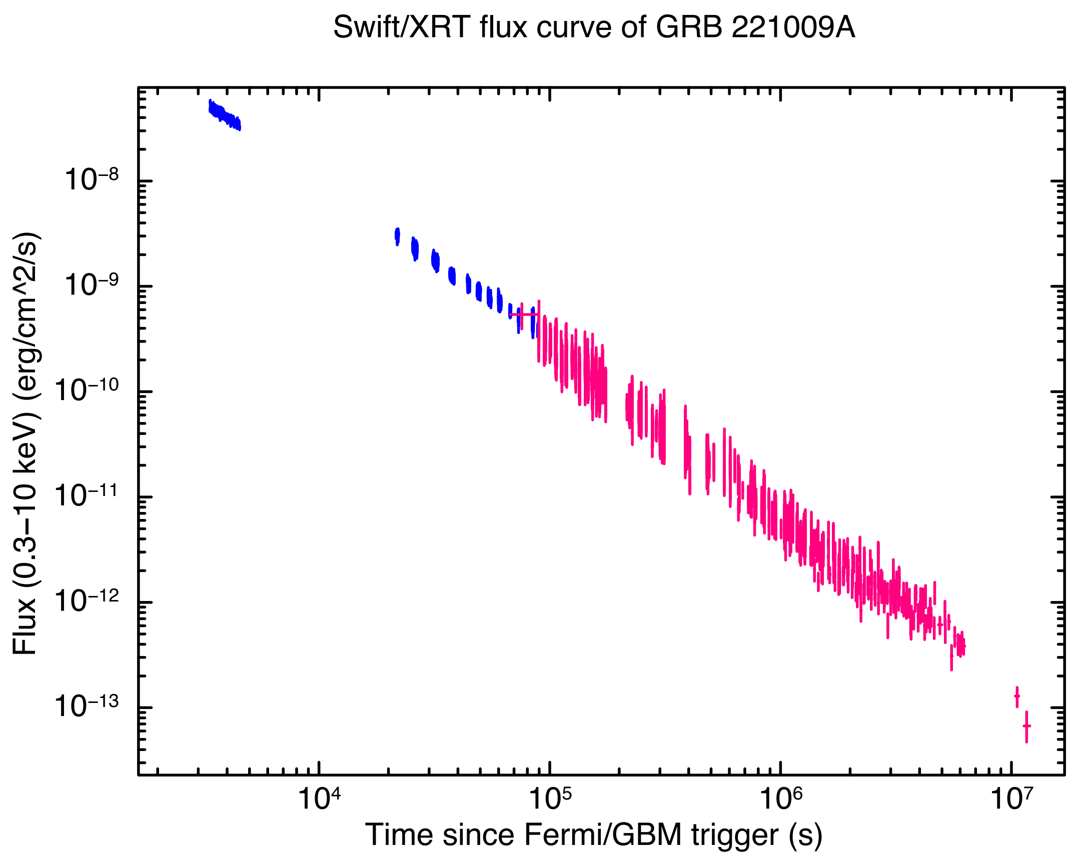

Steep decay + plateau

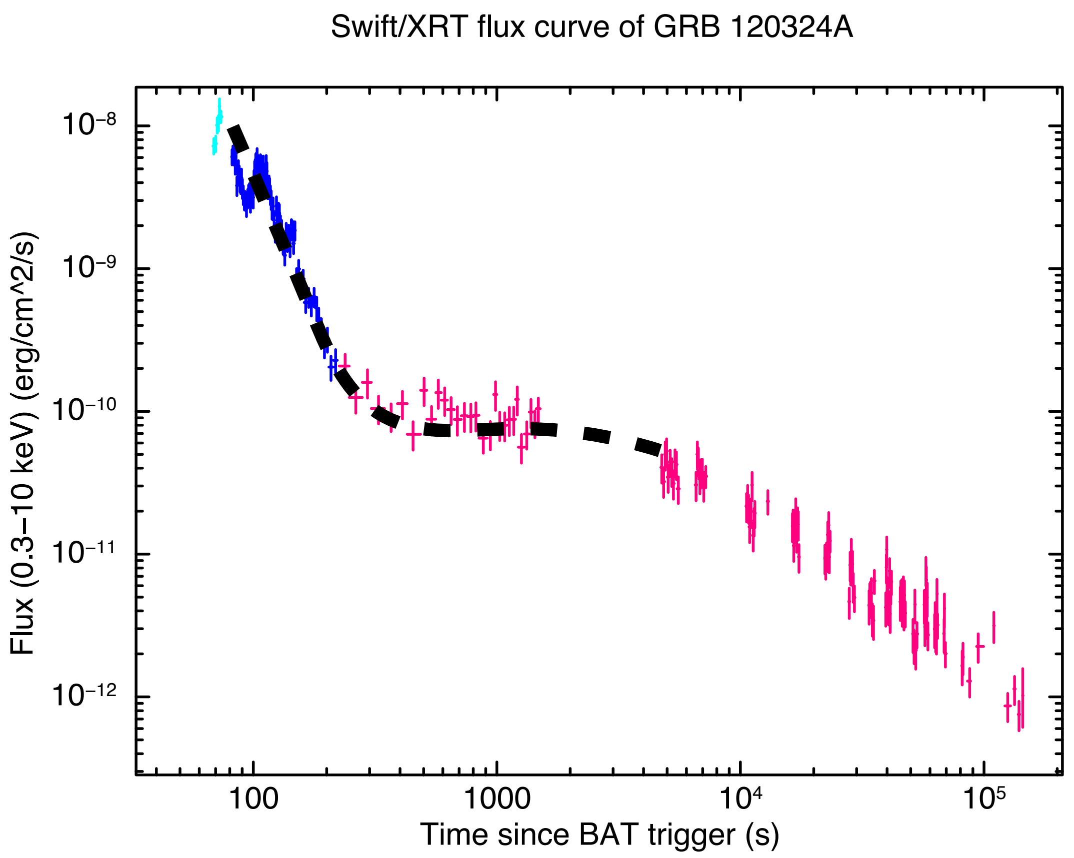

Flares

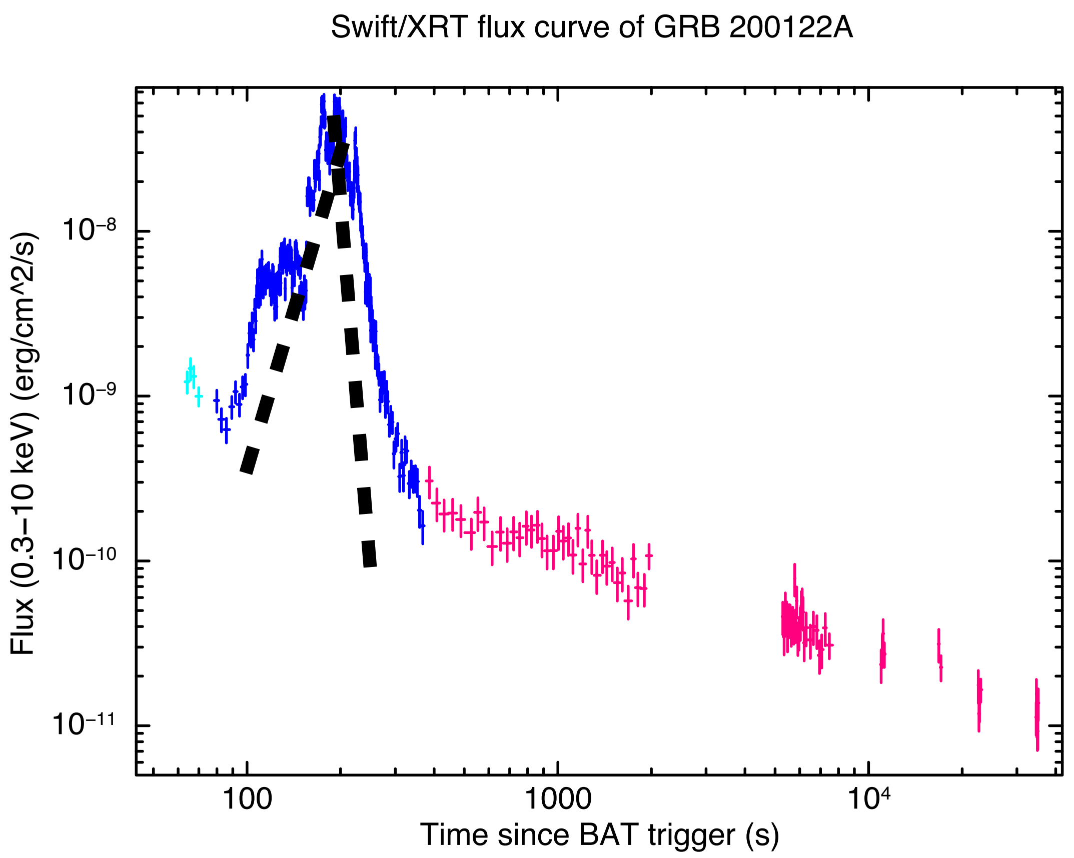

Plateau + steep drop

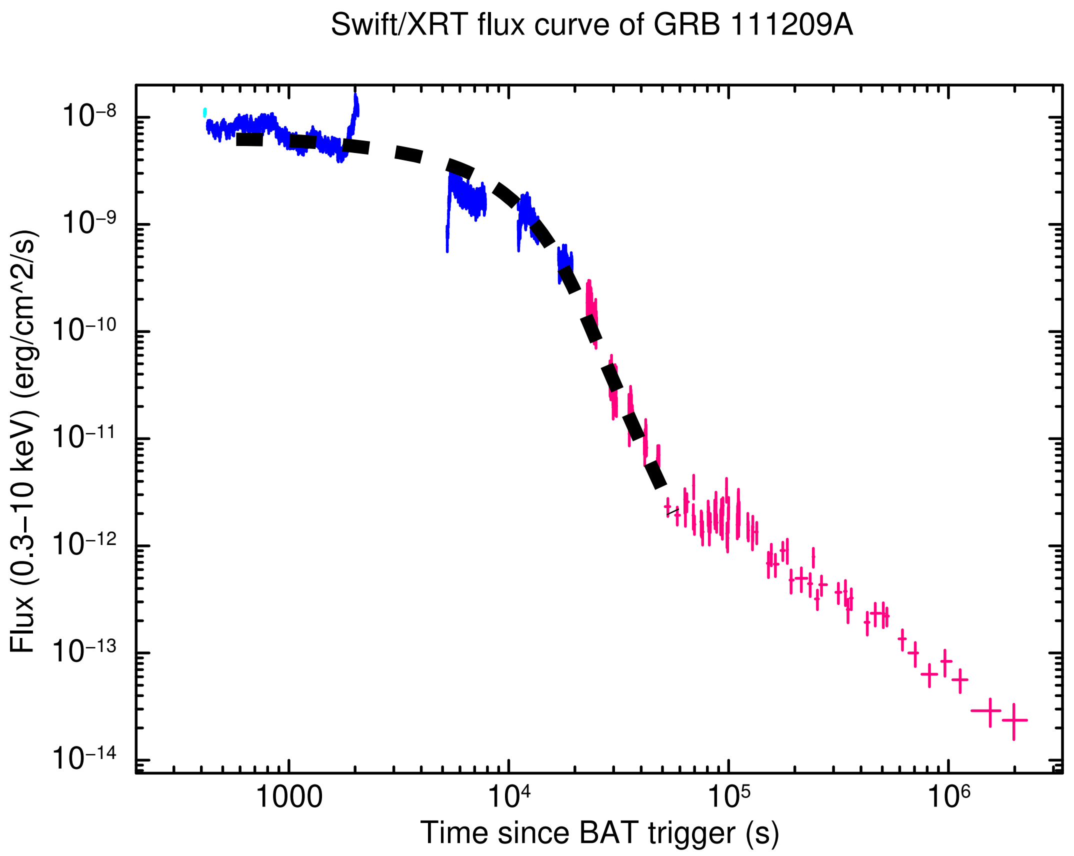

Re-brightening

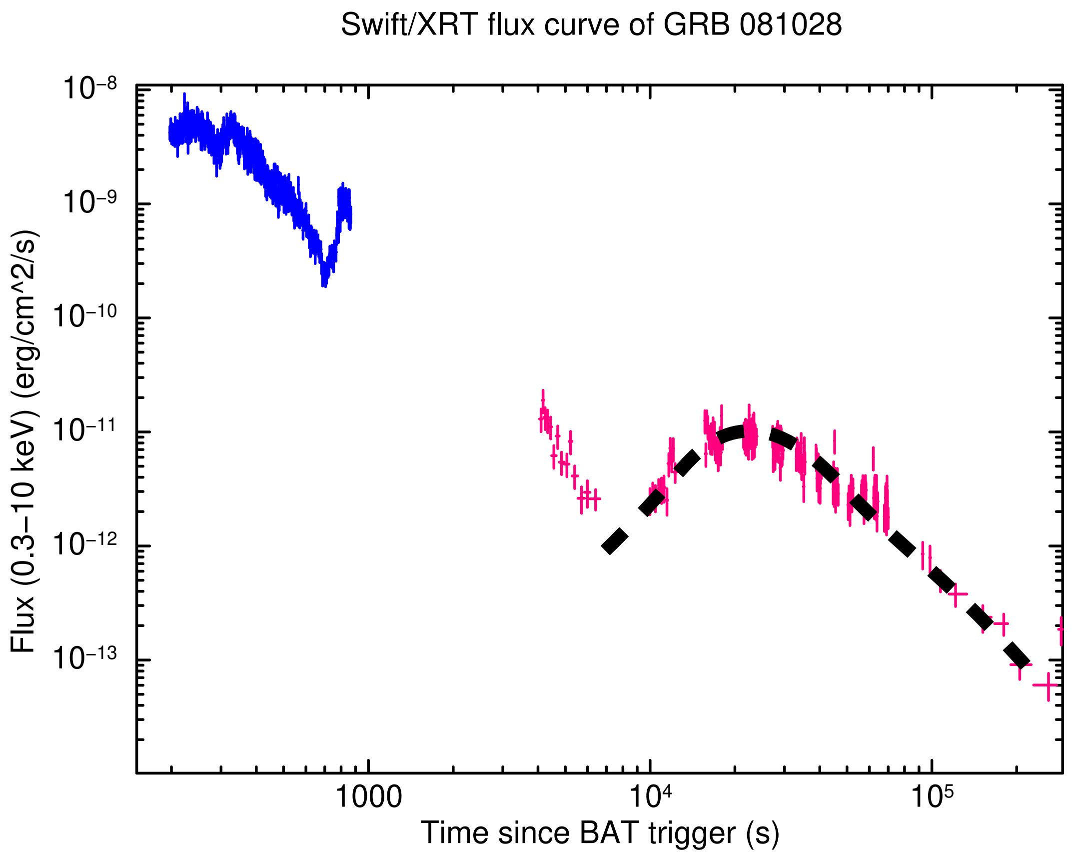

(*) natural outcome of a jet decelerating in the ISM

Blandford McKee 1976,
Meszaros & Rees 1997,
Sari, Piran & Narayan 1998

The multi-messenger revolution

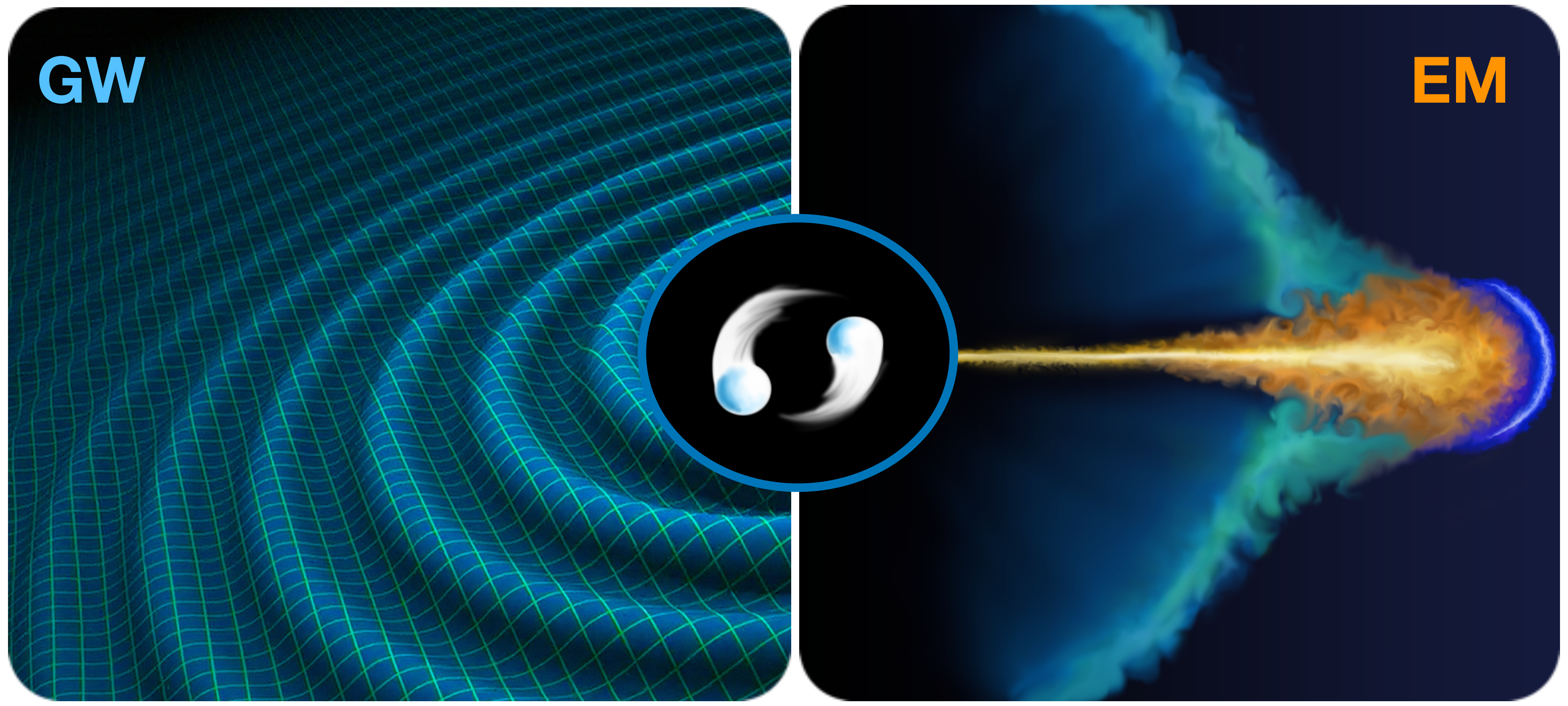

The **first smoking gun** of BNS merger / sGRB / KN association: GW170817, GRB 170817A and AT2017gfo

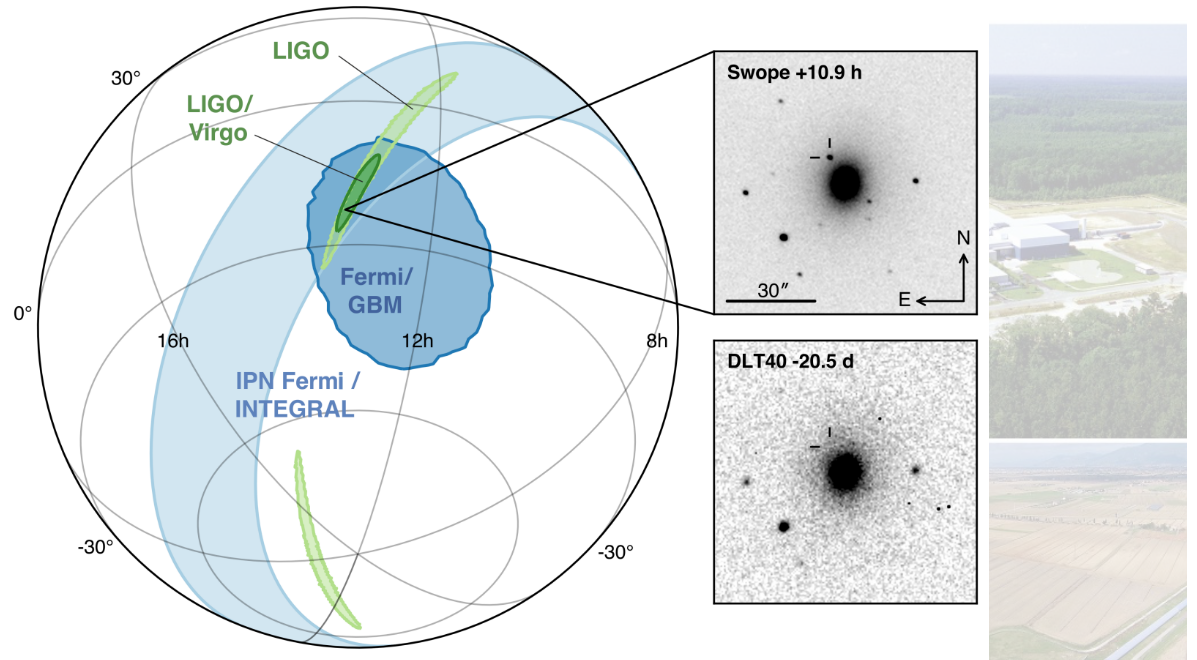

e.g. Abbott+ 2017, Goldstein+ 2017, Pian+ 2017, Smartt+ 2017, Villar + 2017, D'Avanzo+ 2018, Ghirlanda+ 2019

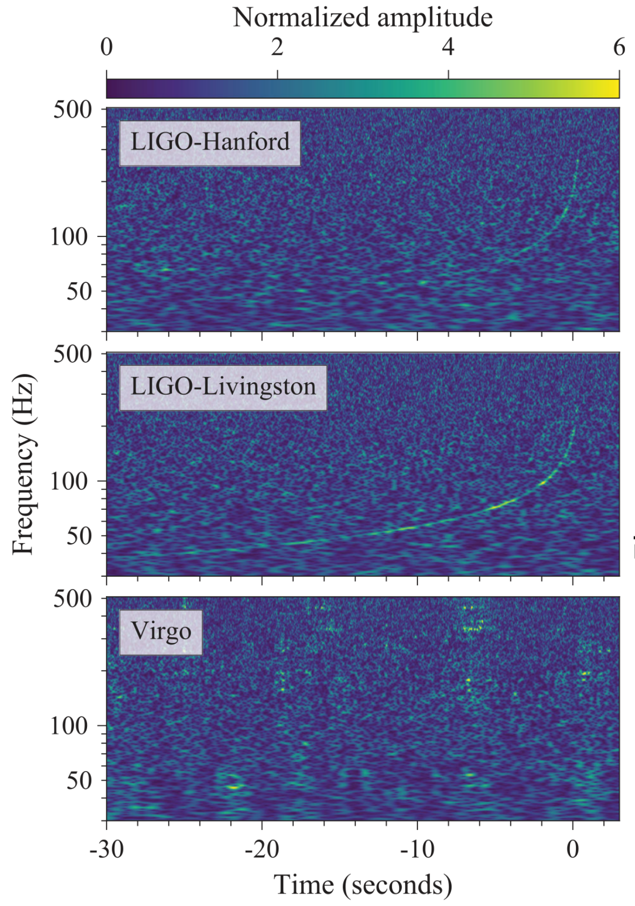

KN spectra

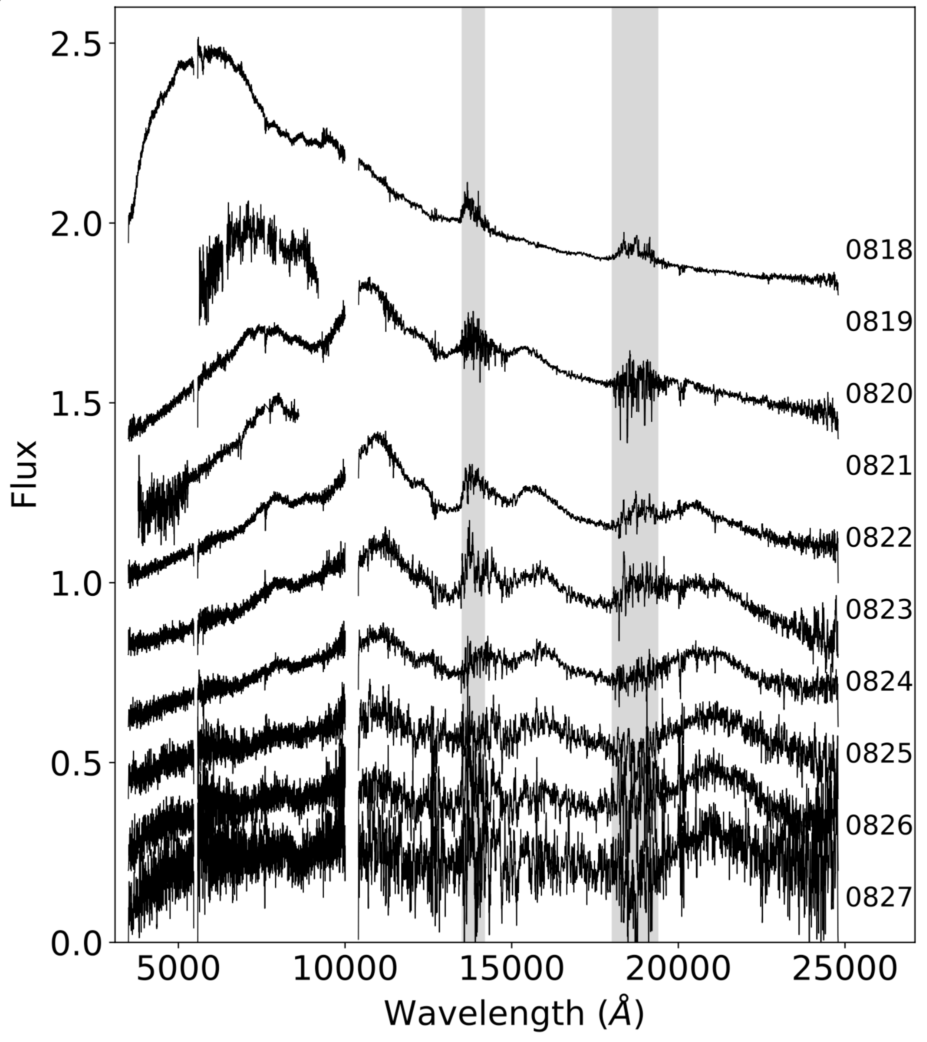

- First association between binary neutron star (**BNS**) mergers and **short GRBs**

- Heavy elements are synthesized in the ejecta of BNS mergers —> their radioactive decay powers the **kilonova** (KN) emission (Li & Paczynski 1998)

- Evidence of a **relativistic jet with an angular structure**, observed **off-axis**

KN light curve

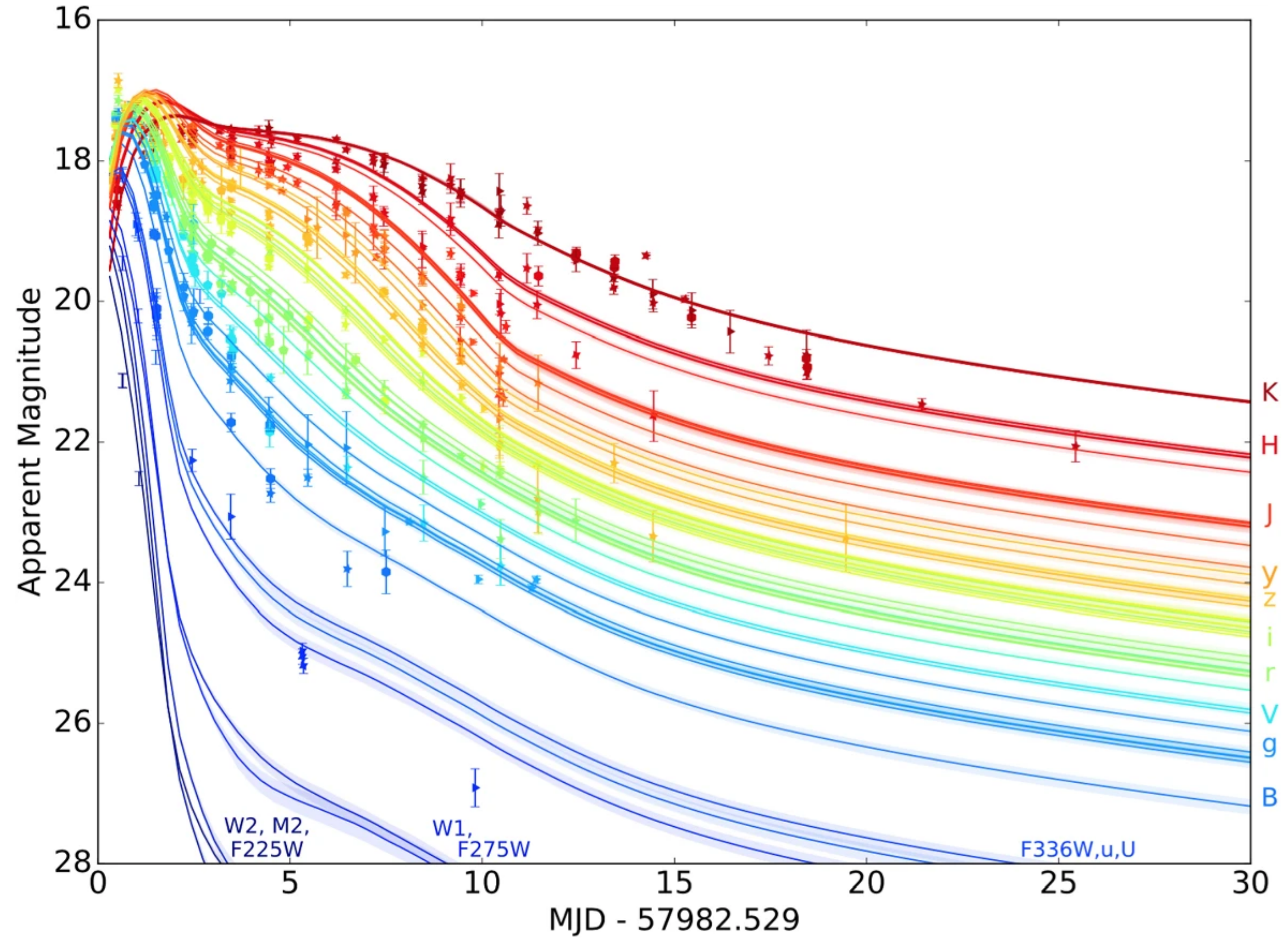

Radio to X-ray afterglow

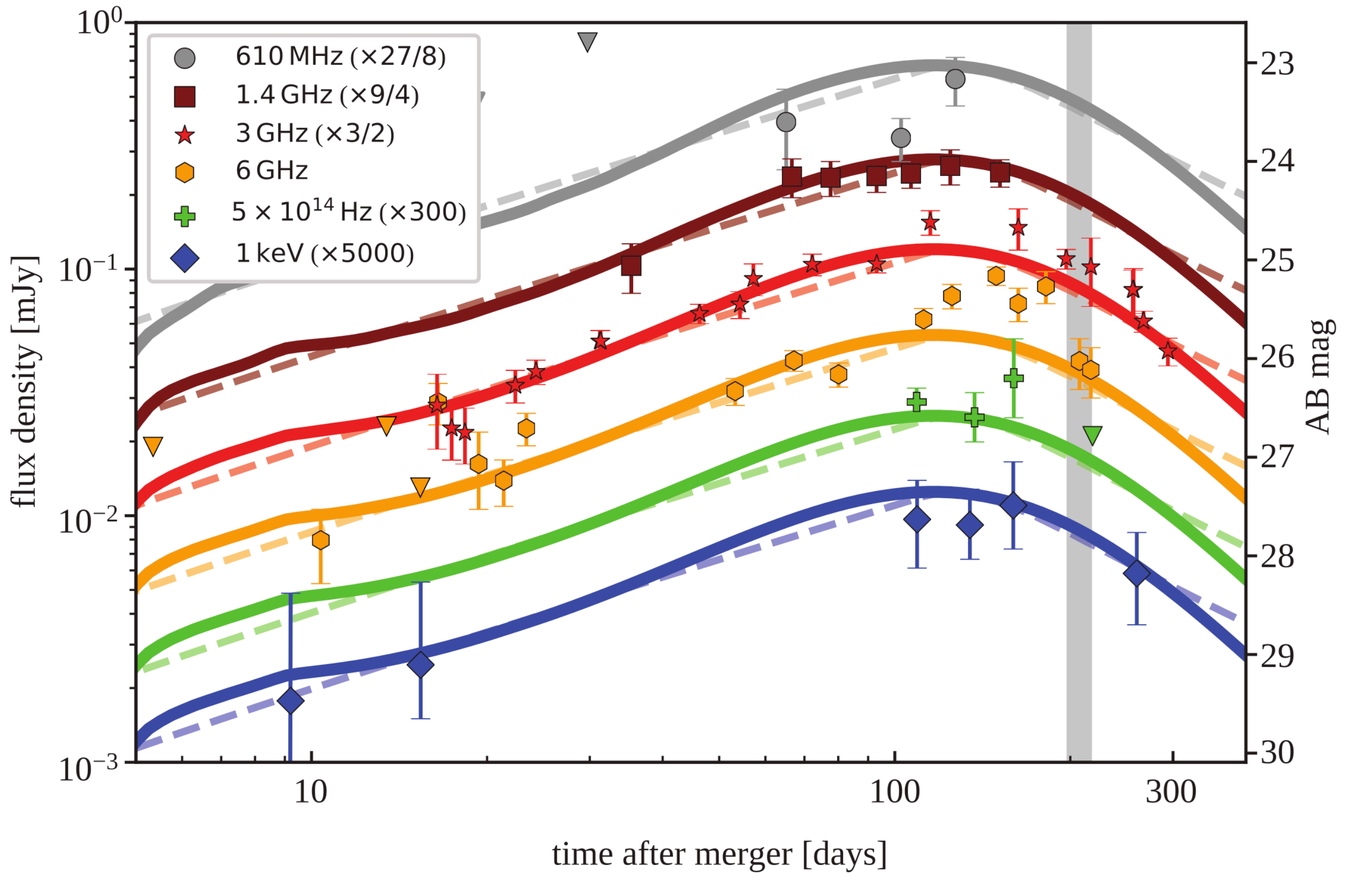

GW170817: discoveries and their impact

Such a wide,
multi-disciplinary impact …

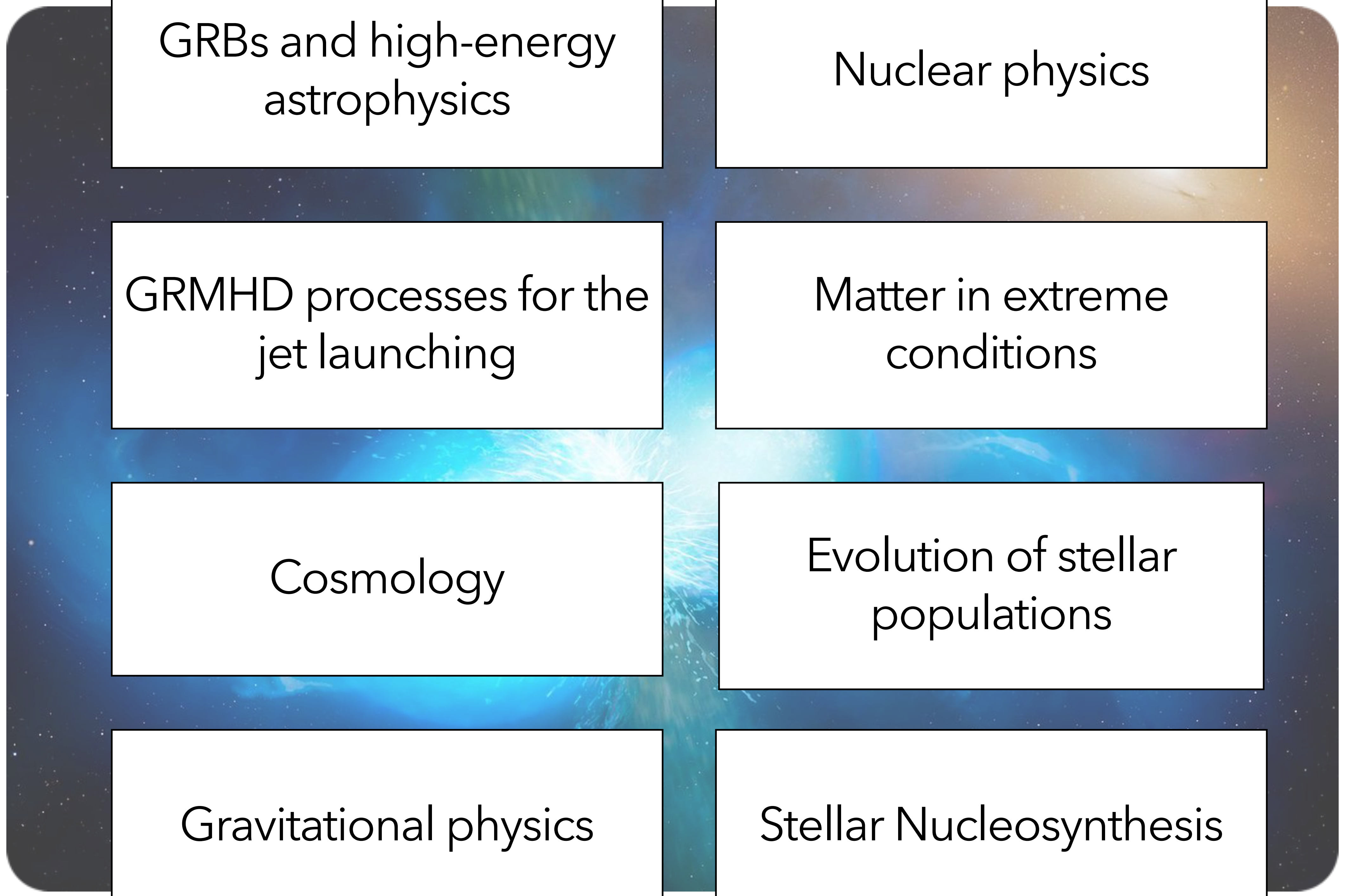

GRBs and high-energy astrophysics

Nuclear physics

GRMHD processes for the jet launching

Matter in extreme conditions

Cosmology

Evolution of stellar populations

Gravitational physics

Stellar Nucleosynthesis

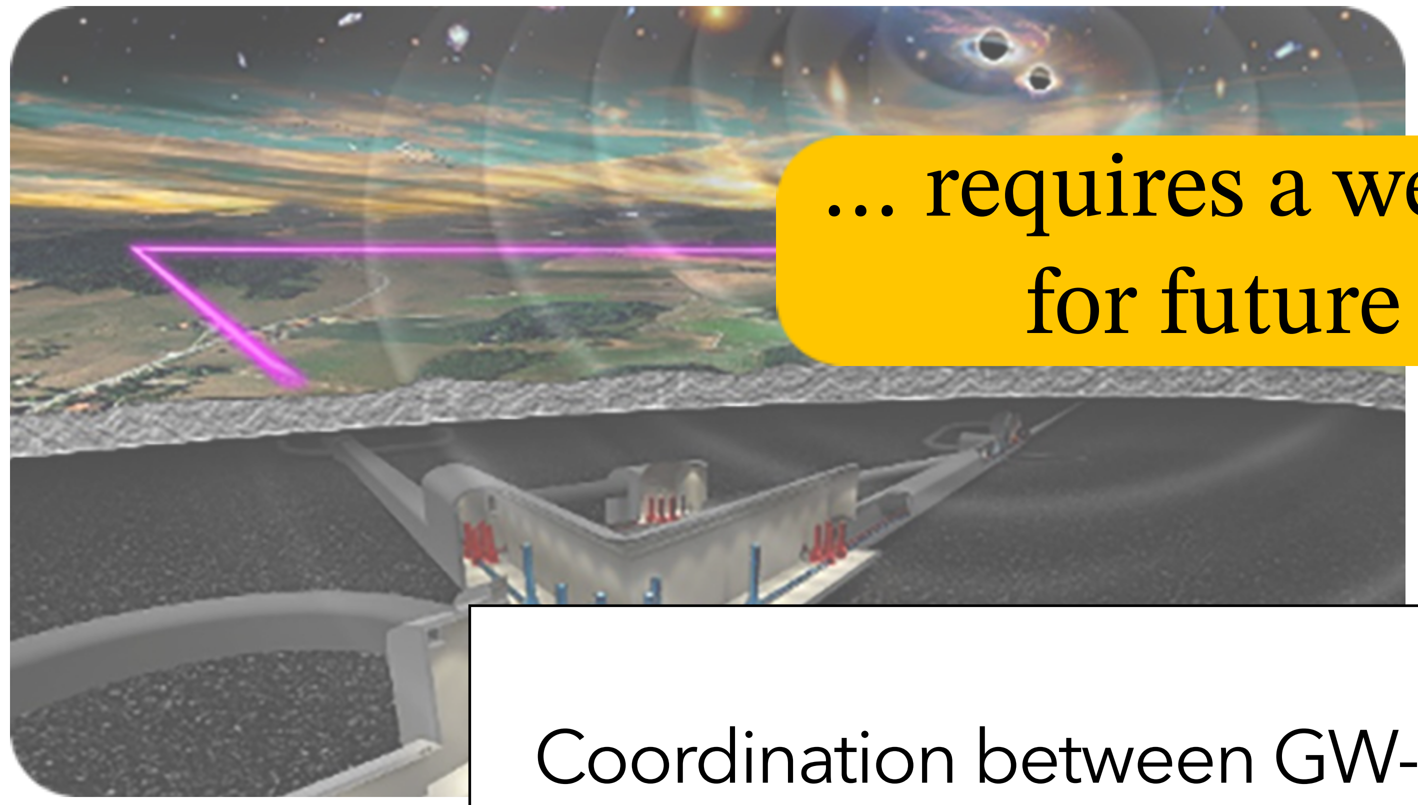

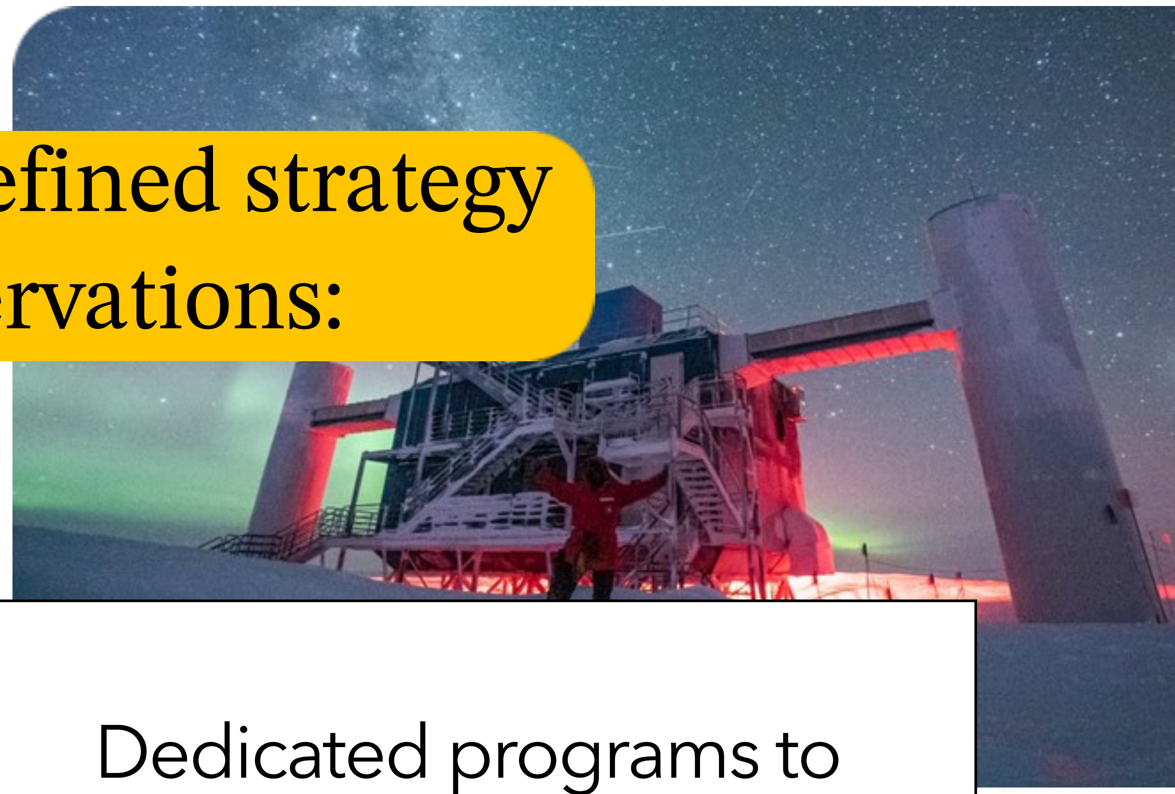

… requires a well defined strategy
for future observations:

- Coordination between GW-EM community
- Dedicated programs to follow-up the GW events
- Optimized observational strategies
- Design next generation telescopes and GW detectors to maximize the multi-messenger science output

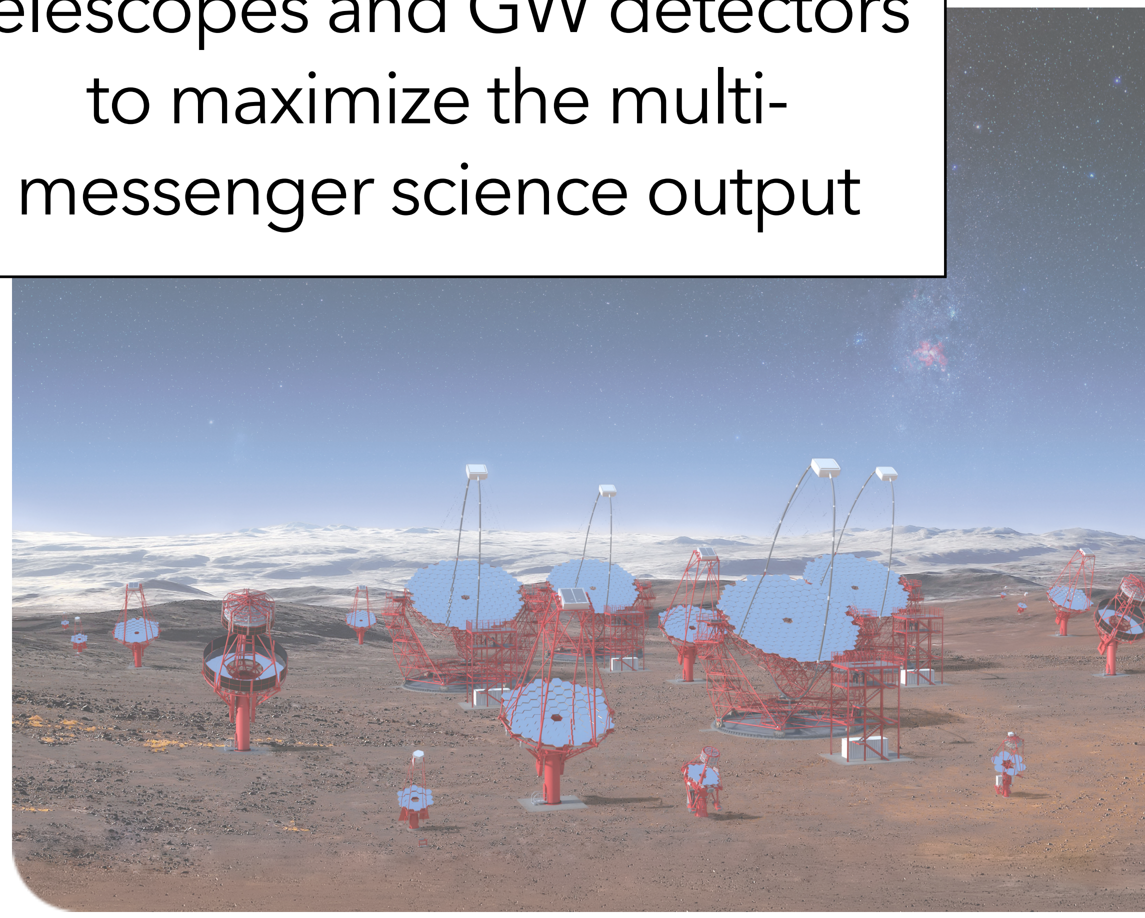

The standard picture

Massive star collapse

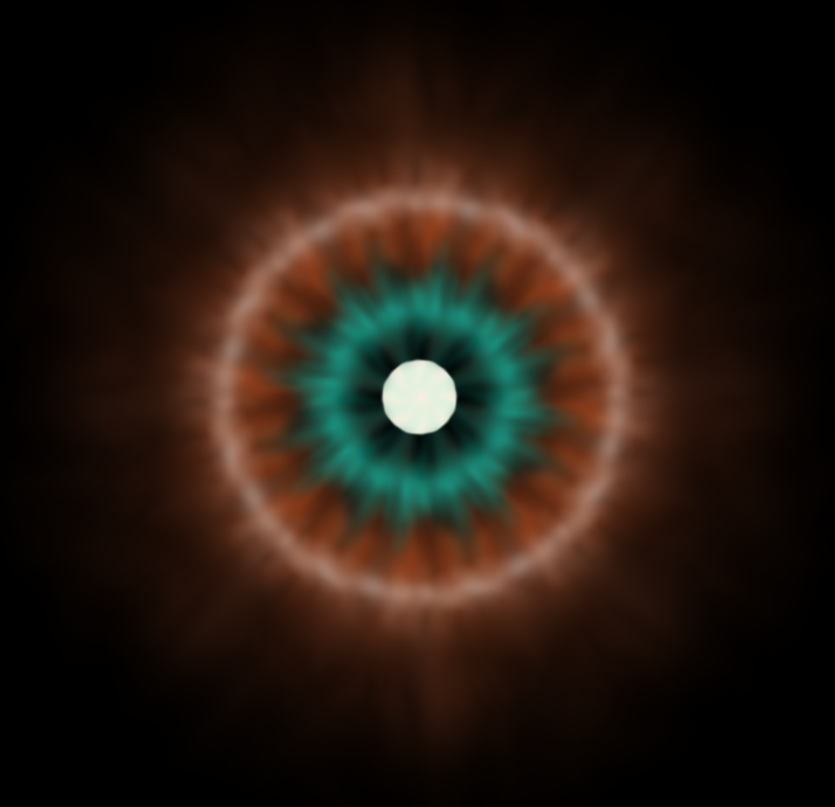

Central engine

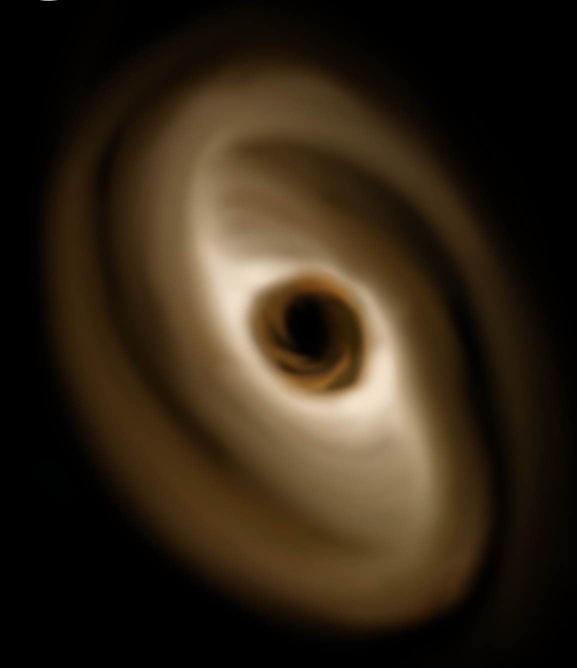

Several prompt emission scenarios

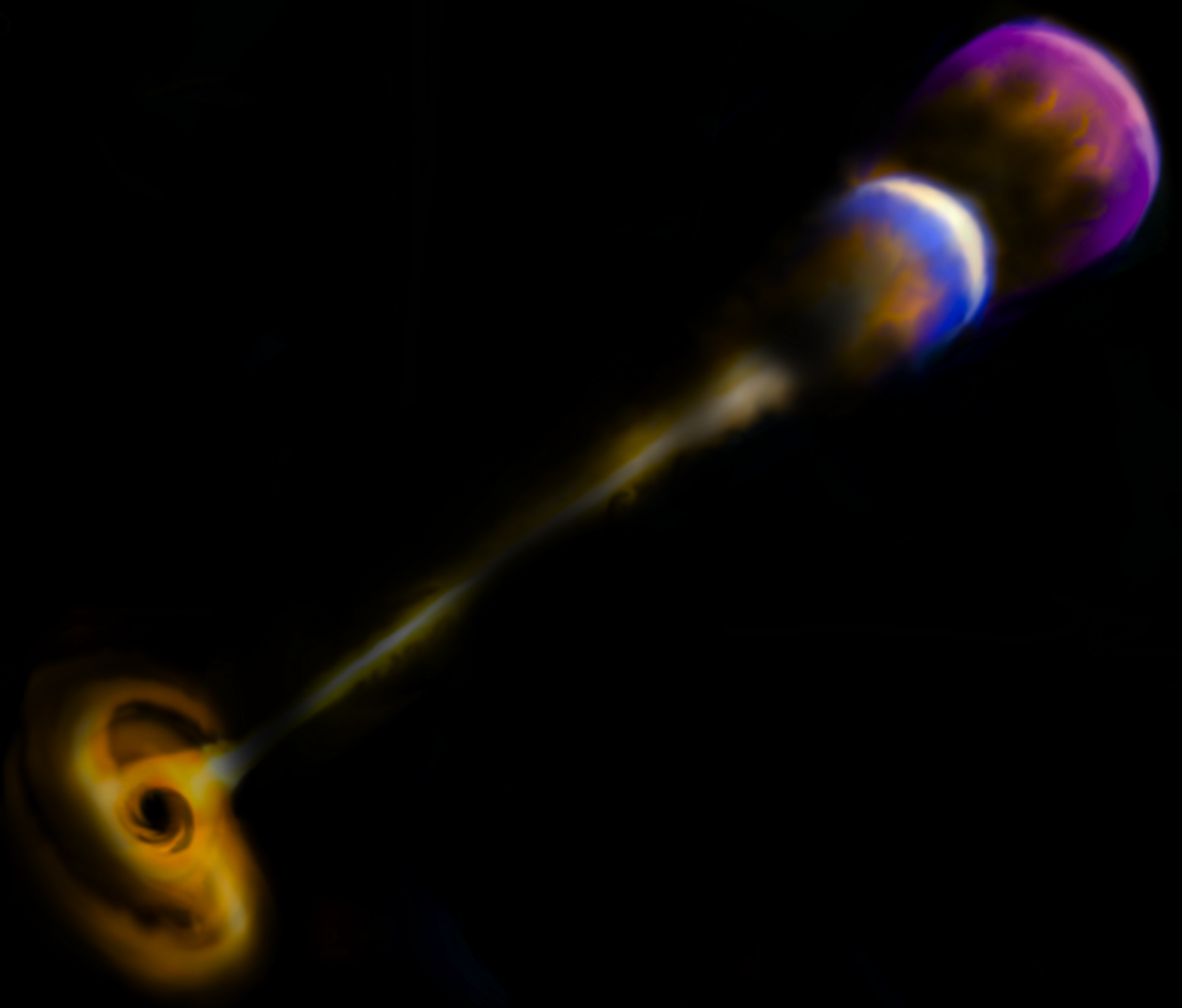

Compact binary merger, containing at least one neutron star

The standard picture

Massive star collapse

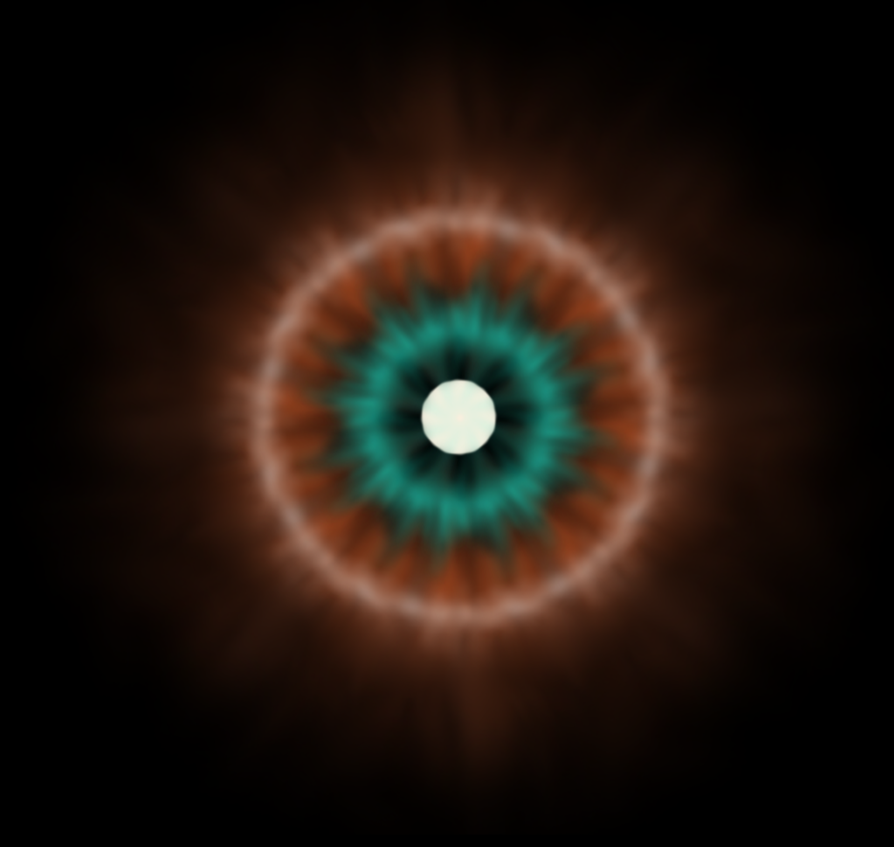

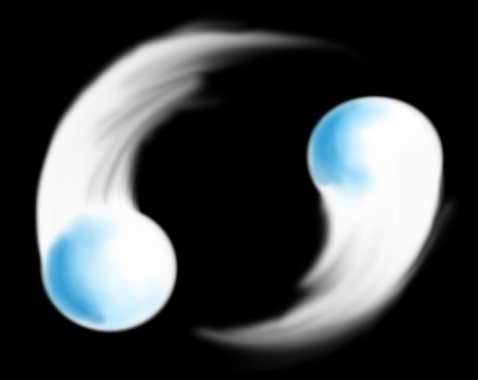

Compact binary merger, containing at least one neutron star

Central engine

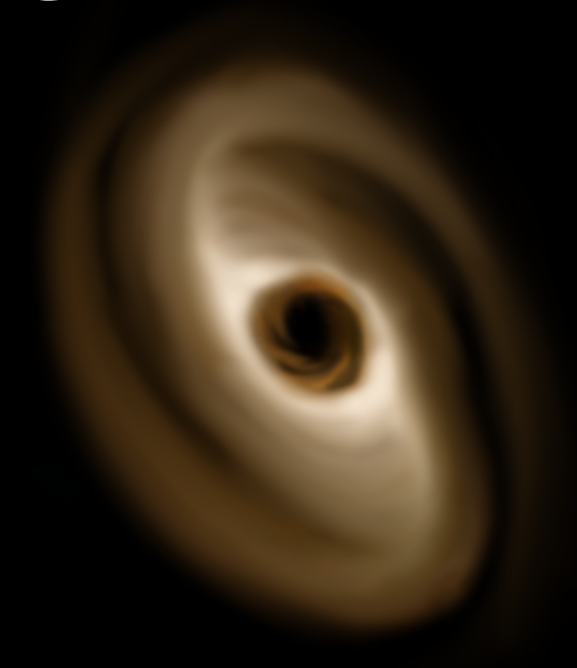

Several prompt emission scenarios

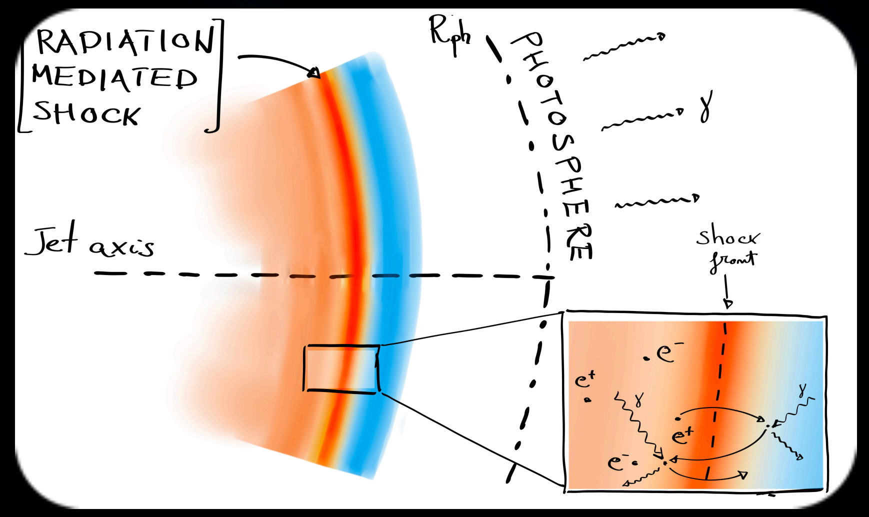

Photospheric emission

Eichler + 2000,
Ryde + 2005,
Pe'er + 2006

The standard picture

Massive star collapse

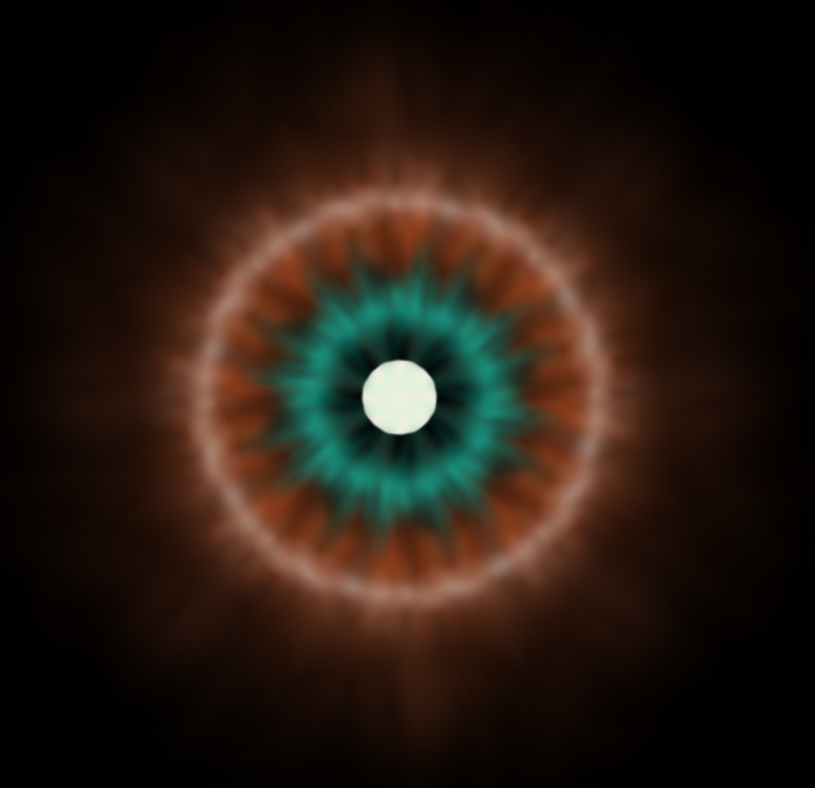

Central engine

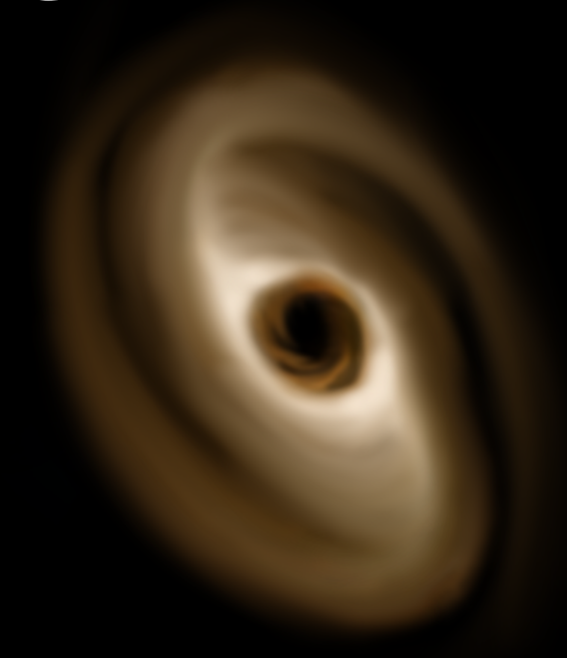

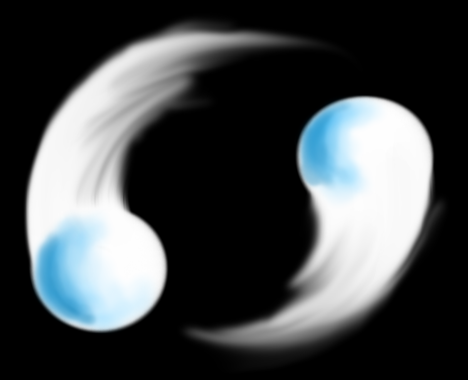

Compact binary merger, containing at least one neutron star

Several prompt emission scenarios

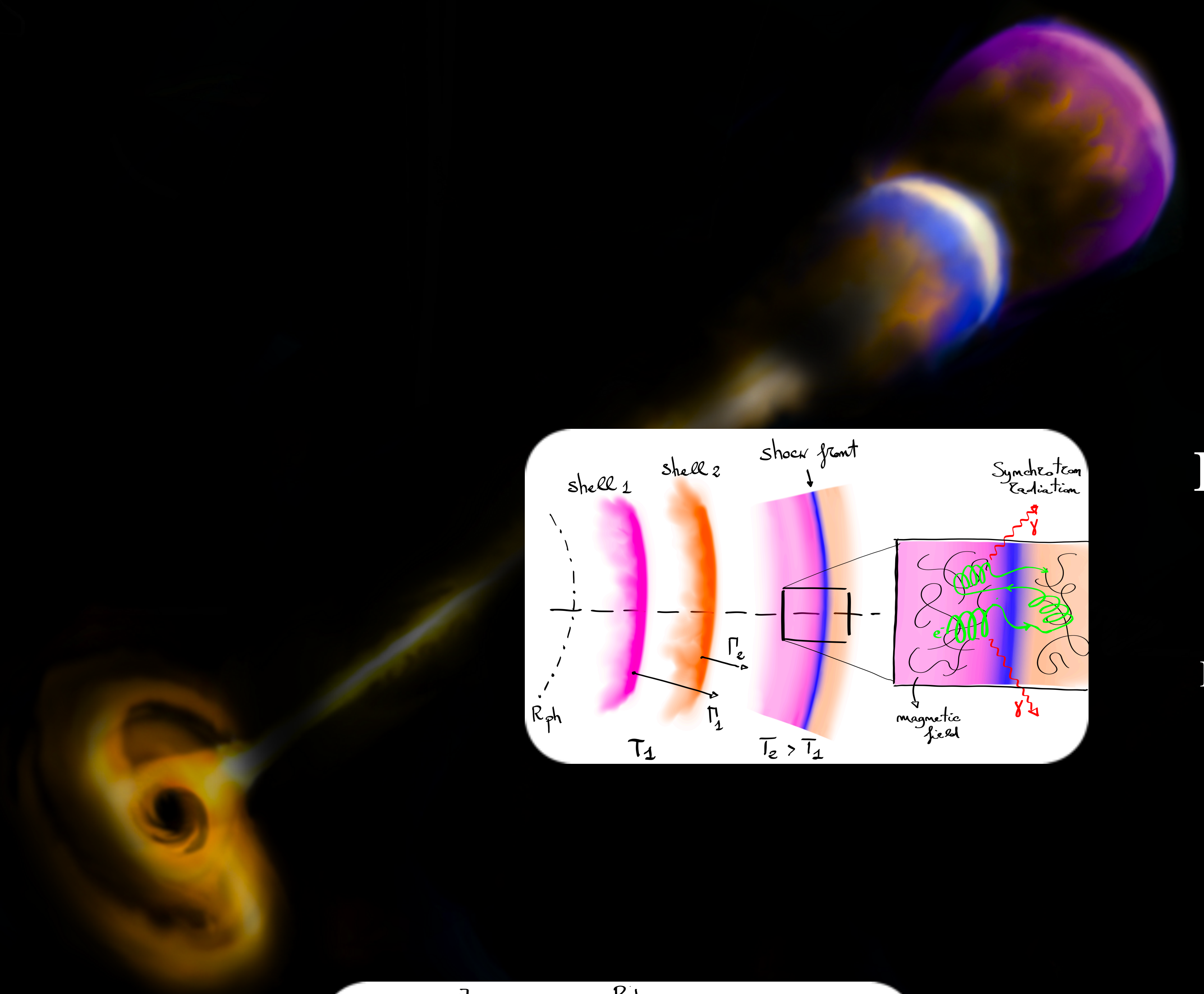

Internal shocks

Rees & Mezsaros 1994
Kobayashi + 1997
Daigne & Mochkovich 1998

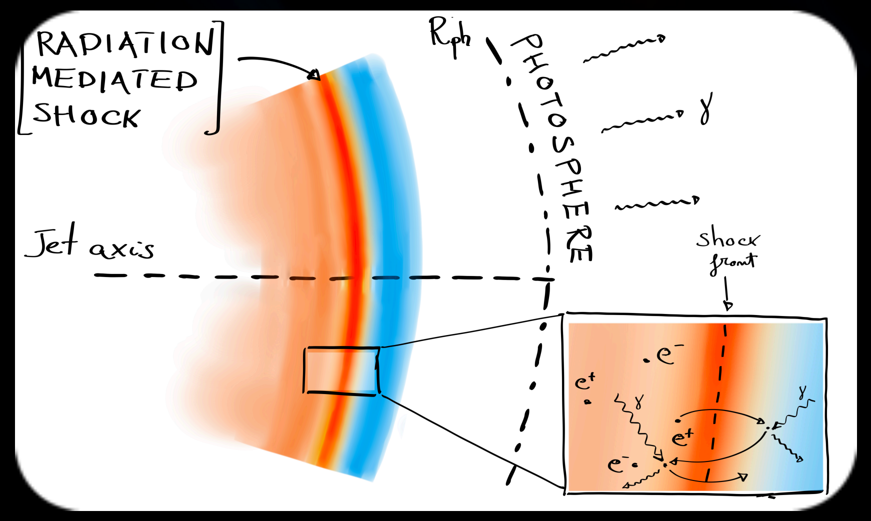

Photospheric emission

Eichler + 2000,
Ryde + 2005,
Pe'er + 2006

Massive star collapse

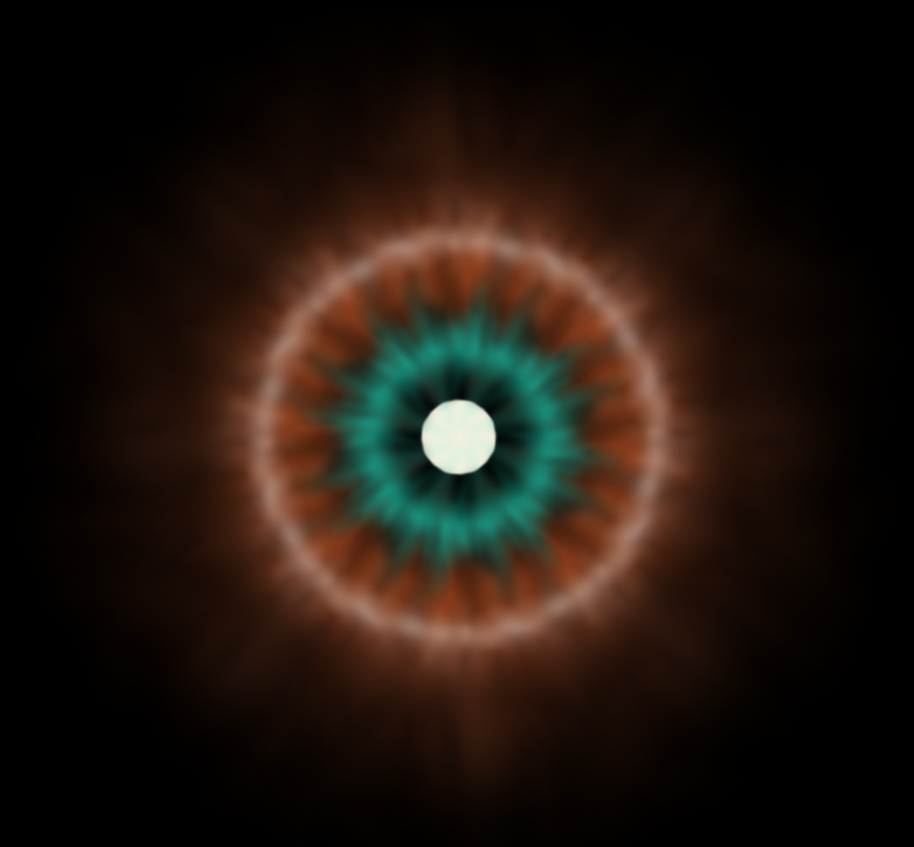

Compact binary merger, containing at least one neutron star

Central engine

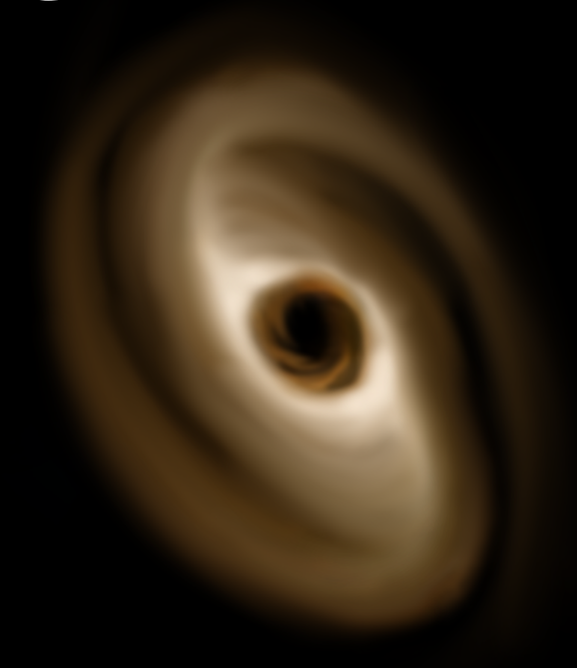

Several prompt emission scenarios

Magnetic reconnections

Drenkhahn 2002,
Lyutikov & Blandford 2003
Zhang 2011

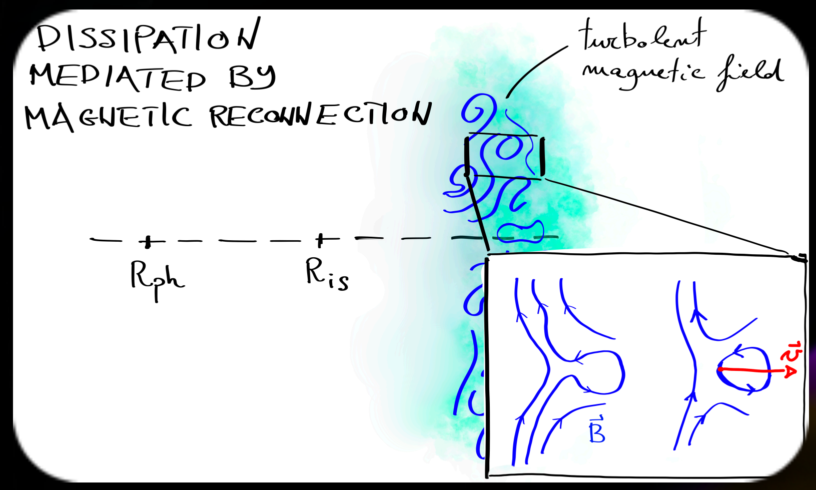

Internal shocks

Rees & Mezsaros 1994
Kobayashi + 1997
Daigne & Mochkovich 1998

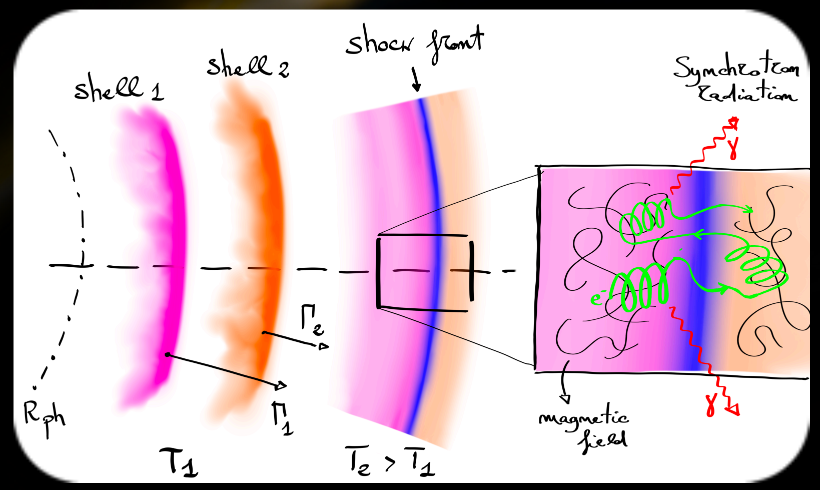

Photospheric emission

Eichler + 2000,
Ryde + 2005,
Pe'er + 2006

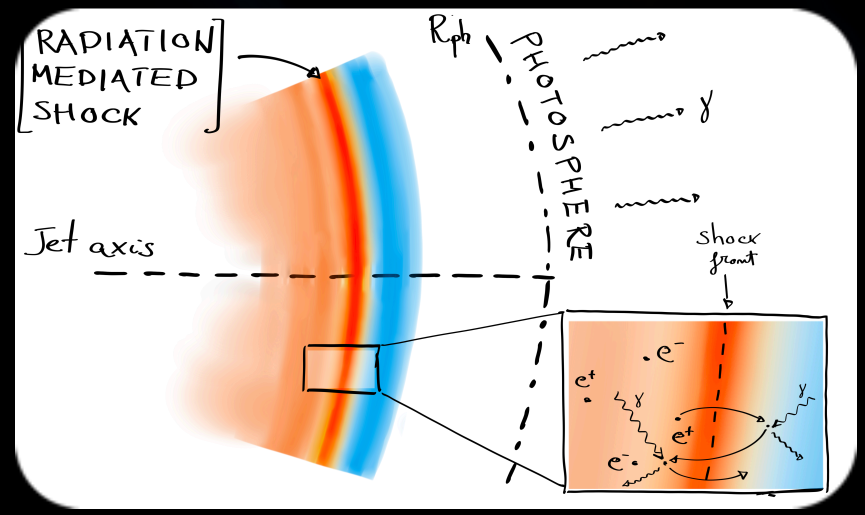

The standard picture

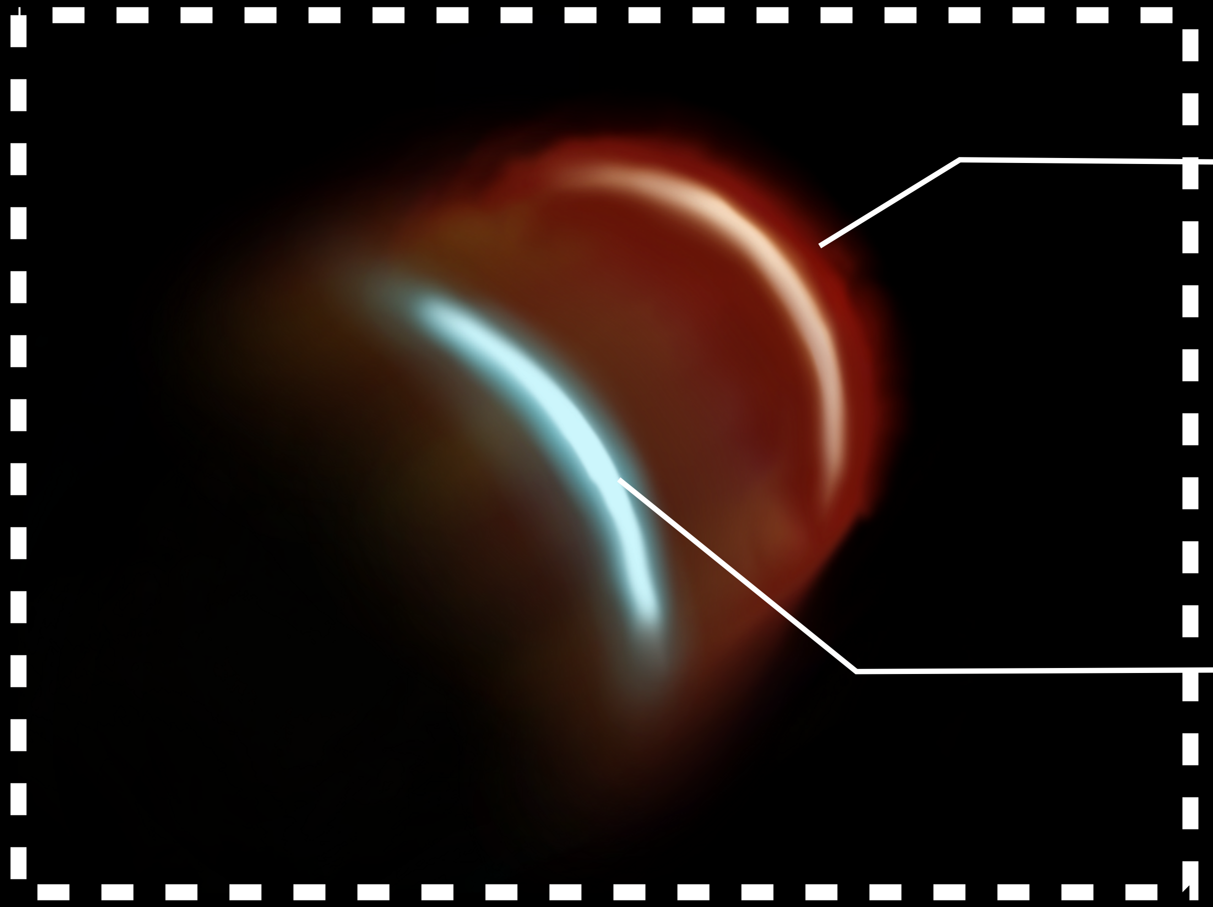

Forward shock —> long lasting, visible from radio to VHE

Reverse shock —> duration limited by shock crossing time, visible mainly in optical and radio

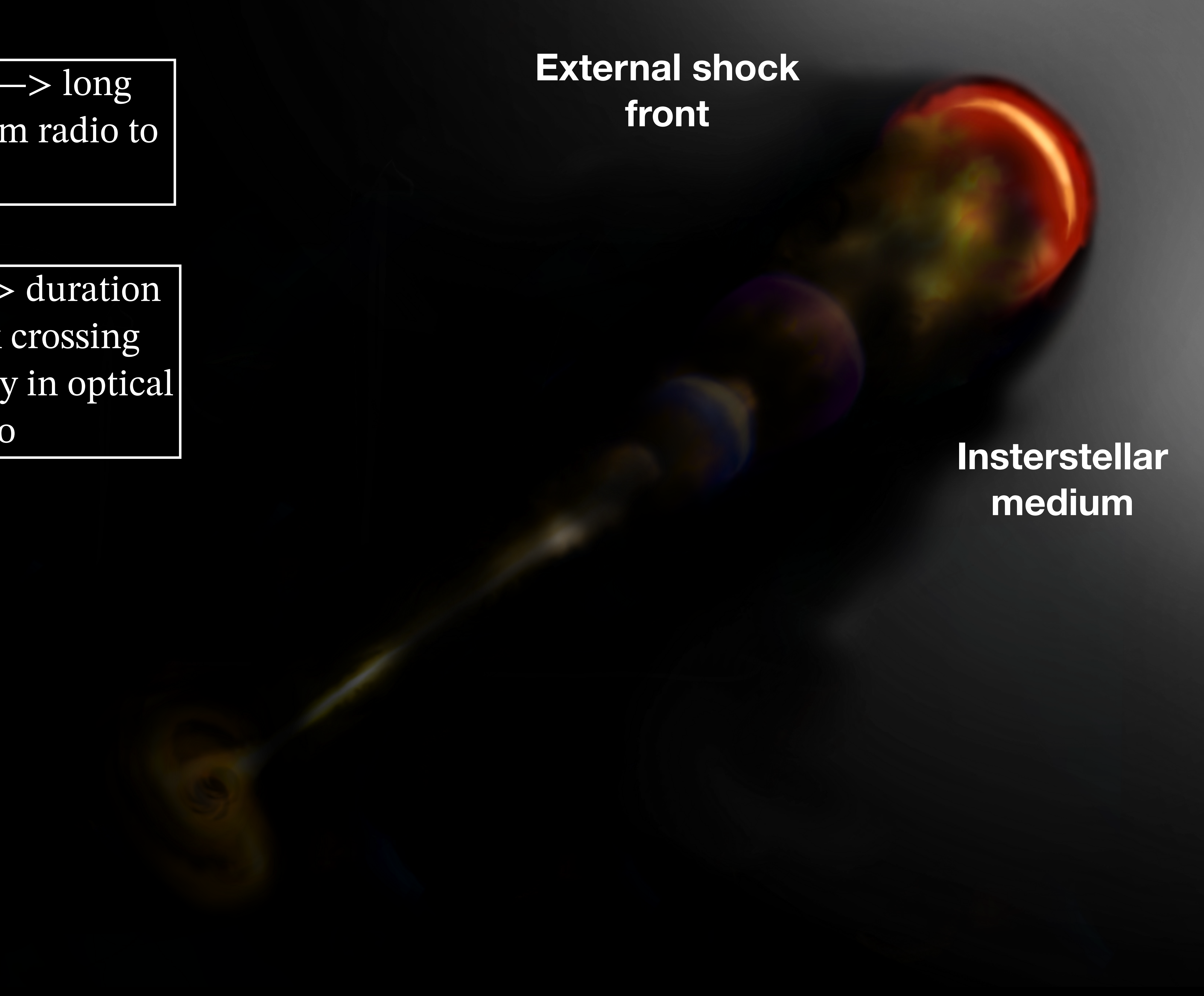

The standard picture

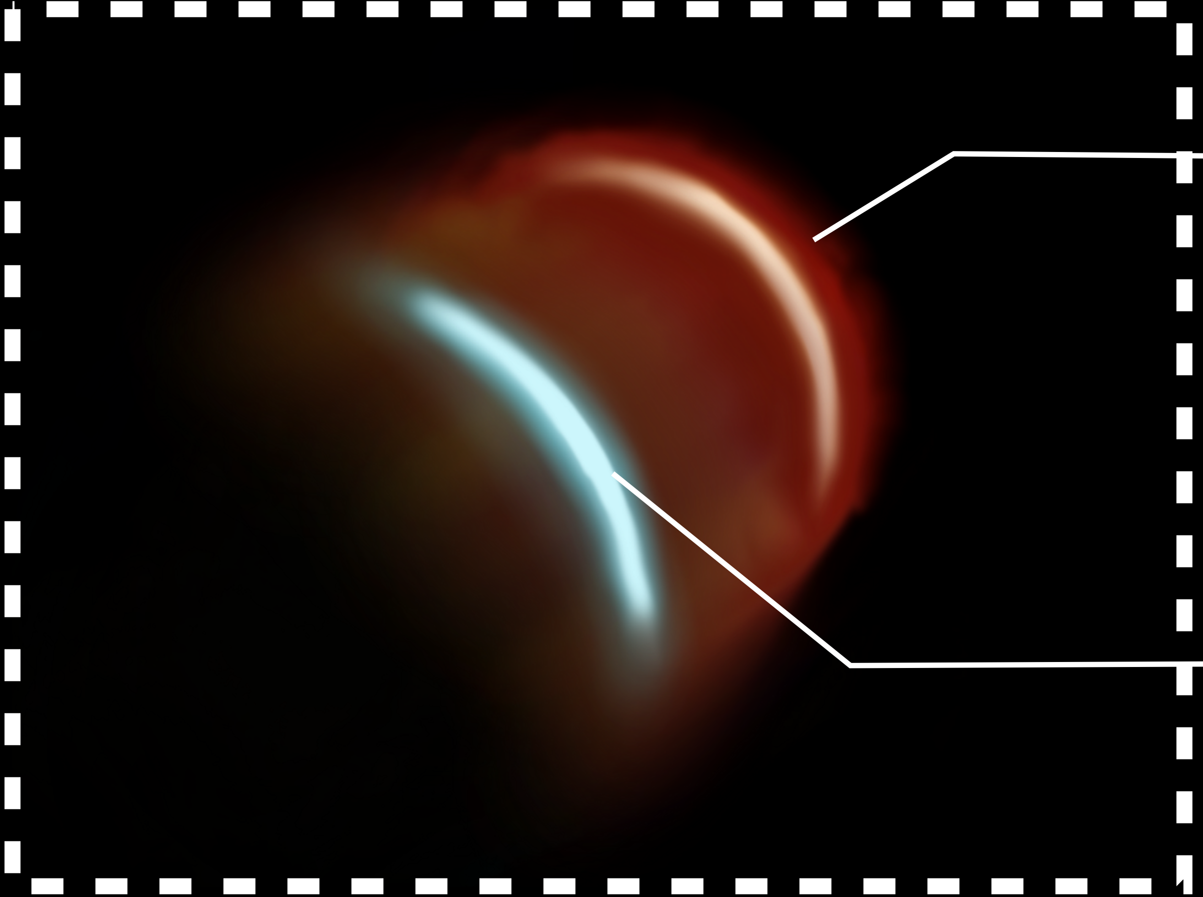

Forward shock —> long lasting, visible from radio to VHE

Reverse shock —> duration limited by shock crossing time, visible mainly in optical and radio

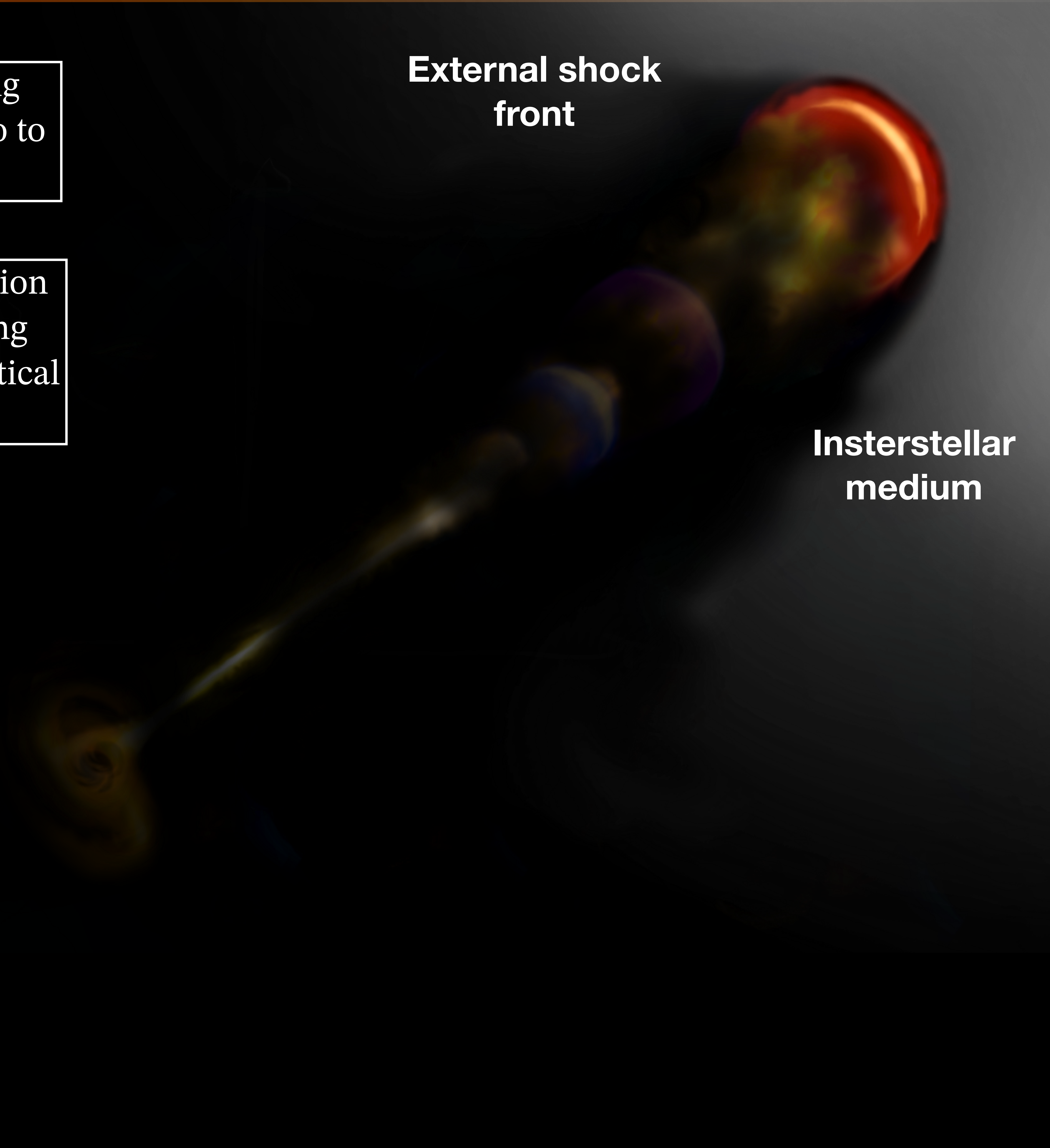

On-axis

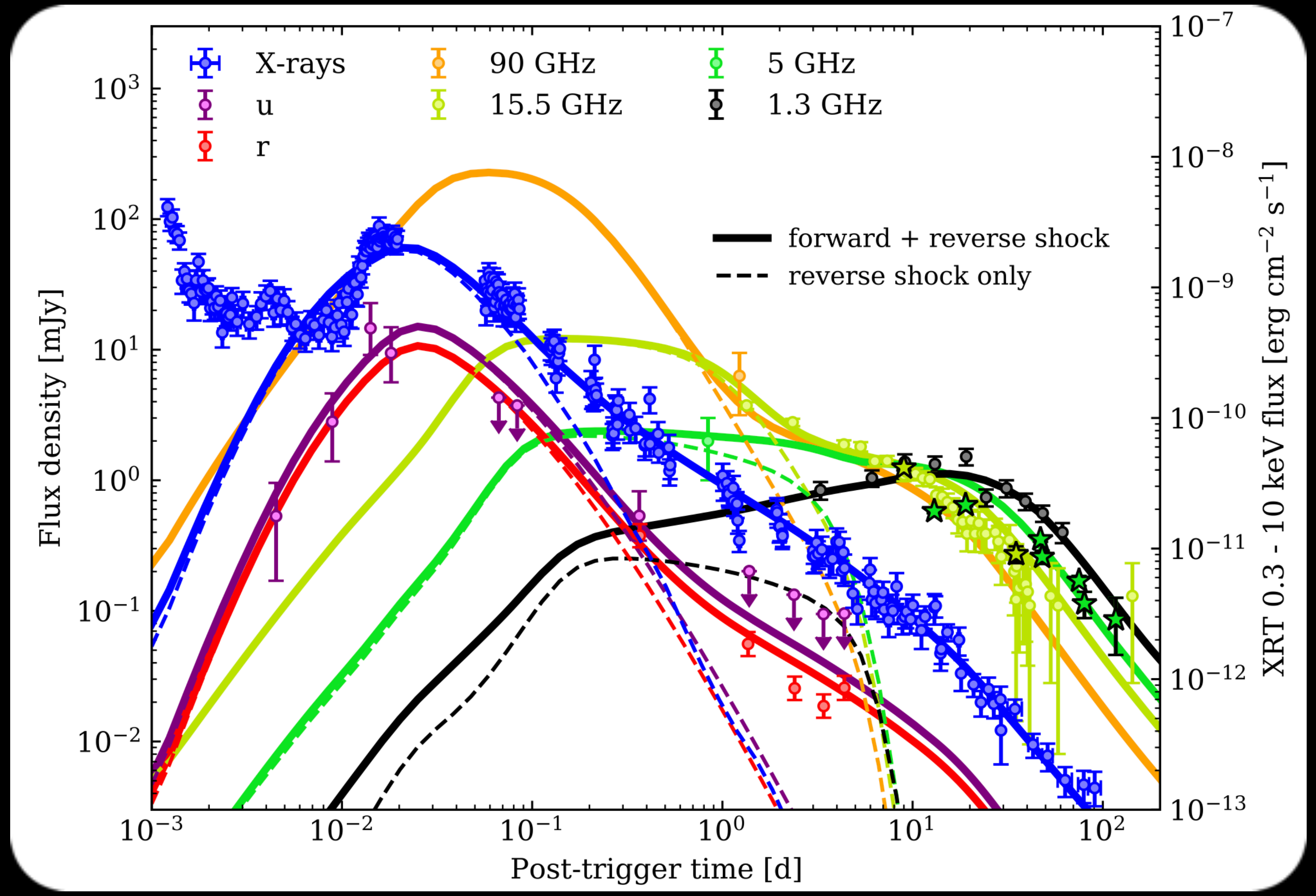

e.g., Salafia 2022

The standard picture

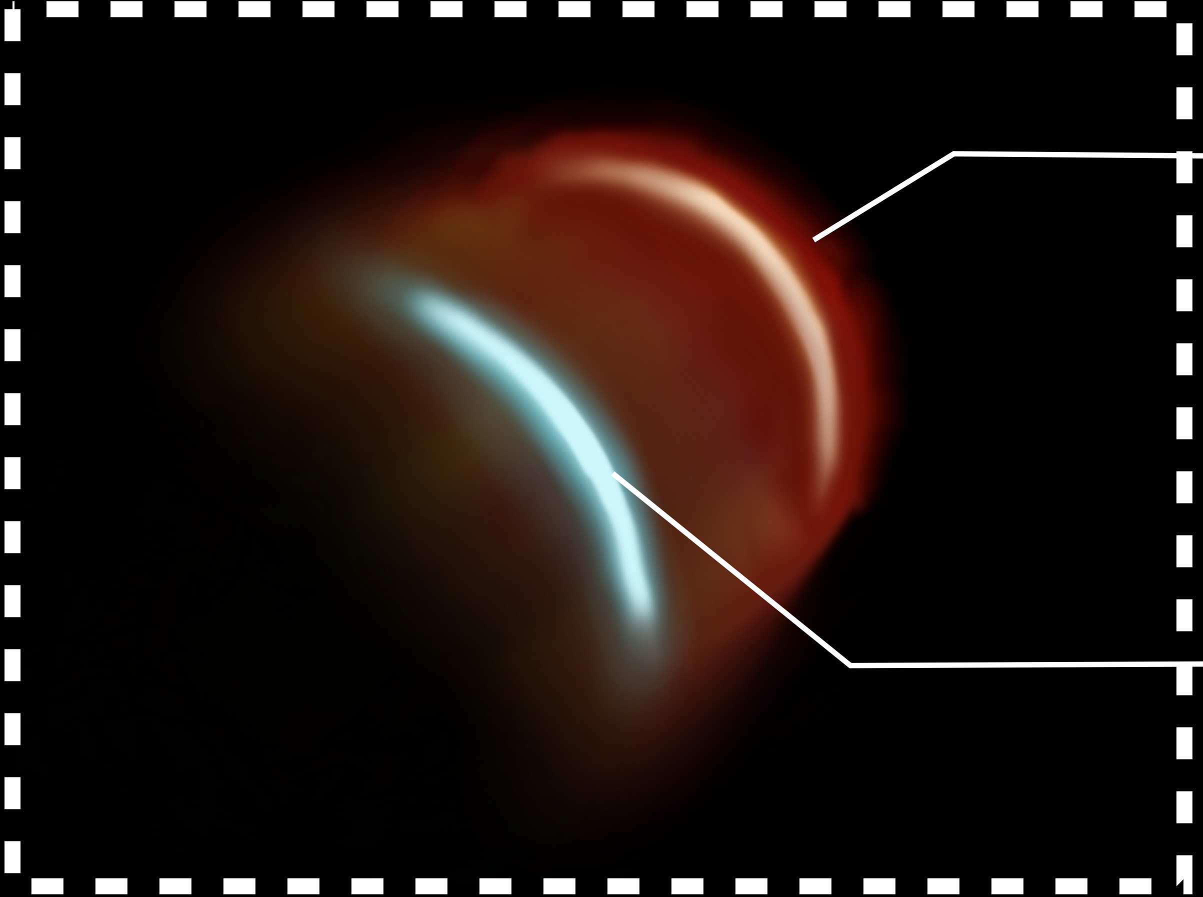

Forward shock —> long lasting, visible from radio to VHE

Reverse shock —> duration limited by shock crossing time, visible mainly in optical and radio

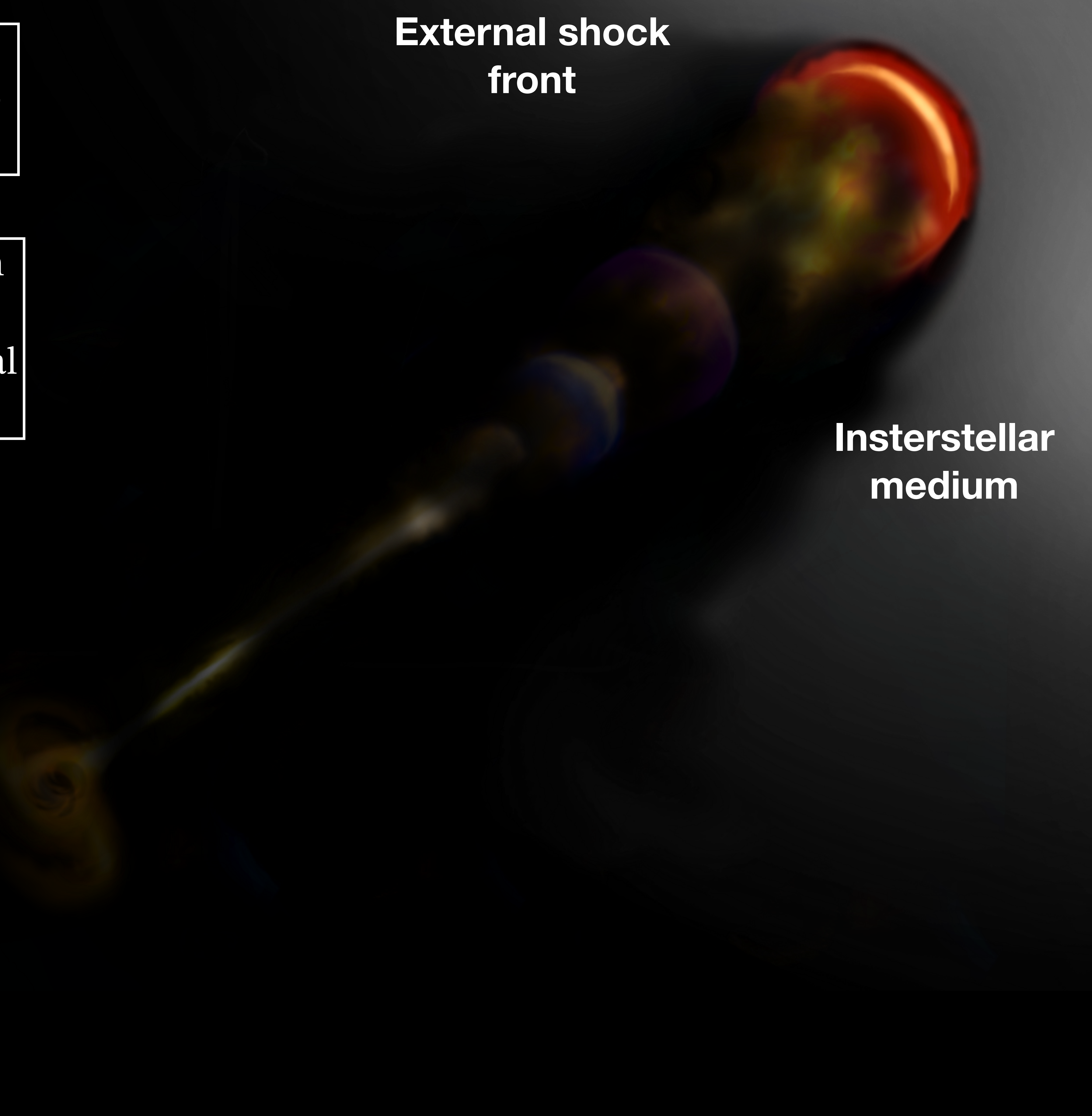

On-axis

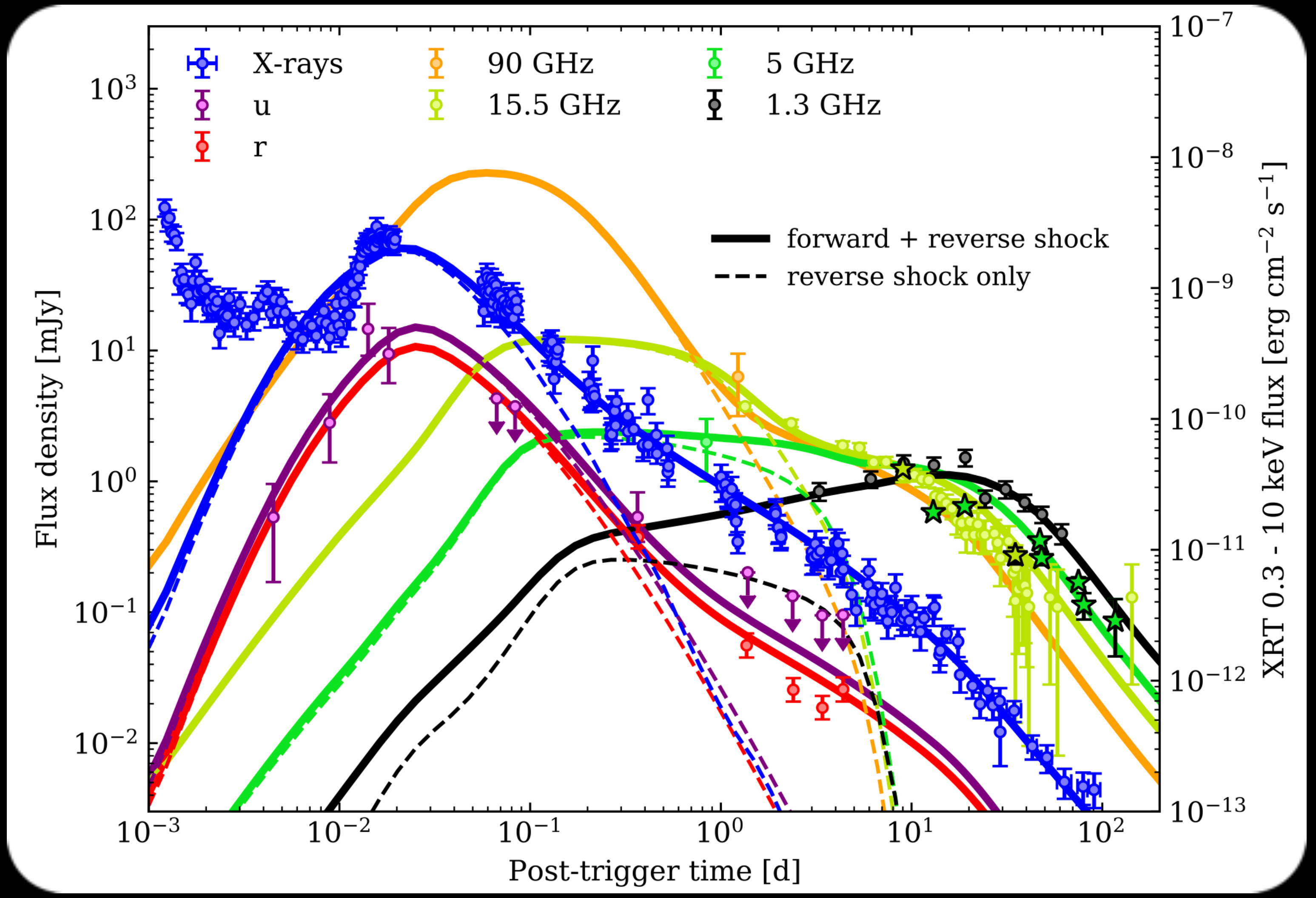

e.g., Salafia 2022

Off-axis

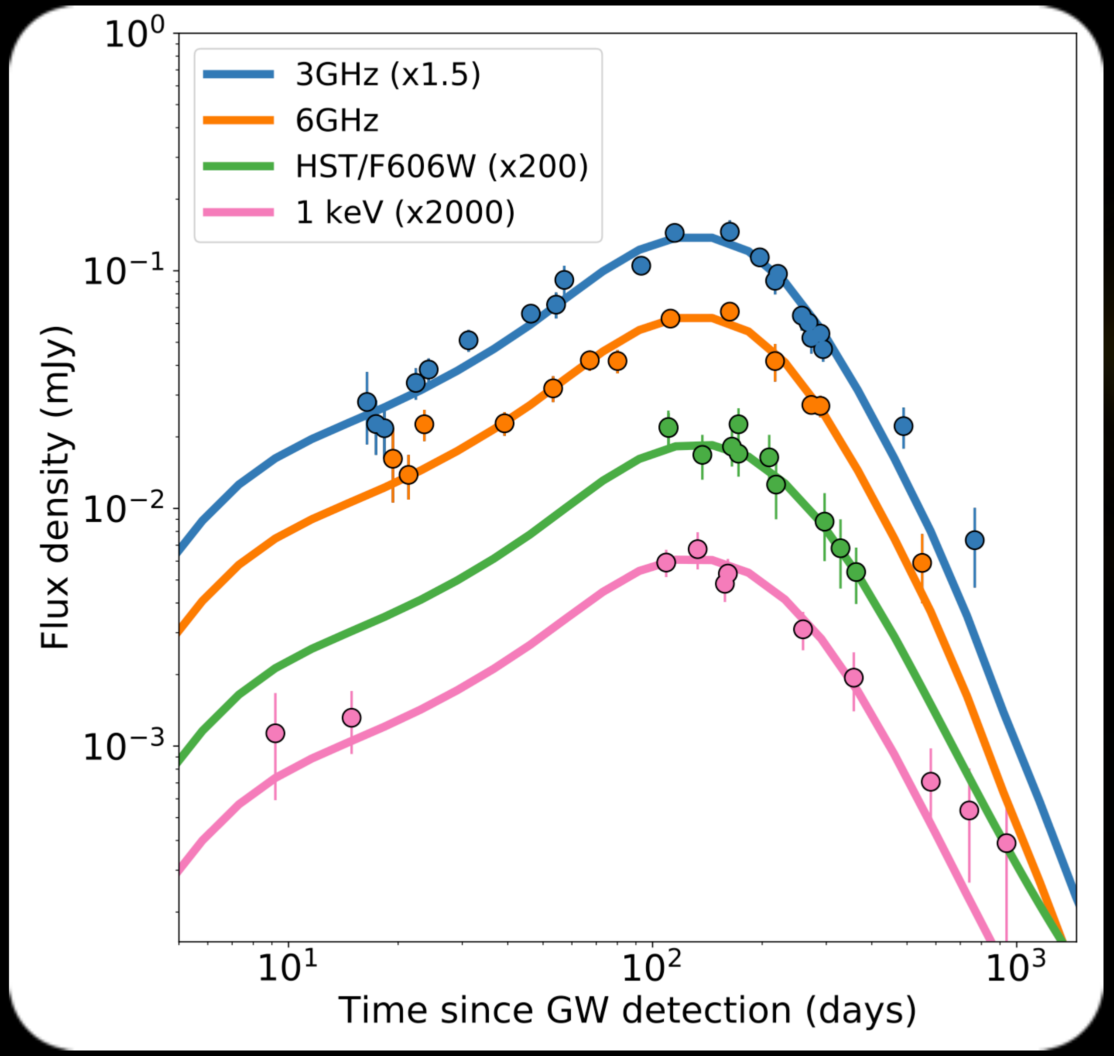

e.g., Makhathini 2021

The standard picture

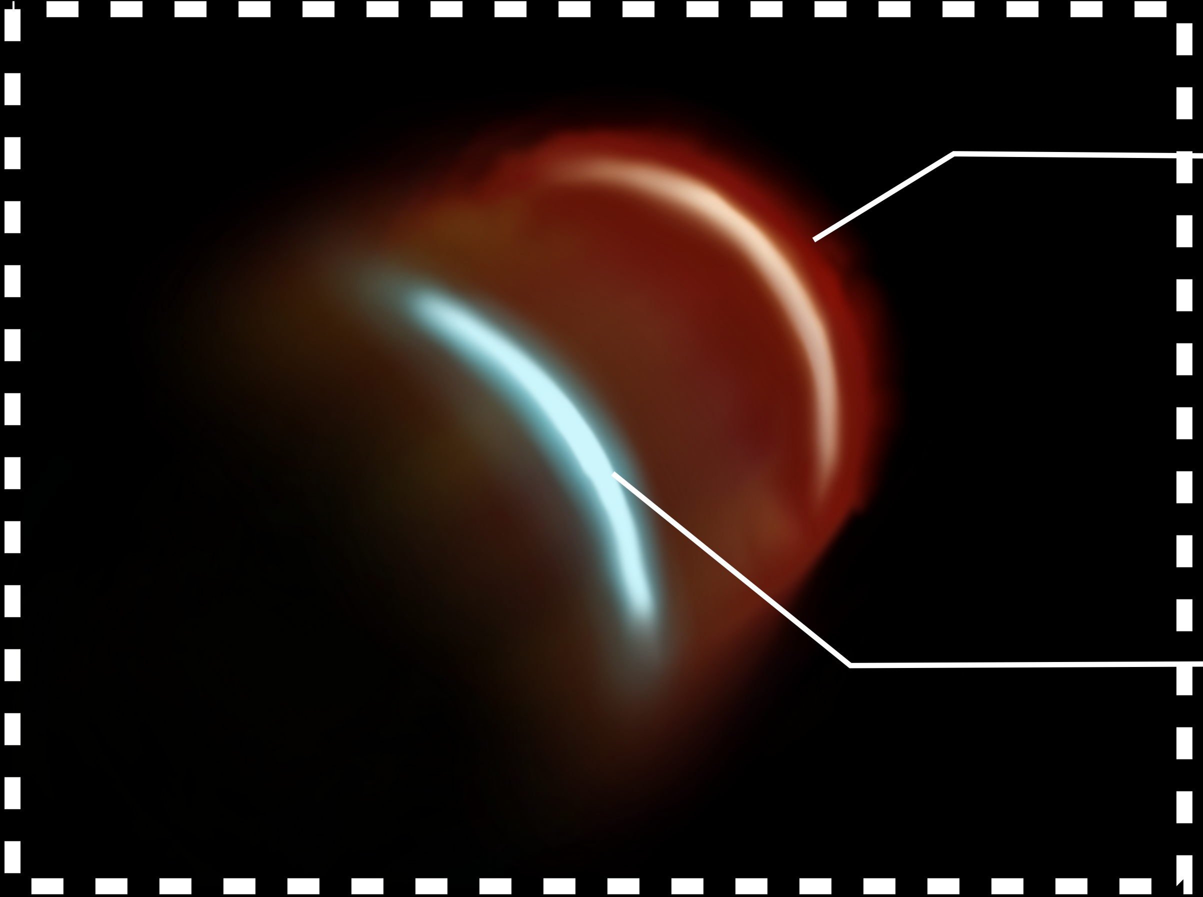

Forward shock —> long lasting, visible from radio to VHE

Reverse shock —> duration limited by shock crossing time, visible mainly in optical and radio

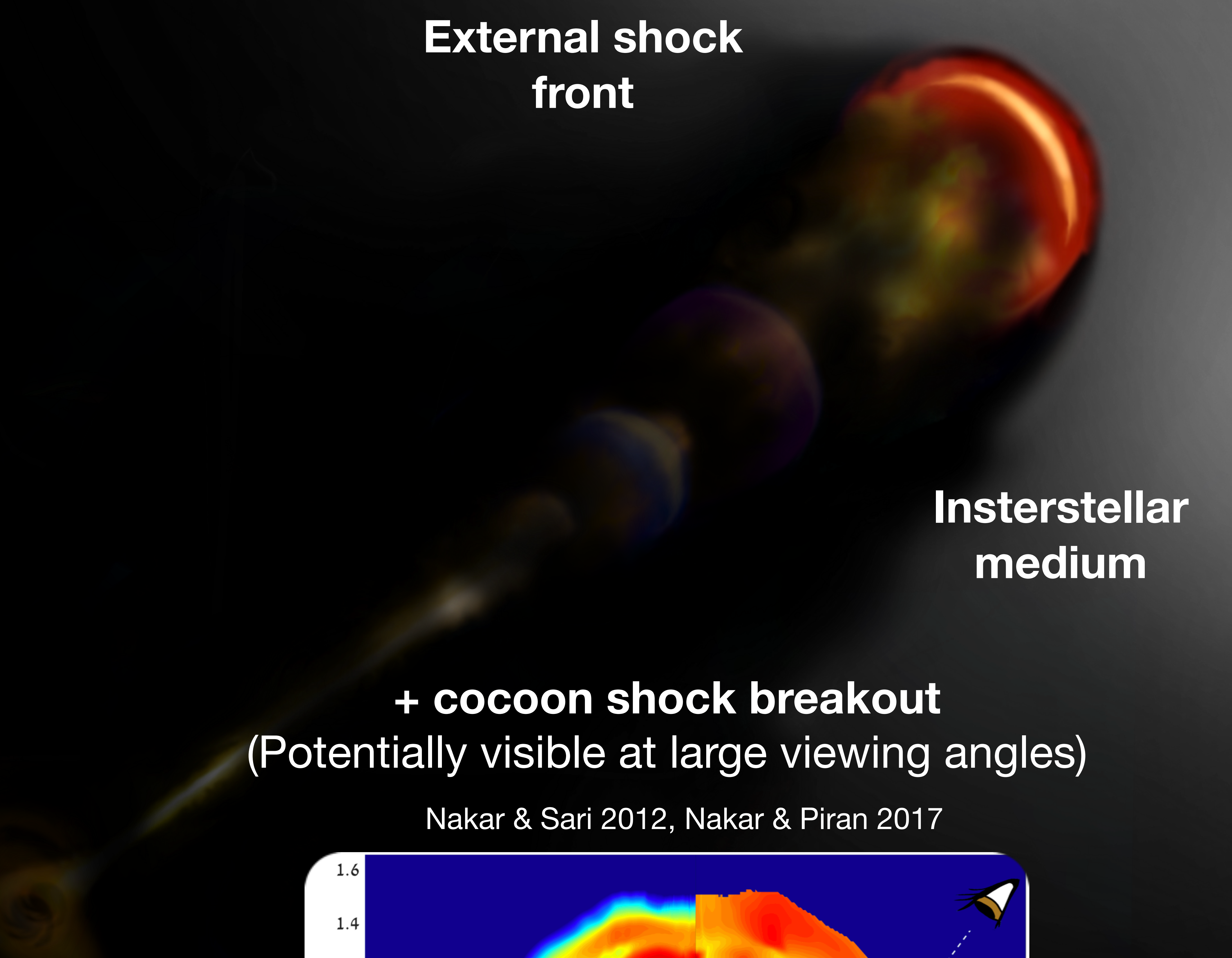

+ cocoon shock breakout
(Potentially visible at large viewing angles)

Nakar & Sari 2012, Nakar & Piran 2017

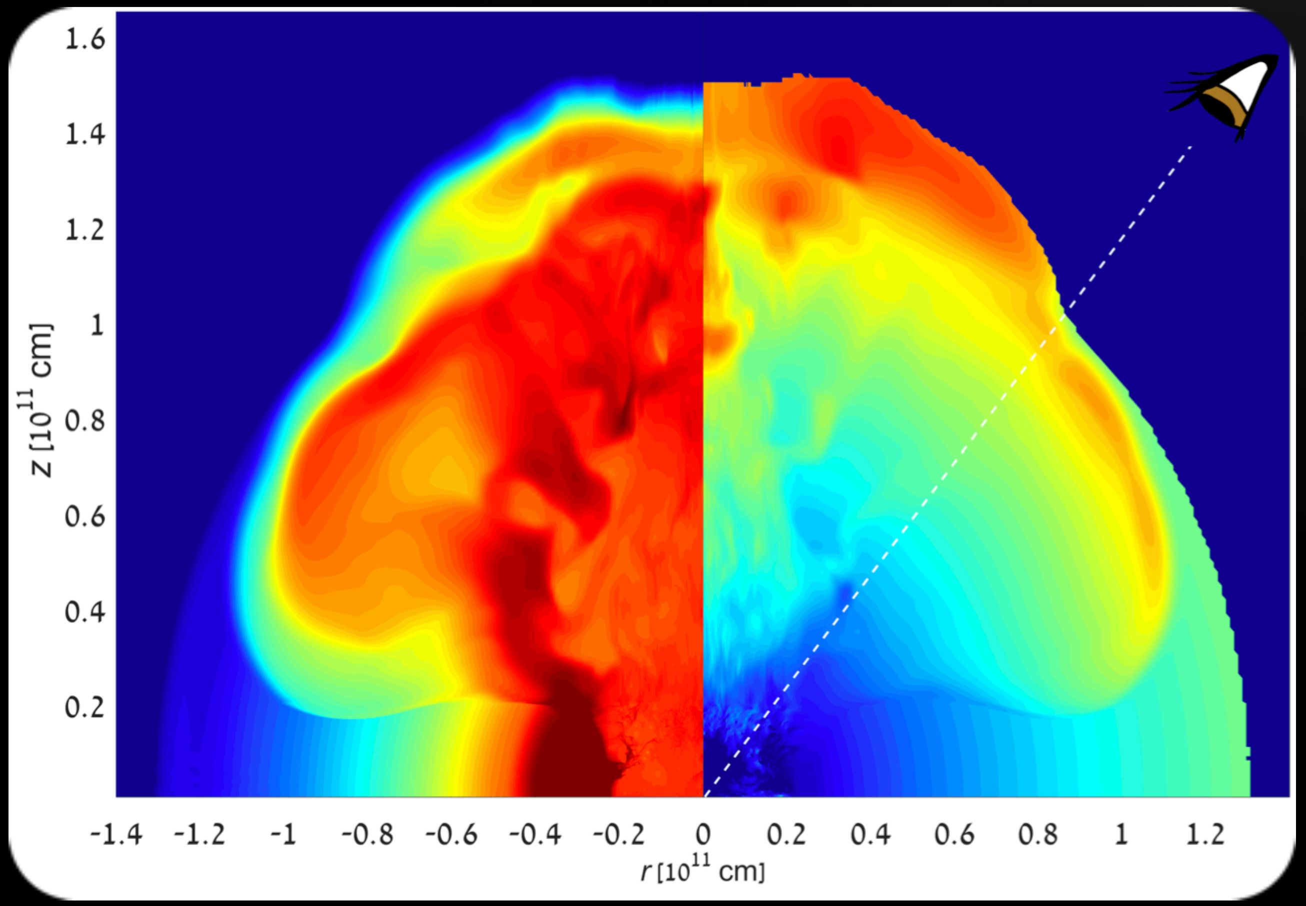

On-axis

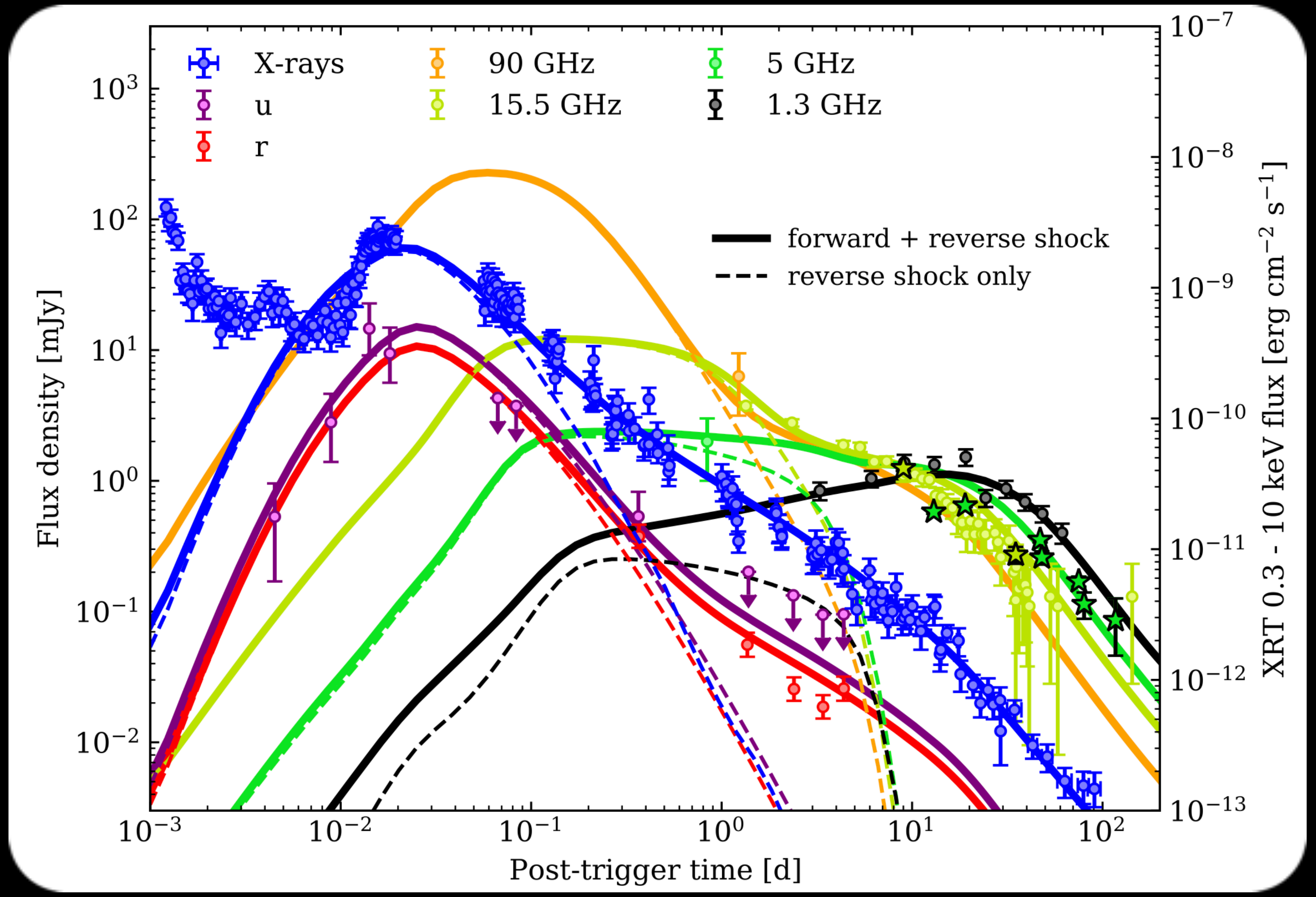

e.g., Salafia 2022

Off-axis

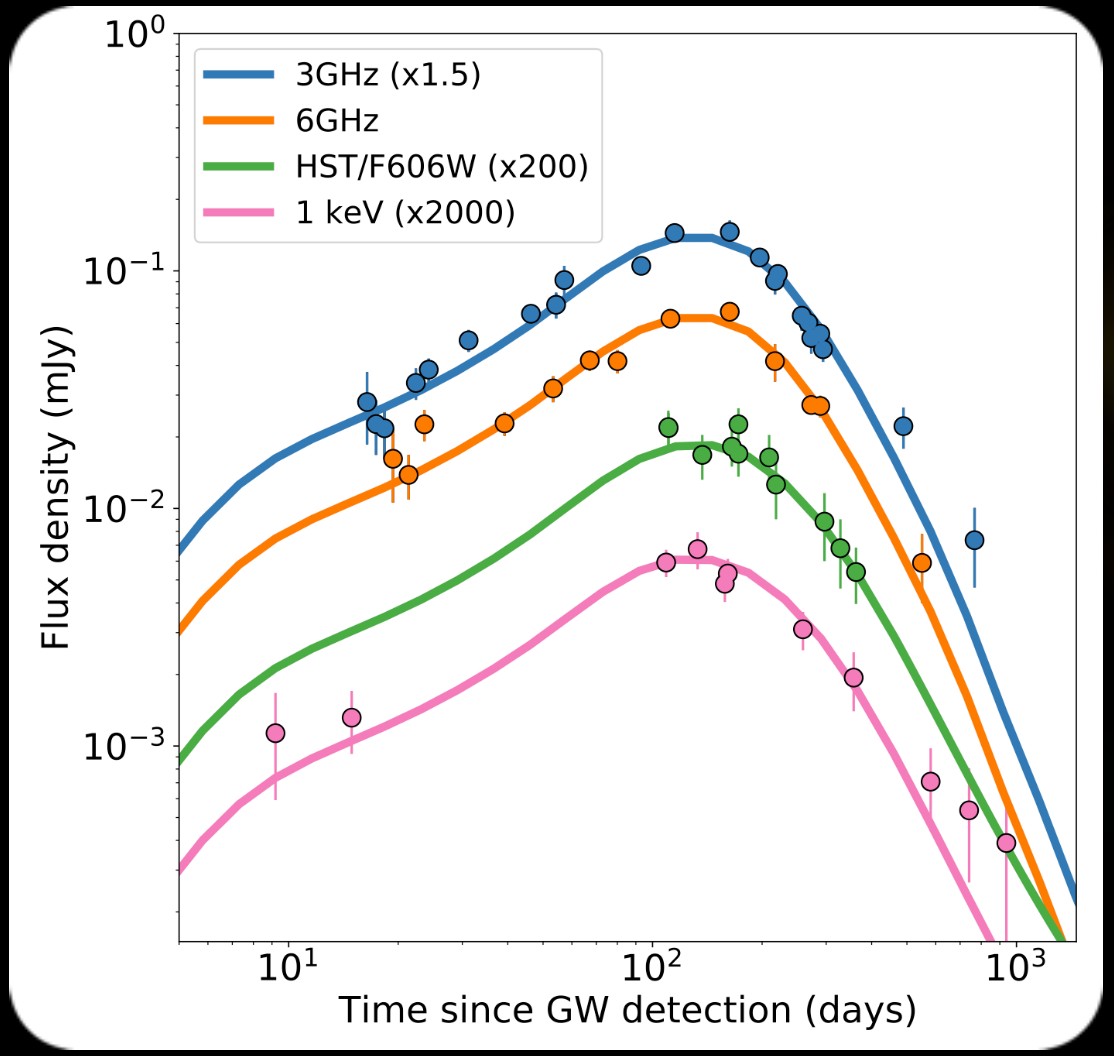

e.g., Makhathini 2021

Open questions about γ-ray bursts physics

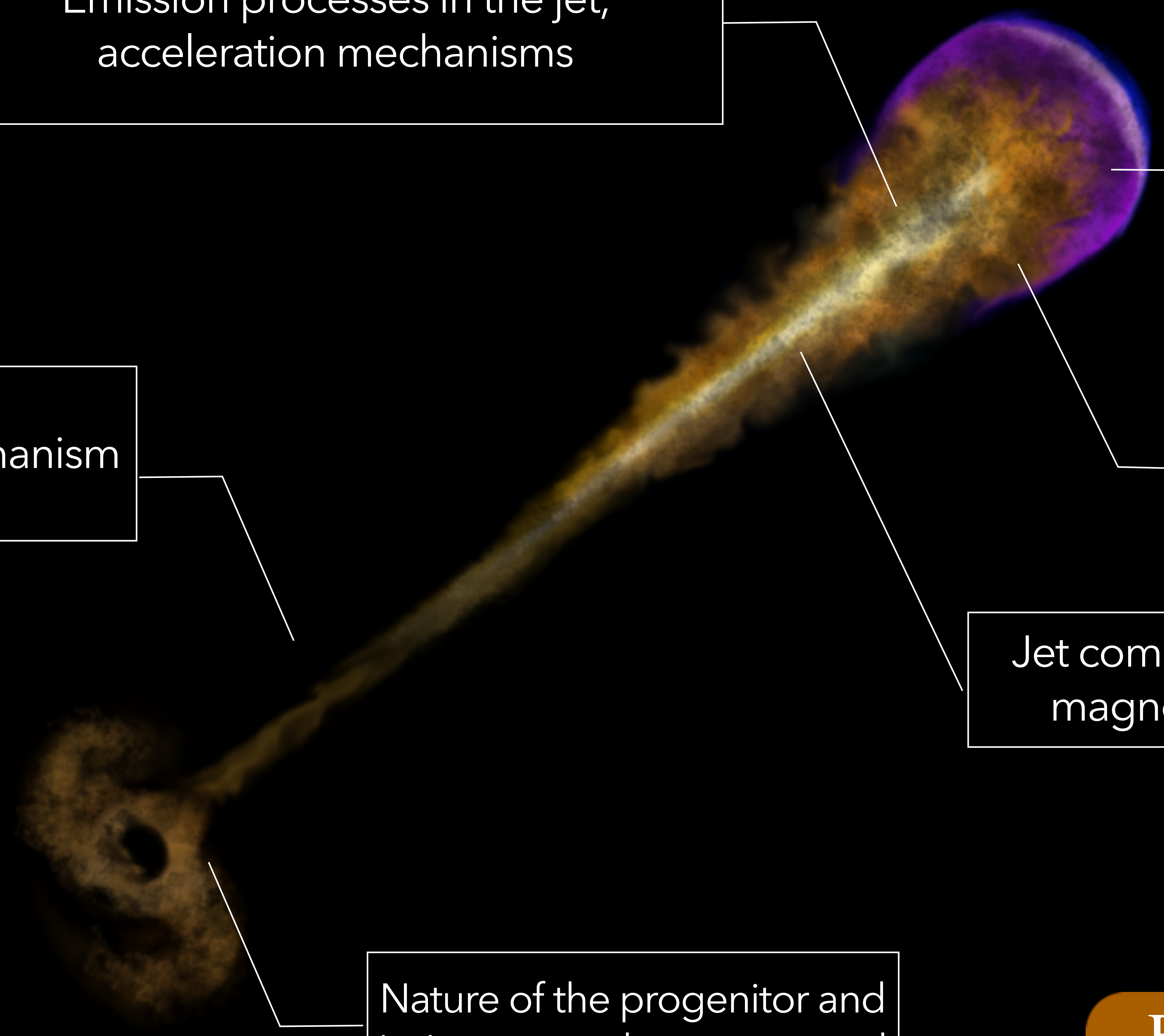

First goal of my work:

Exploit the archival data from *Swift* to give new insights about these open issues

Multi-messenger perspectives

What GW data can tell about the remnant and the GRB progenitor:

- NS-NS or NS-BH?
- constraints on exotic scenarios (GRBs from BBH)
- central engine: BH vs NS paradigm
- fraction of binary mergers able to produce a relativistic jet

Joint GW+EM detection:

- a fundamental tool to test alternative theories of gravity
- critical to probe the physics of the launching mechanism and the jet break-out through the circum-burst ejecta

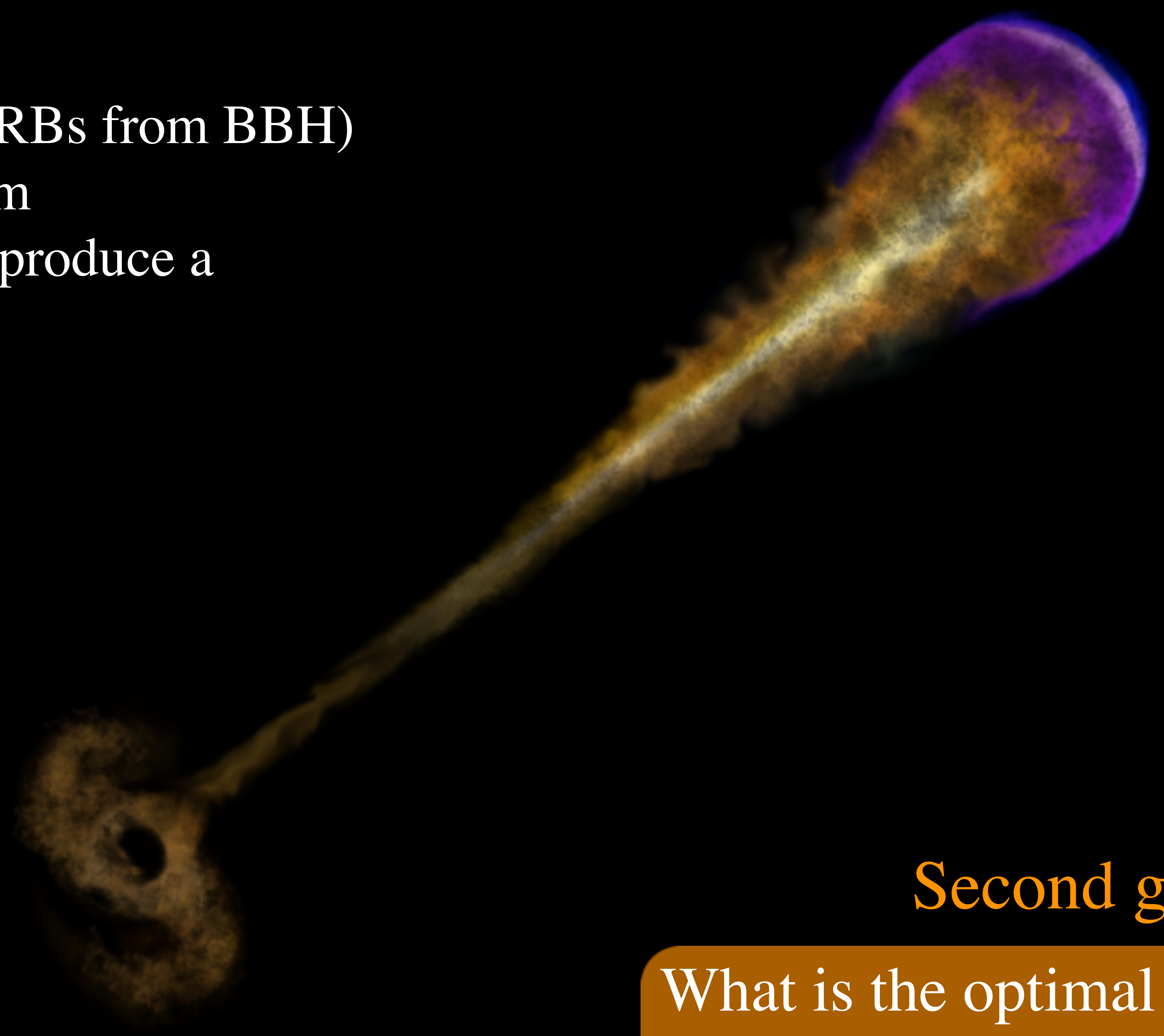

The missing messenger:

- Where are high-energy neutrinos from CBMs?

Properties of the KN ejecta:

- geometrical and dynamical structure
- neutron richness
- Heavy elements nucleosynthesis
- Probe the Jet-KN interaction

Second goal of my work:

What is the optimal combination of **future GW networks and high-energy EM probes** to answer to these questions?

Part I

On the origin of spectral evolution in the steep decay of GRBs

Ronchini et al. 2021, Nature Communications, 12, 4040

The steep decay: the transition between the prompt and afterglow phase

- Observed very often at the beginning of the light curves of Swift-XRT
- Typical duration of few 10^2 sec
- Temporal decay index ≈ 2-3
- Usually characterized by a gradual softening of the X-ray spectrum

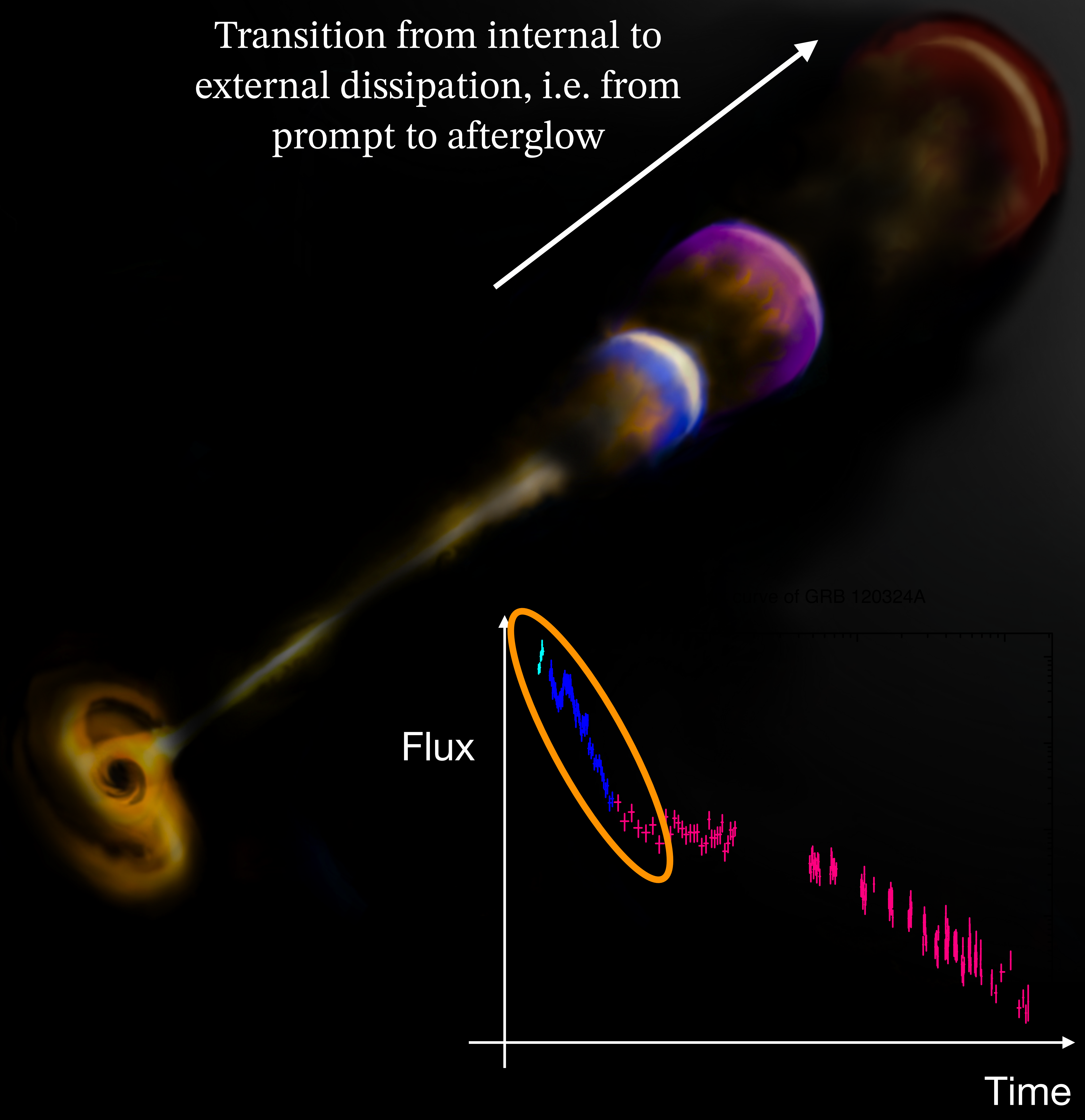

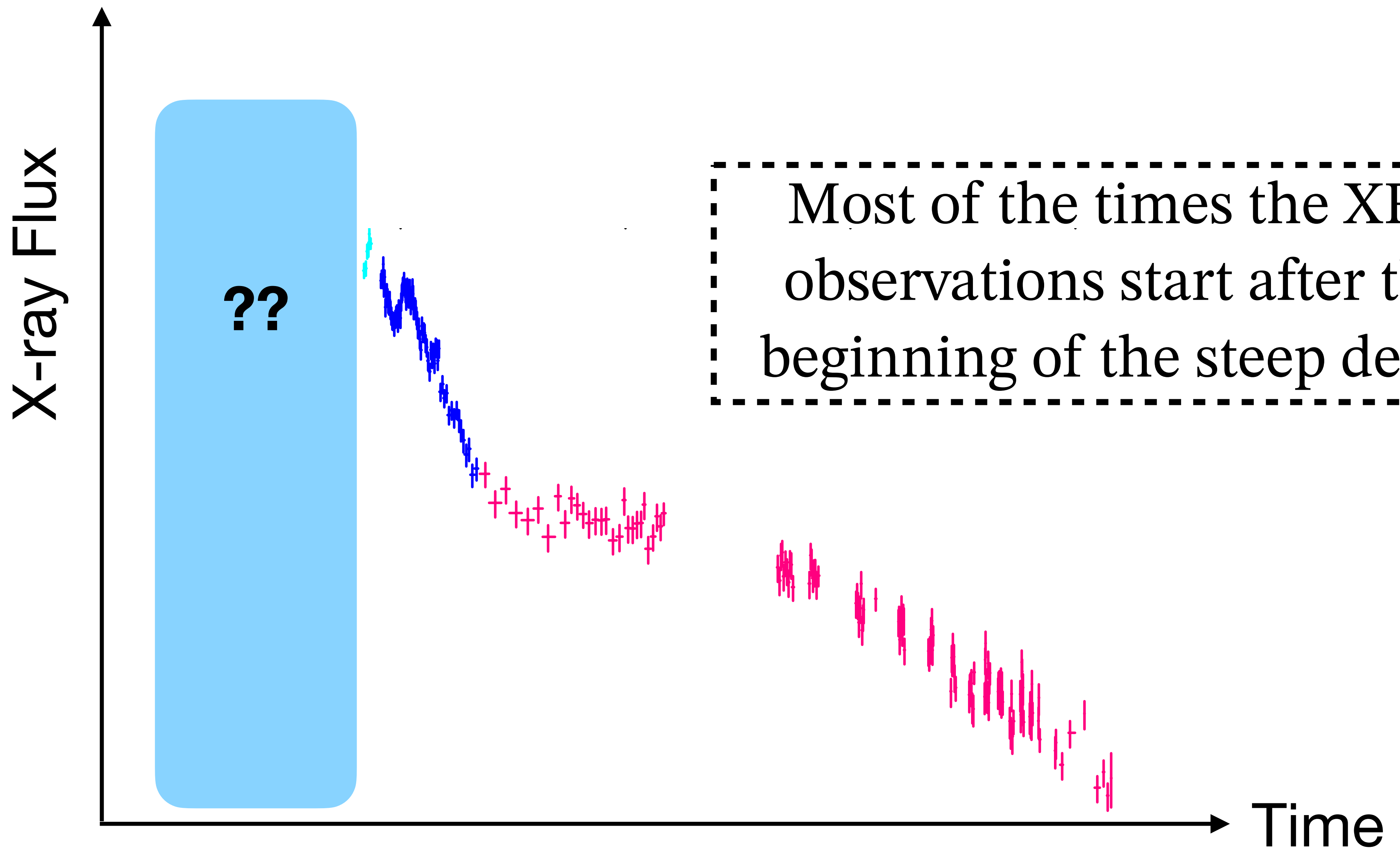

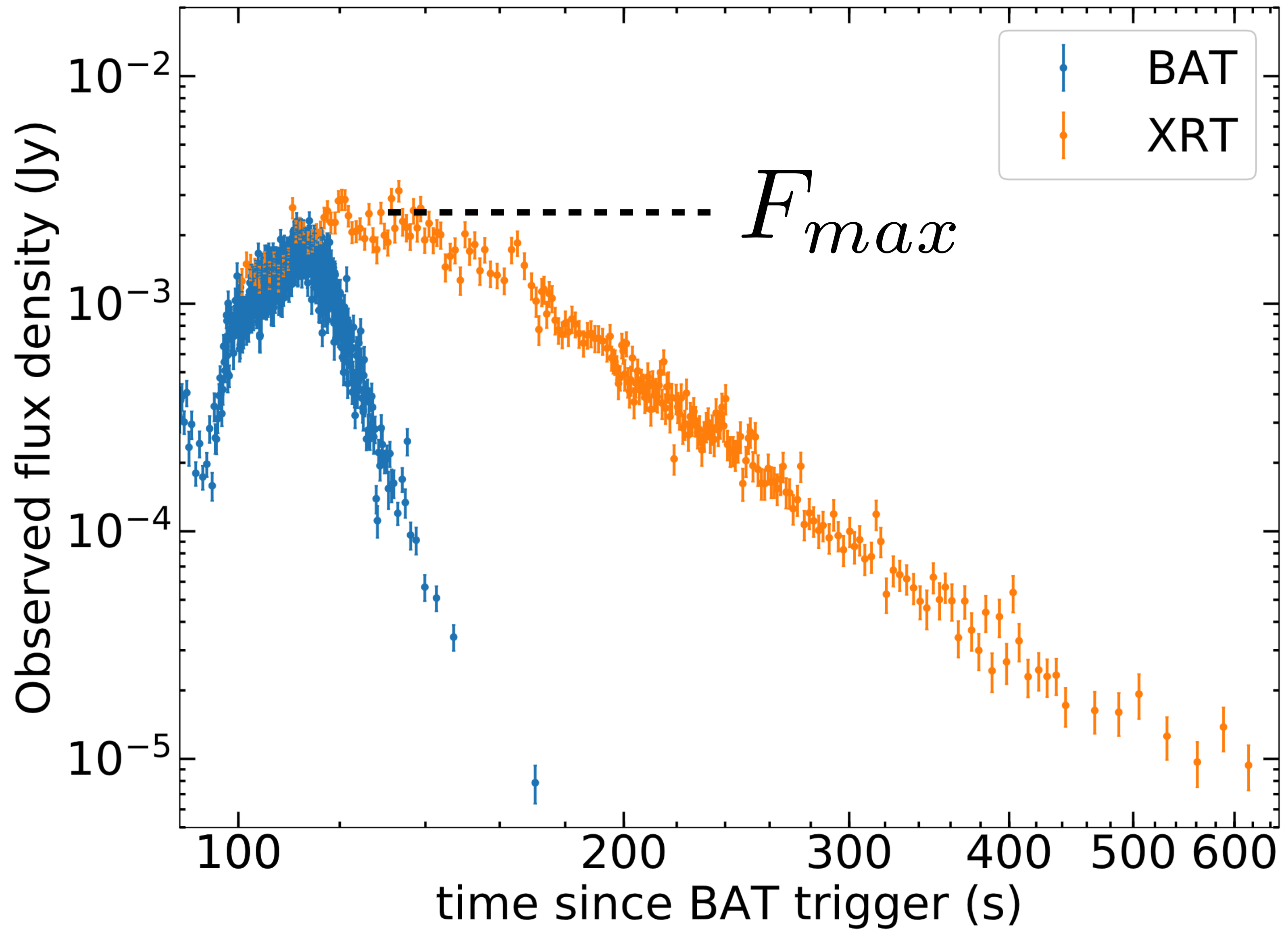

Ensures that the spectral peak is above the XRT band and hence we can monitor its transition as the flux decays

Goal of the work:

- perform a systematic spectral analysis during the steep decay observed with Swift-XRT
- Compare the spectral evolution for a well defined sample of events

Sample selection

- Bright enough events, for a time resolved analysis
- Events characterized by a well defined peak time of the decay
- Bright emission in the BAT instrument at the moment of the peak

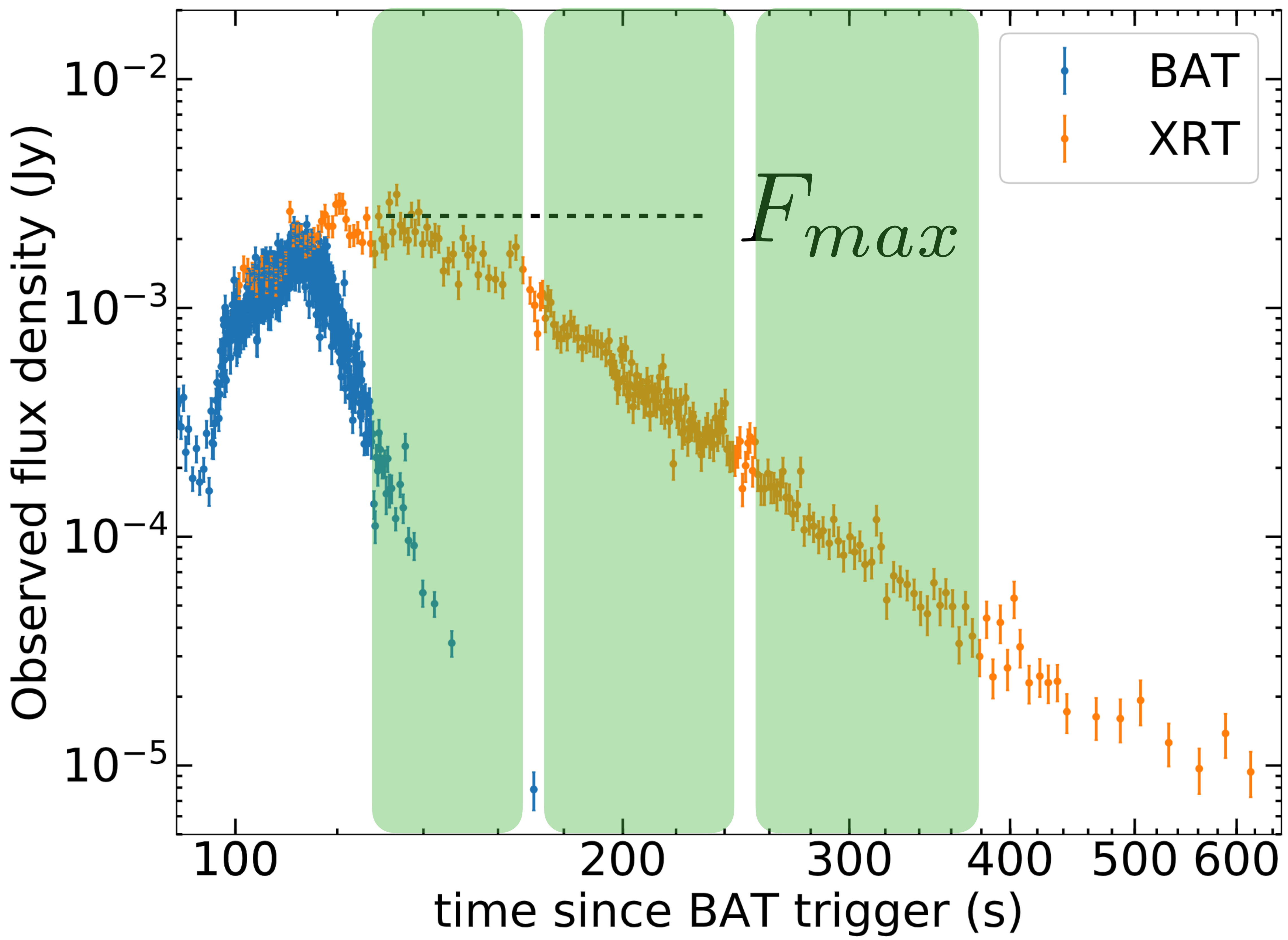

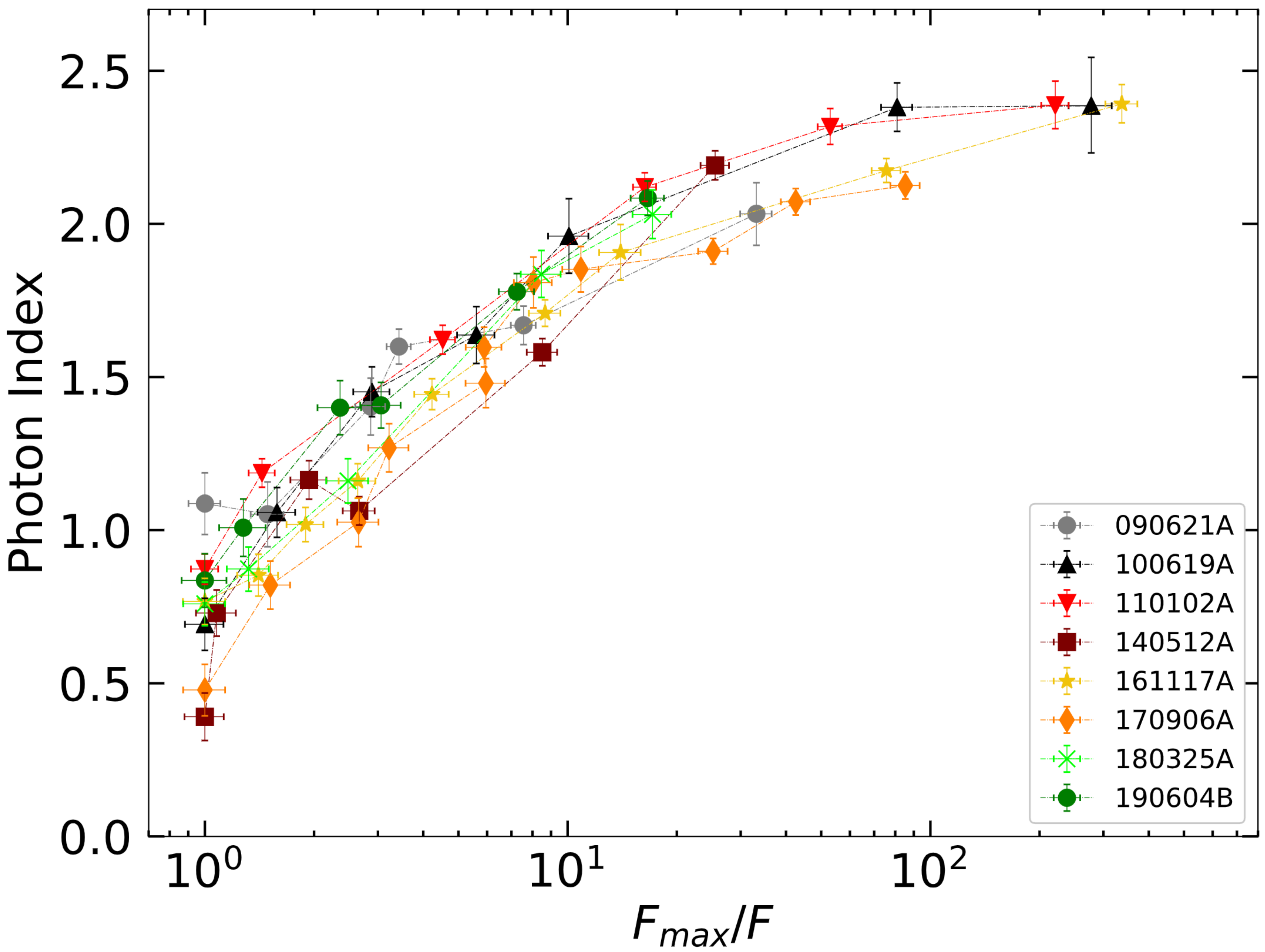

$$N(E) \propto A(E) \times E^{-\alpha}$$

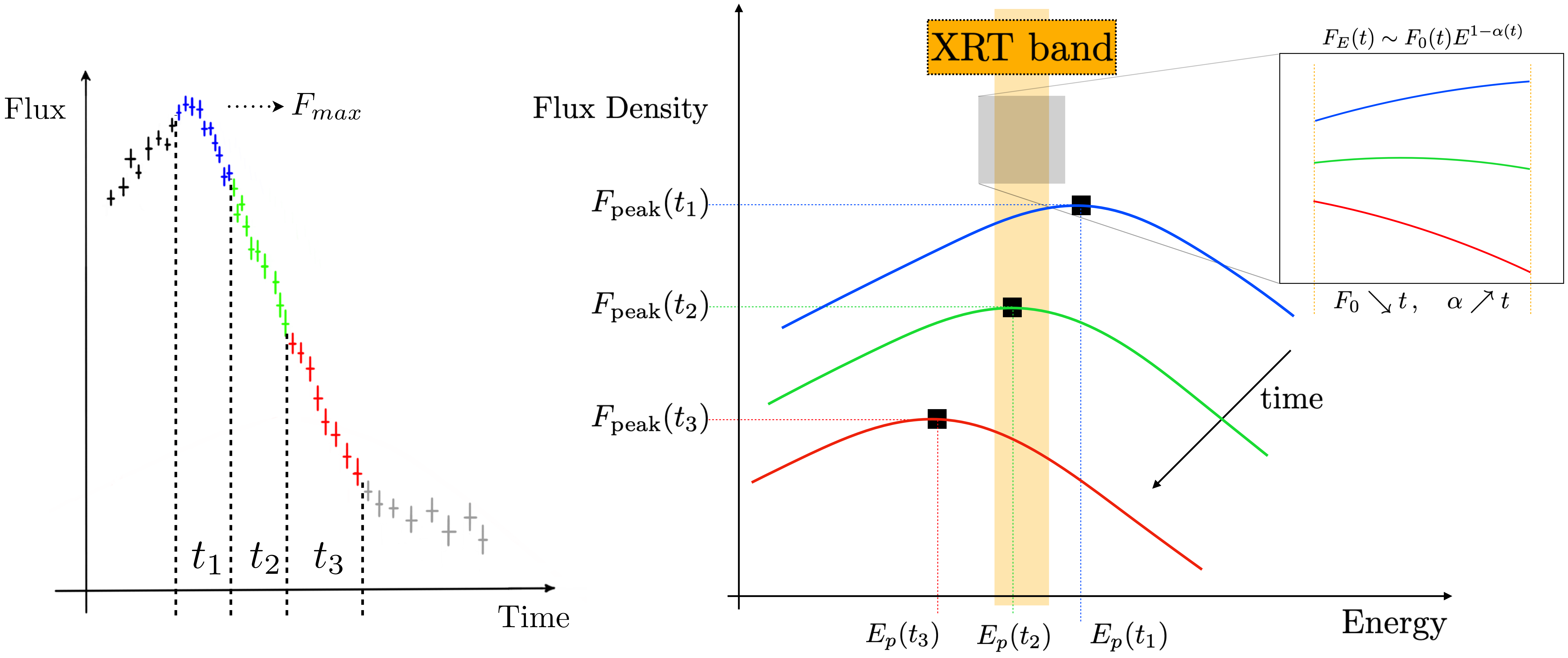
Flux
F_{max}
t_1 t_2 t_3
Time
Flux Density
XRT band
$F_E(t) \sim F_0(t)E^{1-\alpha(t)}$
$F_{\rm peak}(t_1)$
$F_{\rm peak}(t_2)$
$F_{\rm peak}(t_3)$
$F_0 \searrow t\,,\quad \alpha \nearrow t$
time
$E_p(t_3)$ $E_p(t_2)$ $E_p(t_1)$
Energy

The theoretical approach

$$\frac{\partial}{\partial t}\left(\frac{dN_{\rm e}}{d\gamma_{\rm e}}\right)+\frac{\partial}{\partial \gamma_{\rm e}}\left[\dot{\gamma}_{\rm e}\left(\frac{dN_{\rm e}}{d\gamma_{\rm e}}\right)\right]=Q\left(\gamma_{\rm e},t\right)$$

$$\dot{\gamma}_e=\dot{\gamma}_{\rm syn}+\dot{\gamma}_{\rm IC}+\dot{\gamma}_{\rm ad}=-\frac{\sigma_{\rm T}B^2\gamma^2}{6\pi m_e c}-\frac{P_{\rm IC}(\gamma)}{m_e c^2}-\frac{2\gamma}{3t}$$

$$\tau_{rad}=\min\left(\tau_{Syn},\tau_{IC},\ldots\right)$$

$$\tau_{dyn}=\frac{R}{2c\Gamma^2}$$

The high latitude emission dominates in the radiative regime

Radiative regime

$$\tau_{rad}\ll\tau_{dyn}$$

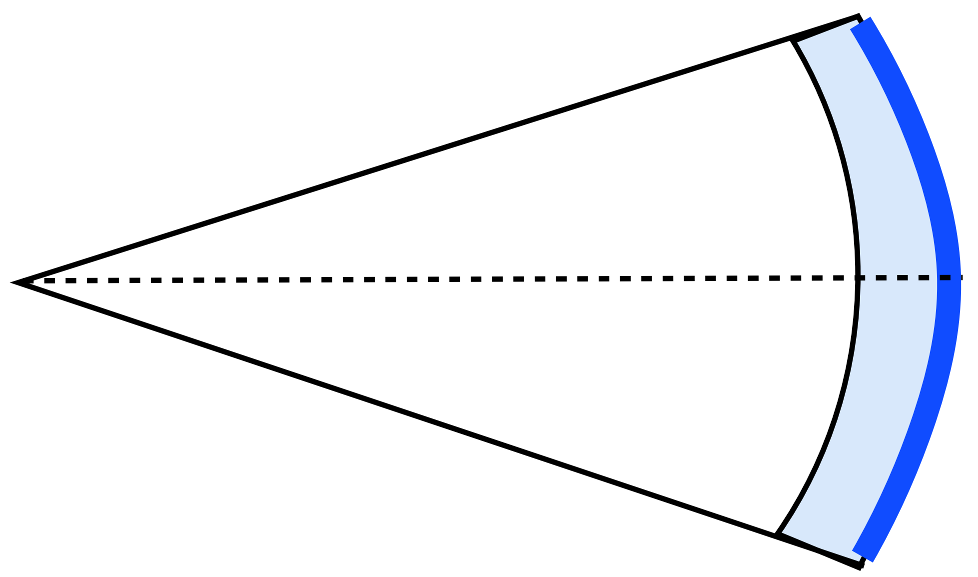

The tail emission is dominated by the last emitting surface

Spectral softening dominated by the Doppler shift due to high latitude emission

Adiabatic regime

$$\tau_{rad}\gg\tau_{dyn}$$

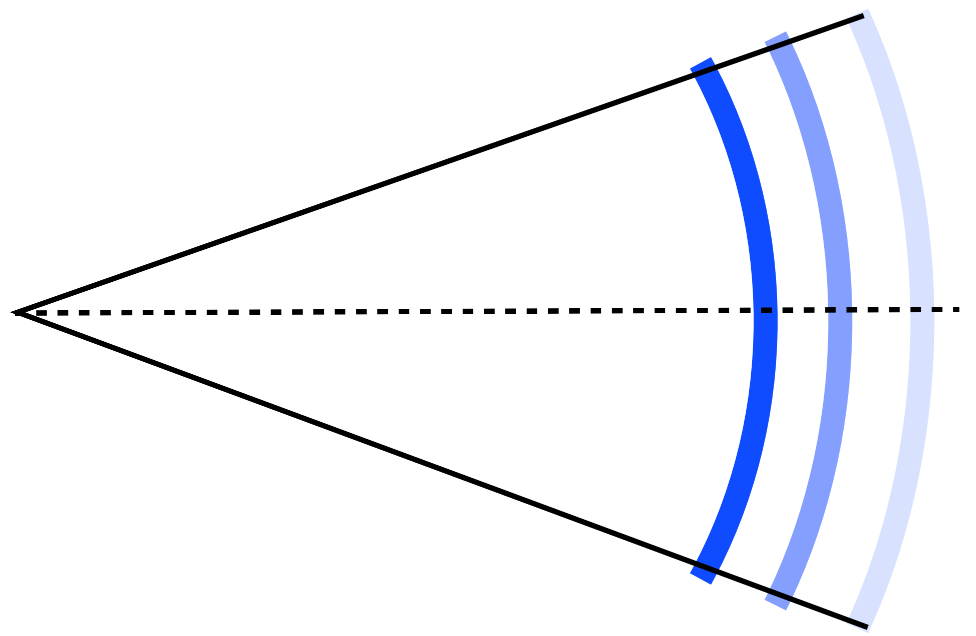

The spectrum undergoes to an intrinsic shift due to the adiabatic cooling of particles

Spectral evolution dominated by HLE

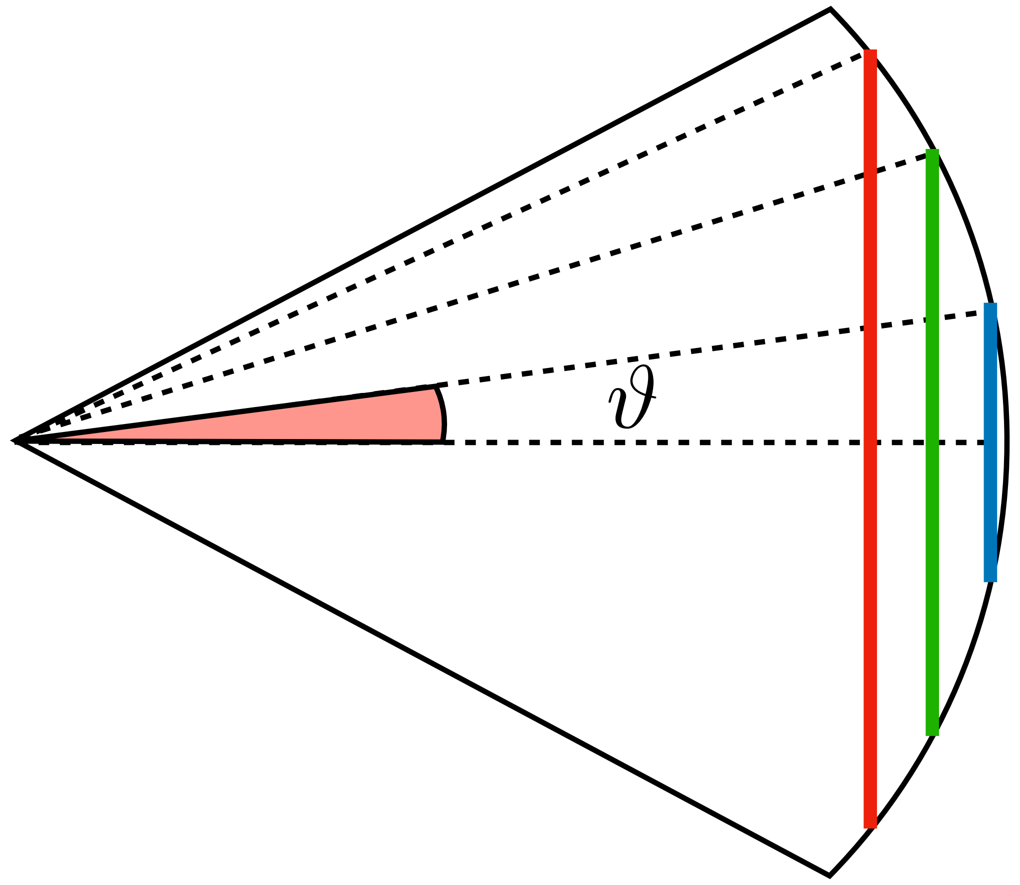

The HLE emission predicts a simultaneous flux decline and a spectral softening, if the spectral peak crosses the band

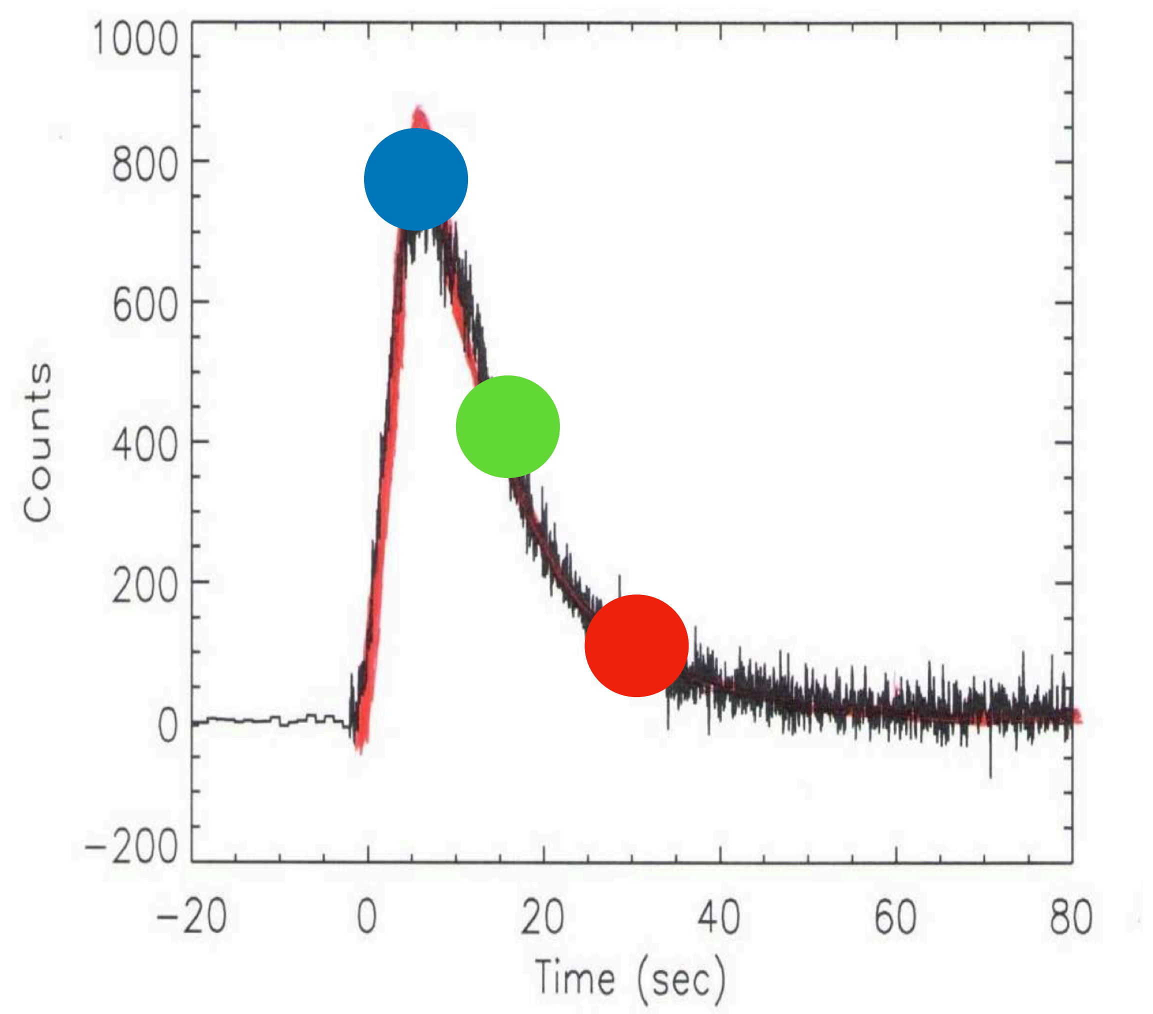

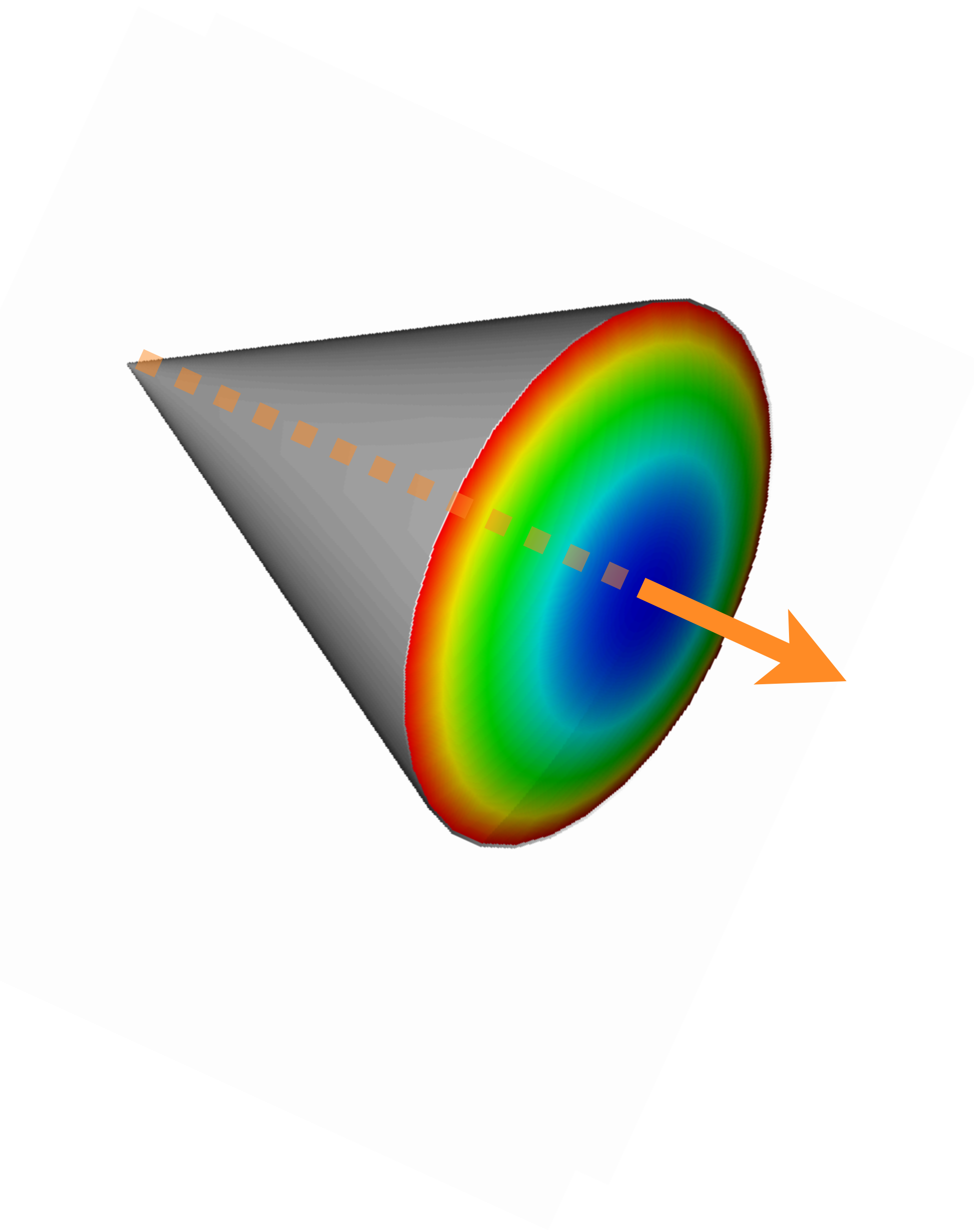

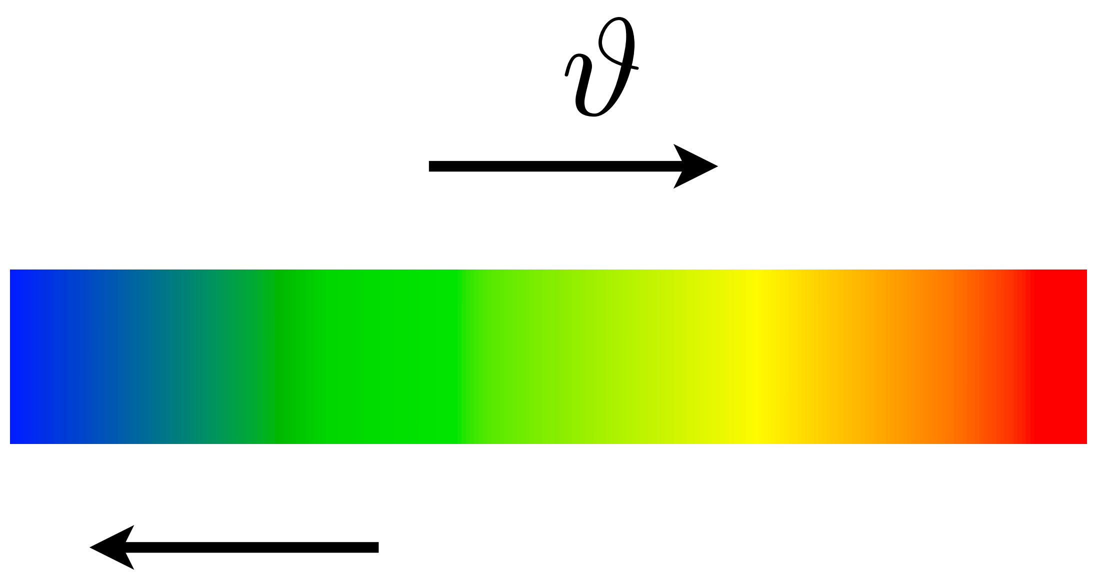

$$\mathcal{D}(\vartheta) = \frac{1}{\Gamma(1-\beta\cos(\vartheta))}$$

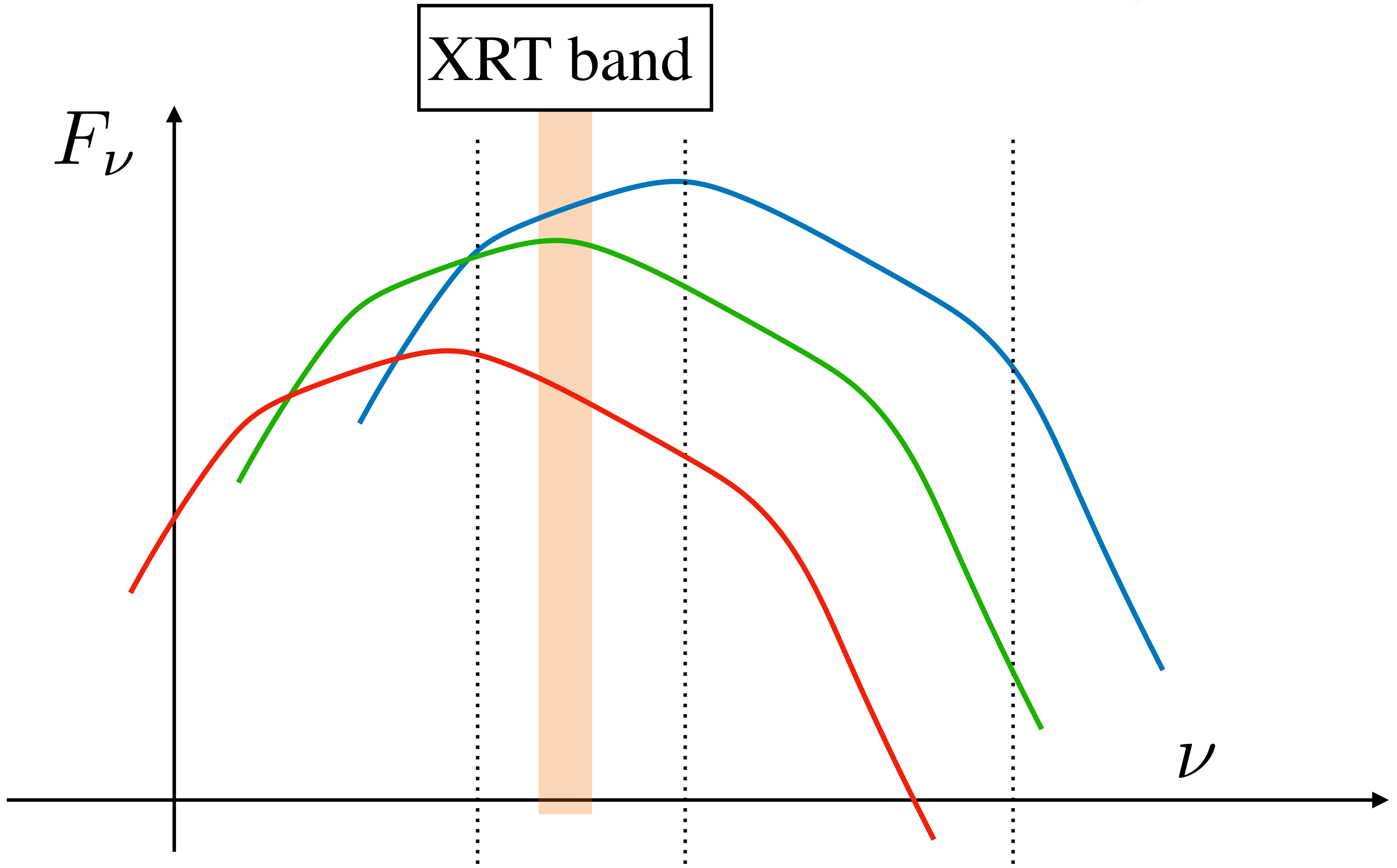

High Latitude Emission

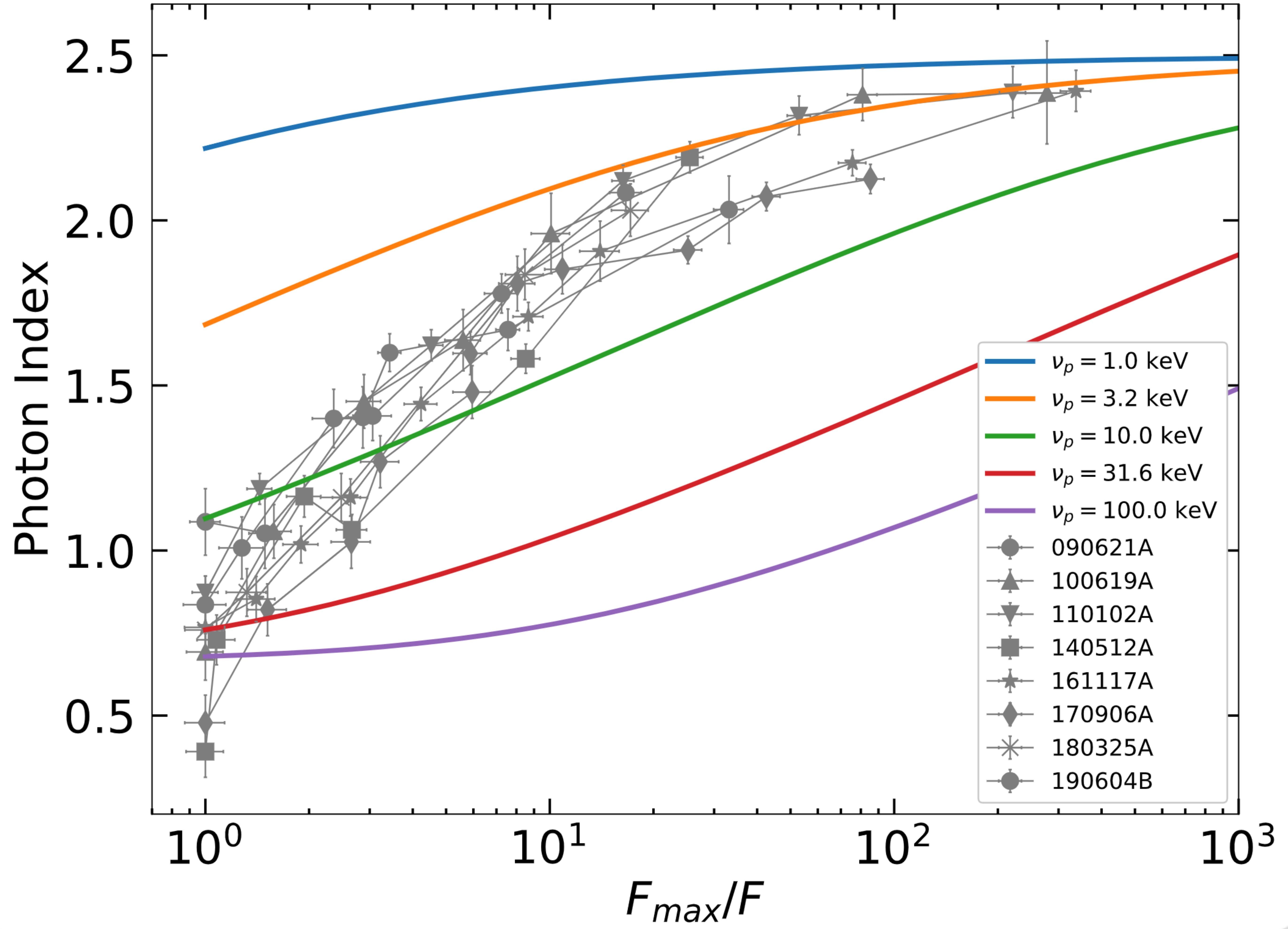

From Ronchini et al. 2021

Several variations tested:

- Assuming different spectral shapes
- Including the jet structure
- Including finite width emitting shell
- Including time-dependent shell dynamics
- Including time-dependent evolution of magnetic field and particle injection rate

In all cases, the predicted spectral evolution is shallower than the observed one

Spectral evolution dominated by adiabatic cooling

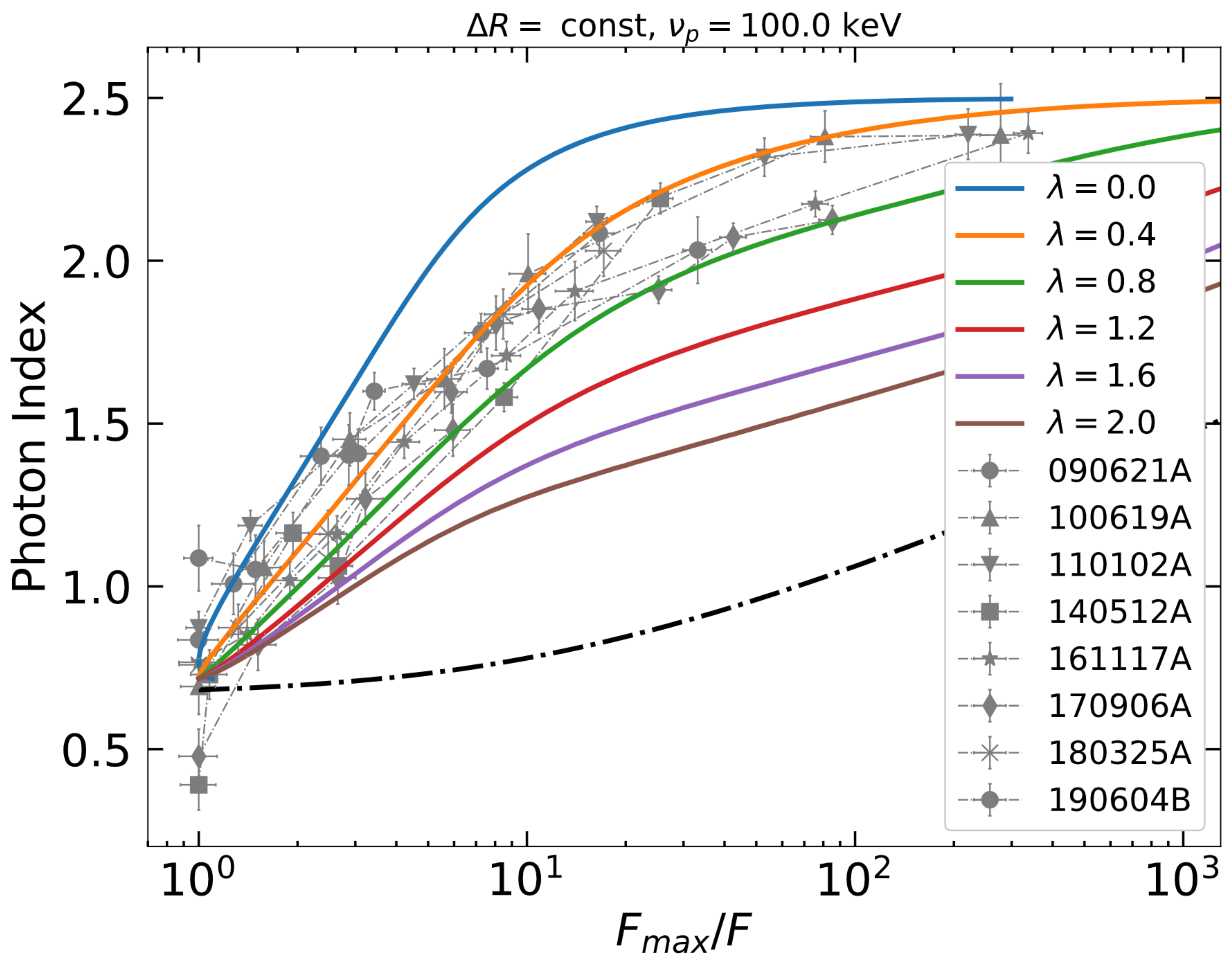

From Ronchini et al. 2021

Conservation of entropy

$$\langle\gamma\rangle^3 V' = \text{ const}$$

For a synchrotron spectrum

$$\nu_p \propto \langle\gamma\rangle^2 B$$

Prescription for magnetic field evolution

$$B = B_0 \left(\frac{R}{R_0}\right)^{-\lambda}$$

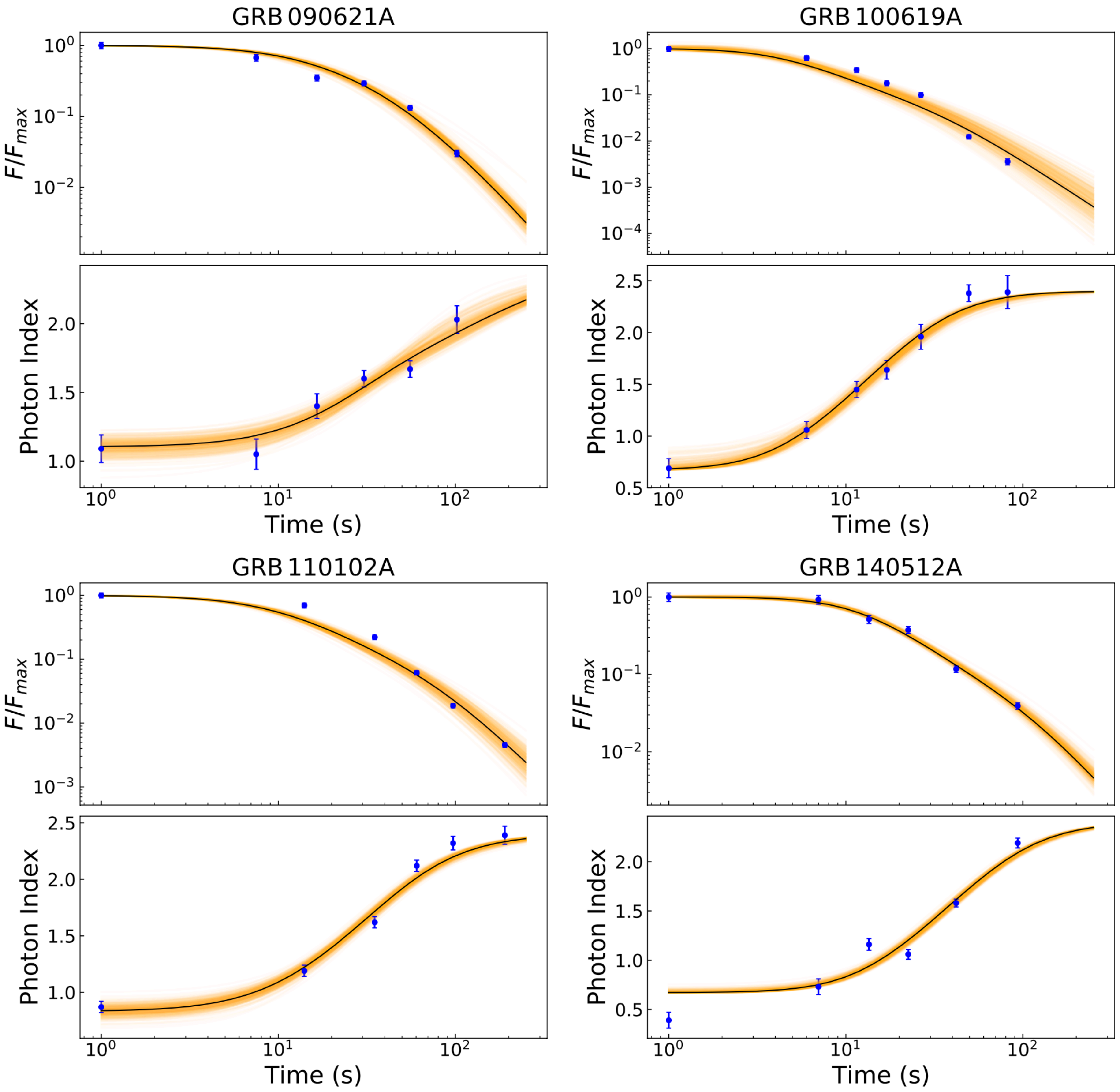

Joint spectral - temporal fit allows us to constrain:

- the radius of the last emitting region

$$1.8 \times 10^{14} (\Gamma/100)^2 \text{ cm} \lesssim R_0 \lesssim 1.4 \times 10^{16} (\Gamma/100)^2 \text{ cm}$$

- the decay index of B

GRB	E_{peak} (keV)	λ	τ_{ad} (s)
090621A	18^{+3}_{-2}	$2.11^{+0.56}_{-0.54}$	$24.4^{+4.7}_{-3.0}$
100619A	>129	$0.47^{+0.11}_{-0.07}$	$0.3^{+1.0}_{-0.2}$
110102A	46^{+15}_{-9}	$0.61^{+0.10}_{-0.10}$	$5.8^{+1.9}_{-1.1}$
140512A	>323	$0.48^{+0.04}_{-0.03}$	$0.9^{+0.9}_{-0.4}$
161117A	80^{+55}_{-21}	$0.69^{+0.10}_{-0.10}$	$6.2^{+2.0}_{-2.3}$
170906A	135^{+204}_{-53}	$0.66^{+0.10}_{-0.09}$	$3.0^{+1.6}_{-1.5}$
180325A	>122	$0.39^{+0.06}_{-0.05}$	$0.8^{+1.3}_{-0.5}$
190604B	54^{+227}_{-20}	$0.45^{+0.25}_{-0.15}$	$3.5^{+2.6}_{-2.8}$

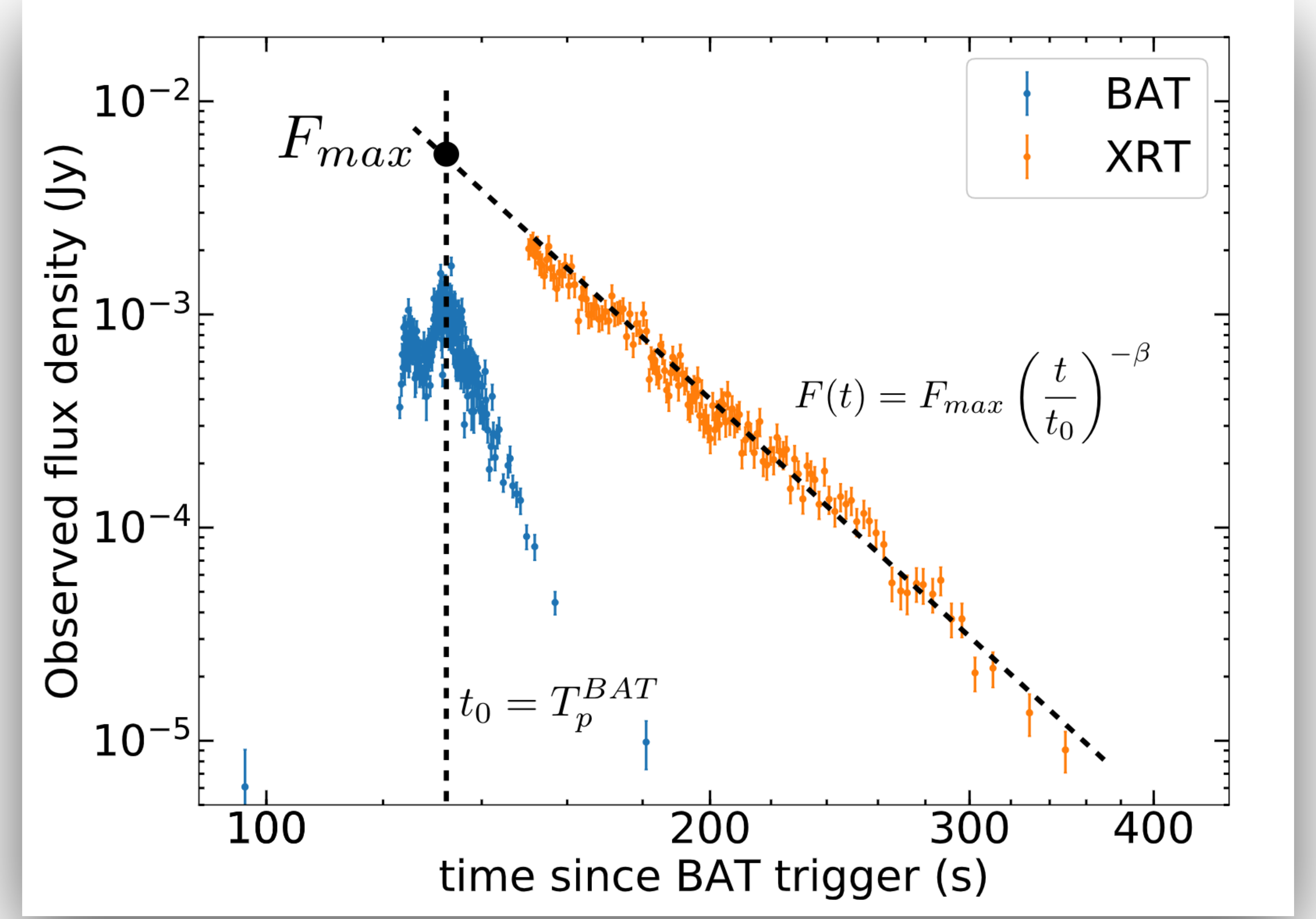
BAT
XRT
F_{max}
$F(t) = F_{max}\left(\frac{t}{t_0}\right)^{-\beta}$
$t_0 = T_p^{BAT}$
Observed flux density (Jy)
time since BAT trigger (s)
10^{-2}
10^{-3}
10^{-4}
10^{-5}
100
200
300
400

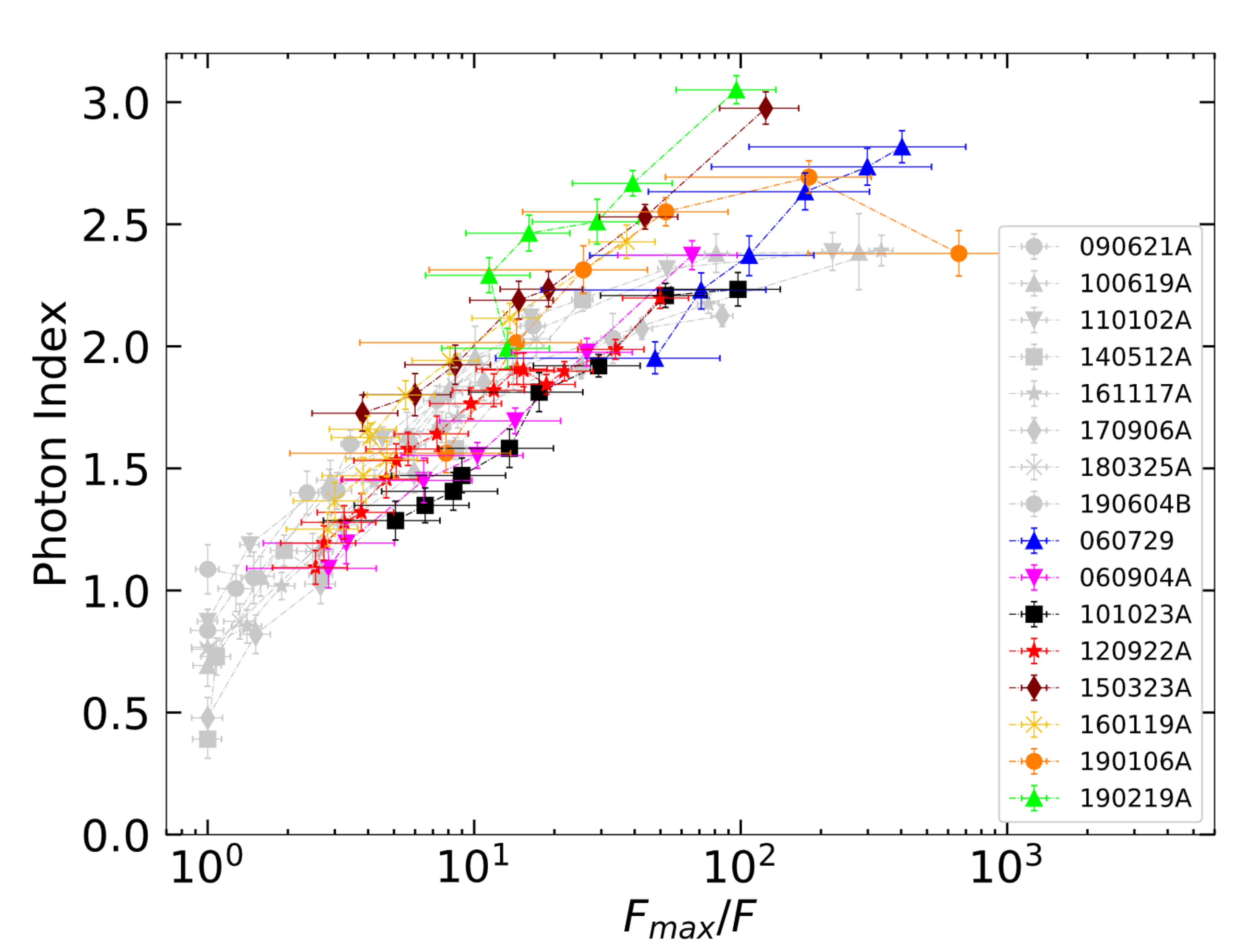
Photon Index
F_{max}/F
3.0
2.5
2.0
1.5
1.0
0.5
0.0
10^0
10^1
10^2
10^3
090621A
100619A
110102A
140512A
161117A
170906A
180325A
190604B
060729
060904A
101023A
120922A
150323A
160119A
190106A
190219A

Transient High-Energy Sky and Early Universe Surveyor

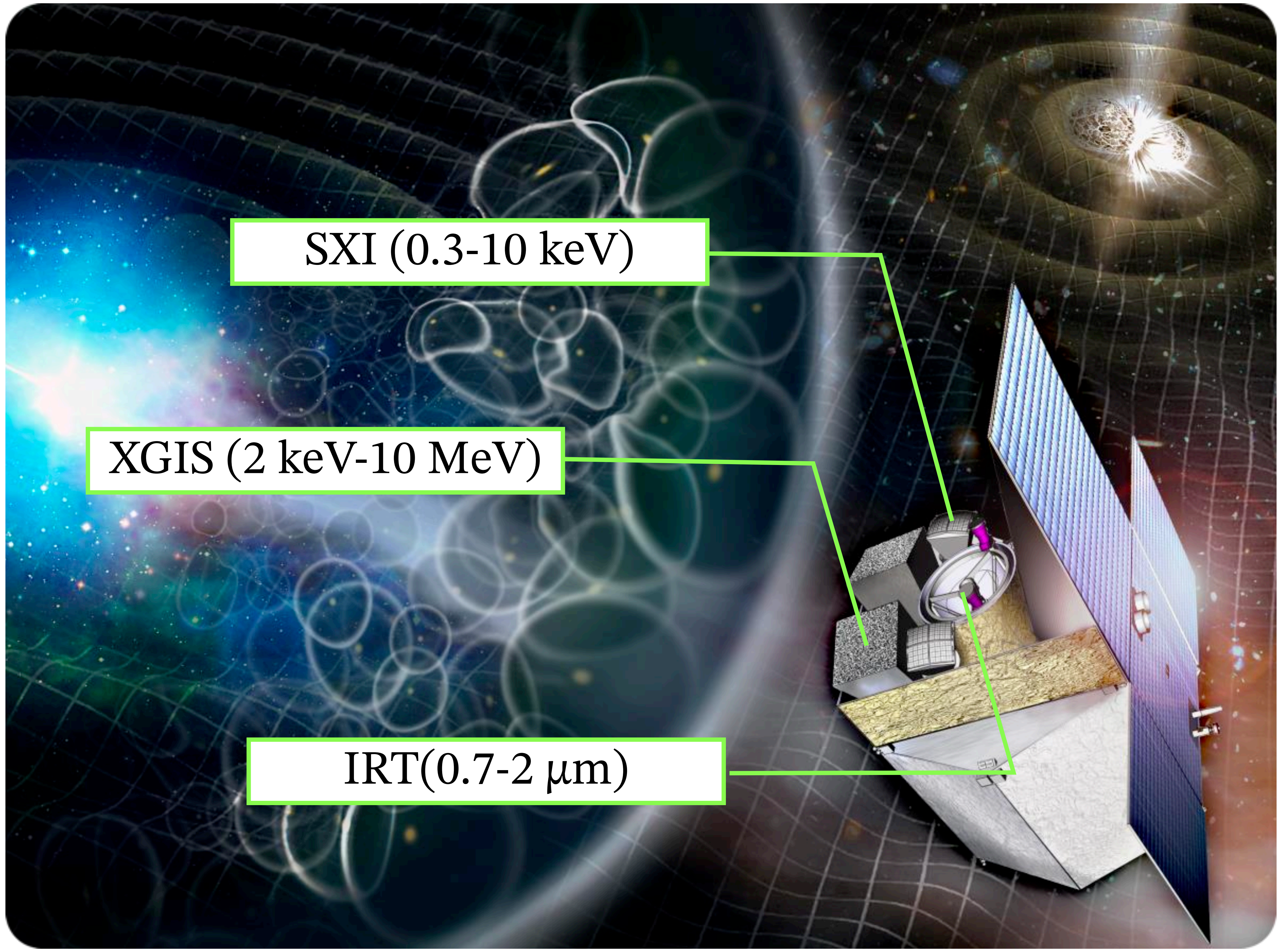

Mission concept optimized for:

1. Multi-messenger studies, follow up and identification of EM counterpart of GW and neutrino events
2. Detection and characterization of GRBs up to redshifts close to the re-ionization epoch of the Universe
3. Systematic survey of the transient sky in the high-energy

Soft X-ray Imager (SXI)

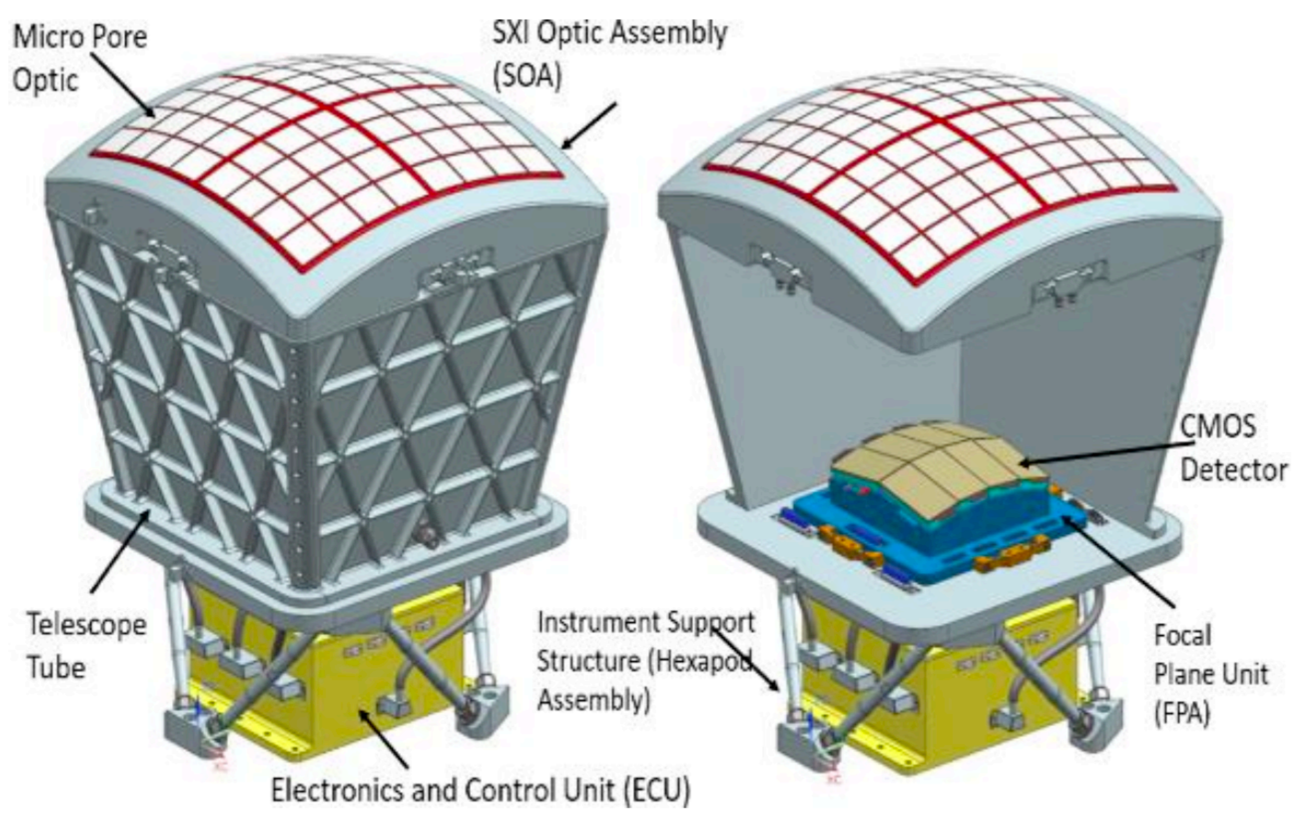

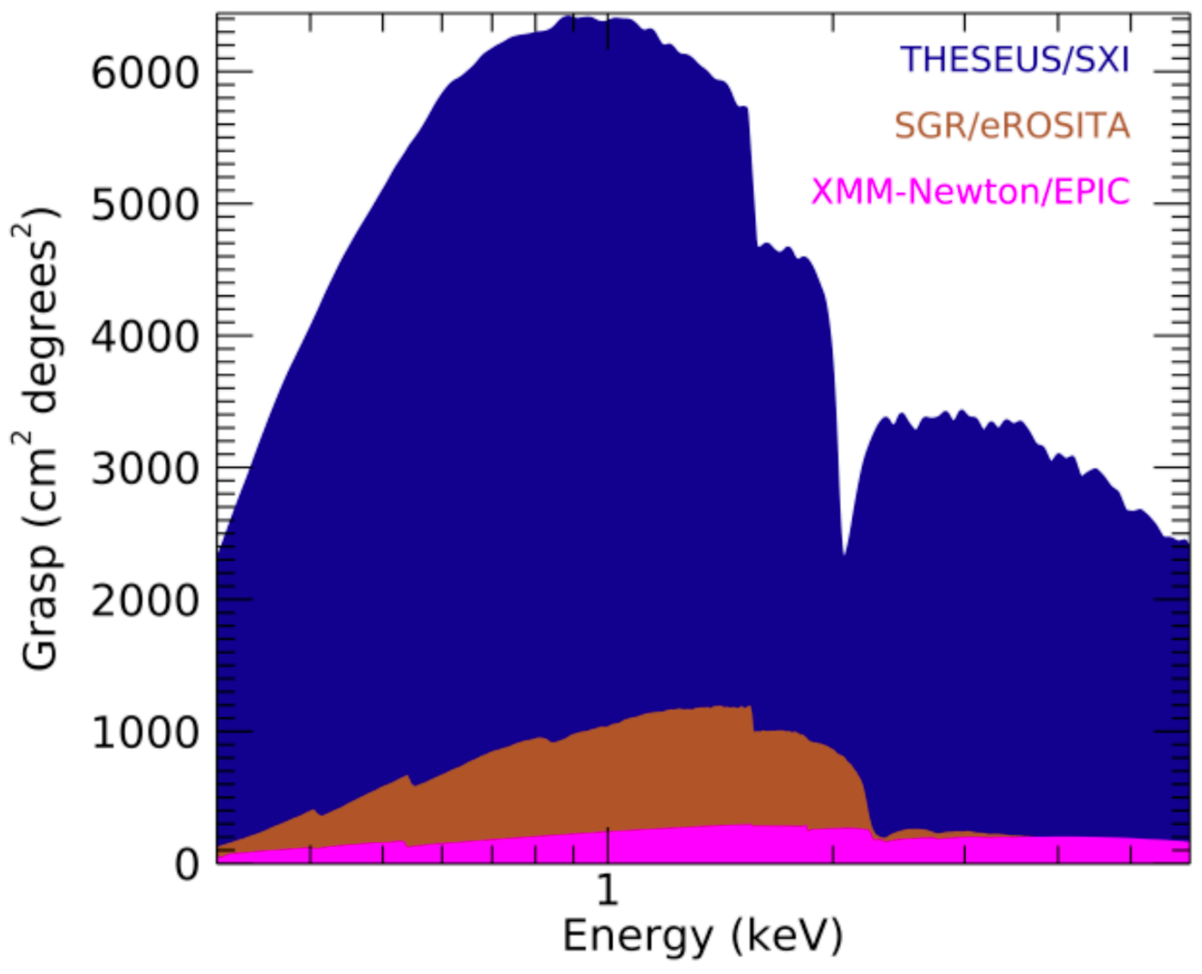

Large Grasp

X/gamma-ray Imaging spectrometer (XGIS)

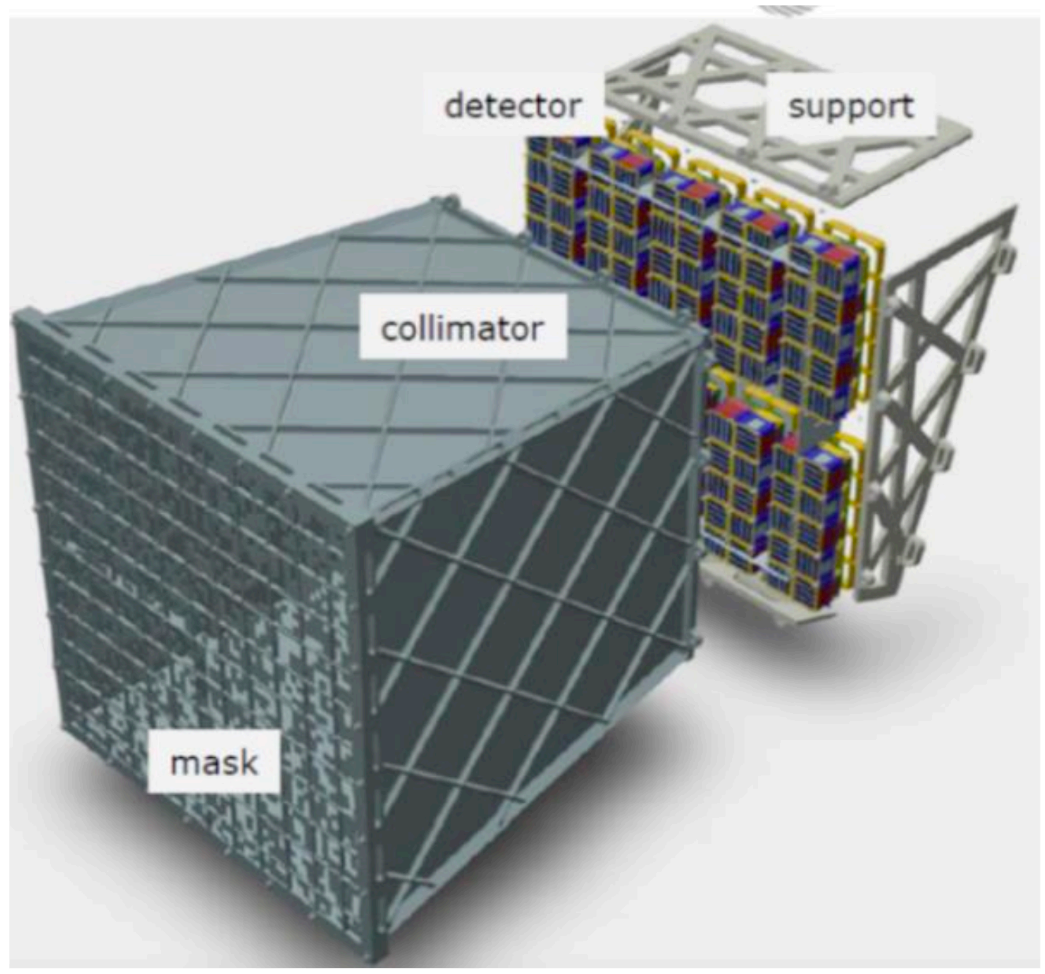

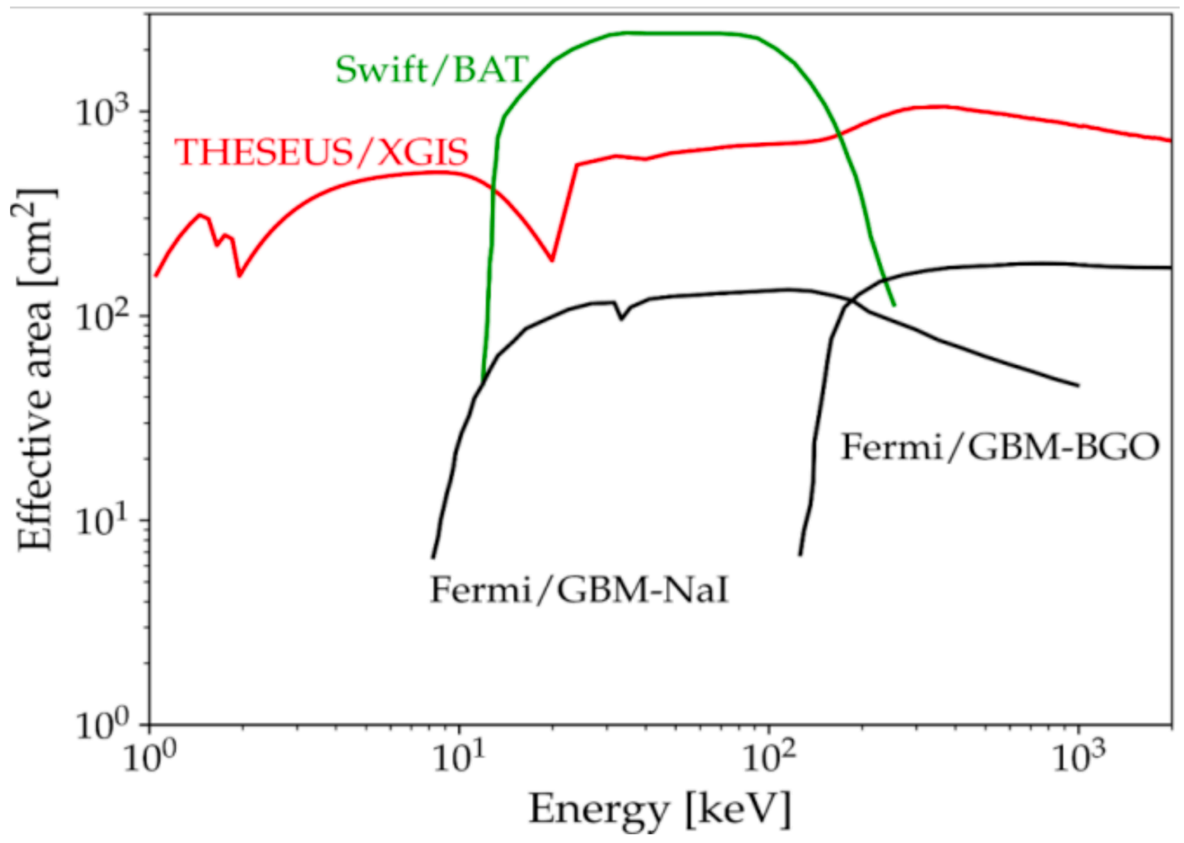

Very wide spectral coverage

Key advantages:

1. Wide coverage of the sky
2. Very extended energy range, from 0.3 keV to 10 MeV
3. Arcmin localisation

	FOV	Position accuracy
SXI	0.5 sr	< 2 arcmin
XGIS	2 sr (2 - 150 keV) 4 sr (>150 keV)	< 15 arcmin
IRT	15’ x 15’	< 1 arcsec

Predicted performance of THESEUS for the monitoring of the steep decay

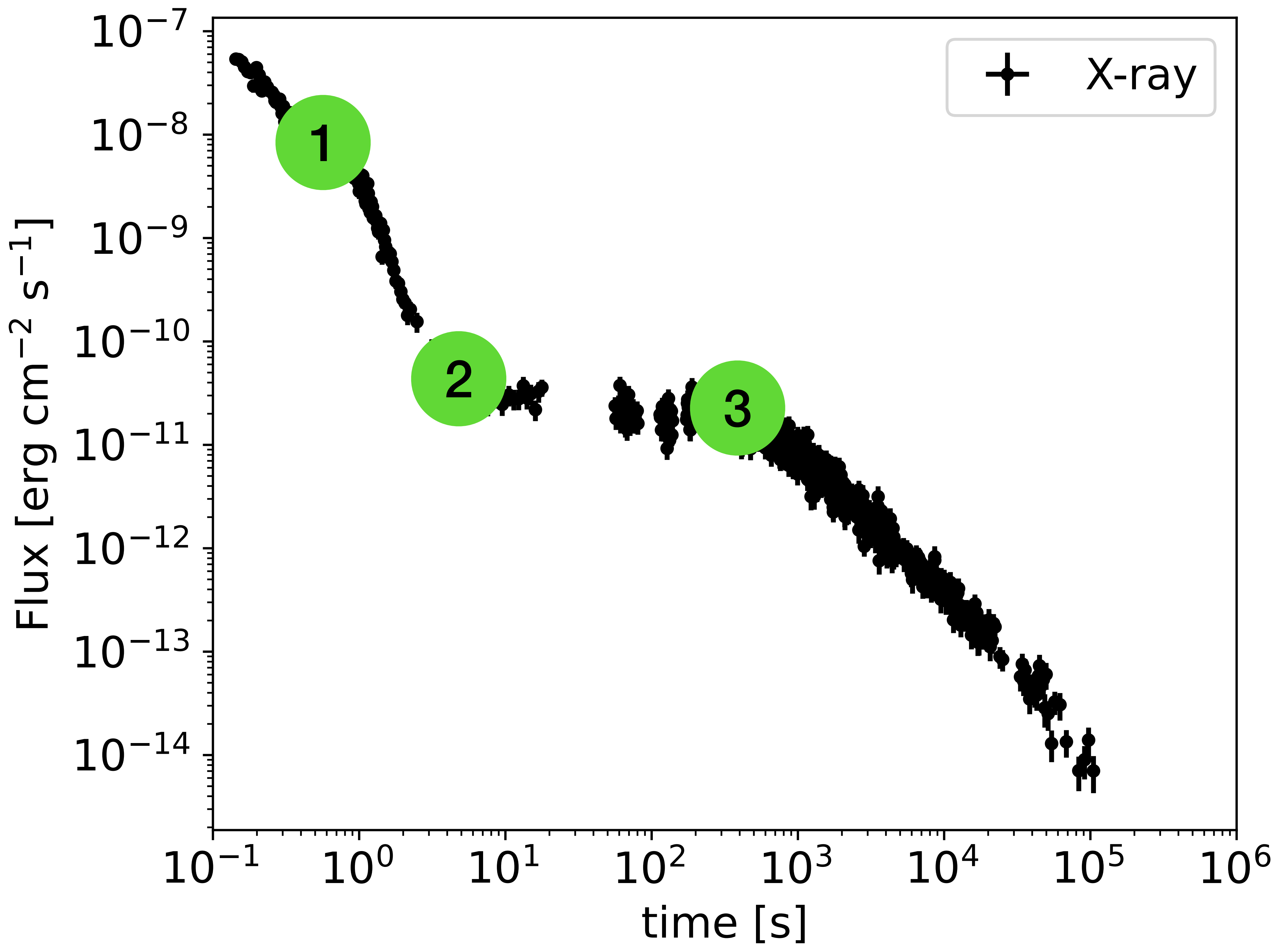

$L_{\rm iso} \sim 10^{52} erg/s, \quad z = 0.5$

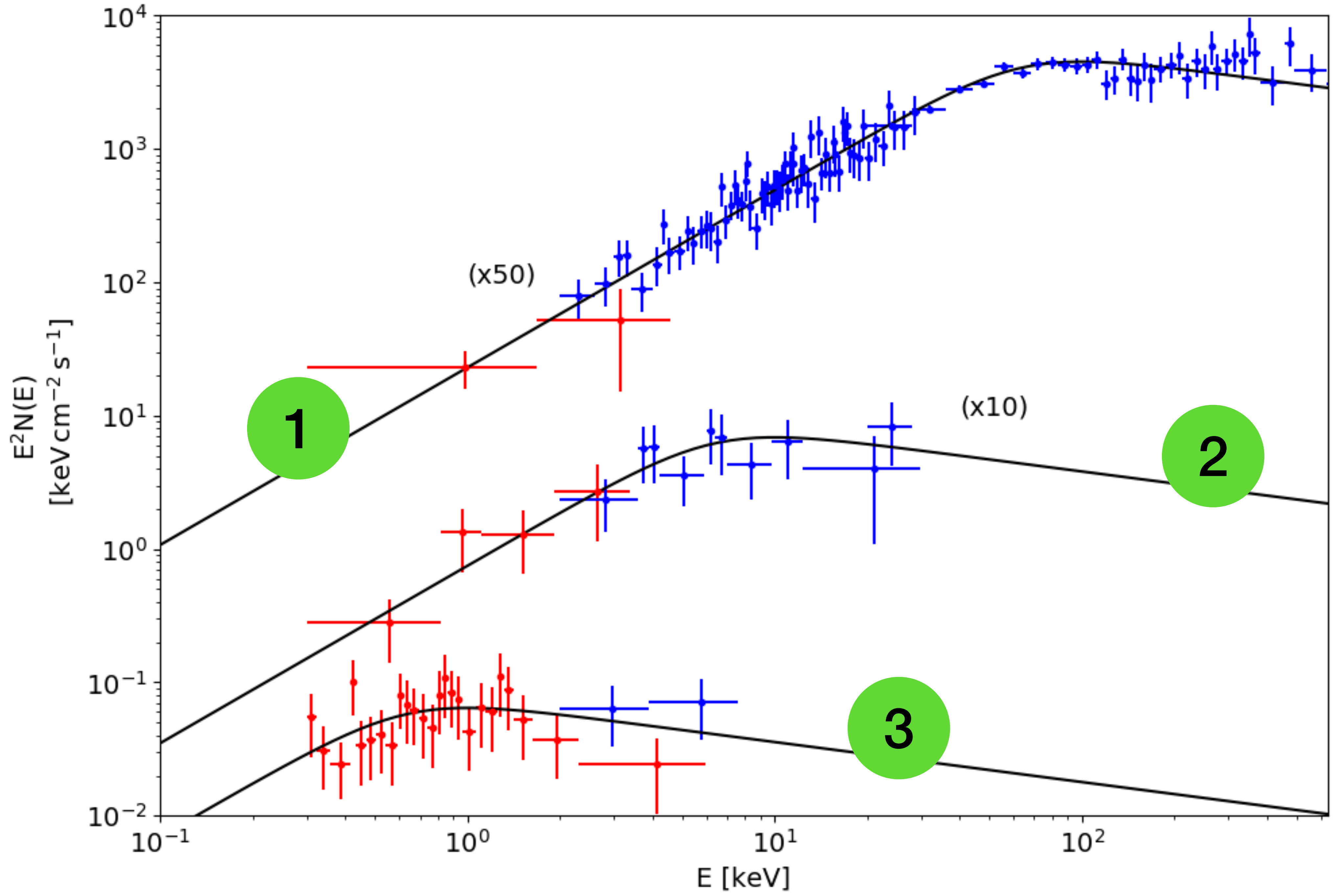

Time $[s]$	$\alpha_{\rm Input}$	$\beta_{\rm Input}$	$E_{\rm p,\,Input}$ [keV]	α	β	$E_{\rm p}$ [keV]
10	-0.67	-2.3	100	-0.74 ± 0.04	-2.27 ± 0.08	120^{+10}_{-8}
100	-0.67	-2.3	10	$-0.72^{+0.27}_{-0.25}$	< -2.20	$7.8^{+3.5}_{-1.6}$
1000	-0.67	-2.3	1	$-1.12^{+0.50}_{-0.28}$	< -2.3	$1.87^{+0.58}_{-0.47}$

Published in Ghirlanda + 2021

Conclusions Part I

- The spectral evolution during the steep decay of prompt-like pulses in GRBs is characterized by a **unique relation**
- The standard **high latitude emission** scenario cannot account for the spectral evolution during the steep decay.
- Our results **disfavor an efficient cooling** of particles
- The inclusion of **adiabatic cooling** of particles well explains the observed alpha-F relation
- The **inefficient radiative cooling** of particles in GRB outflows is in contrast with energy dissipations from electrons (proton-synchrotron could be a solution)
- Future wide field X-ray instruments, such as **THESEUS**, will be able to **monitor the full prompt-to-afterglow transition**, systematically probing the spectral evolution during the steep decay

Part II

On the origin of plateau emission in the X-ray afterglow of GRBs

Ronchini et al. 2023, Astronomy & Astrophysics, accepted

Observational evidences:

- Duration 10^2 - 10^4 s
- Typical temporal slope s<0.7-0.8
- Found in both short and long GRBs.
- Luminosity and duration anti-correlated
- Diverse behavior in optical: both chromatic and achromatic

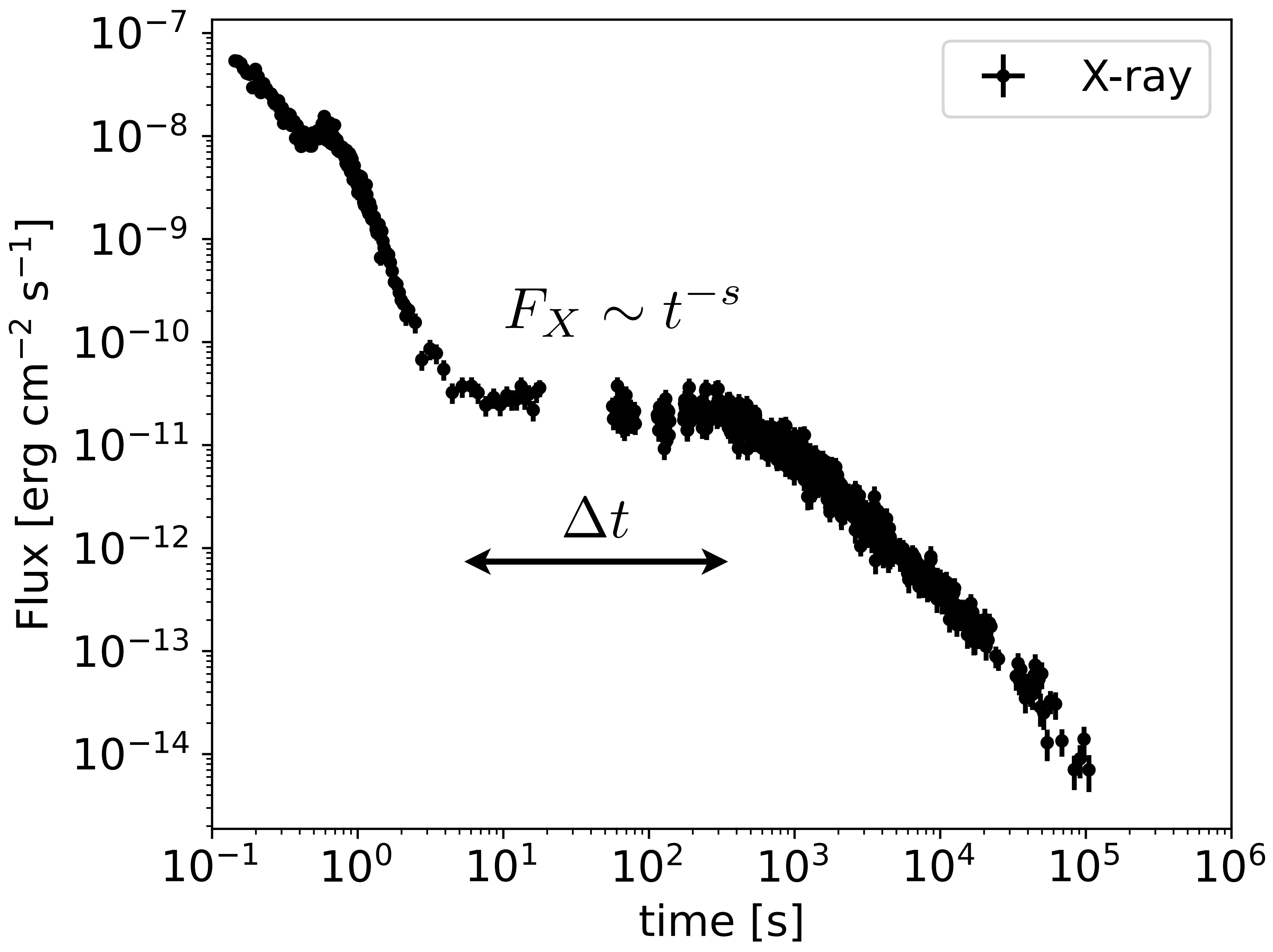

Achromatic

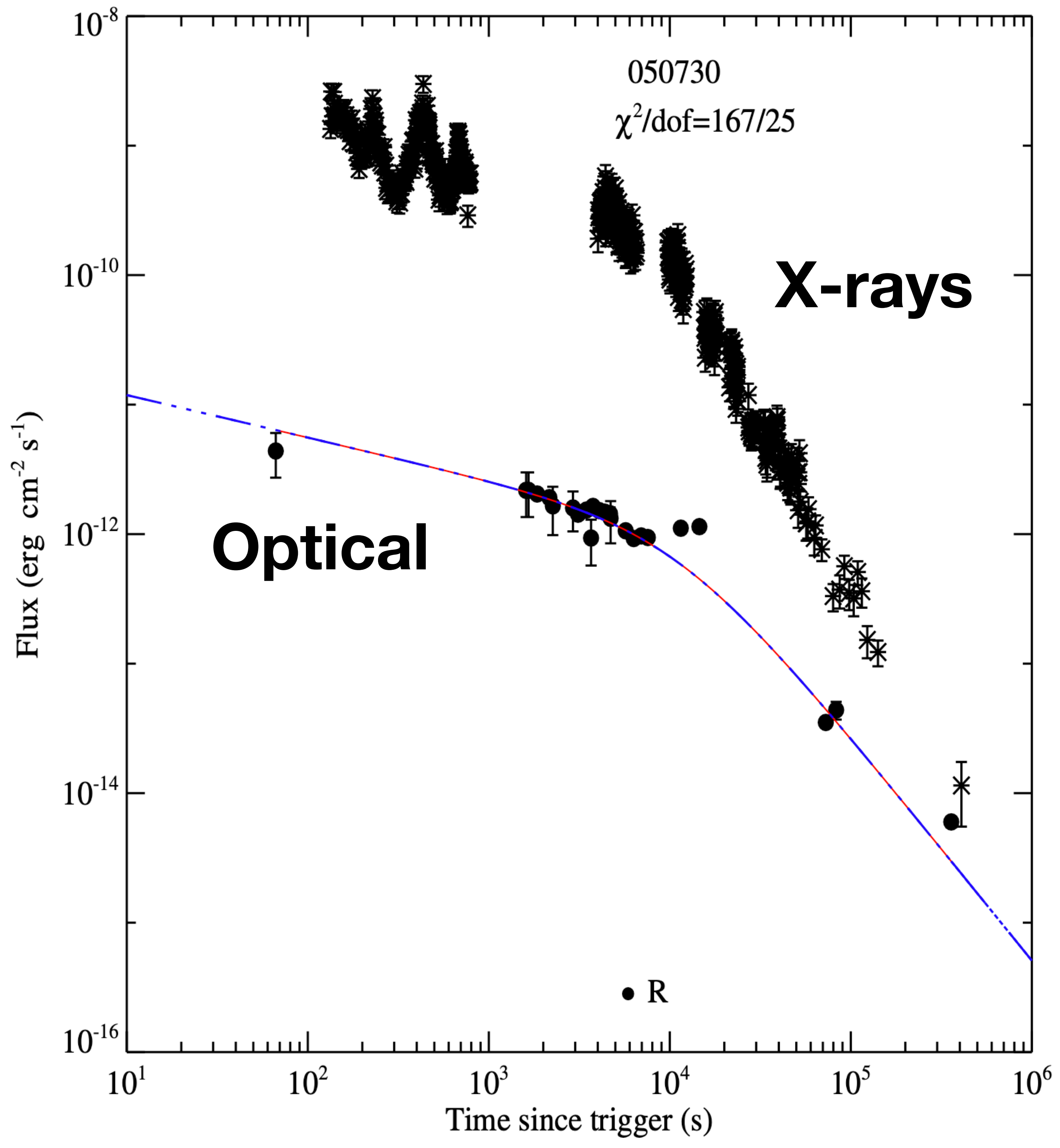

Chromatic

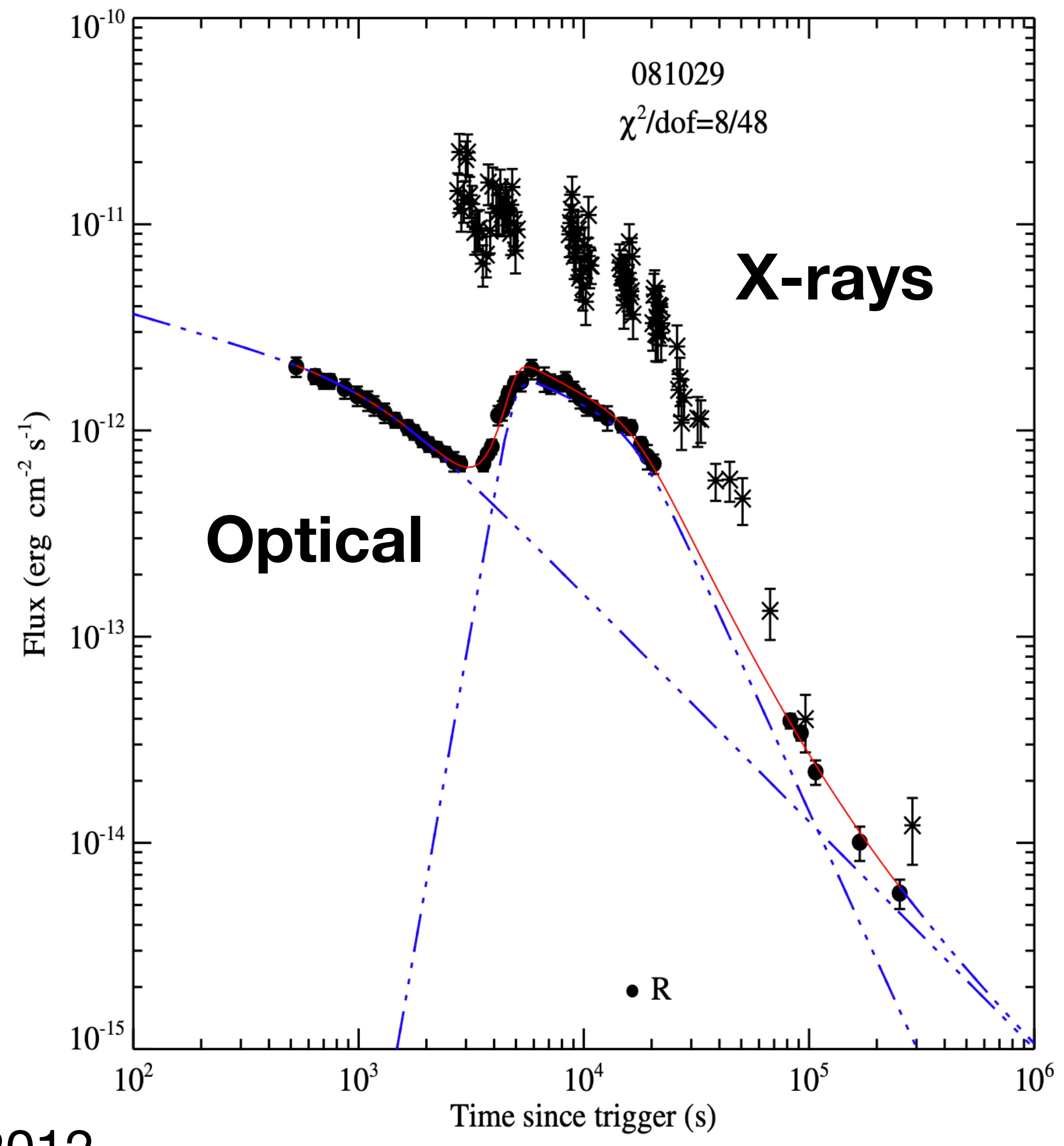

Li et al. 2012

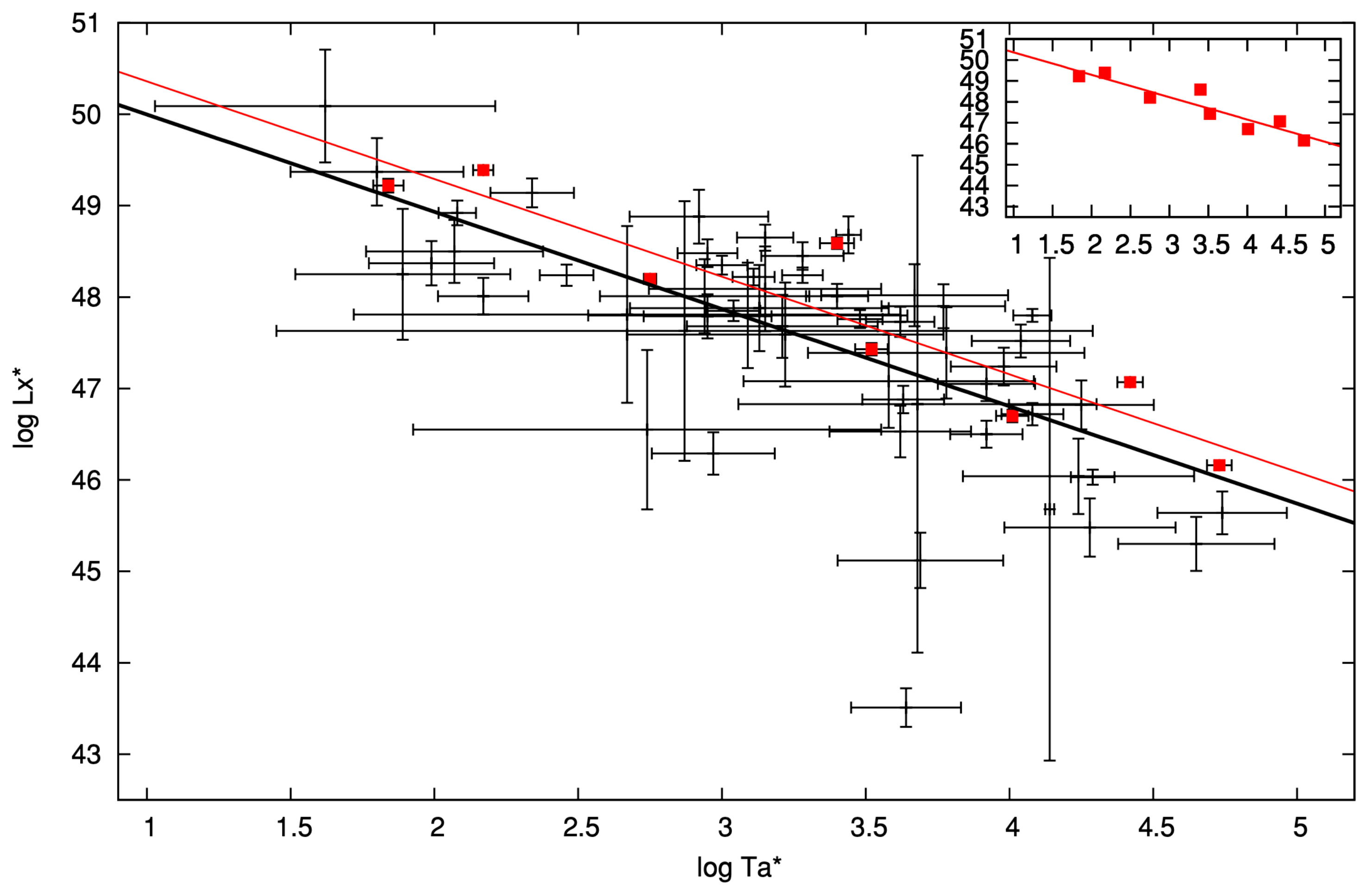

Dainotti et al. 2010

The X-ray plateau challenges the decelerating fireball paradigm

In the assumption that synchrotron radiation is the dominant process, the temporal decay depends:

1. On the medium density profile
2. On the shape of the particle energy distribution
3. On the microphysical parameters

No combination of these factors can account for such a shallow decay

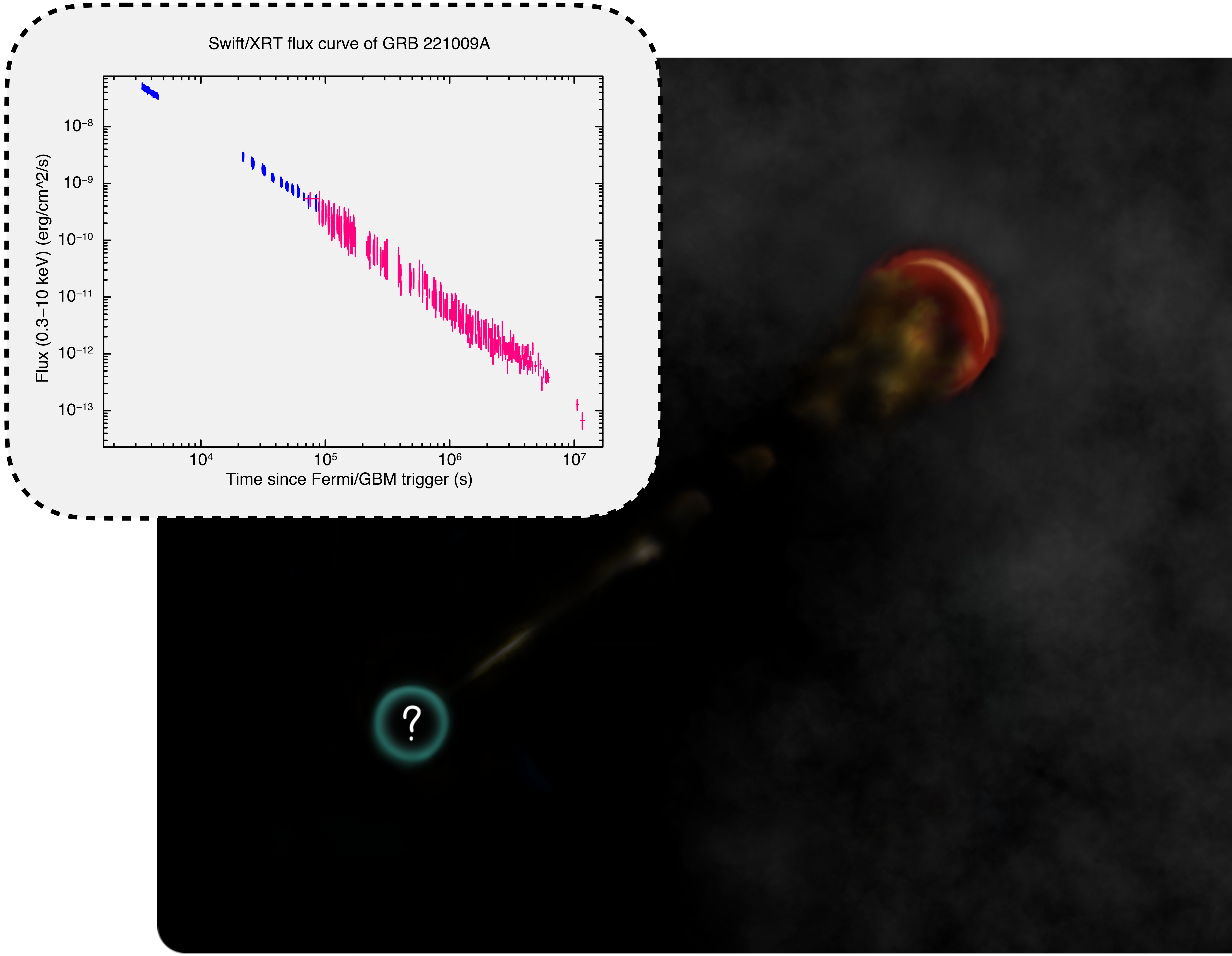

The magnetar scenario

If the central engine is a **fast rotating** (P~1 ms) **highly magnetized** (B~10^{14} G) **neutron star**, the rotational energy is lost via spin down radiation

The energy released can:

1. **Refresh the forward shock**, injecting additional energy in the accelerated particles

   (e.g., Dai & Lu 1998, Zhang & Mészáros 2001, Rowlinson + 2014)

2. Create a quasi-isotropic particle **wind**, which shocks the ISM and by itself emits in X-rays

   (e.g. Fan & Xu 2006, Yu + 2010, You + 2021)

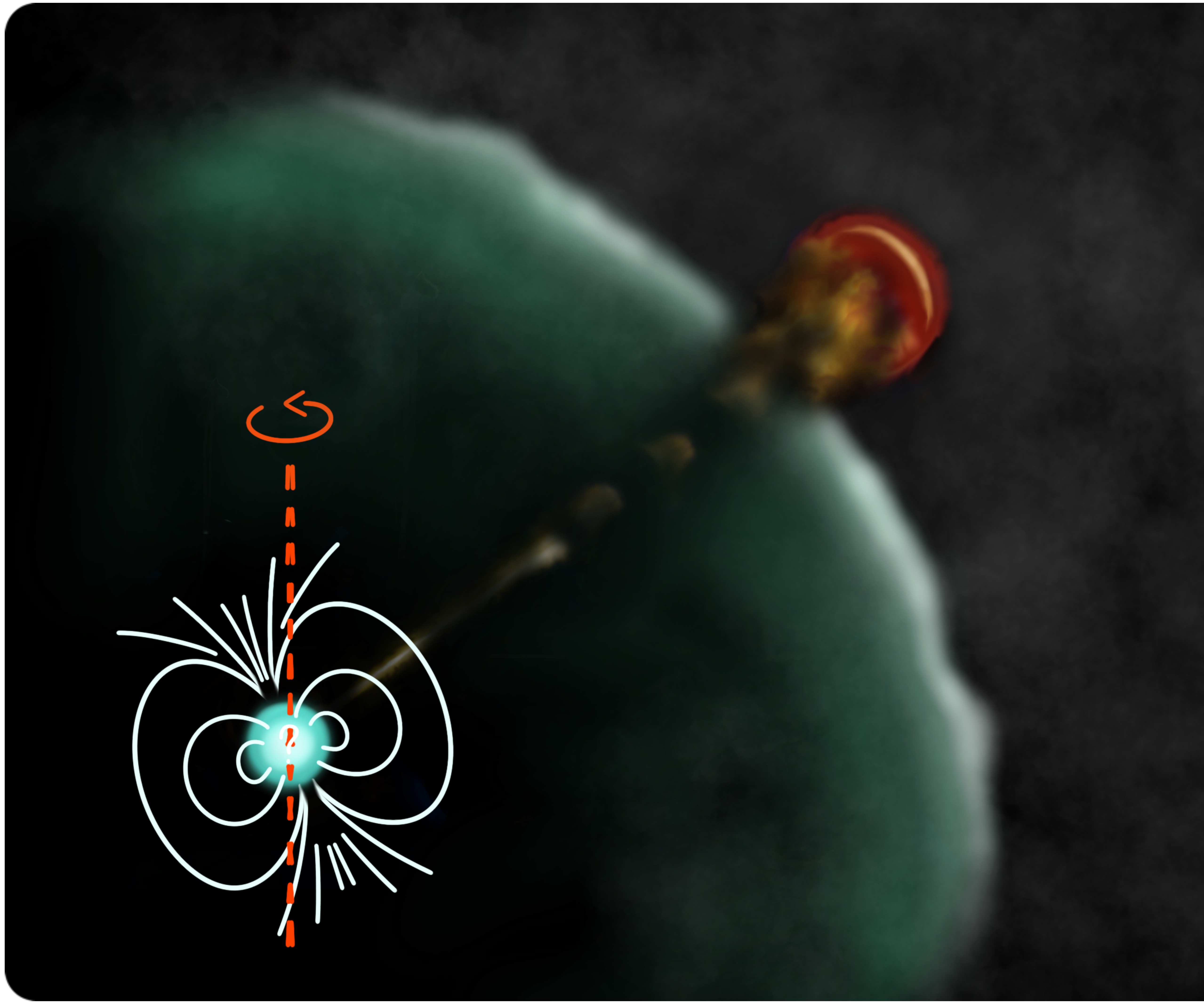

Evidence of internal plateau

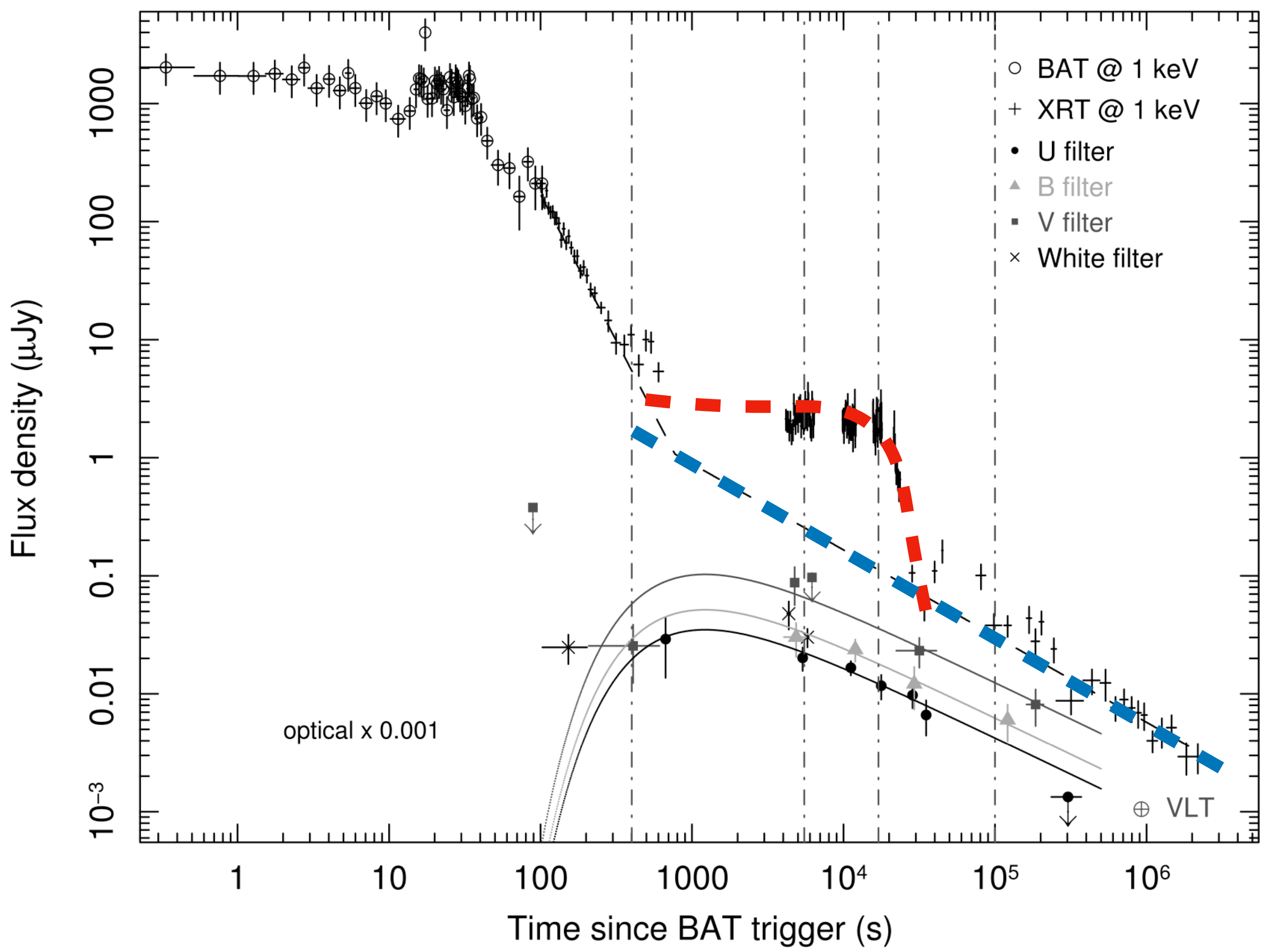

Troja 2007

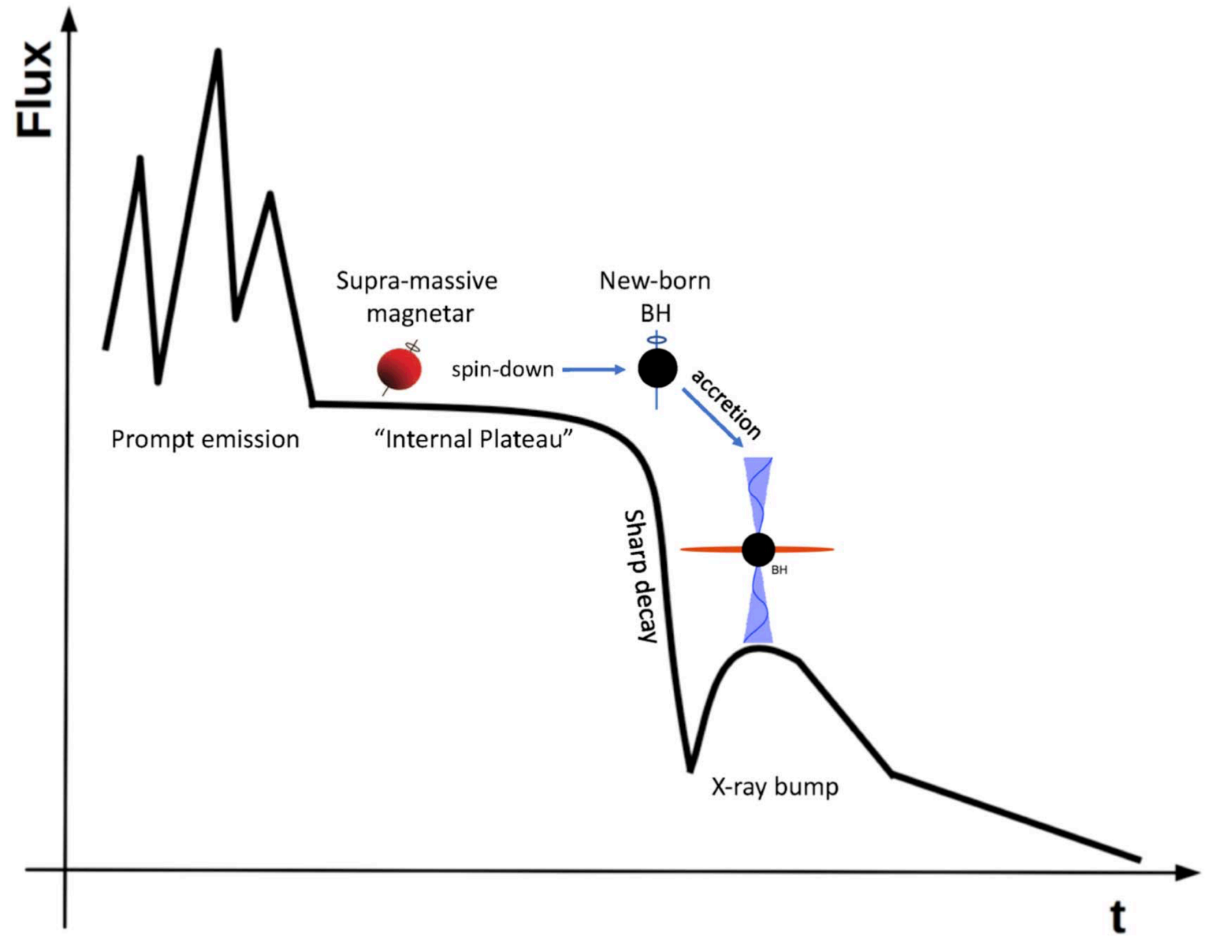

Chen 2017

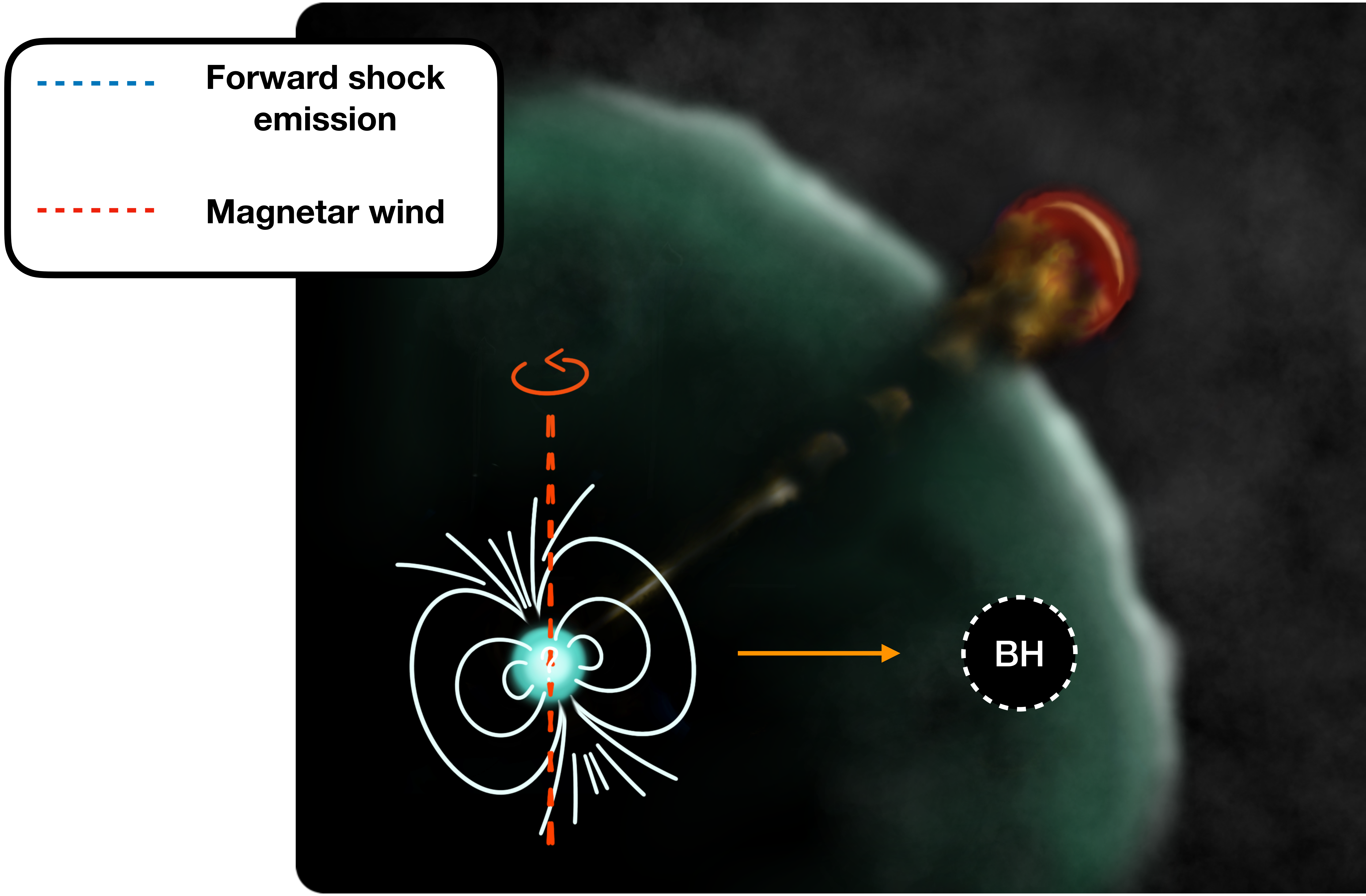

The jet shock front deviates from a spherical geometry

$$\Gamma(\theta) = \text{const}$$

Top hat

$$\Gamma(\theta) = \begin{cases} \sim \Gamma_0, & \theta < \theta_c \\ \sim \Gamma_0 \cdot f_\Gamma(\theta), & \theta > \theta_c \end{cases}$$

Structured

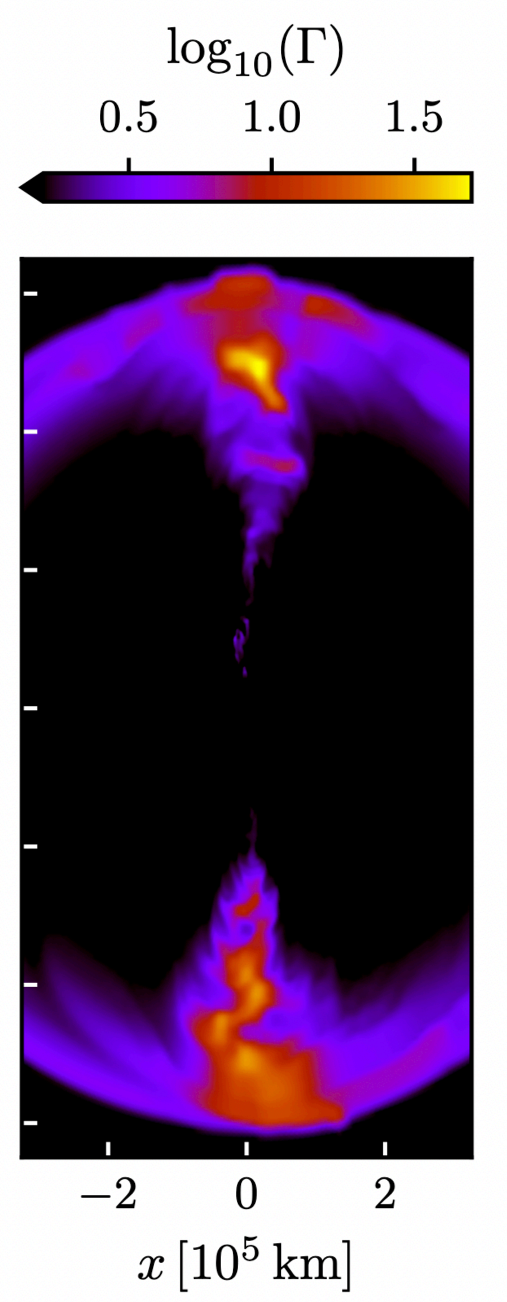

Pavan + 2022

The formation of a jet structure is a natural outcome of the [jet - circumburst medium] interaction, both for merger and collapsar driven GRBs, confirmed by simulations

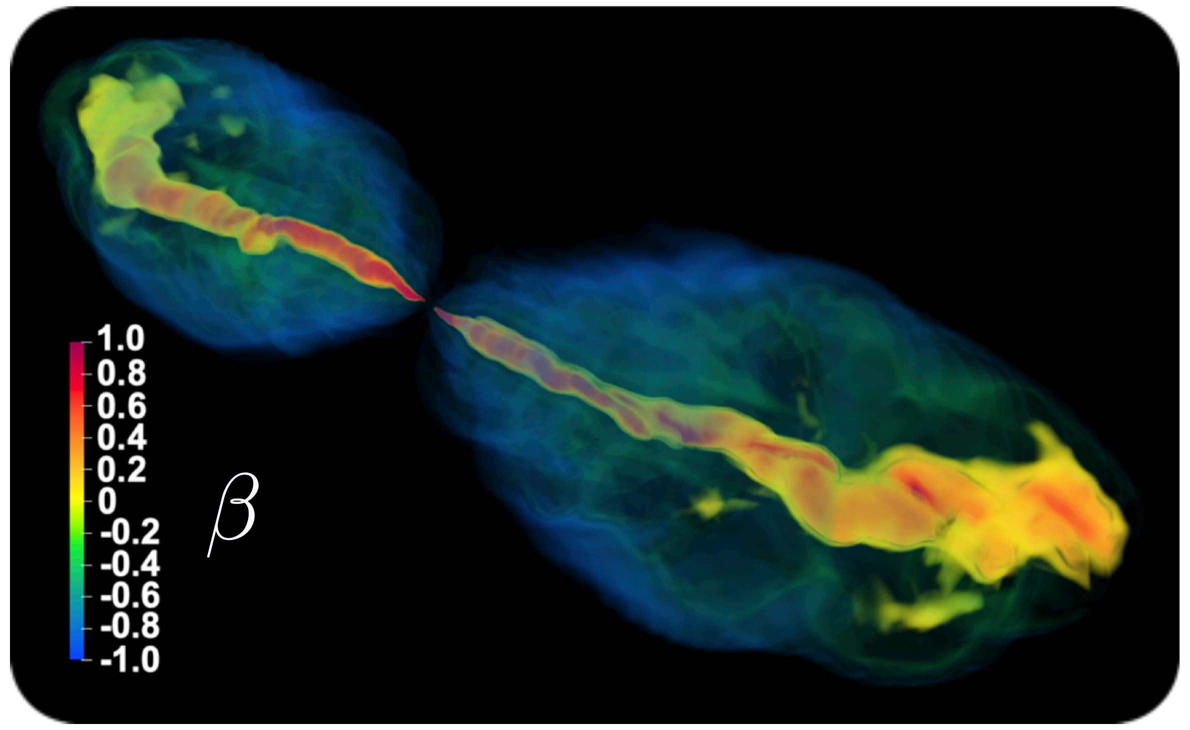

Gotlieb + 2022

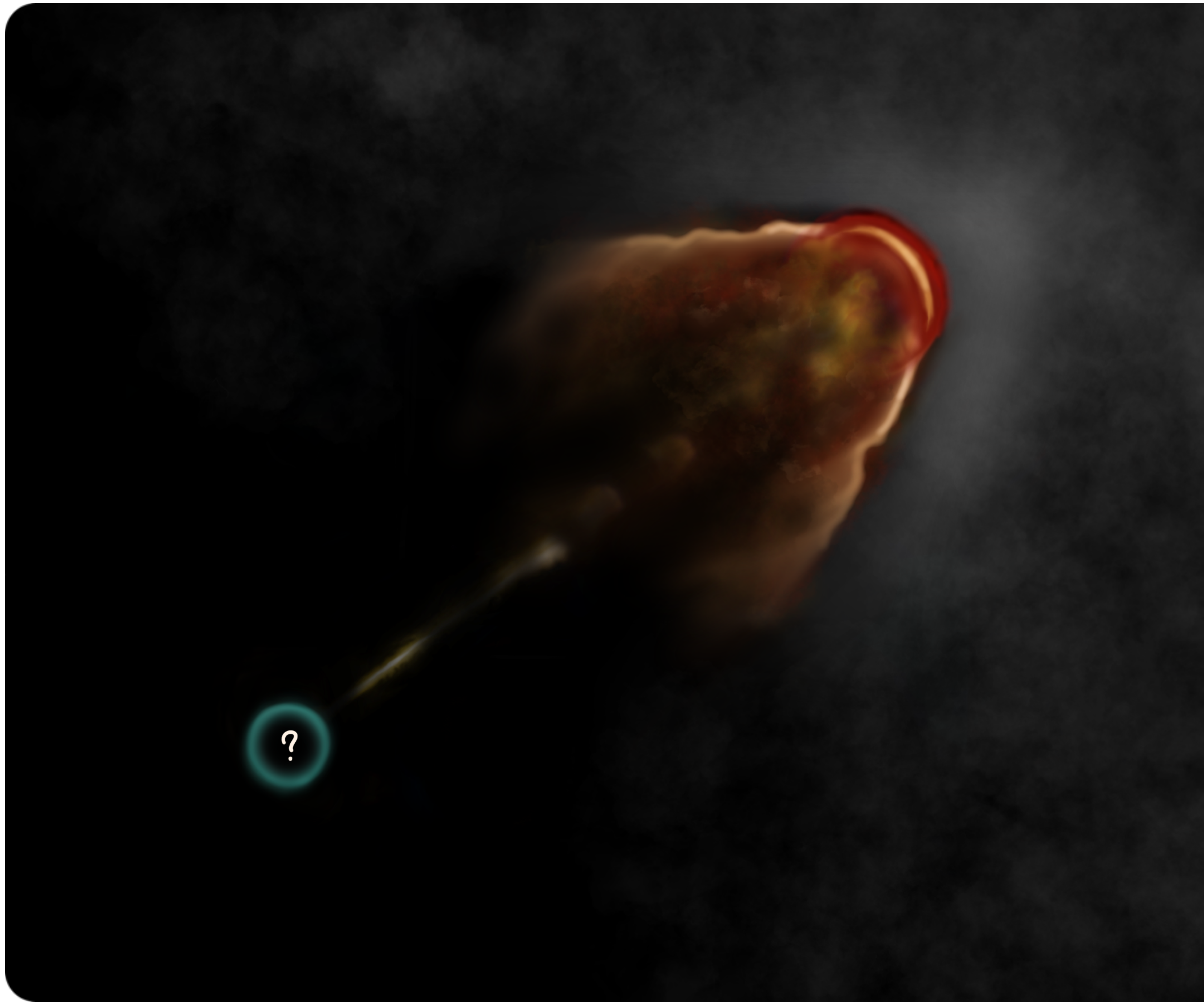

The structured jet scenario

Impact on the afterglow light curve

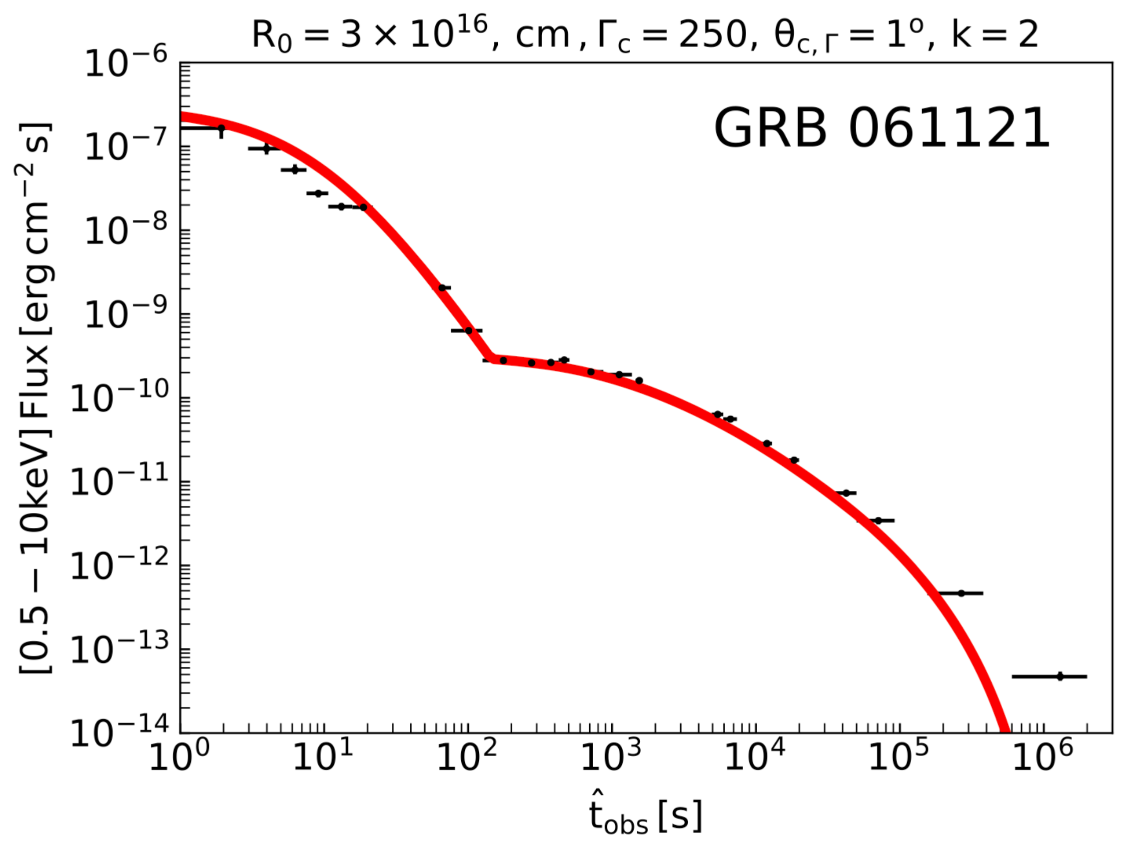

Oganesyan 2020

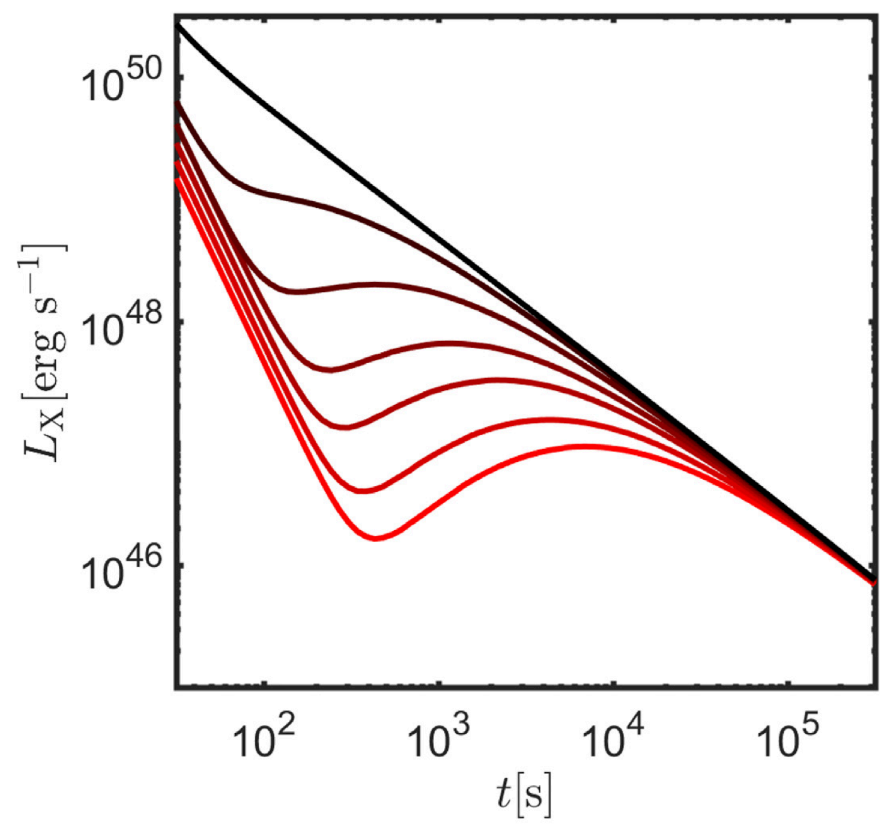

Beniamini 2020

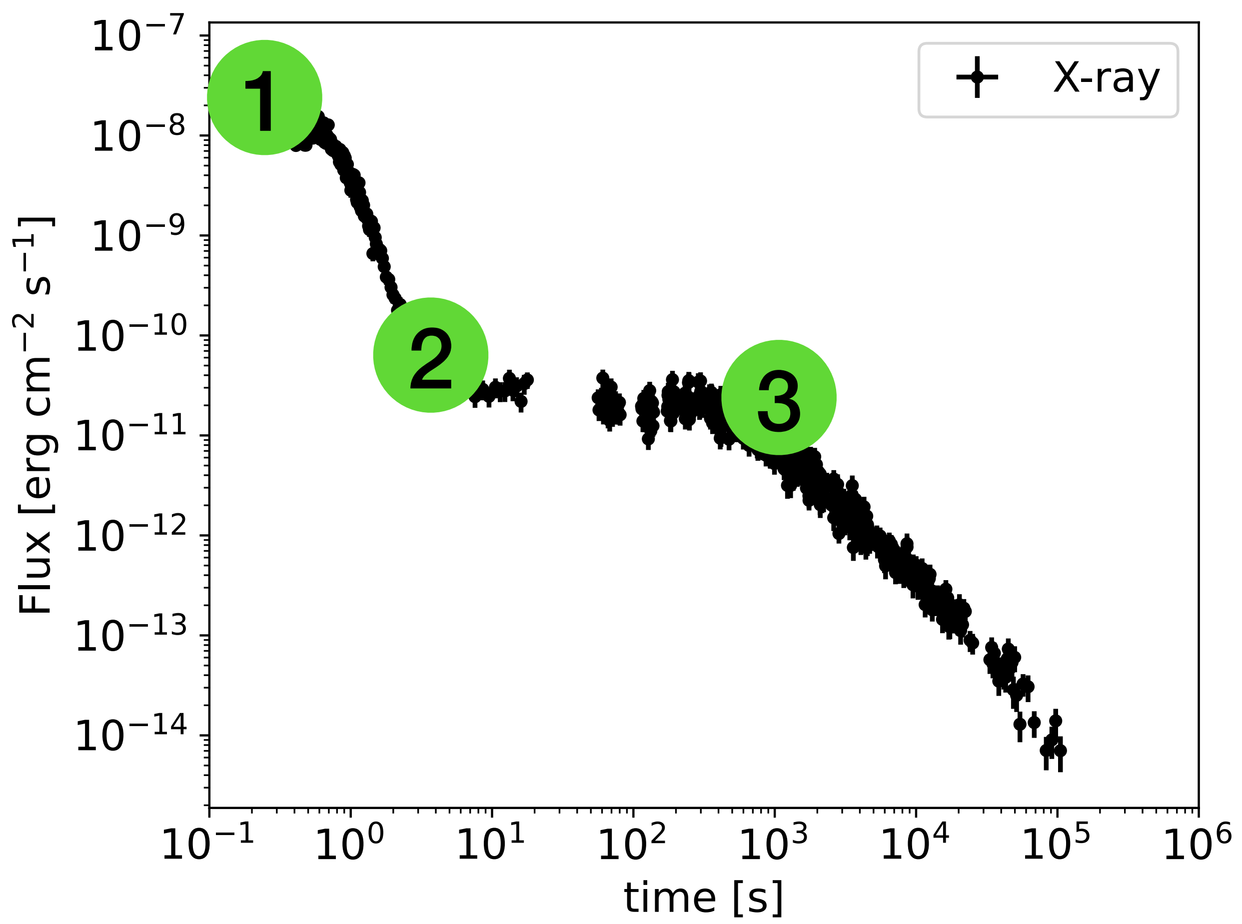

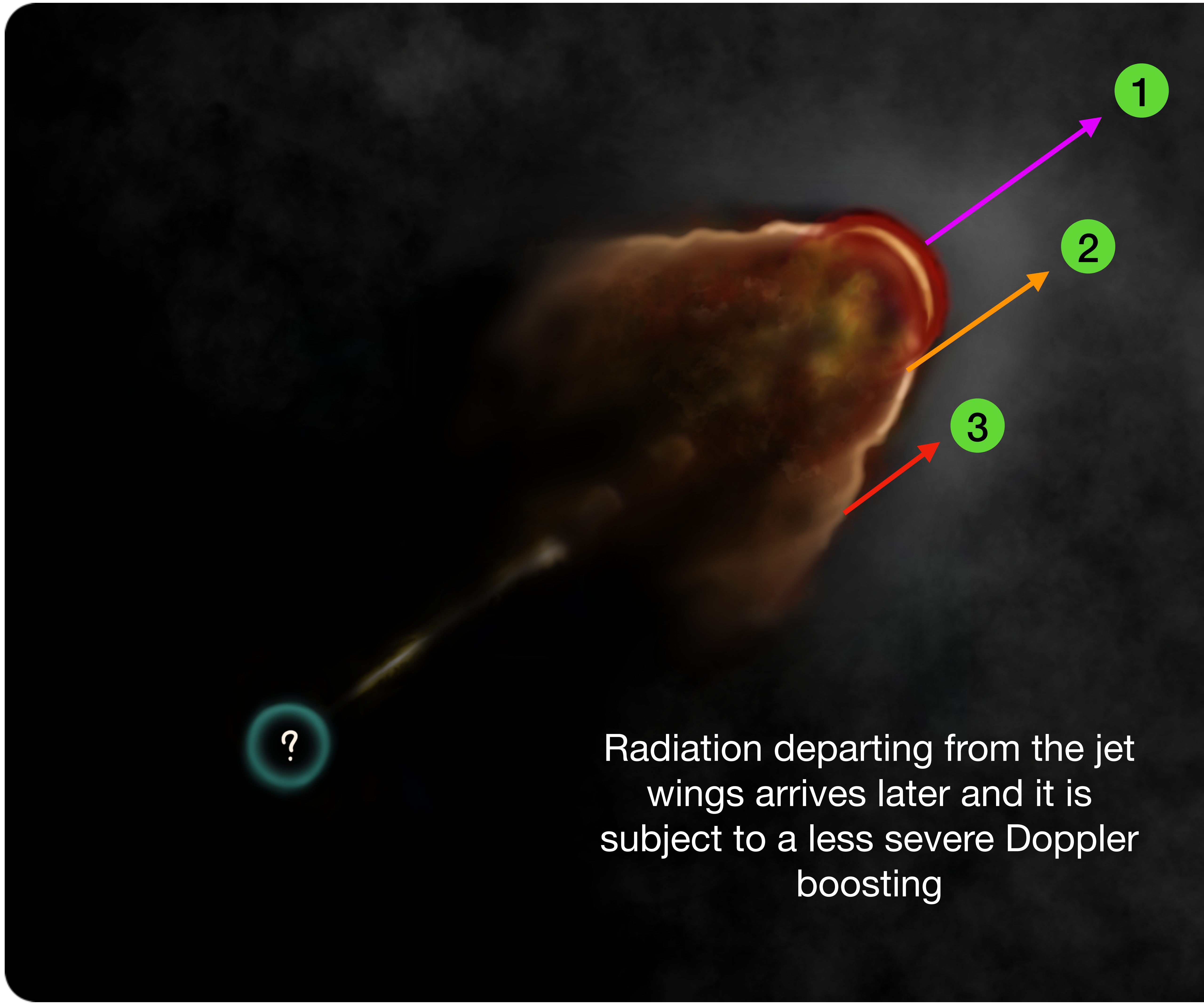

Strategy of our analysis

1. Build a complete **Swift sample** of GRBs with an **X-ray plateau and simultaneous optical data**

2. Study the spectral evolution in the X-rays with a **temporally resolved analysis**

3. Test if, at each time, optical and X-ray are simultaneously compatible with **a single emission region**, dominated by synchrotron radiation

4. Characterize the **multi-band emission** during the X-ray plateau, in the context of available scenarios

We define two samples, based on the comparison between optical and X-ray fluxes

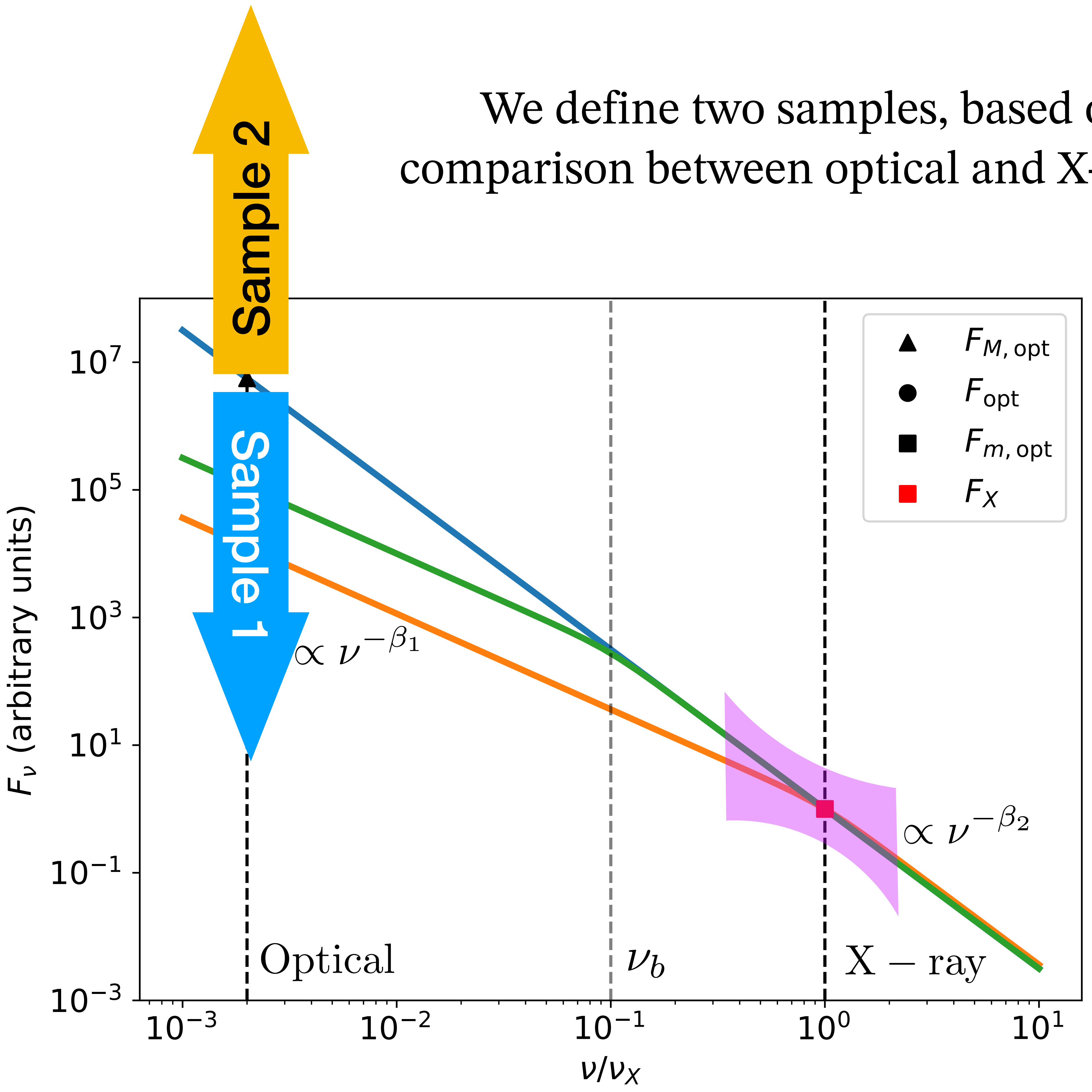

For each temporal bin

1. We derive X-ray flux and photon index
2. We extrapolate down to optical
3. We compare with the observed optical flux

19 GRBs in Sample 1

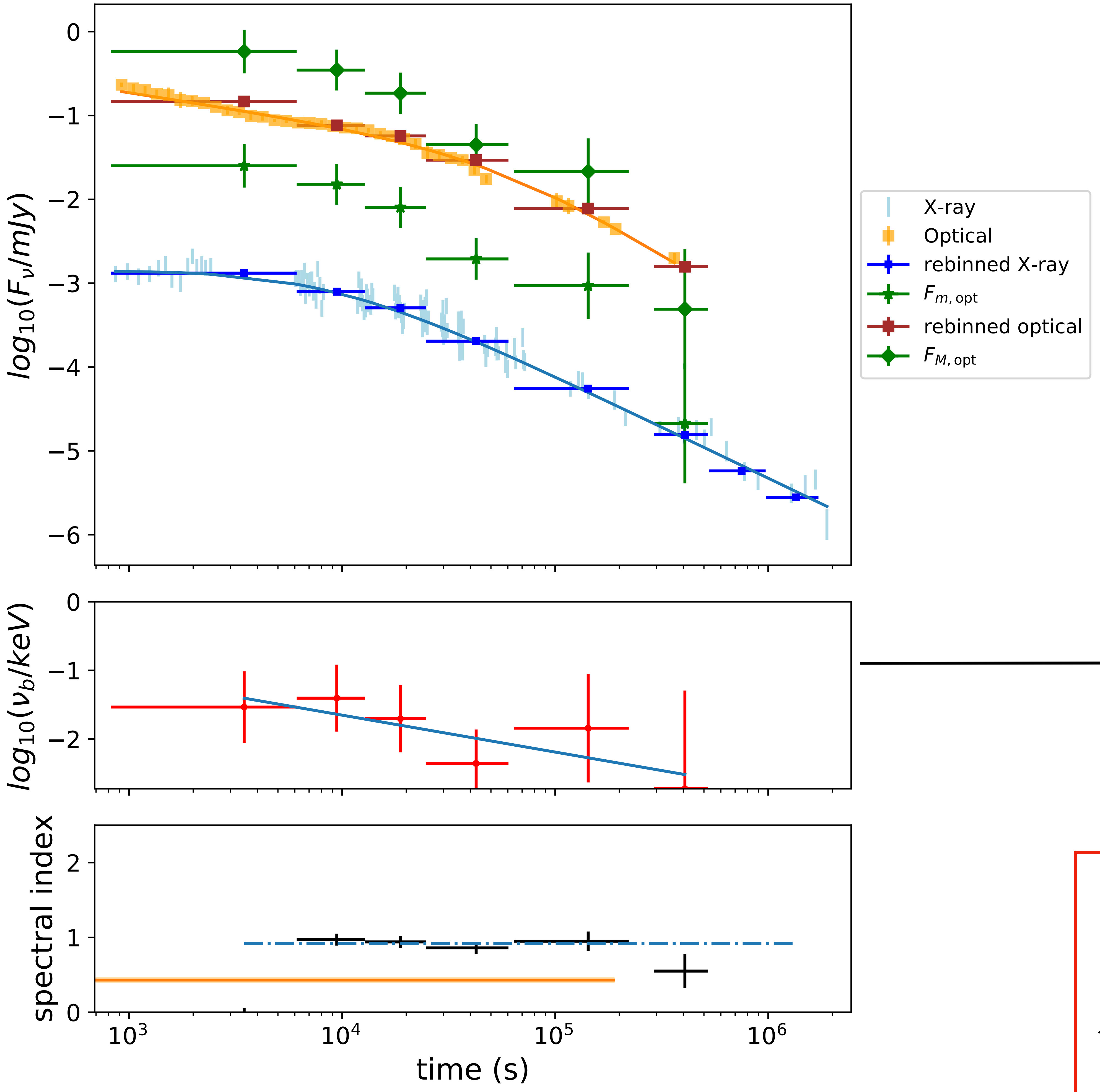

From Ronchini et al. 2023

11 GRBs in Sample 2

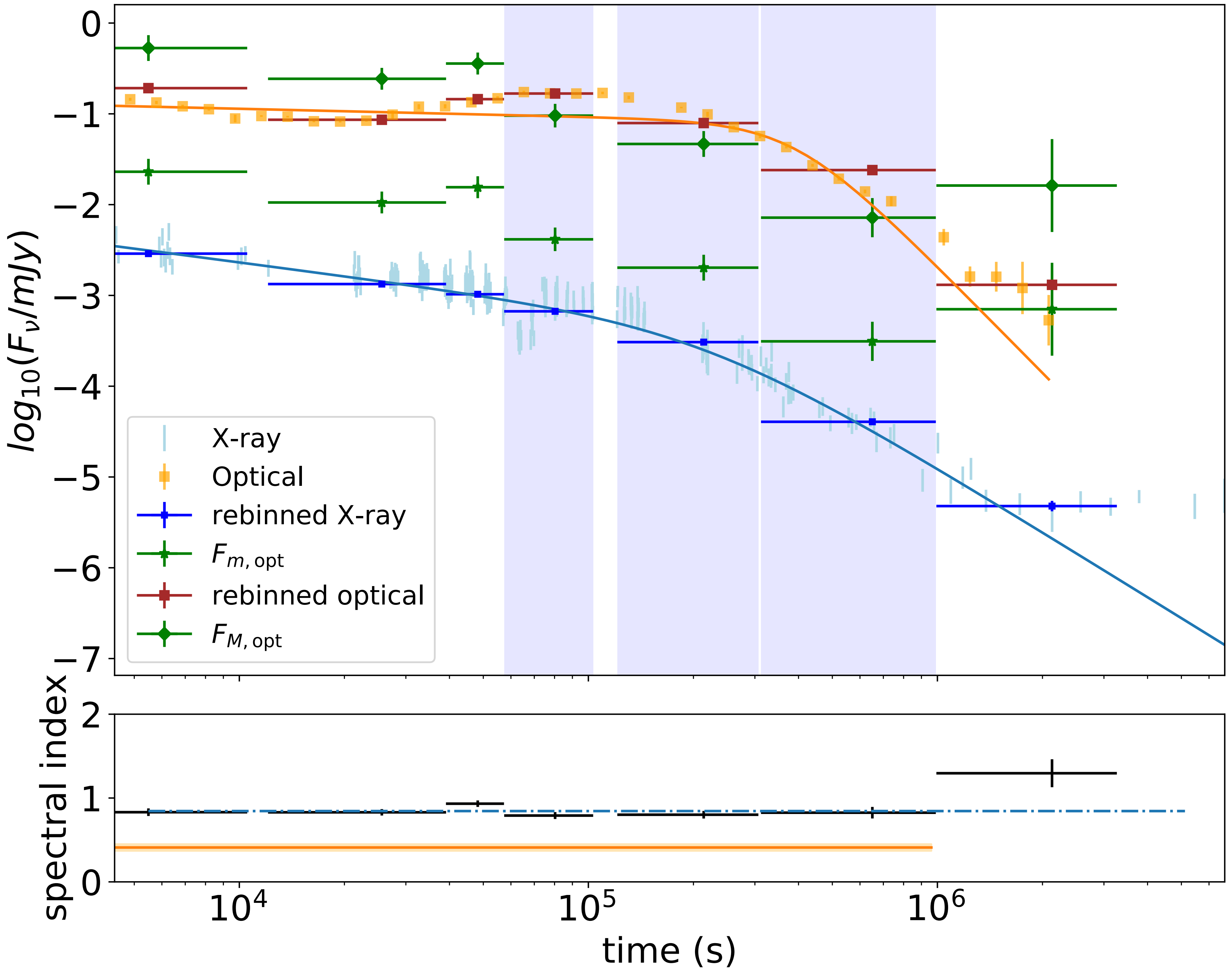

We can derive the evolution of the break frequency and compare it with the behavior expected from different scenarios

Results: Sample 1

The temporal evolution of X-ray and optical flux and break frequency is fitted with a power law

$$\nu_b \propto t^{-s}$$

	s<0	s=0	s>0
# cases	3	5	11

We find:

1. The **standard FS scenario**, even assuming time-dependent micro-physical parameters, **cannot explain the X-ray/optical evolution**
2. The **energy injection scenario can reproduce** the temporal evolution of the spectral break
3. **The structured jet scenario**, as well, **is able to explain the observed spectral evolution**, assuming different possible ISM density profiles

Results: Sample 2

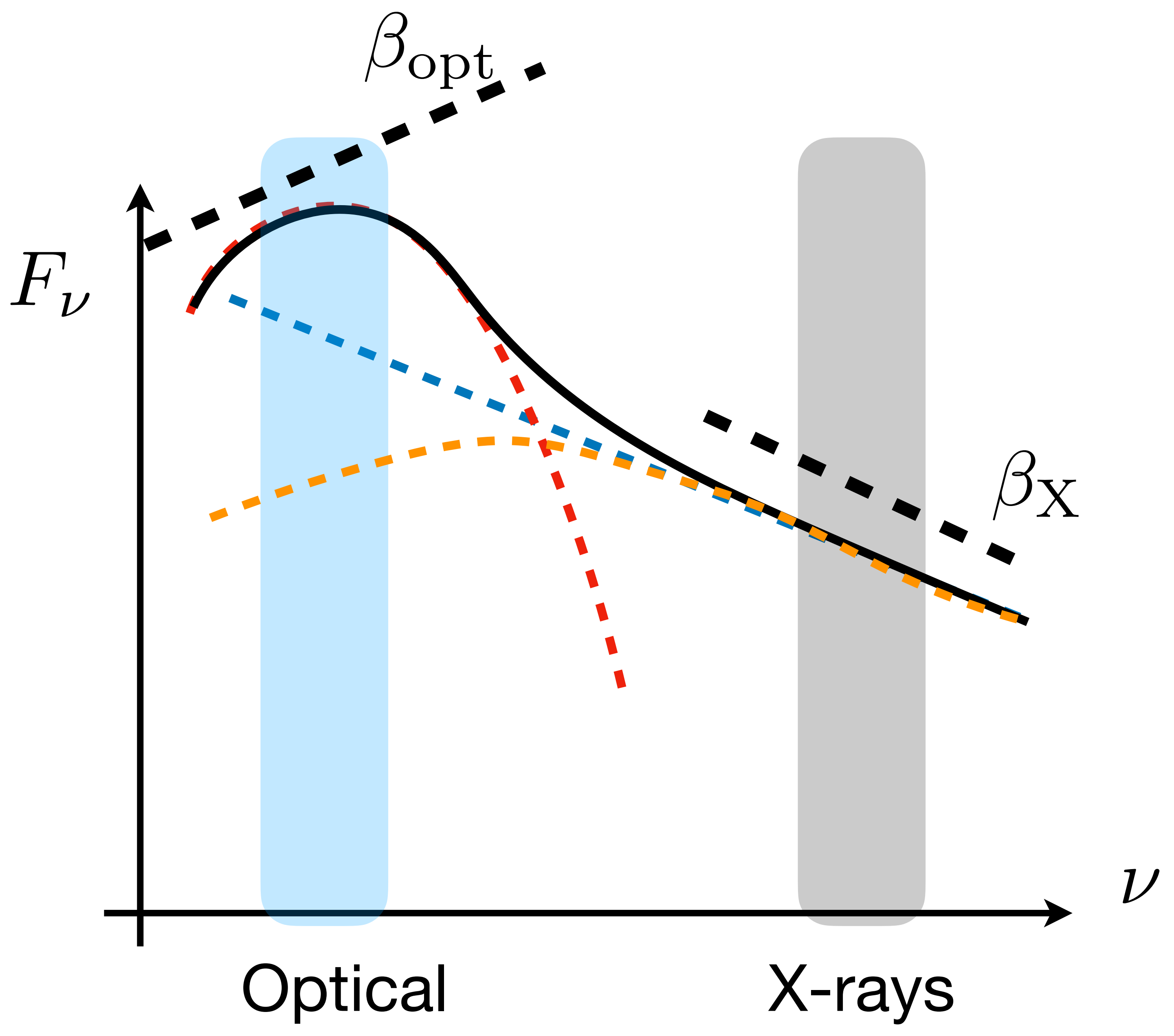

What we know:
A single synchrotron component is excluded

The optical excess requires the presence of two spectral components

Optical always in excess

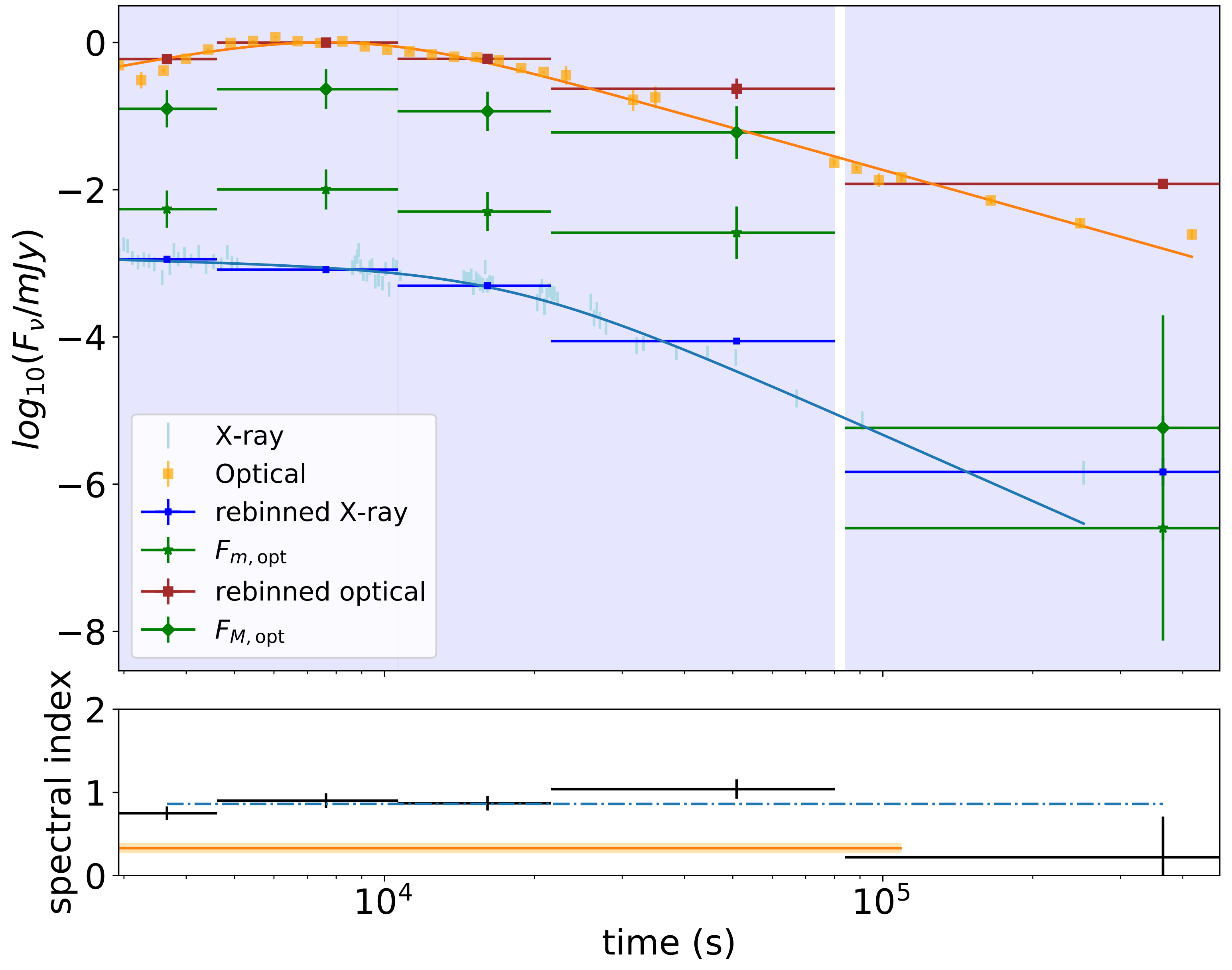

Excess only in a limited temporal window

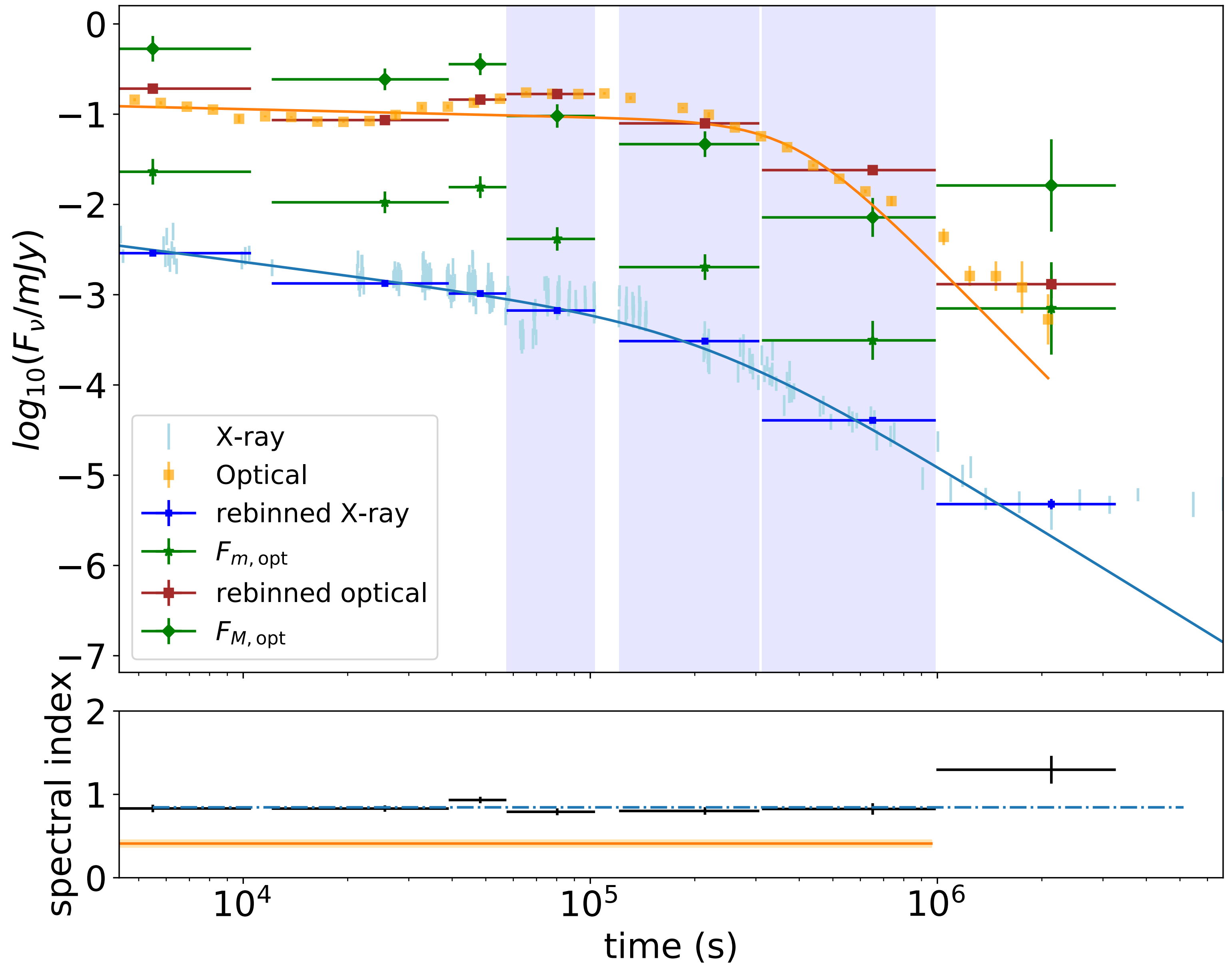

$\beta_{\rm X} > \beta_{\rm opt}$

From Ronchini et al. 2023

Conclusions Part II

1. The **plateau** is a temporal feature often observed in the X-ray light curve of GRBs and the physical origin should involve a **quite common process**, present both in merger- and collapsar-driven GRBs

2. A satisfactory model for the X-ray plateau should be able to explain:
   A. Why the plateau is so common
   B. The observed empirical correlations
   C. The full multi-band emissions and associated spectral evolution

3. For **~2/3** of the analysed GRBs, the multi-wavelength emission during the plateau is **compatible with a single synchrotron spectral component**

4. For the remaining **1/3 the optical emission is in excess**, showing the evidence of the interplay of at least two spectral components during the plateau phase

5. Both the HLE from a structured jet and the magnetar are viable scenarios, possibly contributing in different bands

Part III

Multi-messenger observations of GRBs in the Einstein Telescope era

Ronchini et al. 2022, Astronomy & Astrophysics, 665, A97

Goal of this work:

Provide an exhaustive overview about the **joint detection** of:

1. **gravitational waves (GWs)**
2. Electromagnetic (EM) counterpart in the **high energy domain**

from the coalescence of **NS binaries**, in the era of **3G GW detectors**

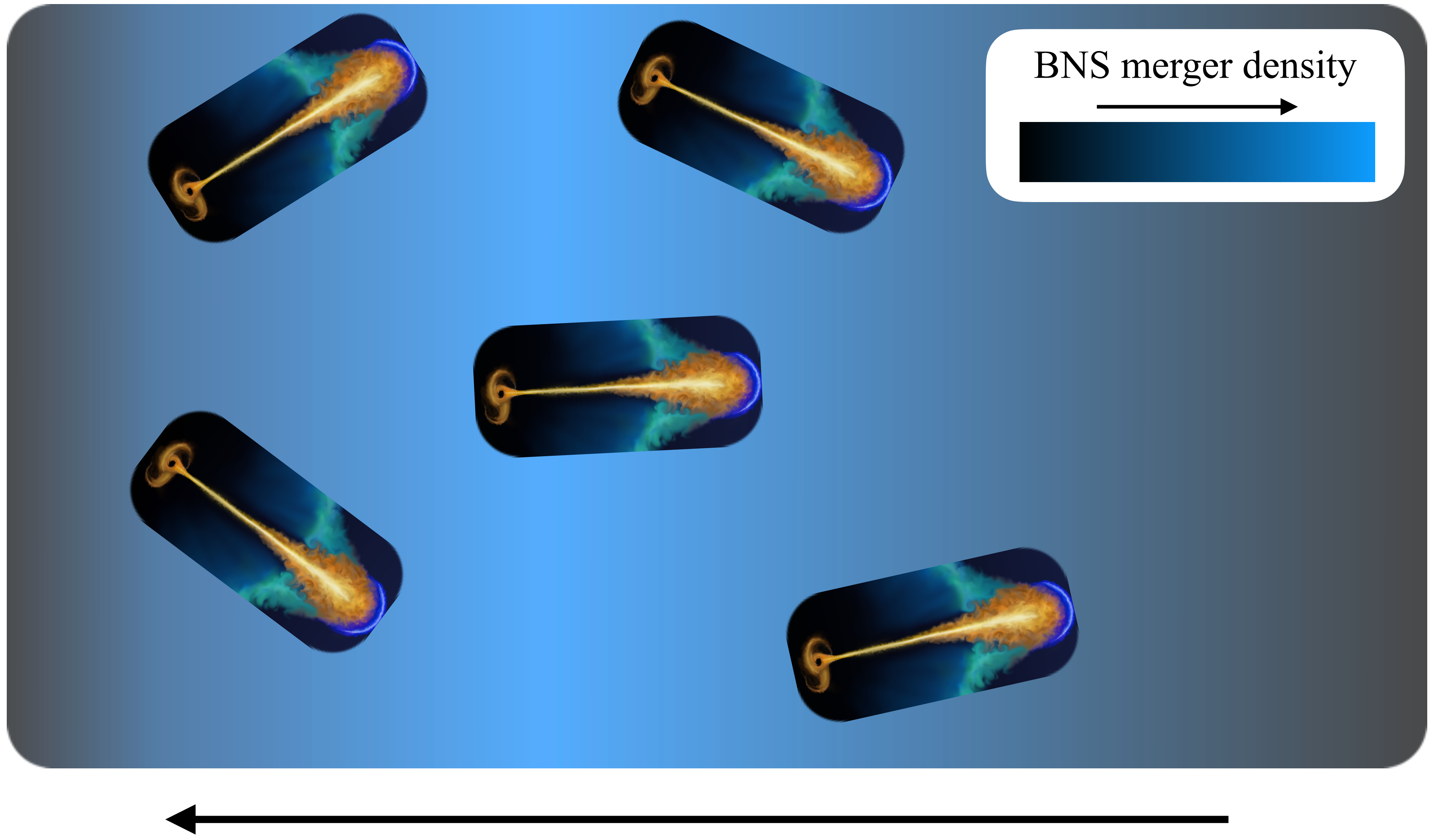

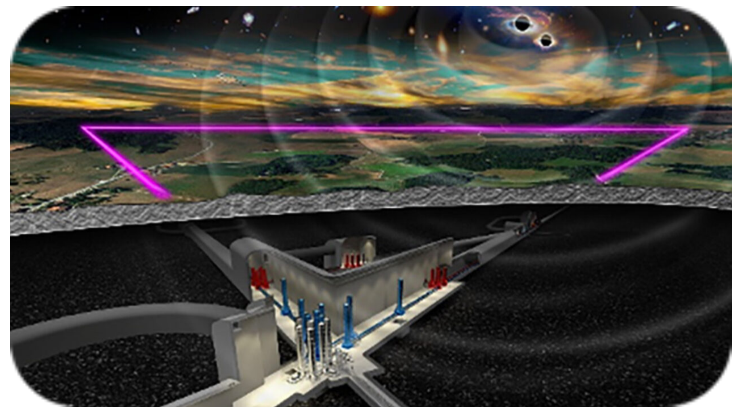
GW

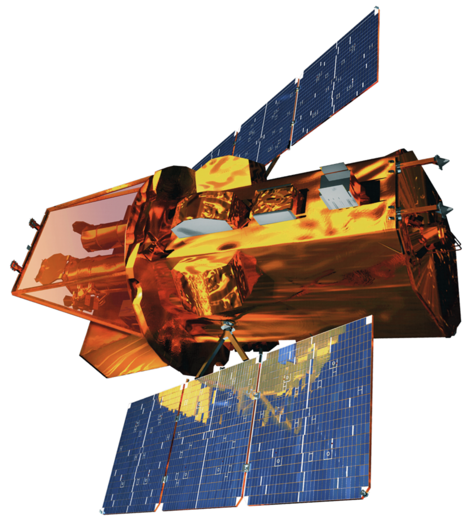
EM

Relevance of this work:

- Highlight the **role of wide field space telescopes** for the identification of the EM counterpart
- Evaluate the **scientific return** of future GW-EM synergies
- **Define the best technical design** of future GW and EM instruments, to optimally achieve the multi-messenger science goals

The 3rd generation of GW detectors: steps forwards

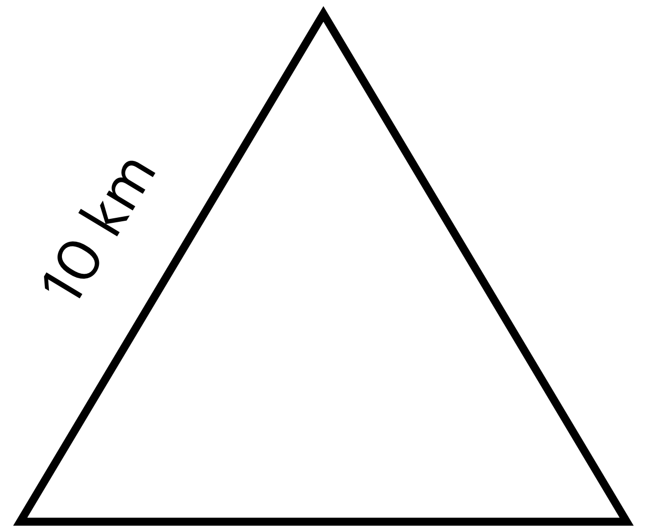

Einstein Telescope
(ET)

- **Triangle** geometry
- Xilophone concept: **low frequency** at cryogenic temperature + **high frequency** at room temperature
- Underground to **minimise seismic noise**

Sensitivity curves

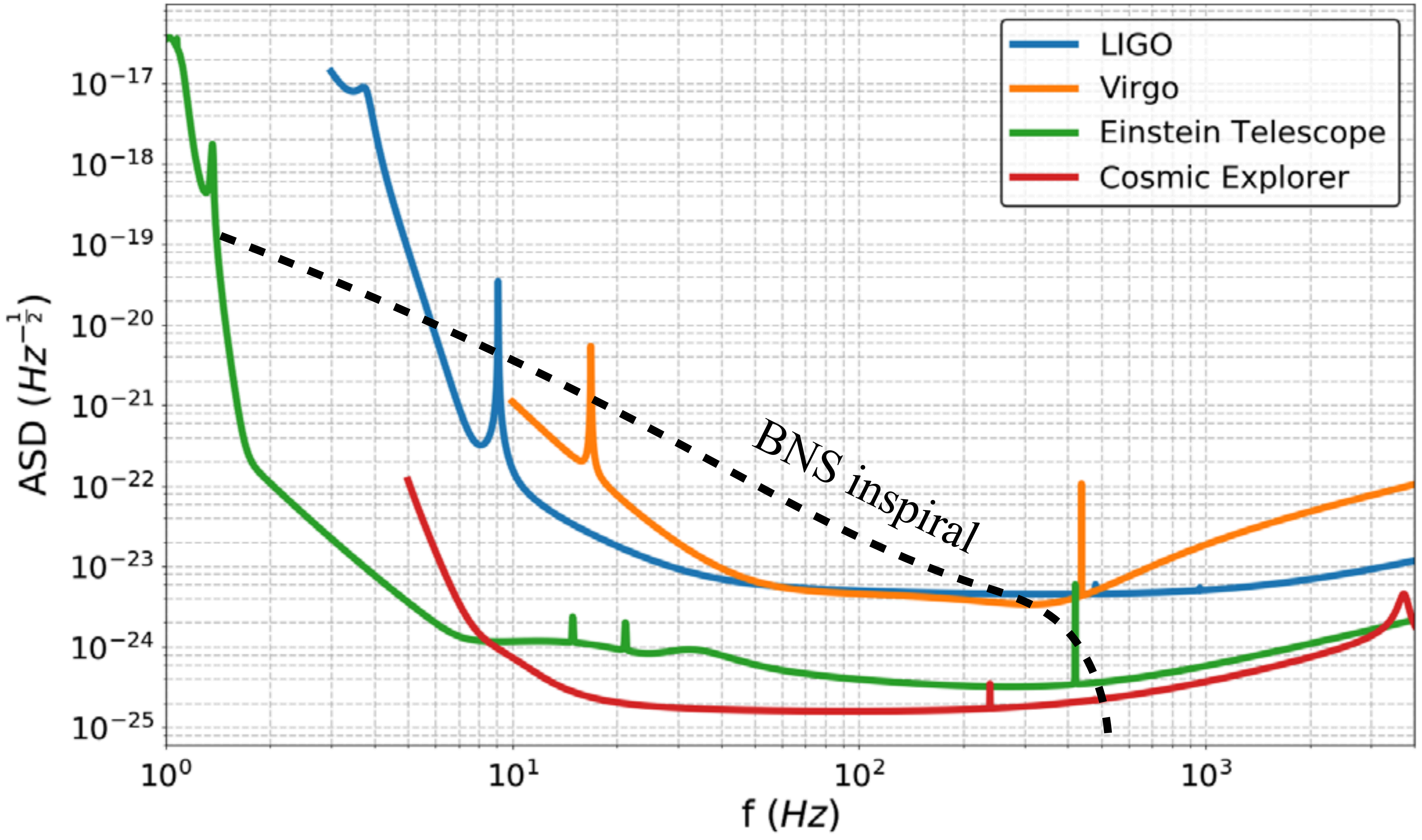

From Chan et al. 2018

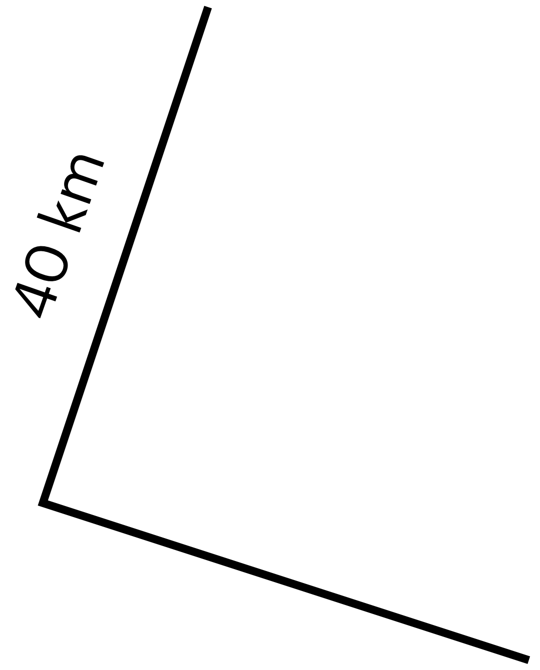

Cosmic Explorer
(CE)

Extension of LIGO concept with **10x longer arms**

The 3rd generation of GW detectors: science case

- 10^5-10^6 detections / yr of stellar mass BH mergers up to z~100
- Detection of primordial BH
- Detection of ~10^5 BNS mergers/yr beyond the star formation peak
  - ET more **sensitive at low frequency** → the inspiral is followed for a longer time → **better sky localisation**
  - Access the **effects of tidal deformations** at the moment of the merger → **NS EoS**
- Test of GR during the inspiral and in the post-merger (e.g. BH ringdown)
- Nature of dark energy and modifications of GR at cosmological distances

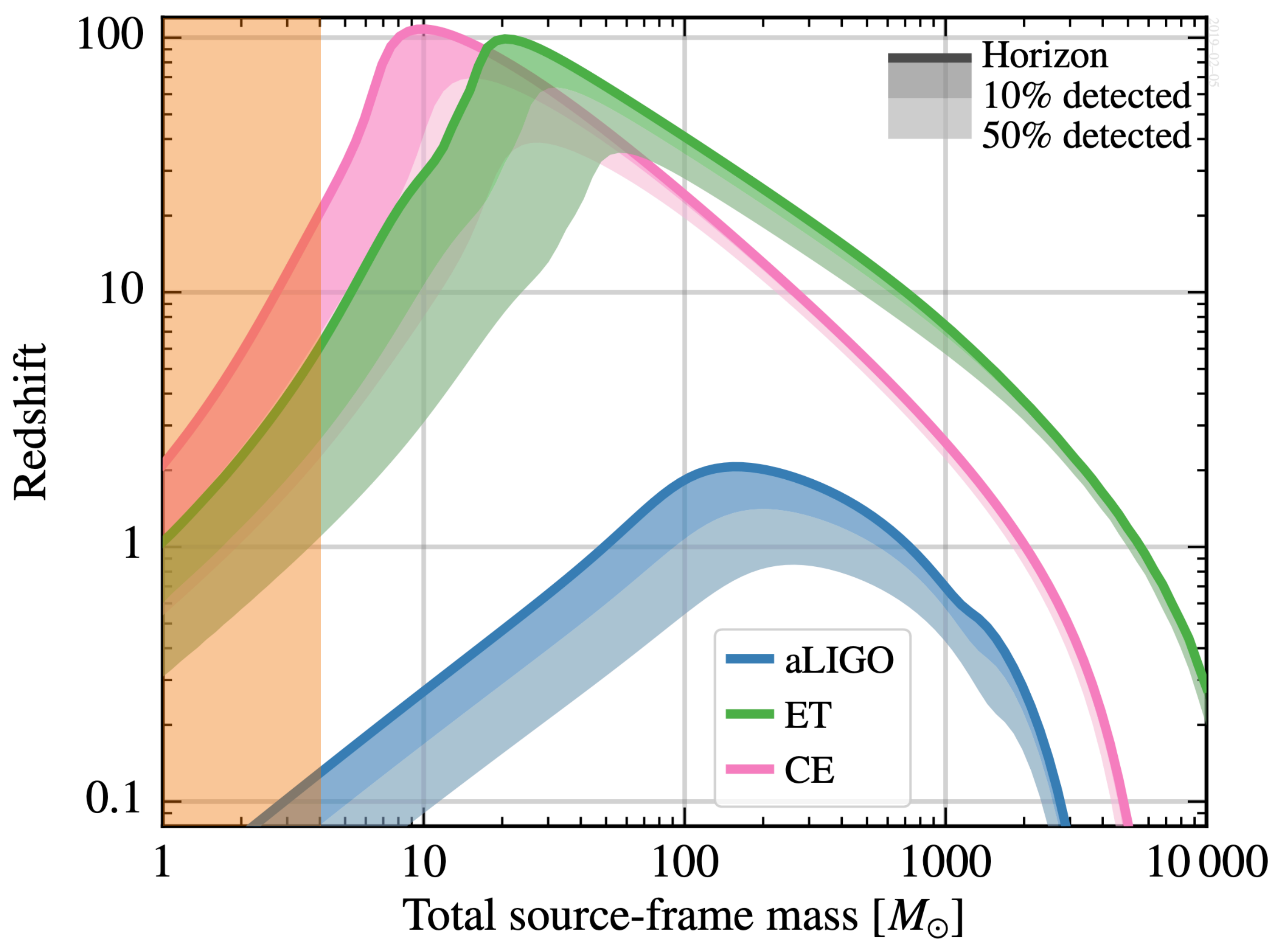

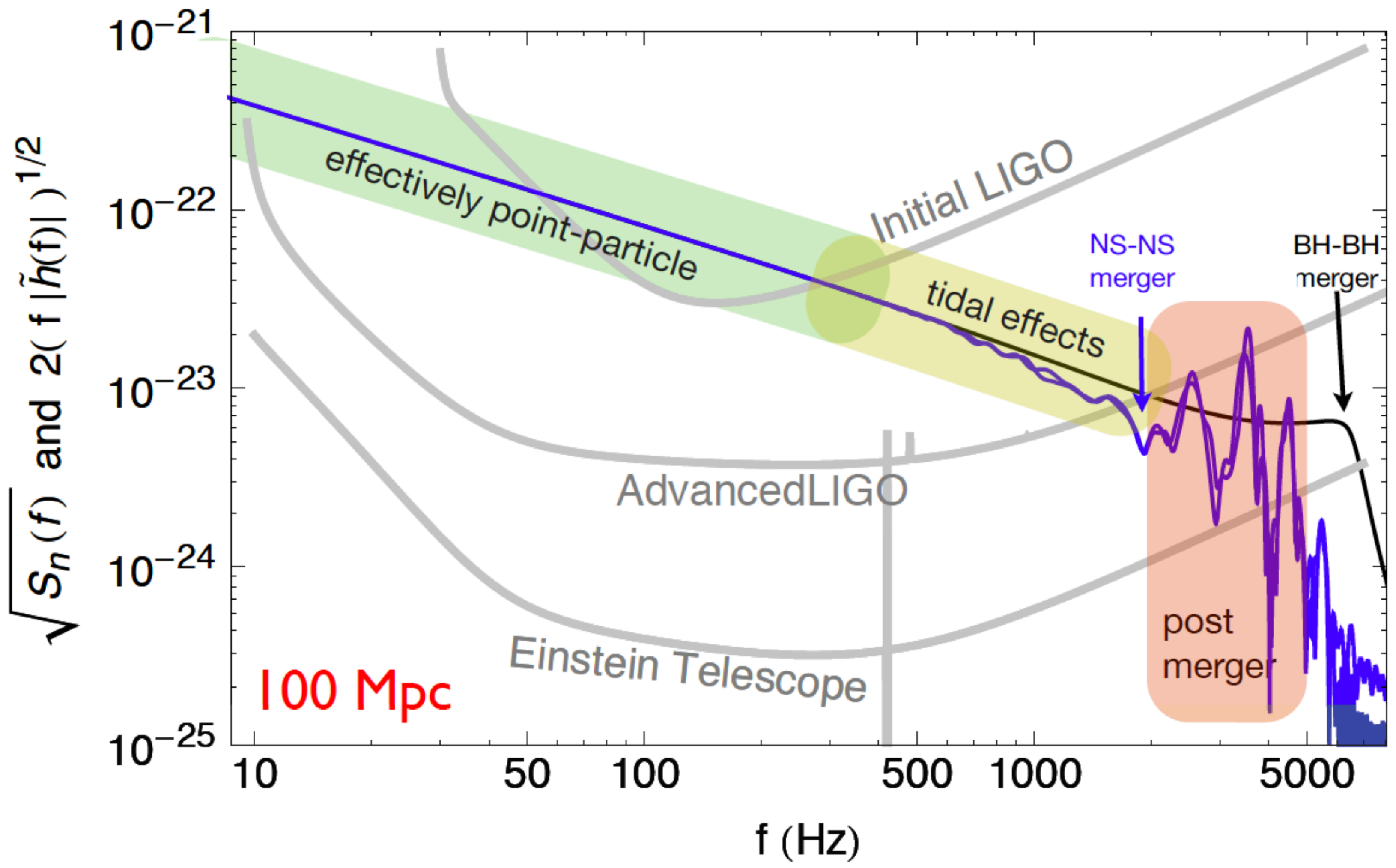

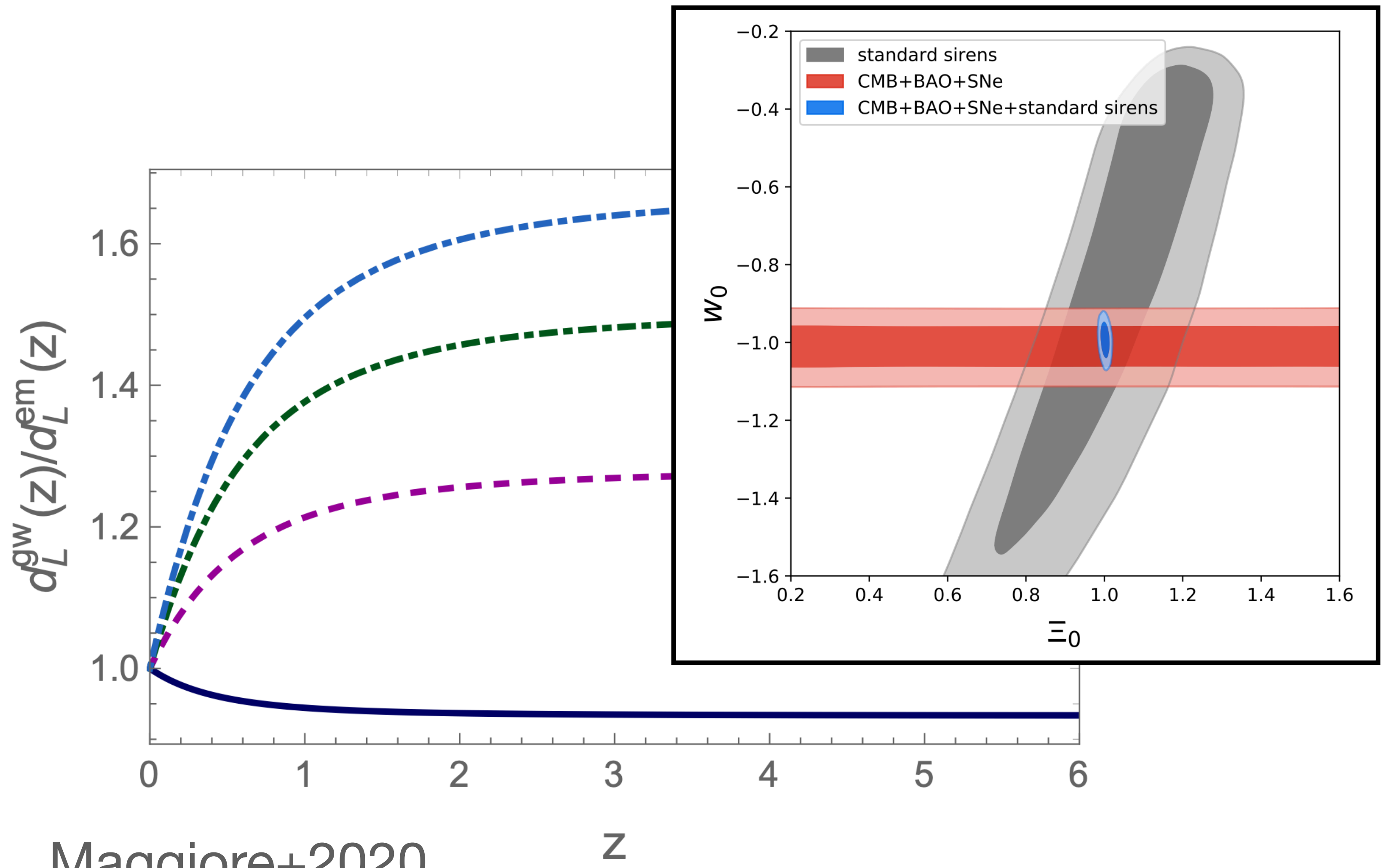

Maggiore+2020

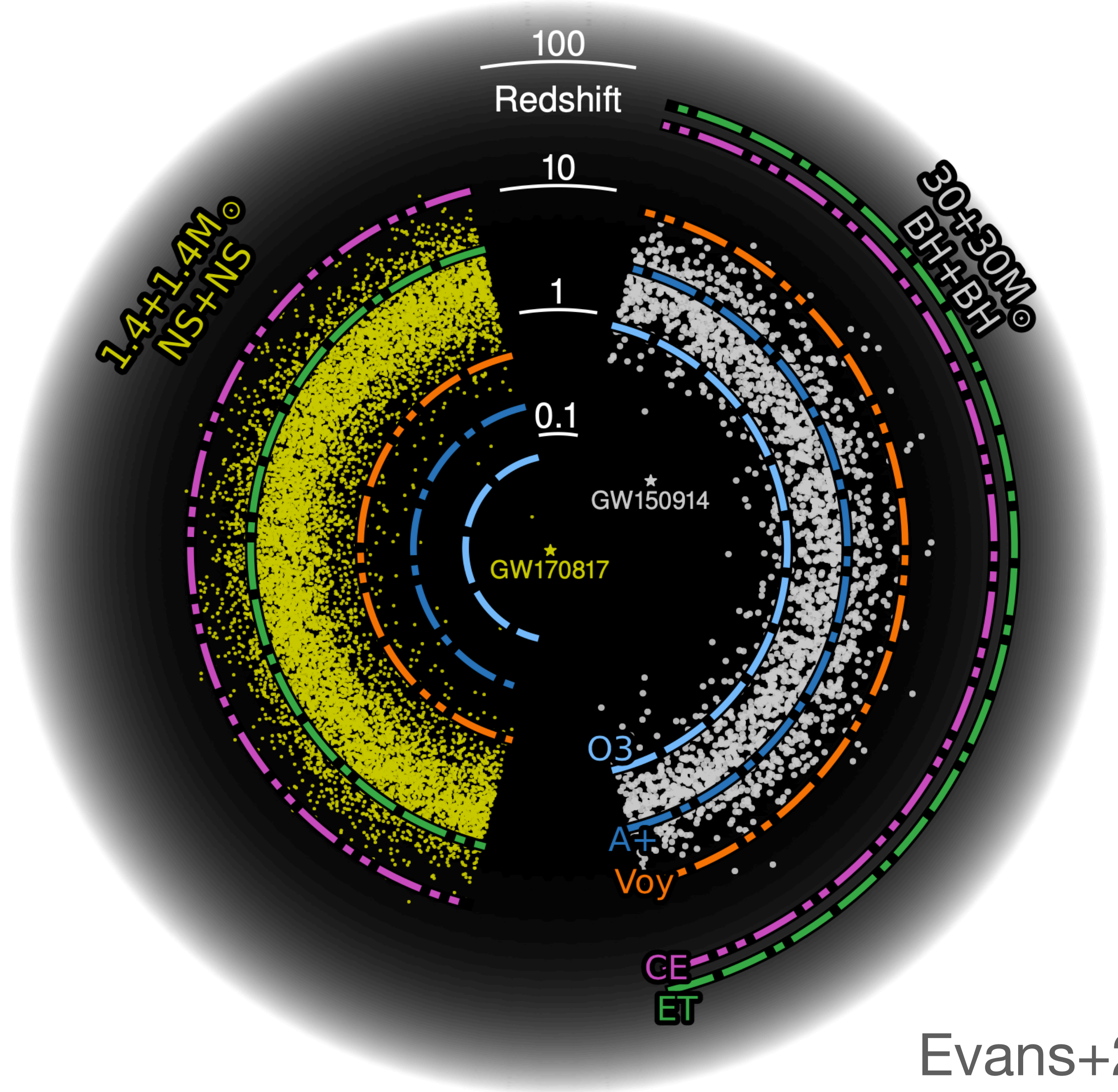

Evans+2021

The 3rd generation of GW detectors: population studies

GWFISH

Dupletsa et al. 2022

Expected number of BNS detections / yr ~ 10^5

↓

Bayesian parameter estimation → Fisher matrix

In the limit of high SNR: quadratic approximation of the likelihood

→

- Parameter estimation based on **Fisher-matrix** approximation
- Includes the effect of **Earth rotation** (not negligible for long-lasting signals)
- Computationally **efficient**
- Ideal to process **large amount of injections** and to obtain average population properties
- Gives robust results in the **limit of high SNR**

Population of BNS mergers from compact binary population synthesis model

Phenomenological model for prompt emission

Comparison with properties of Fermi-GBM sample

Estimation of the prompt and afterglow emission

Prediction of the point detection rate

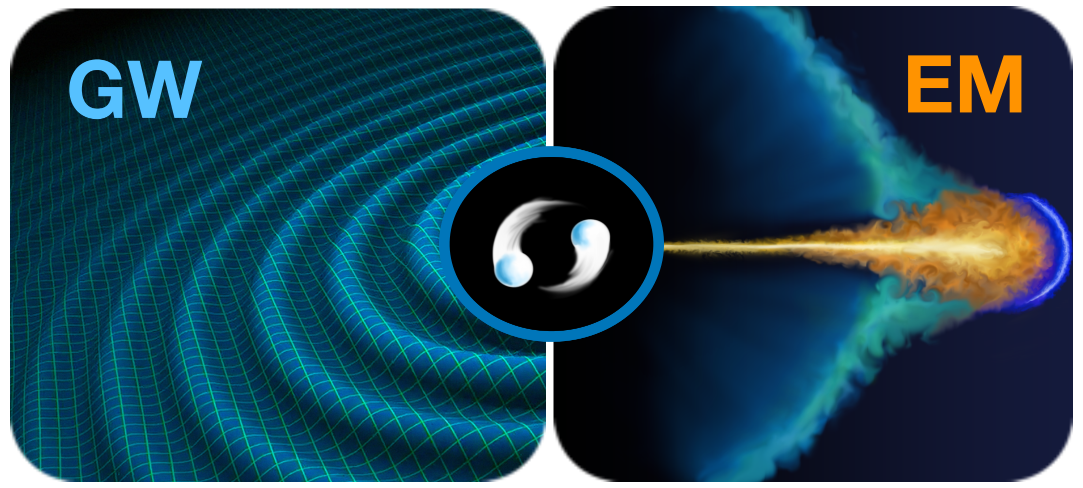

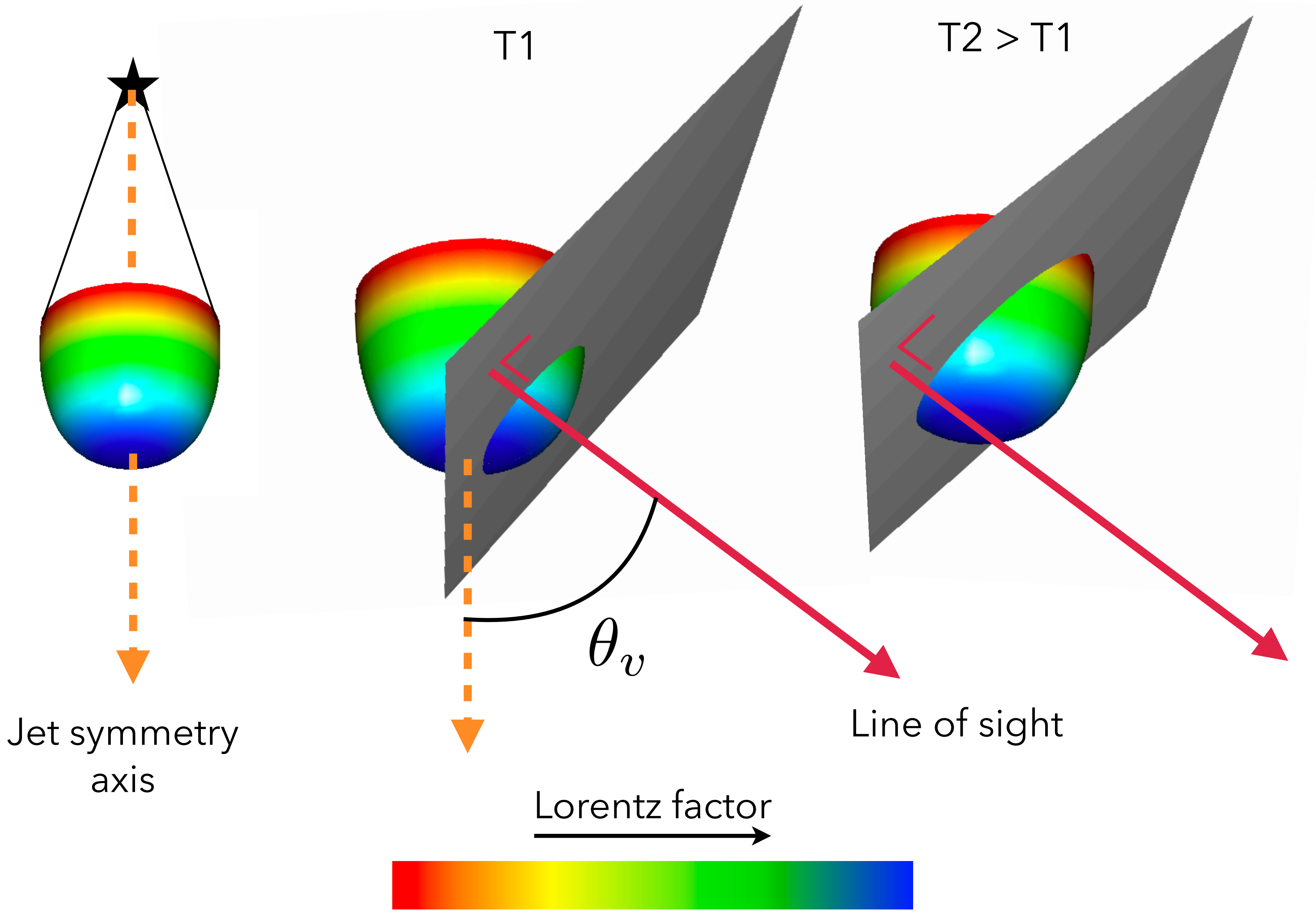

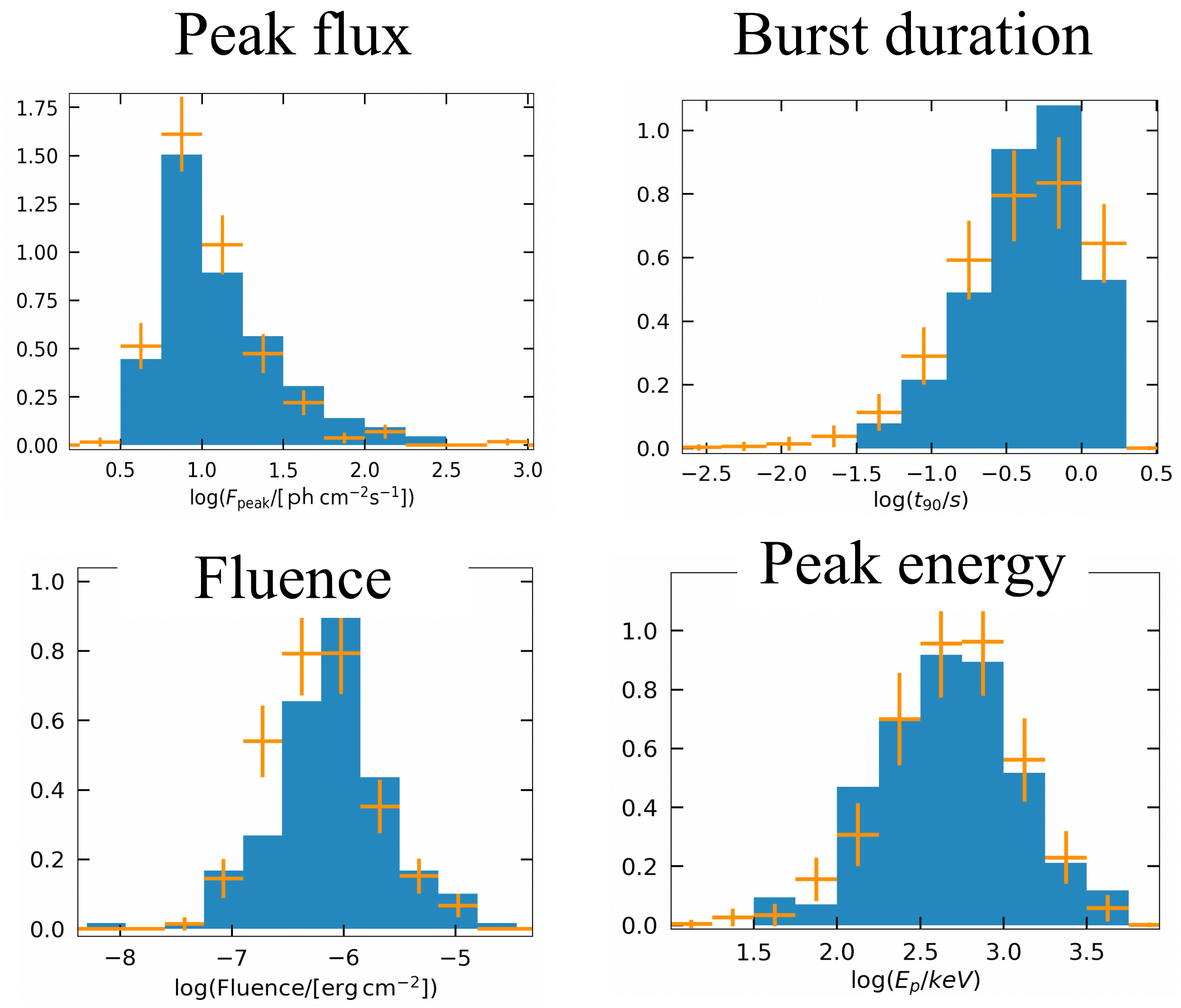

+ Fermi-GBM rate of short GRBs

Joint detection of γ-ray emission and GWs

INSTRUMENT	band MeV	$F_{\rm lim}$ erg cm^{-2} s^{-1}	FOV/4π	loc. acc.	Joint ET +γ-ray	N_{JD}/N_γ	Joint (ET+CE) +γ-ray	N_{JD}/N_γ
Fermi-GBM	0.01 - 25	0.5(*)	0.75	5 deg (^{a})	33^{+14}_{-11}	$68^{+13}_{-18}\%$	47^{+14}_{-14}	$95^{+5}_{-7}\%$
Swift-BAT	0.015 - 0.15	2×10^{-8}	0.11	1-3 arcmin	10^{+3}_{-3}	$62^{+11}_{-14}\%$	13^{+5}_{-4}	$94^{+6}_{-7}\%$
SVOM-ECLAIRs	0.004 - 0.250	1.792(*)	0.16	$<$ 10 arcmin	3^{+1}_{-1}	$69^{+10}_{-9}\%$	4^{+1}_{-1}	$95^{+5}_{-4}\%$
SVOM-GRM	0.03 - 5	0.23(*)	0.16	$\sim$ 5 deg	9^{+4}_{-3}	$59^{+6}_{-6}\%$	14^{+6}_{-4}	$92^{+3}_{-3}\%$
THESEUS-XGIS	0.002 - 10	3×10^{-8}	0.16	$<$ 15 arcmin	10^{+5}_{-4}	$63^{+13}_{-13}\%$	15^{+6}_{-4}	$94^{+6}_{-7}\%$
HERMES	0.05 - 0.3	0.2(*)	1.0	1 deg	84^{+42}_{-30}	$61^{+10}_{-11}\%$	139^{+54}_{-36}	$94^{+6}_{-6}\%$
TAP-GTM	0.01 - 1	1(*)	1.0	20 deg	60^{+24}_{-24}	$67^{+13}_{-14}\%$	84^{+30}_{-24}	$95^{+5}_{-6}\%$

Fermi GBM+ET

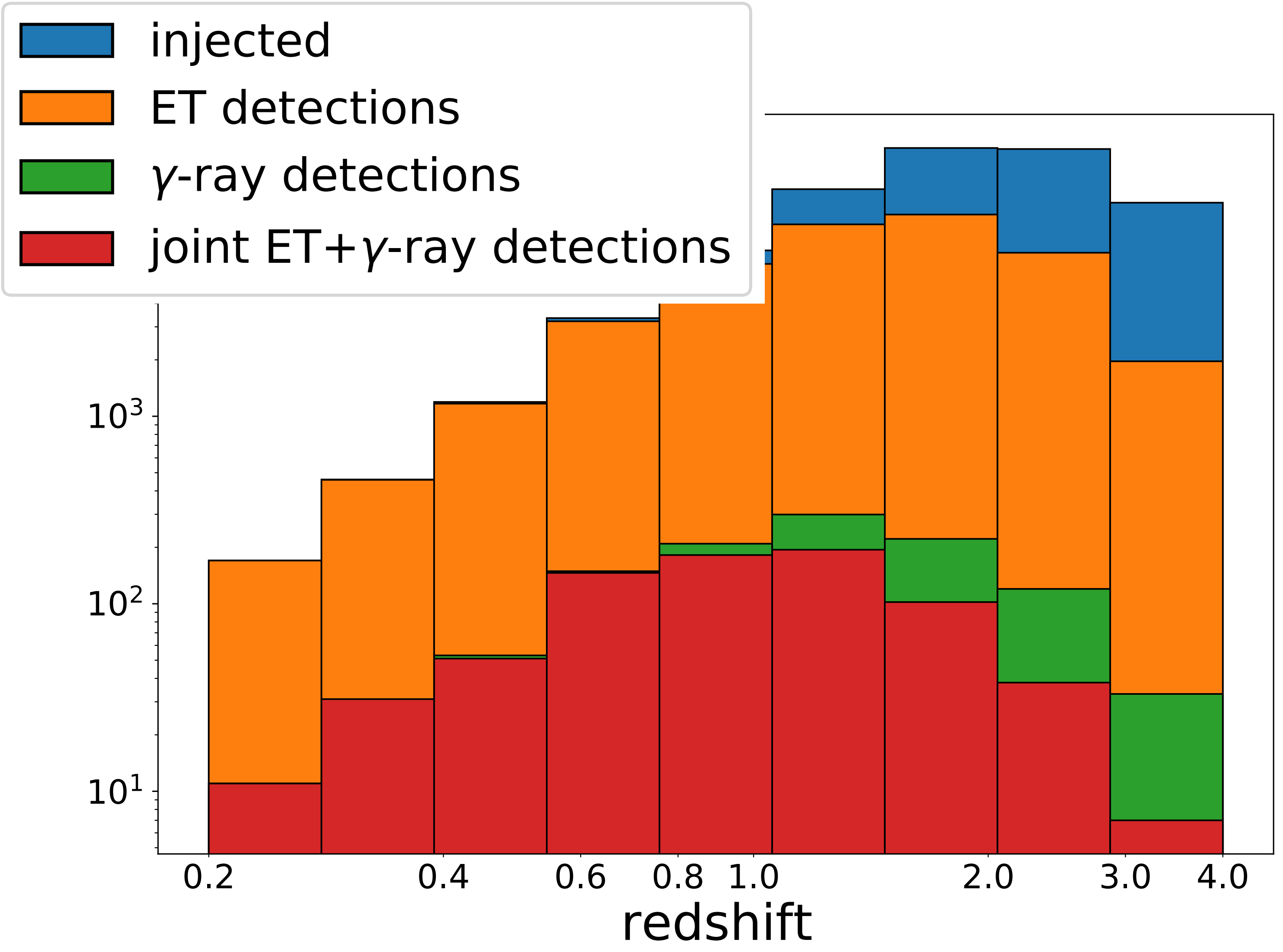

Fermi GBM+(ET&CE)

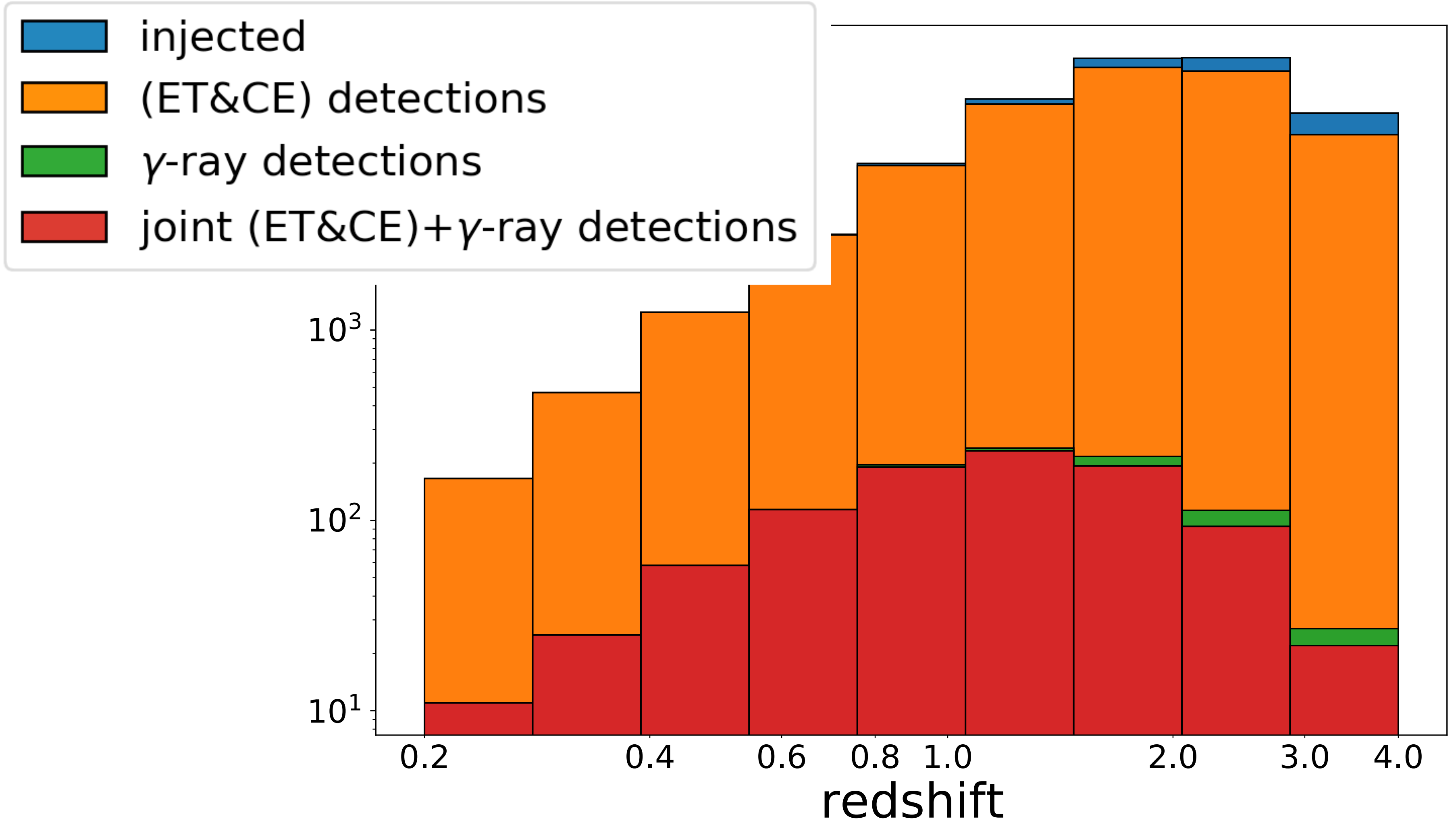

Joint detection of γ-ray emission and GWs

INSTRUMENT	band MeV	$F_{\rm lim}$ erg cm^{-2} s^{-1}	FOV/4π	loc. acc.	Joint ET +γ-ray	N_{JD}/N_γ	Joint (ET+CE) +γ-ray	N_{JD}/N_γ
Fermi-GBM	0.01 - 25	0.5(*)	0.75	5 deg (^{a})	33^{+14}_{-11}	$68^{+13}_{-18}\%$	47^{+14}_{-14}	$95^{+5}_{-7}\%$
Swift-BAT	0.015 - 0.15	2×10^{-8}	0.11	1-3 arcmin	10^{+3}_{-3}	$62^{+11}_{-14}\%$	13^{+5}_{-4}	$94^{+6}_{-7}\%$
SVOM-ECLAIRs	0.004 - 0.250	1.792(*)	0.16	< 10 arcmin	3^{+1}_{-1}	$69^{+10}_{-9}\%$	4^{+1}_{-1}	$95^{+5}_{-4}\%$
SVOM-GRM	0.03 - 5	0.23(*)	0.16	~ 5 deg	9^{+4}_{-3}	$59^{+6}_{-6}\%$	14^{+6}_{-4}	$92^{+3}_{-3}\%$
THESEUS-XGIS	0.002 - 10	3×10^{-8}	0.16	< 15 arcmin	10^{+5}_{-4}	$63^{+13}_{-13}\%$	15^{+6}_{-4}	$94^{+6}_{-7}\%$
HERMES	0.05 - 0.3	0.2(*)	1.0	1 deg	84^{+42}_{-30}	$61^{+10}_{-11}\%$	139^{+54}_{-36}	$94^{+6}_{-6}\%$
TAP-GTM	0.01 - 1	1(*)	1.0	20 deg	60^{+24}_{-24}	$67^{+13}_{-14}\%$	84^{+30}_{-24}	$95^{+5}_{-6}\%$

Fermi GBM+ET

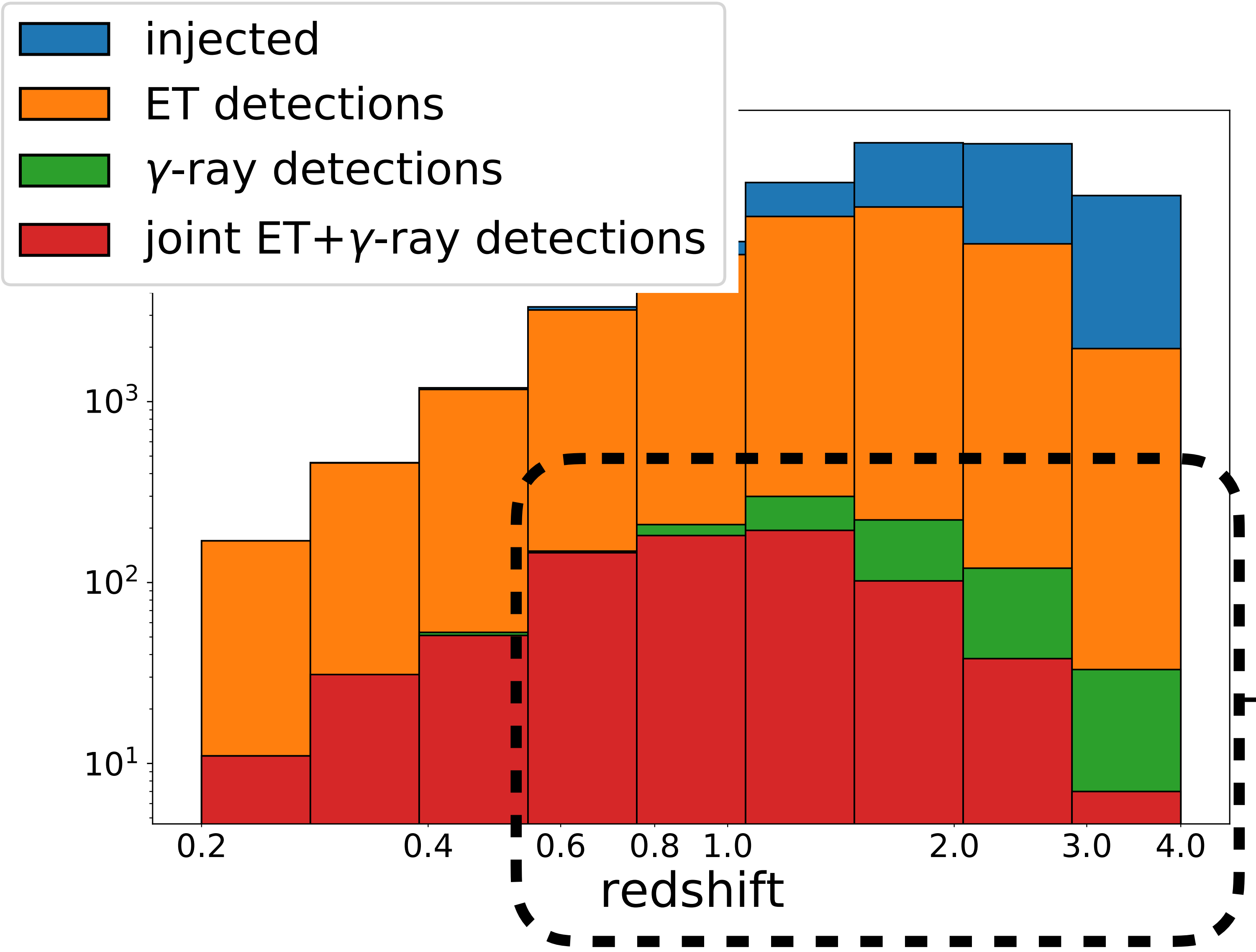

High-z GW counterparts can be detected **only** at high-energy (kilonova intrinsically fainter)

Fermi GBM+(ET&CE)

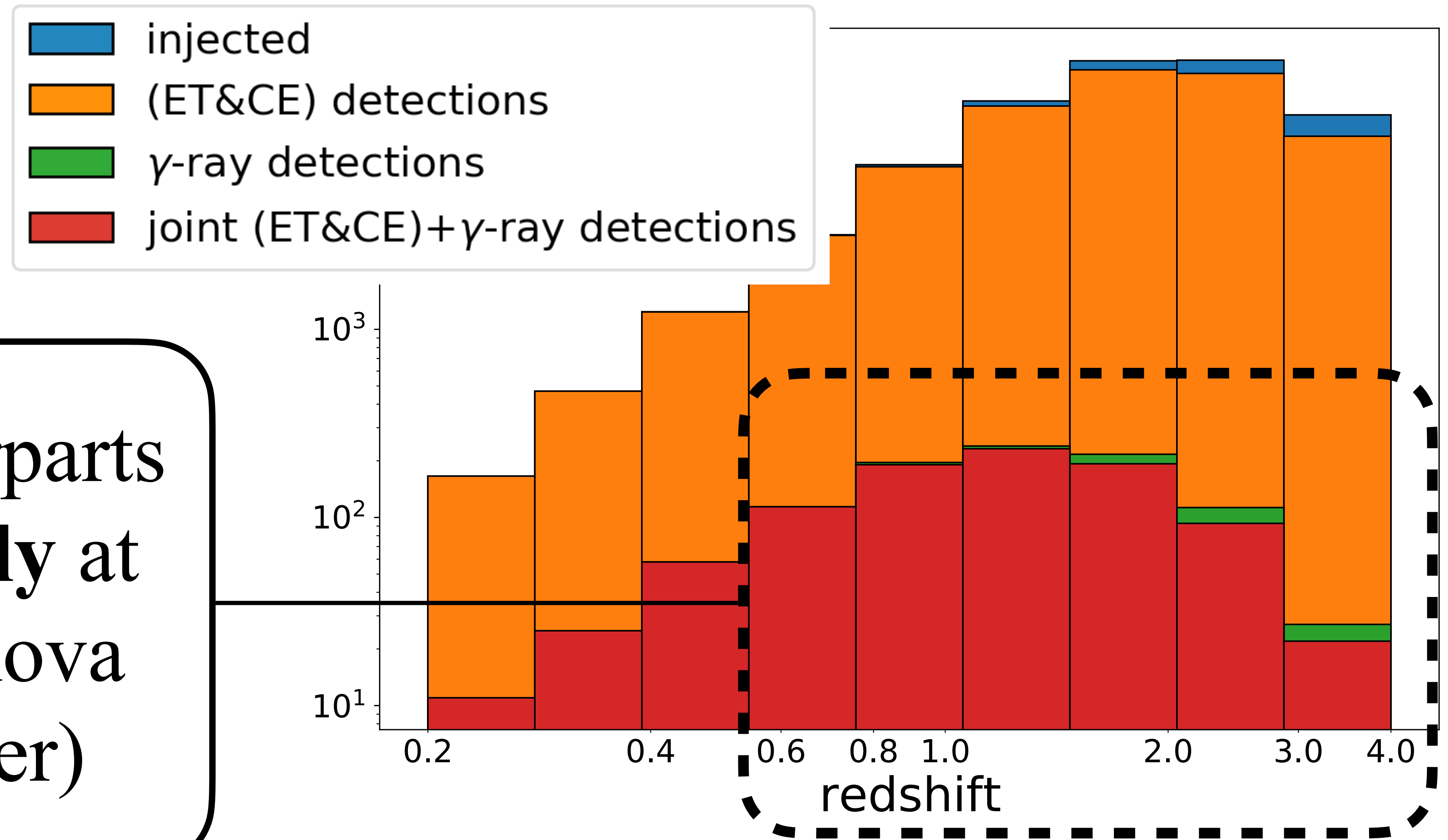

Joint detection of γ-ray emission and GWs

INSTRUMENT	band MeV	$F_{\rm lim}$ erg cm^{-2} s^{-1}	FOV/4π	loc. acc.	Joint ET +γ-ray	N_{JD}/N_γ	Joint (ET+CE) +γ-ray	N_{JD}/N_γ
Fermi-GBM	0.01 - 25	0.5(*)	0.75	5 deg (^{a})	33^{+14}_{-11}	$68^{+13}_{-18}\%$	47^{+14}_{-14}	$95^{+5}_{-7}\%$
Swift-BAT	0.015 - 0.15	2×10^{-8}	0.11	1-3 arcmin	10^{+3}_{-3}	$62^{+11}_{-14}\%$	13^{+5}_{-4}	$94^{+6}_{-7}\%$
SVOM-ECLAIRs	0.004 - 0.250	1.792(*)	0.16	< 10 arcmin	3^{+1}_{-1}	$69^{+10}_{-9}\%$	4^{+1}_{-1}	$95^{+5}_{-4}\%$
SVOM-GRM	0.03 - 5	0.23(*)	0.16	$\sim$ 5 deg	9^{+4}_{-3}	$59^{+6}_{-6}\%$	14^{+6}_{-4}	$92^{+3}_{-3}\%$
THESEUS-XGIS	0.002 - 10	3×10^{-8}	0.16	< 15 arcmin	10^{+5}_{-4}	$63^{+13}_{-13}\%$	15^{+6}_{-4}	$94^{+6}_{-7}\%$
HERMES	0.05 - 0.3	0.2(*)	1.0	1 deg	84^{+42}_{-30}	$61^{+10}_{-11}\%$	139^{+54}_{-36}	$94^{+6}_{-6}\%$
TAP-GTM	0.01 - 1	1(*)	1.0	20 deg	60^{+24}_{-24}	$67^{+13}_{-14}\%$	84^{+30}_{-24}	$95^{+5}_{-6}\%$

Few but **well localised** events

Fermi GBM+ET

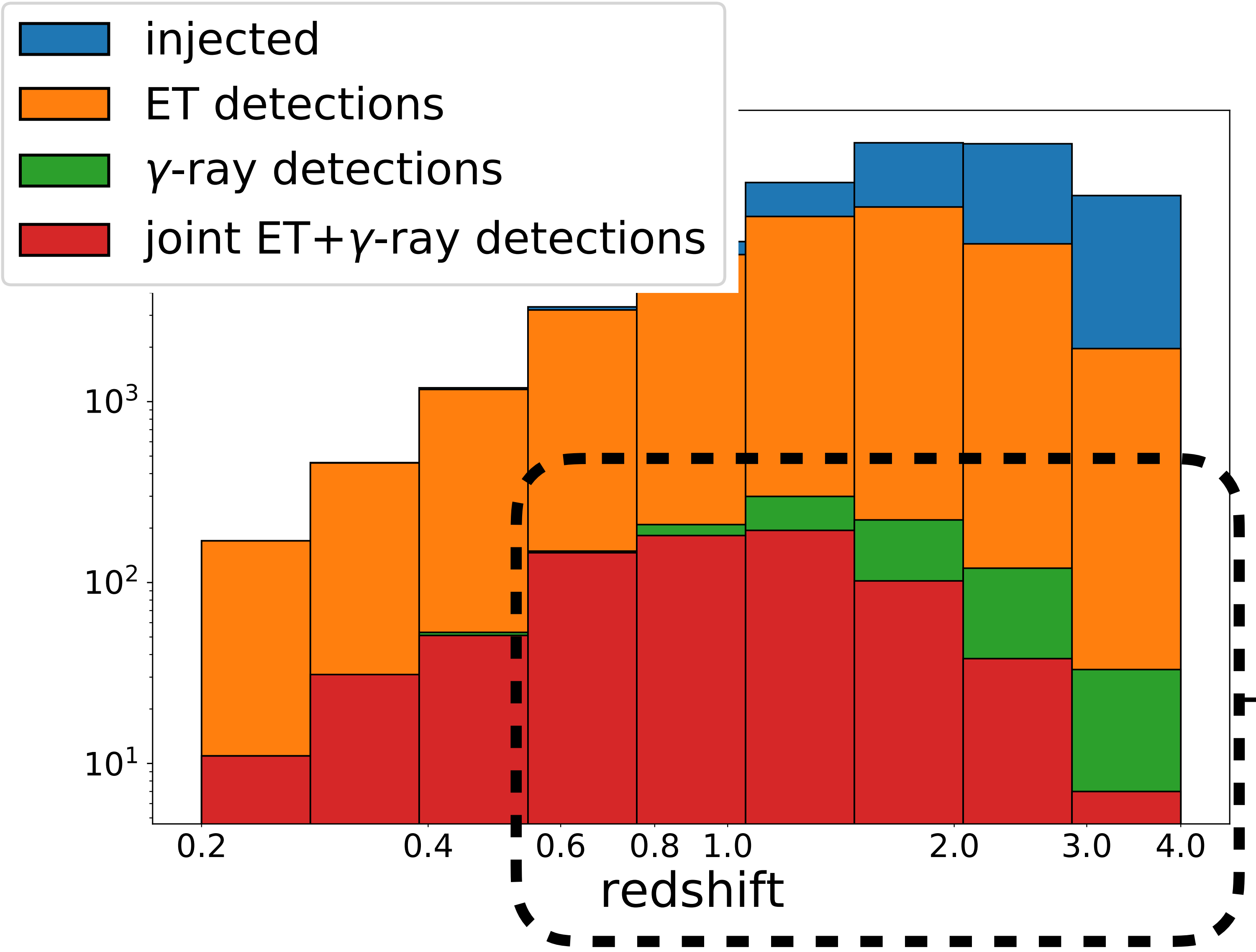

High-z GW counterparts can be detected **only** at high-energy (kilonova intrinsically fainter)

Fermi GBM+(ET&CE)

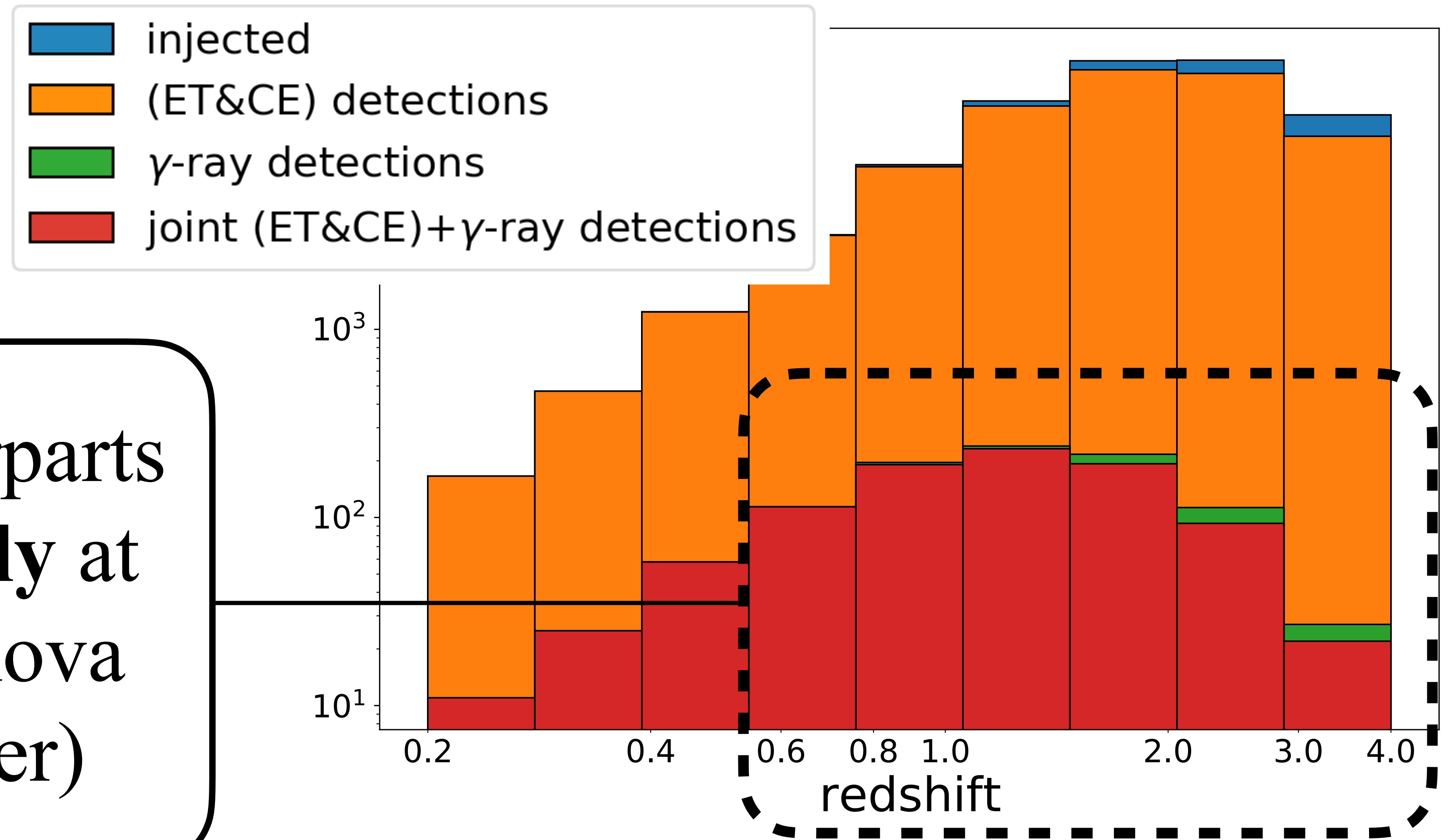

Two kinds of joint detections

Fermi-like telescopes

- ~ **all sky** monitors
- Possibility to build constellations at fairly low cost
- **Best sensitivity** around the sGRB **peak energy**
- ~ deg location accuracy

PROS

- Confirm the spatial and temporal coincidence with the GW
- Characterise the spectral shape up to high energies
- High number of joint detections ⇒ **statistical studies**

Swift-like telescopes

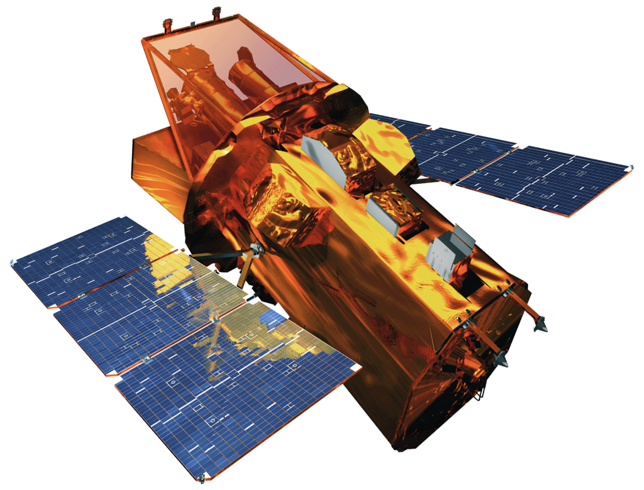

- Good sky coverage
- **Arcmin location accuracy**
- Possibility to promptly follow up with ground-based telescopes

PROS

- Identification of the host galaxy
- Determination of the redshift
- Detection of X-ray counterparts (standard GRB afterglow, jet-KN ejecta interaction, SBO, wind from magnetar…)
- Less number of events but with **deeper understanding of the GRB physics**

GW sky localisation

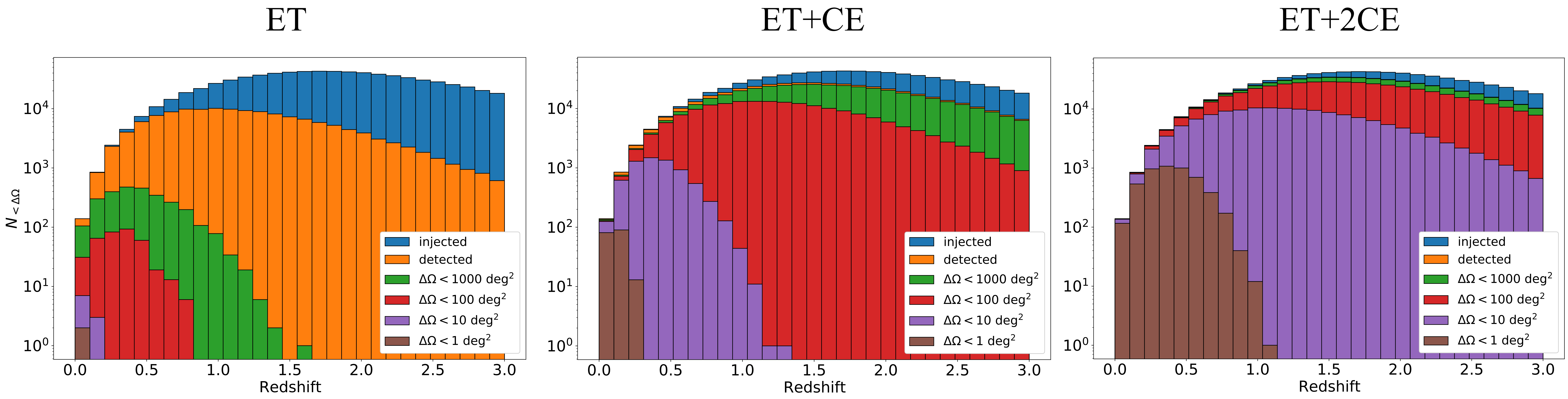

	ET	ET+CE	ET+2CE
$N_{\rm det}$	143970	458801	592565
$N_{\rm det}(\Delta\Omega < 1\ {\rm deg}^2)$	2	184	5009
$N_{\rm det}(\Delta\Omega < 10\ {\rm deg}^2)$	10	6797	154167
$N_{\rm det}(\Delta\Omega < 100\ {\rm deg}^2)$	370	192468	493819
$N_{\rm det}(\Delta\Omega < 1000\ {\rm deg}^2)$	2791	428484	585317

From Ronchini et al. 2022

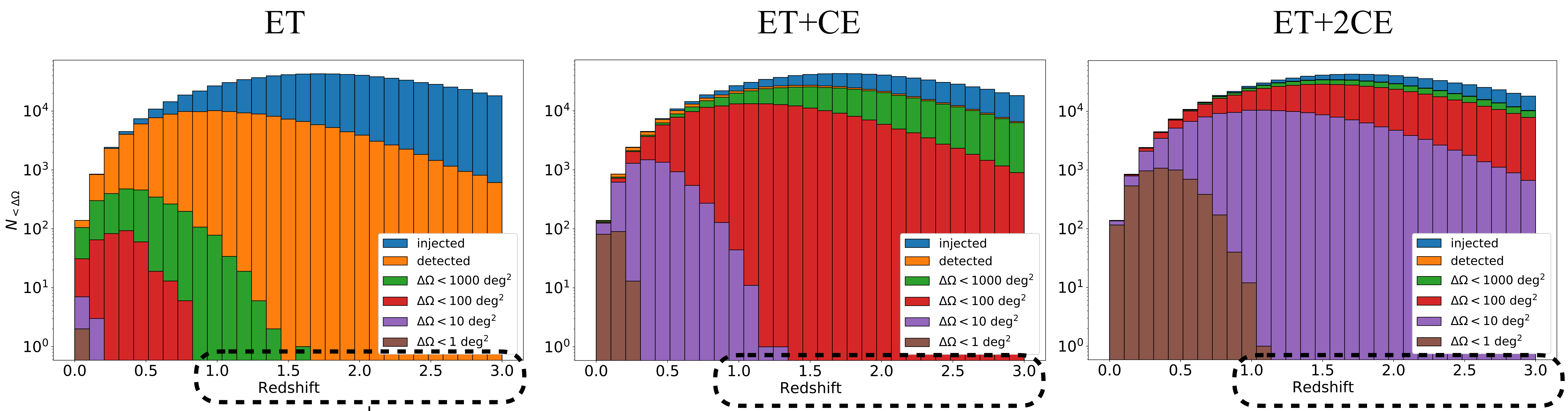

	ET	ET+CE	ET+2CE
N_{det}	143970	458801	592565
$N_{\mathrm{det}}(\Delta\Omega < 1\ \mathrm{deg}^2)$	2	184	5009
$N_{\mathrm{det}}(\Delta\Omega < 10\ \mathrm{deg}^2)$	10	6797	154167
$N_{\mathrm{det}}(\Delta\Omega < 100\ \mathrm{deg}^2)$	370	192468	493819
$N_{\mathrm{det}}(\Delta\Omega < 1000\ \mathrm{deg}^2)$	2791	428484	585317

High-z GW source localisation is given by counterparts detected by **wide field X-ray and γ-ray telescopes** with arcmin localisation capabilities

From Ronchini et al. 2022

Detectability of the afterglow emission: survey vs pointing

How to detect X-ray emission:

1. In **survey mode**: probability ~FOV/4π of detecting by chance the source
2. In **pointing mode**: selection of the sources with $\Delta\Omega$ < 100 deg^2

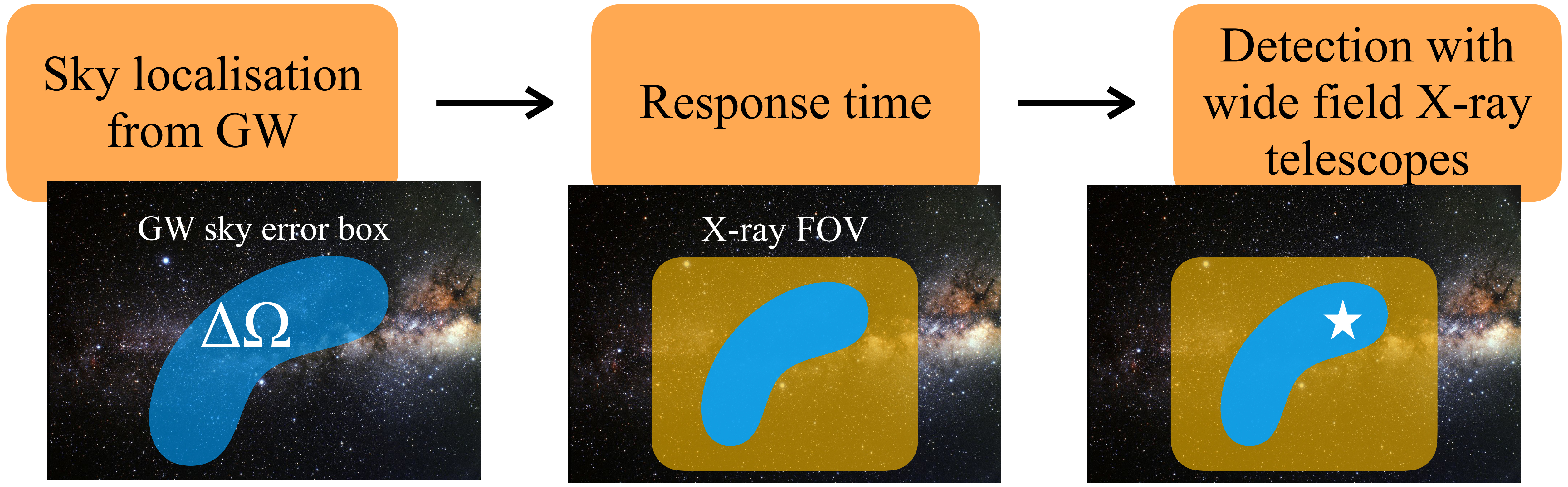

	THESEUS-SXI	TAP	Einstein Probe	Gamow
Energy band	0.3-5 keV	0.3-5 keV	0.5-4 keV	0.3-5 keV
Field of view	0.5 sr	0.4 sr	1.1 sr	0.4 sr

Number of BNS mergers / yr detected in GWs and X-rays

Survey mode

	ET	ET+2CE
EP	50^{+15}_{-16}	64^{+12}_{-20}
Gamow	9^{+2}_{-2}	10^{+3}_{-3}
THESEUS-SXI	11^{+3}_{-3}	13^{+4}_{-3}
THESEUS-(SXI+XGIS)	23^{+6}_{-5}	27^{+7}_{-5}
TAP-WFI	16^{+3}_{-4}	17^{+6}_{-3}

Pointing mode

	ET	ET+CE	ET+2CE
EP	9^{+5}_{-3}	294^{+80}_{-59}	359^{+168}_{-110}
THESEUS-SXI/ *Gamow*	7^{+5}_{-3}	95^{+43}_{-14}	122^{+41}_{-23}
TAP-WFI	8^{+5}_{-3}	182^{+43}_{-31}	225^{+76}_{-72}

For 2-3 GW detectors active, pointing better than survey, but…

Caveats about the pointing strategy

	ET	ET+CE	ET+2CE
EP	9^{+5}_{-3}	294^{+80}_{-59}	359^{+168}_{-110}
THESEUS-SXI/ *Gamow*	7^{+5}_{-3}	95^{+43}_{-14}	122^{+41}_{-23}
TAP-WFI	8^{+5}_{-3}	182^{+43}_{-31}	225^{+76}_{-72}

	100 s	1 hr	4 hr
Einstein Probe	359^{+168}_{-110}	48^{+24}_{-15}	17^{+15}_{-10}
THESEUS-SXI/ *Gamow*	122^{+41}_{-23}	12 ± 7	< 9
TAP-WFI	225^{+76}_{-72}	50^{+20}_{-10}	17^{+10}_{-5}

A **rapid response** is necessary to catch the brighter phase of the afterglow

Following-up all the sources with $\Delta\Omega < 100$ deg^2 is **unfeasible**

Other GW parameters should be exploited to restrict the selection:

- **SNR**
- **Viewing angle** and relative error
- **Luminosity distance** and relative error

Pre-merger sky localisation

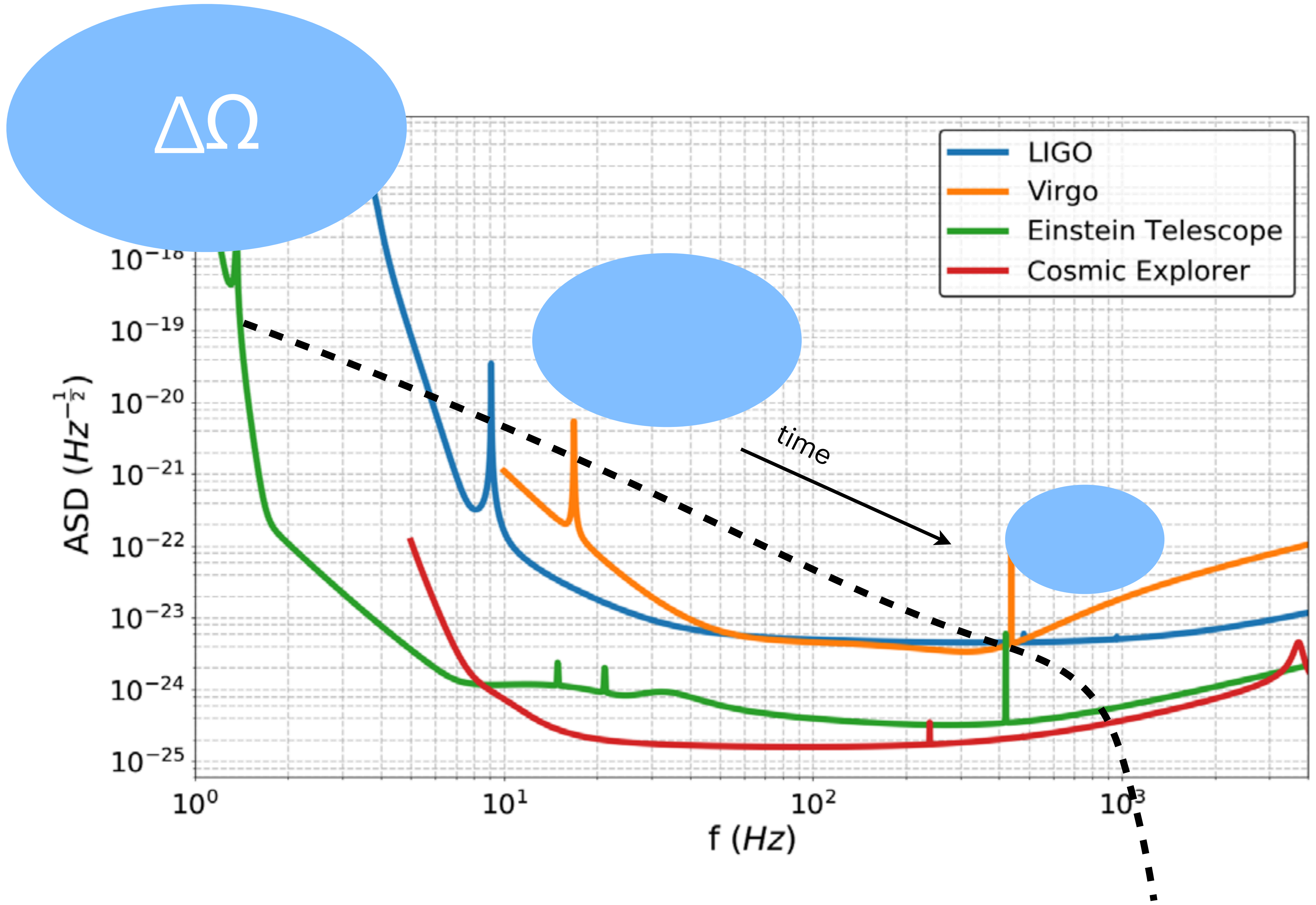

For some golden cases, enough SNR can be accumulated already **before the merger**

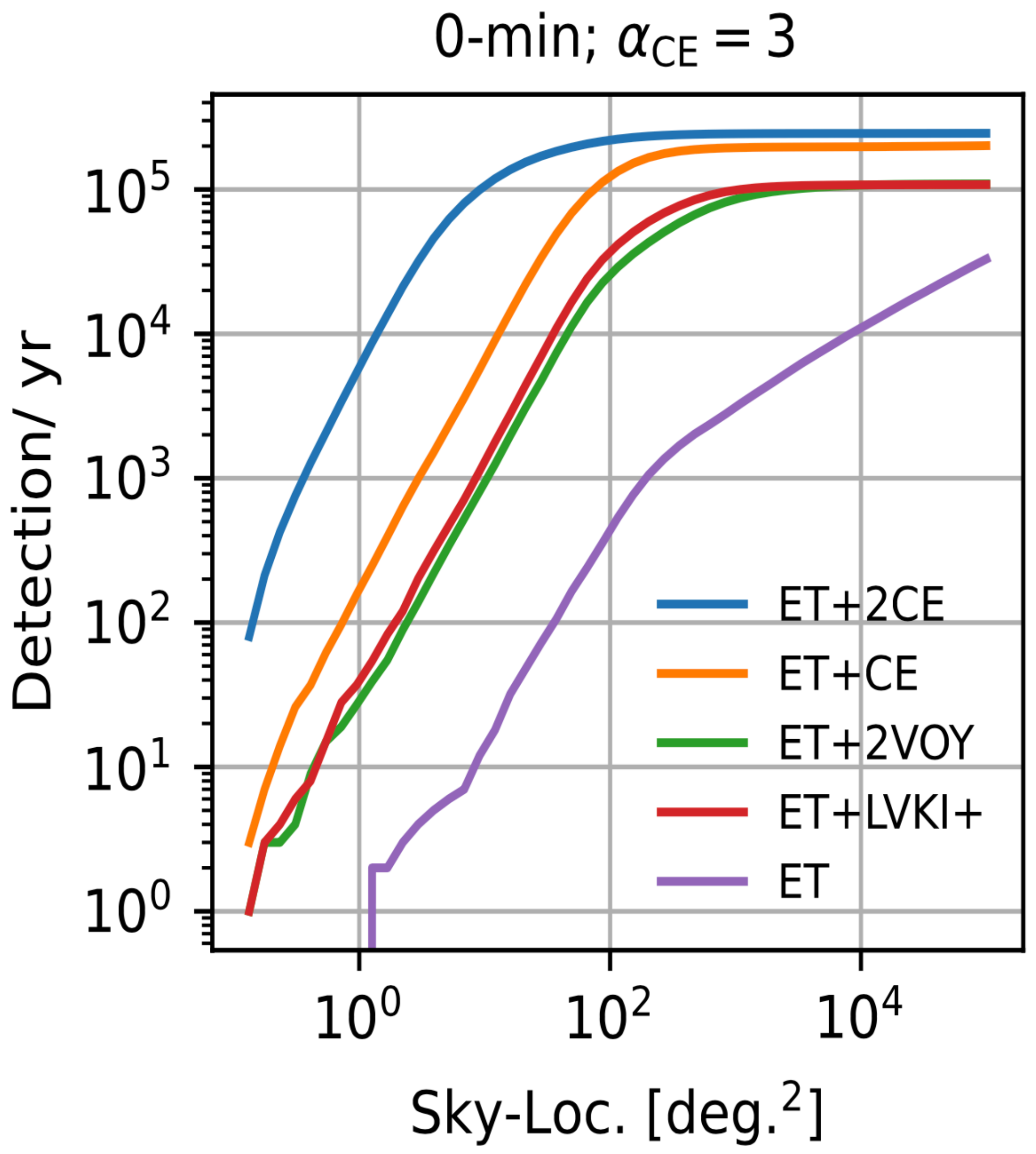

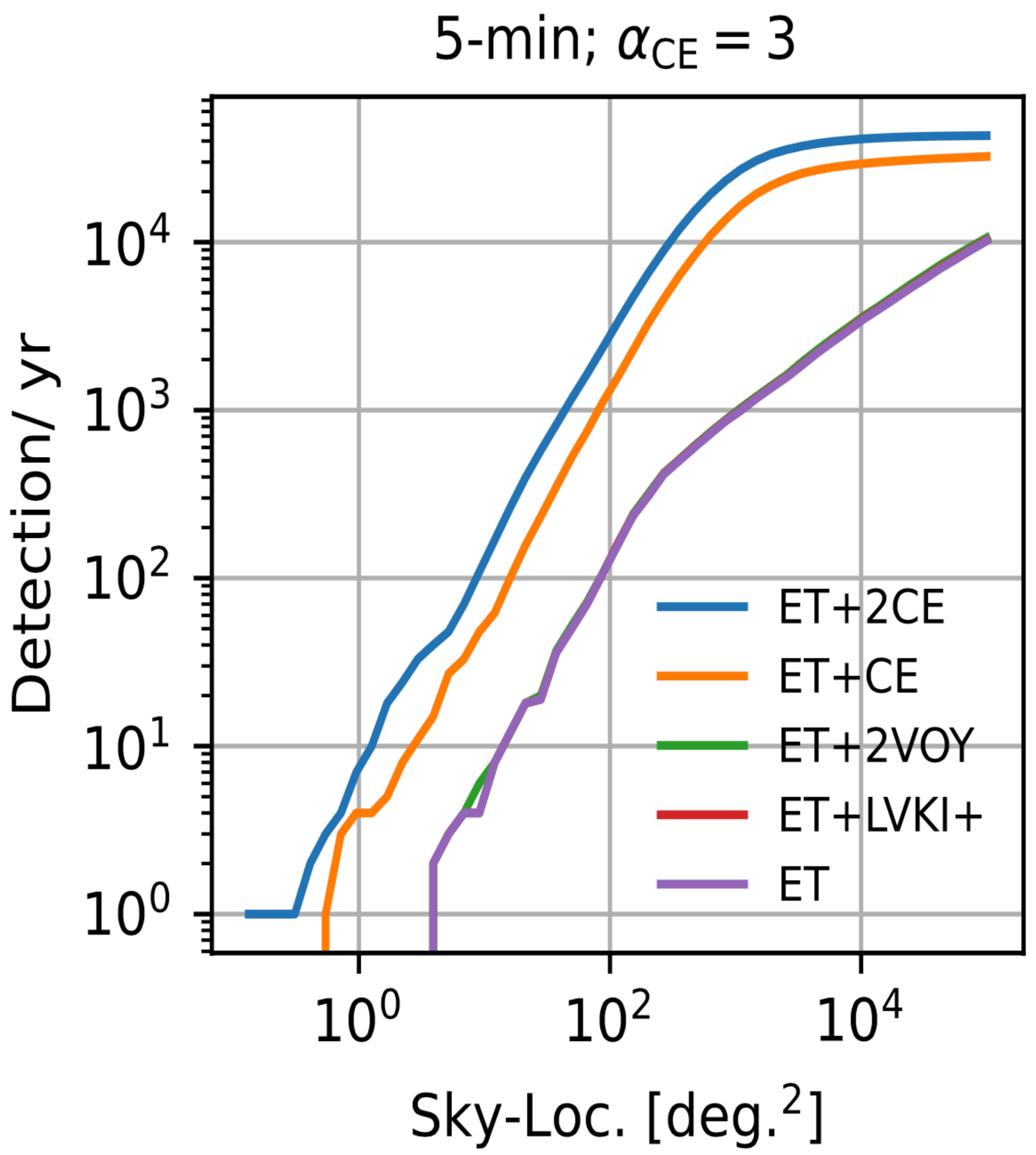

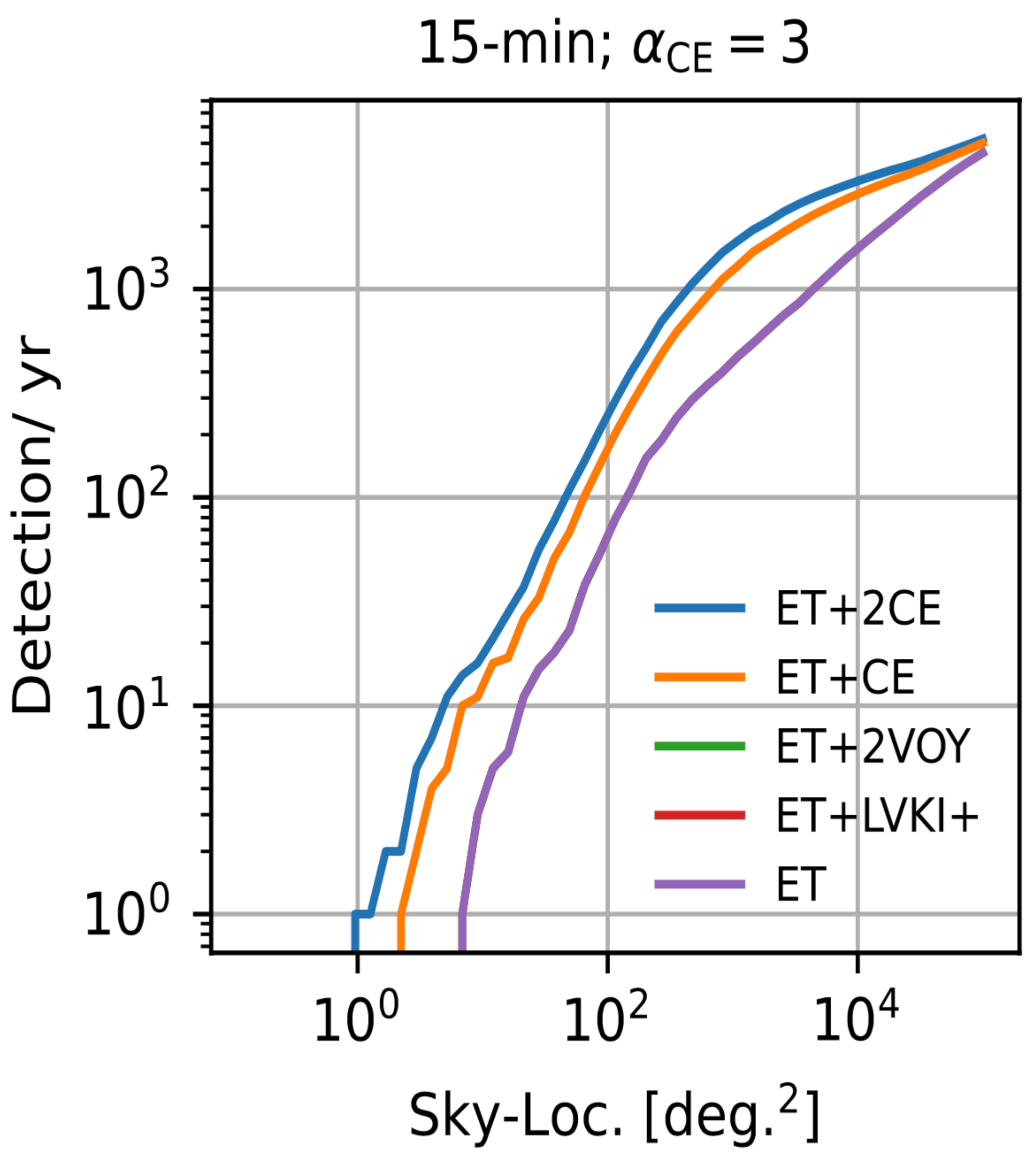

ET+2CE	$N_{det}(\Delta\Omega<100\ deg^2)$
t_m	$\sim 10^5$
t_m-5 min	$\sim 10^3$
t_m-15 min	$\sim 10^2$

From Banerjee et al. 2023 (under review)

The importance of WFX-ray telescopes

Joint γ-ray+GW
detection efficiency (ET+Fermi-GBM)

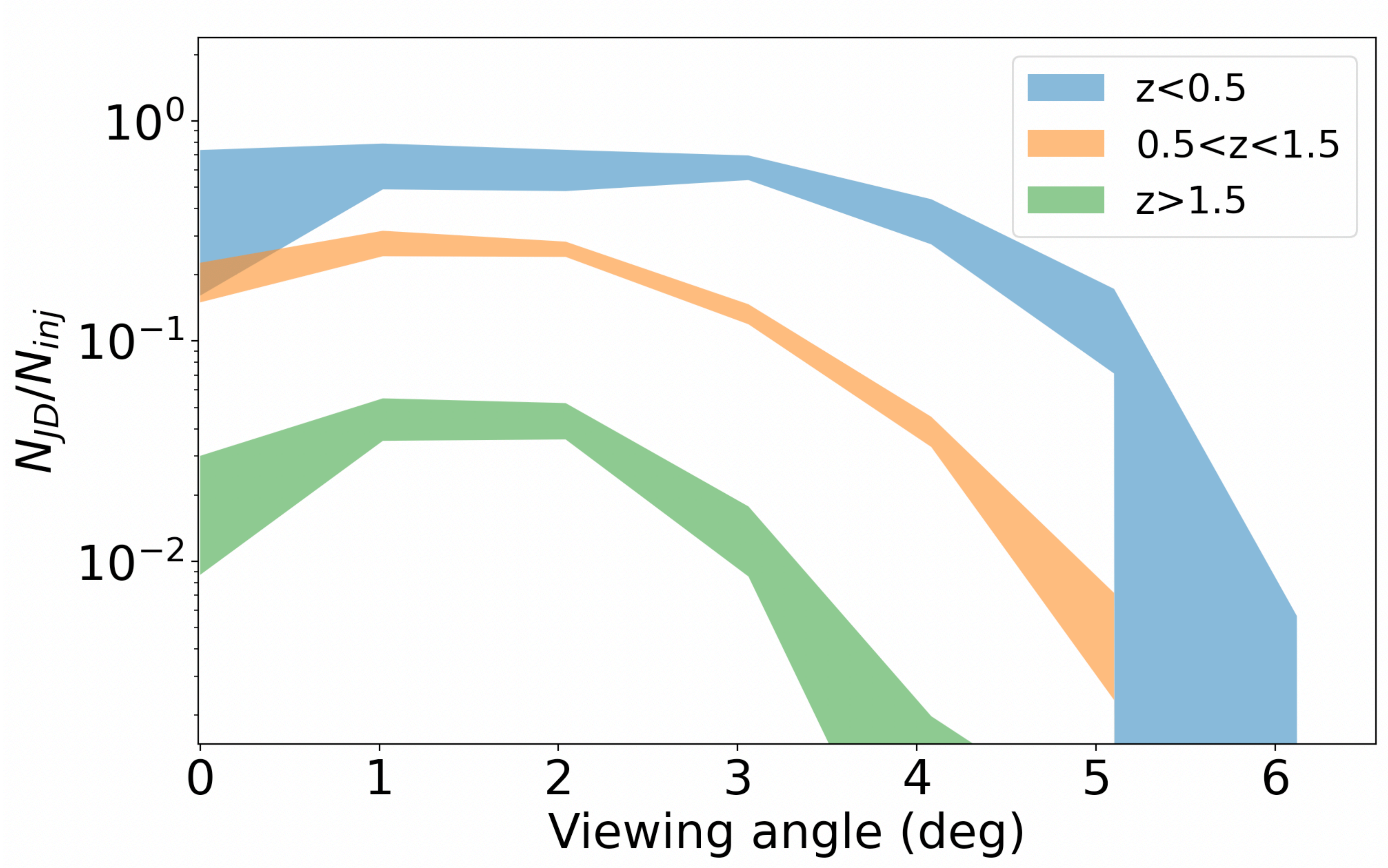

From Ronchini et al. 2022

Redshift distribution of
joint X-ray+GW detections, in pointing mode

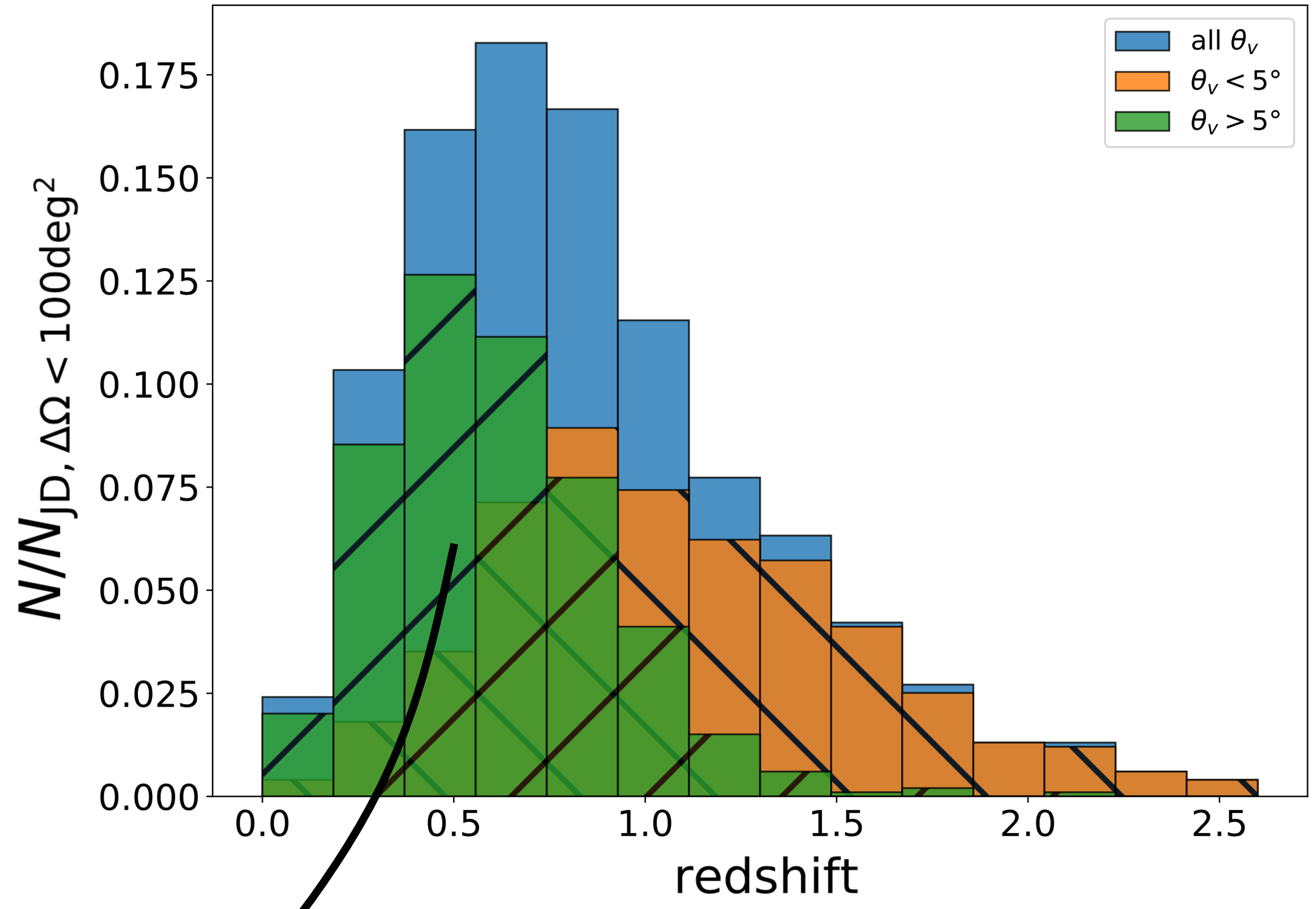

Too off-axis to have a detectable γ-ray emission

WFX-ray telescopes can significantly **enhance the probability of a joint detection**

Assessment of the science case for different the ET design

Delta: 10 km or 15 km

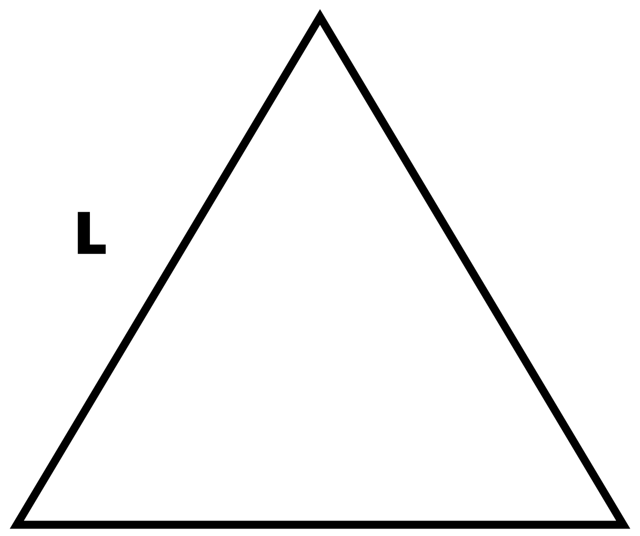

Sardinia

2L misaligned: 15 km or 20 km

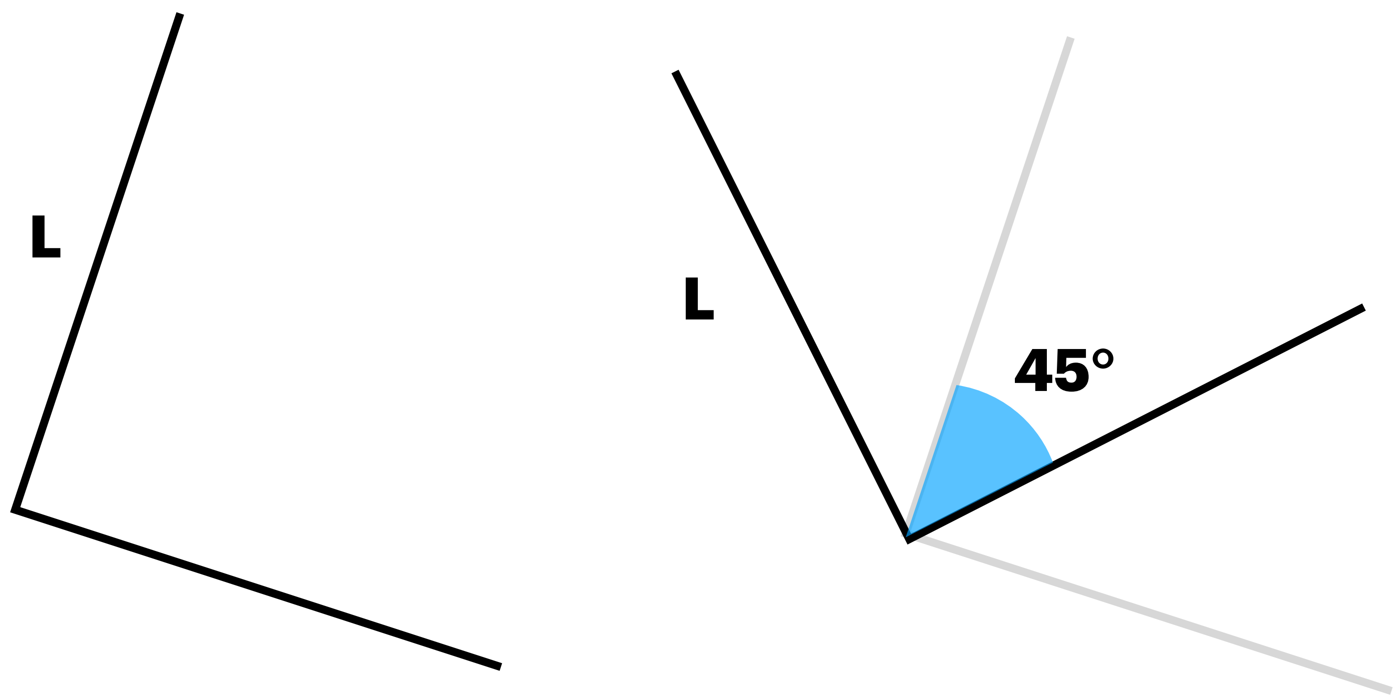

Sardinia

Meuse-Rhine

GOAL: Detailed comparison of the scientific return of the ET with several proposed designs

- CBMs
- Multi-messenger
- Stochastic background
- Nuclear physics
- GR tests
- Population studies
- Cosmology

Branchesi et al. 2023 (under review)

Assessment of the science case for different the ET design

Joint GW + prompt emission

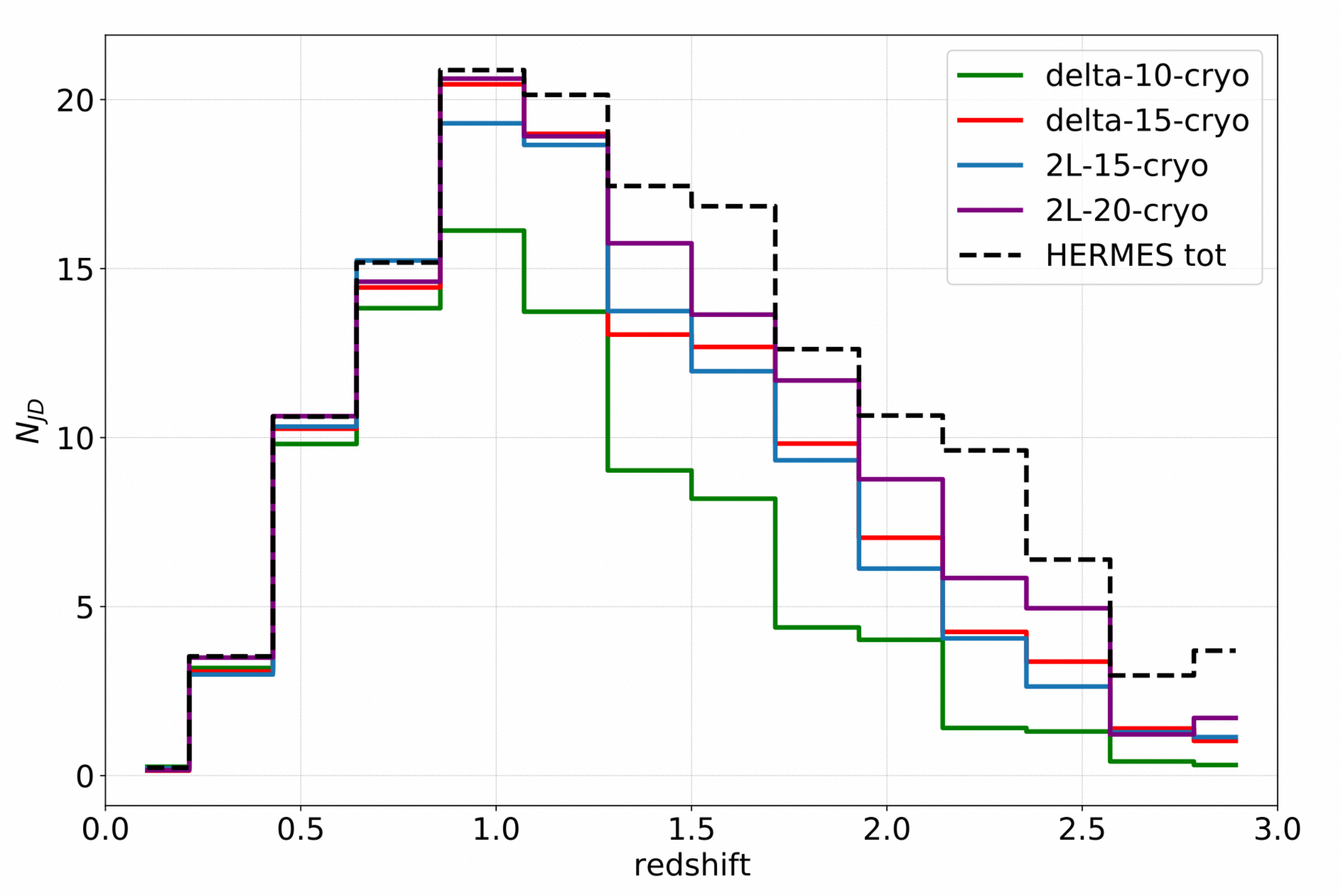

Assessment of the science case for different the ET design

Joint GW + prompt emission

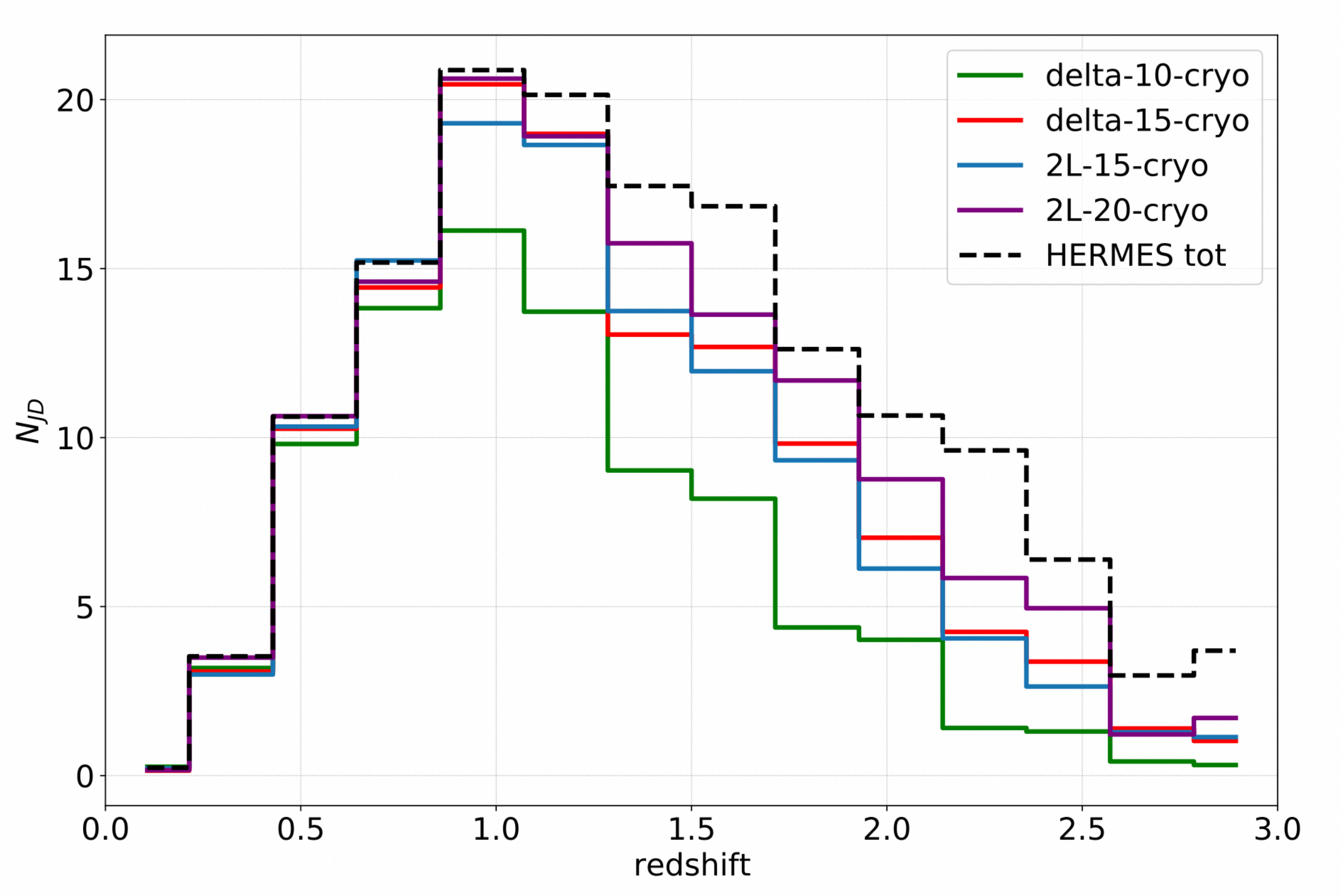

Joint GW + afterglow emission

Full (HFLF cryo) sensitivity detectors

Instrument	Δ10	Δ15	2L 15	2L 20
THESEUS-SXI survey	10^{+3}_{-2}	13^{+3}_{-4}	12^{+3}_{-3}	12^{+3}_{-3}
THESEUS-(SXI+XGIS) survey	21^{+6}_{-7}	21^{+8}_{-6}	20^{+7}_{-5}	21^{+7}_{-7}

Joint GW + prompt emission

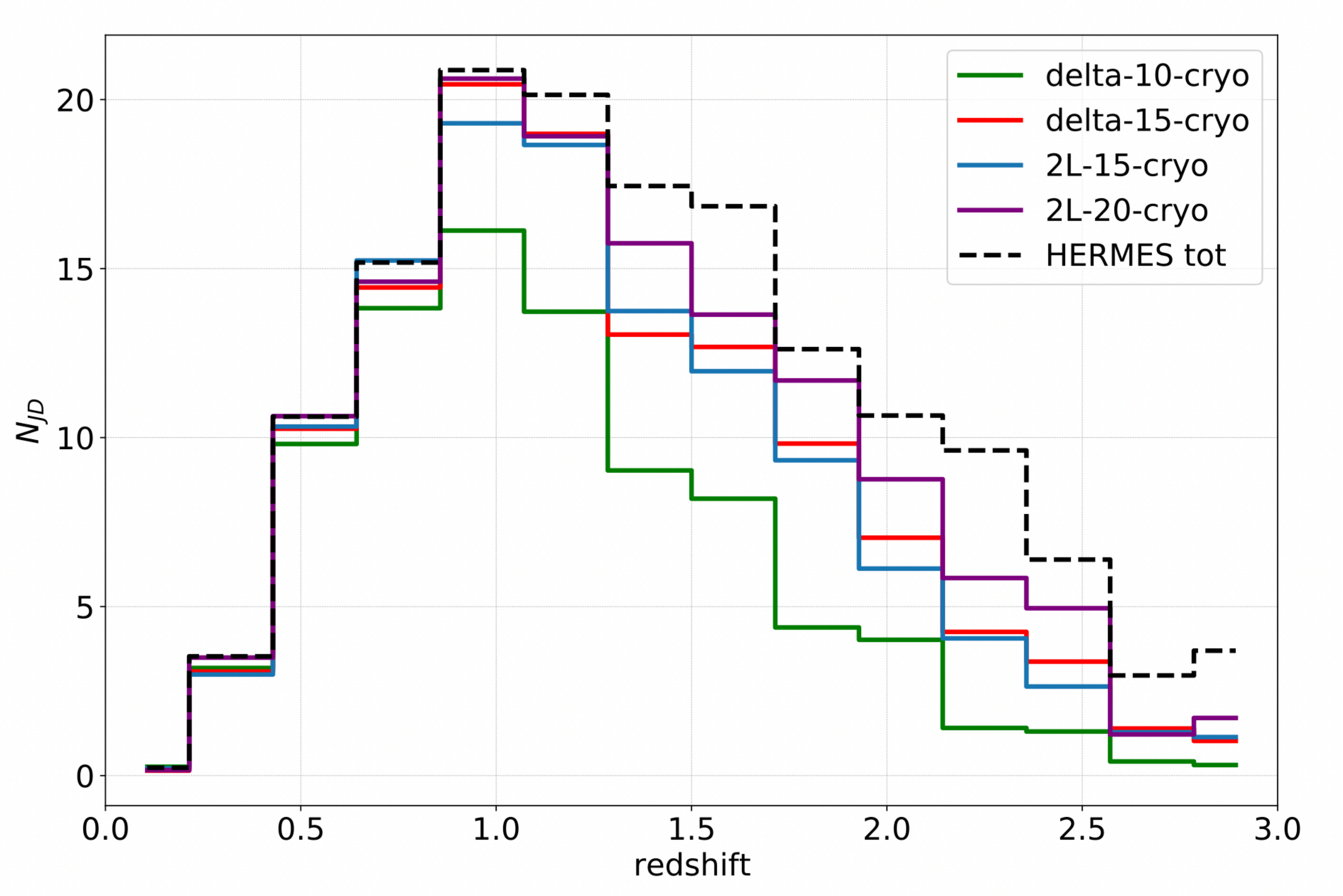

Sky localization

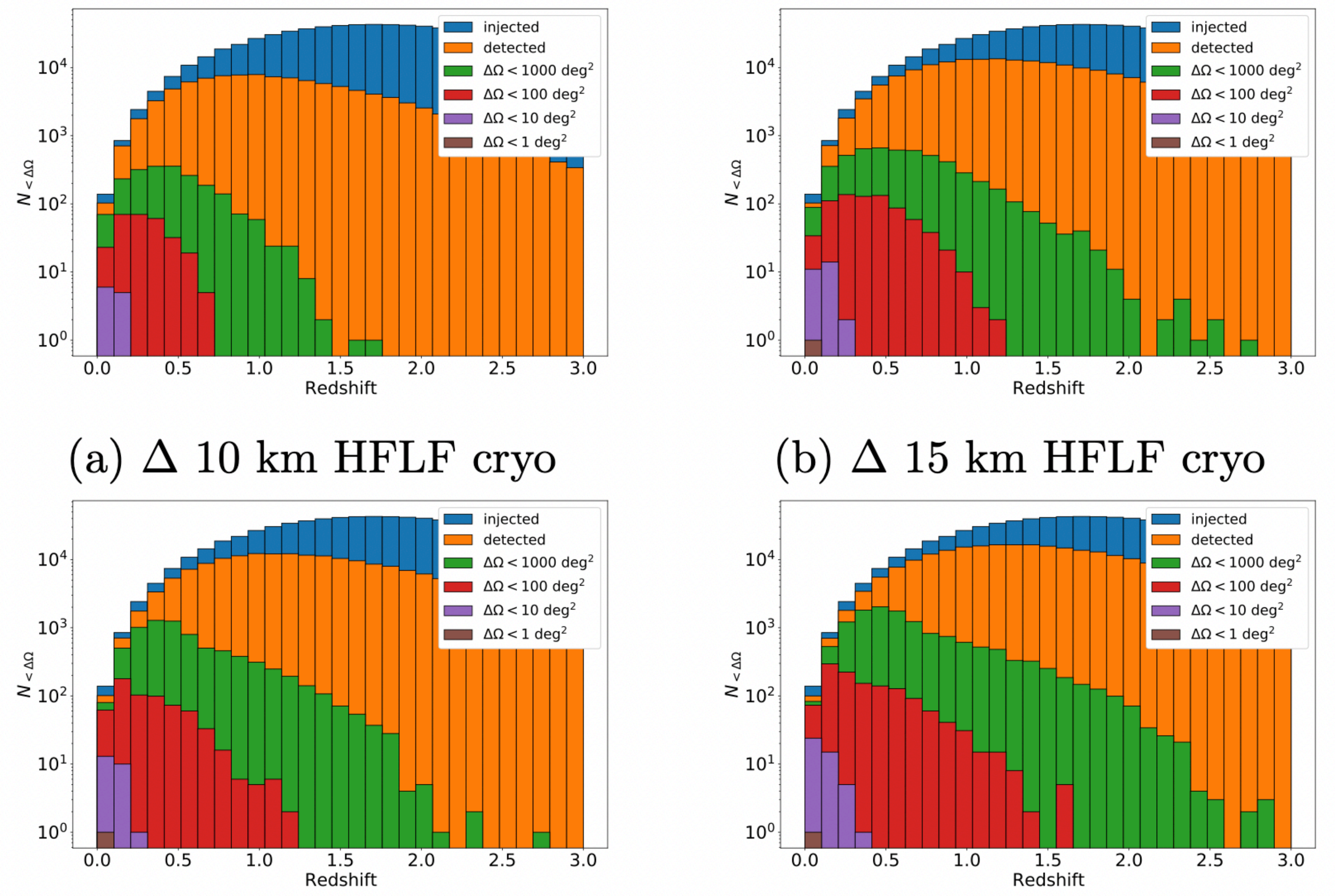

(a) Δ 10 km HFLF cryo
(b) Δ 15 km HFLF cryo
(d) 2L 15 km HFLF cryo
(e) 2L 20 km HFLF cryo

Joint GW + afterglow emission

Full (HFLF cryo) sensitivity detectors

Instrument	Δ10	Δ15	2L 15	2L 20
THESEUS-SXI survey	10^{+3}_{-2}	13^{+3}_{-4}	12^{+3}_{-3}	12^{+3}_{-3}
THESEUS-(SXI+XGIS) survey	21^{+6}_{-7}	21^{+8}_{-6}	20^{+7}_{-5}	21^{+7}_{-7}

Joint GW + prompt emission

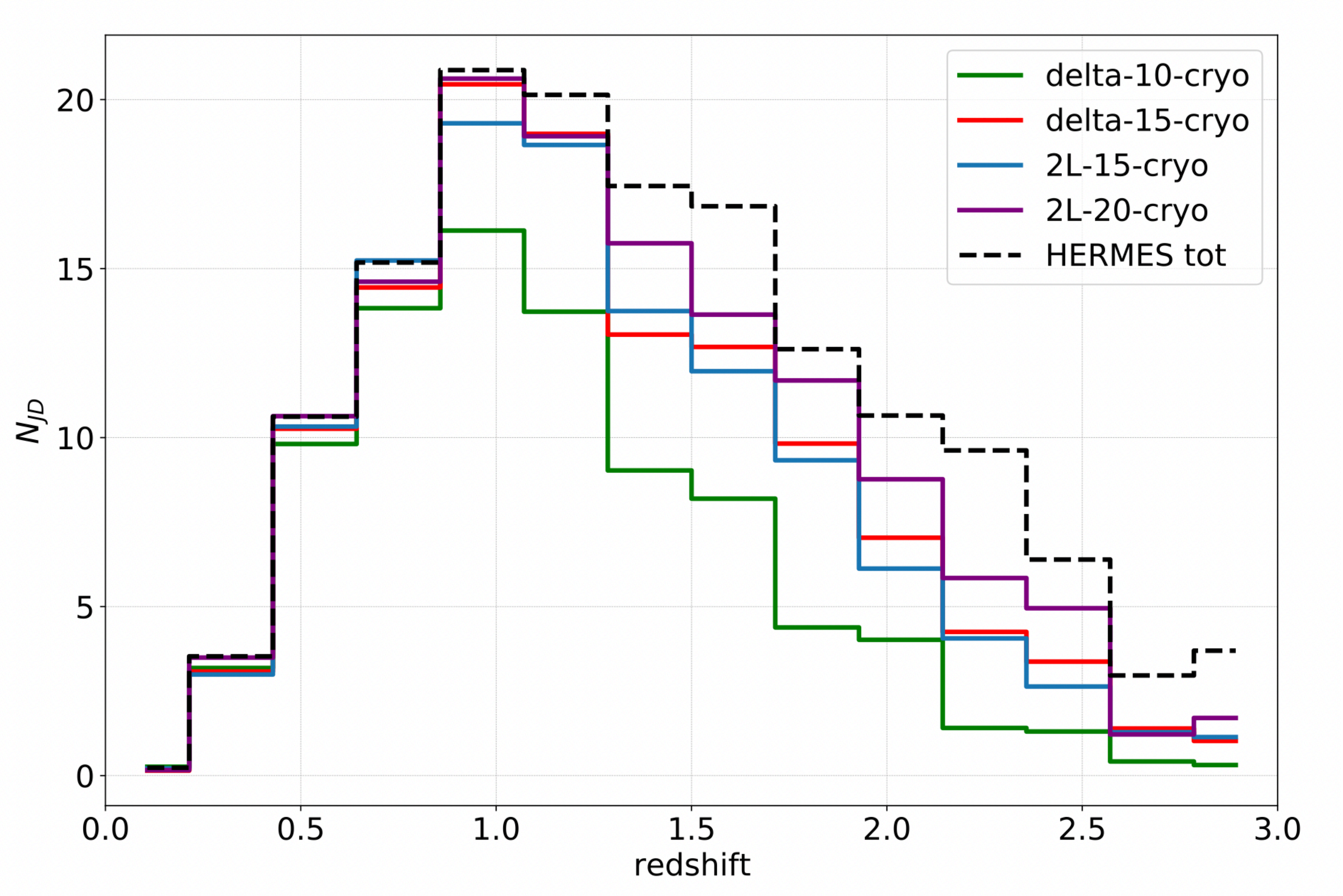

Sky localization

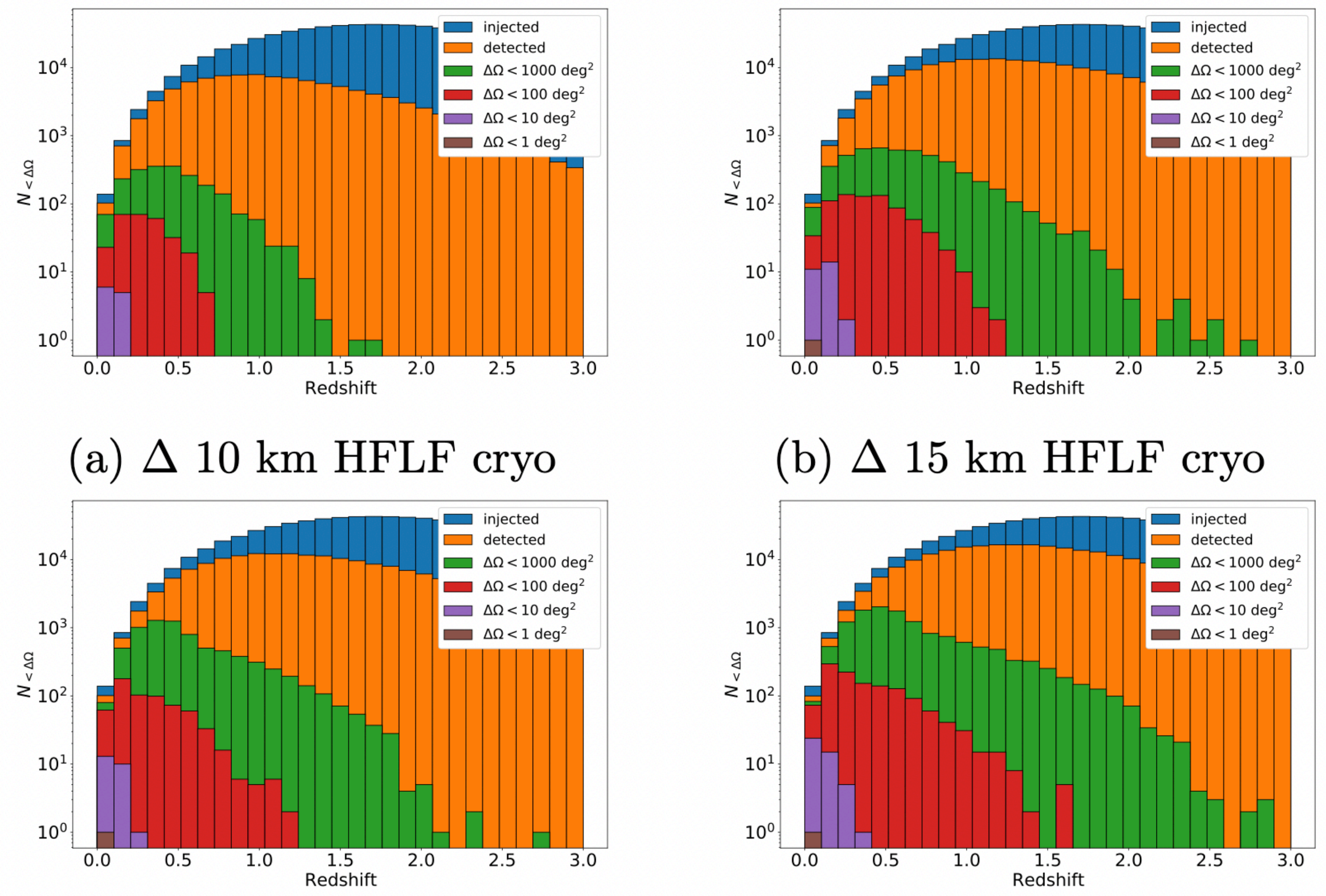

(a) Δ 10 km HFLF cryo (b) Δ 15 km HFLF cryo

(d) 2L 15 km HFLF cryo (e) 2L 20 km HFLF cryo

Joint GW + afterglow emission

Full (HFLF cryo) sensitivity detectors

Instrument	Δ10	Δ15	2L 15	2L 20
THESEUS-SXI survey	10^{+3}_{-2}	13^{+3}_{-4}	12^{+3}_{-3}	12^{+3}_{-3}
THESEUS-(SXI+XGIS) survey	21^{+6}_{-7}	21^{+8}_{-6}	20^{+7}_{-5}	21^{+7}_{-7}

Hubble constant

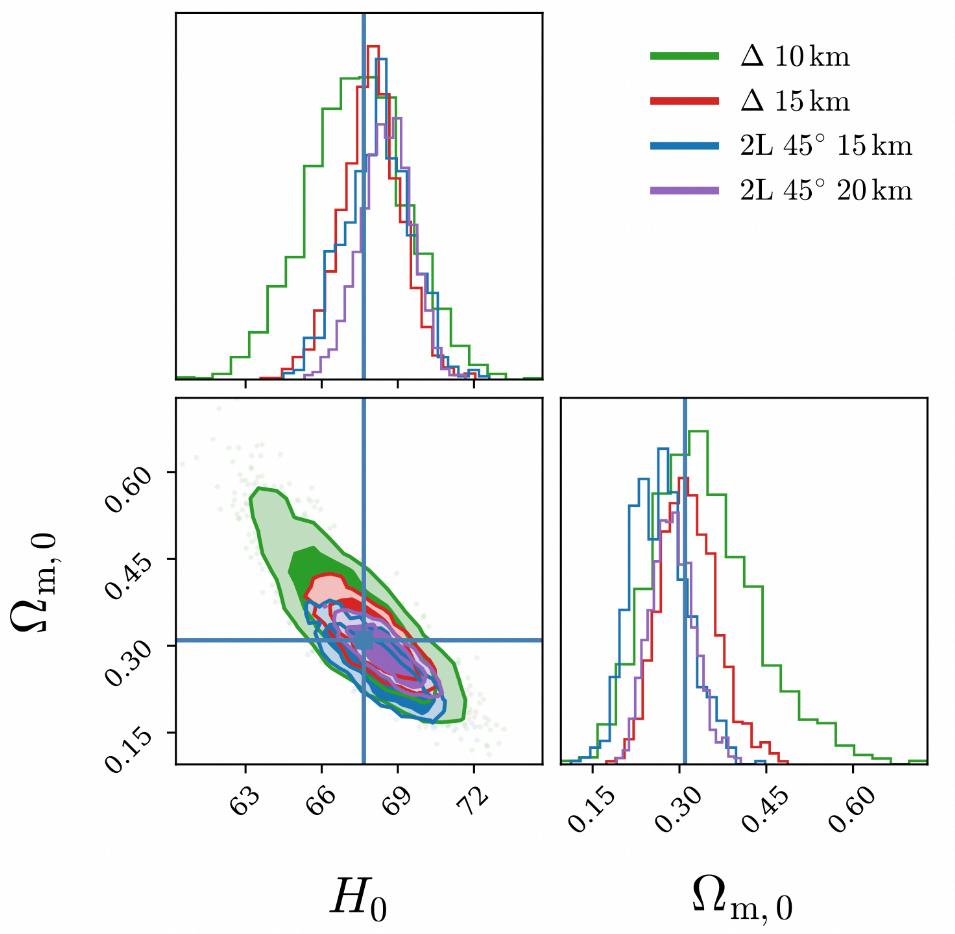

Dark energy EoS

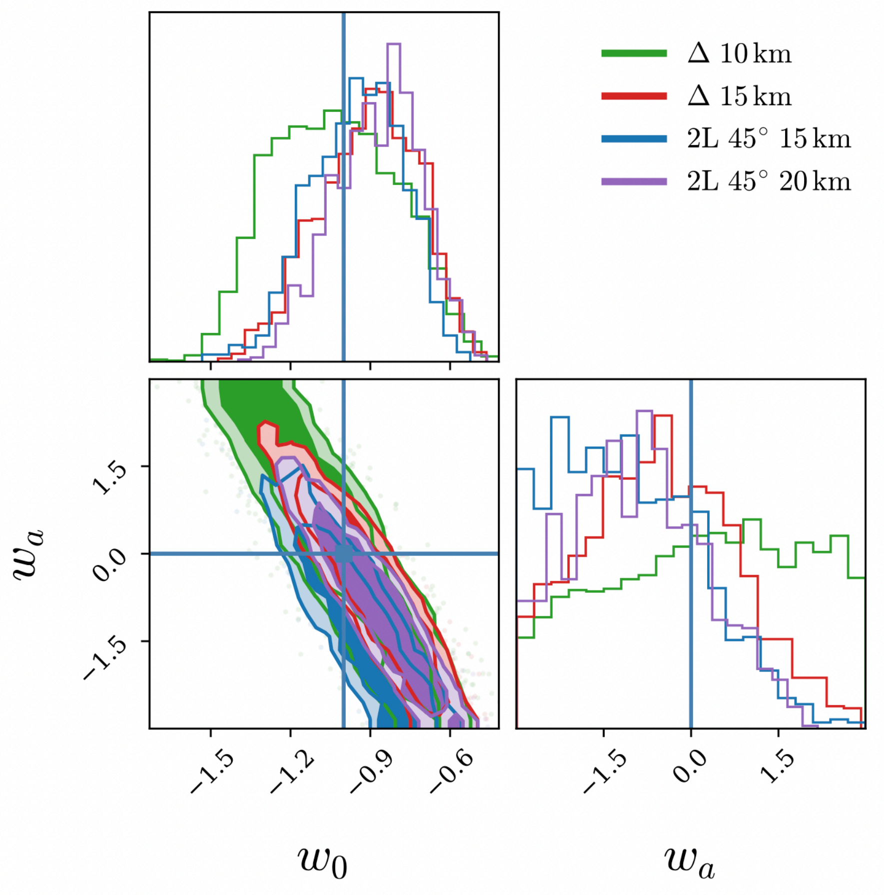

Modified GW propagation

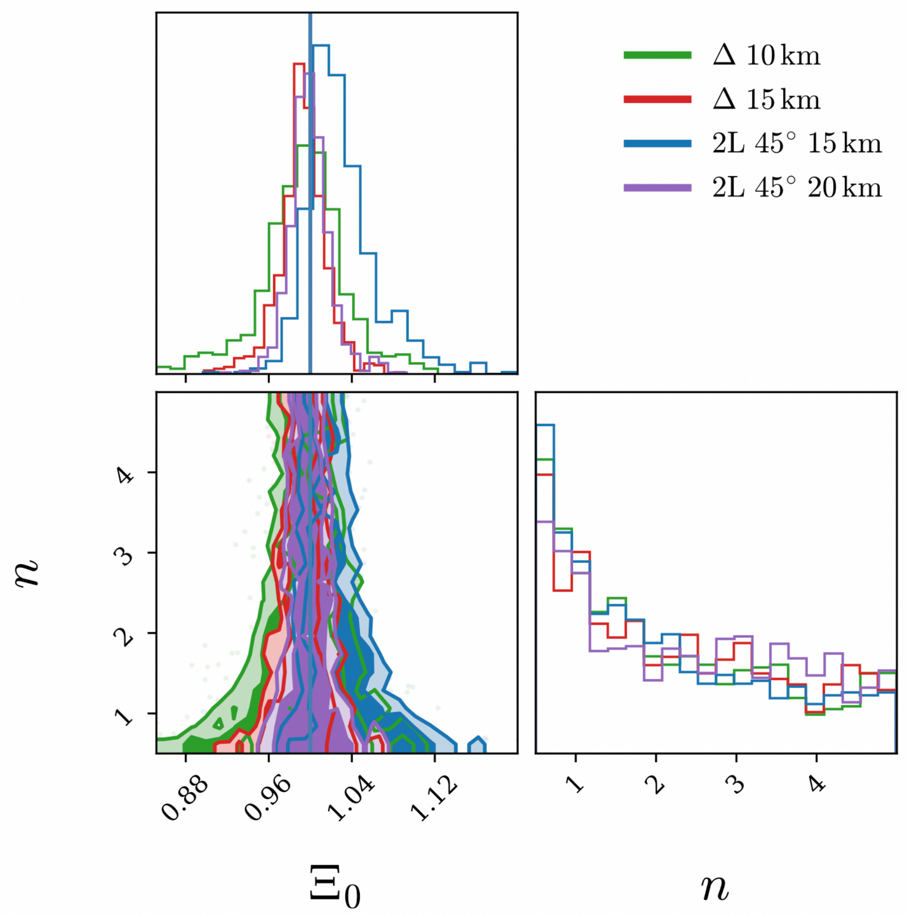

Assessment of the science case for different the ET design

Pre-merger sky localization

HF sensitivity detectors

Configuration	$\Delta\Omega_{90\%}$ [deg^2]	All orientation BNSs 30 min	10 min	1 min
Δ10km	100	0	0	0
	1000	0	0	4
	All detected	0	3	317

Full (HFLF cryo) sensitivity detectors

Configuration	$\Delta\Omega_{90\%}$ [deg^2]	All orientation BNSs 30 min	10 min	1 min
Δ10km	10	0	1	5
	100	10	39	113
	1000	85	293	819
	All detected	905	4343	23597

In terms of detection efficiency and precision in the parameter estimation:

$$\Delta\, 10\, km < \Delta\, 15\, km \sim 2L\, 15\, km < 2L\, 20\, km$$

The inclusion of **the low frequency has a deep impact** on the vast majority of the ET science cases

Horizon for equal mass mergers

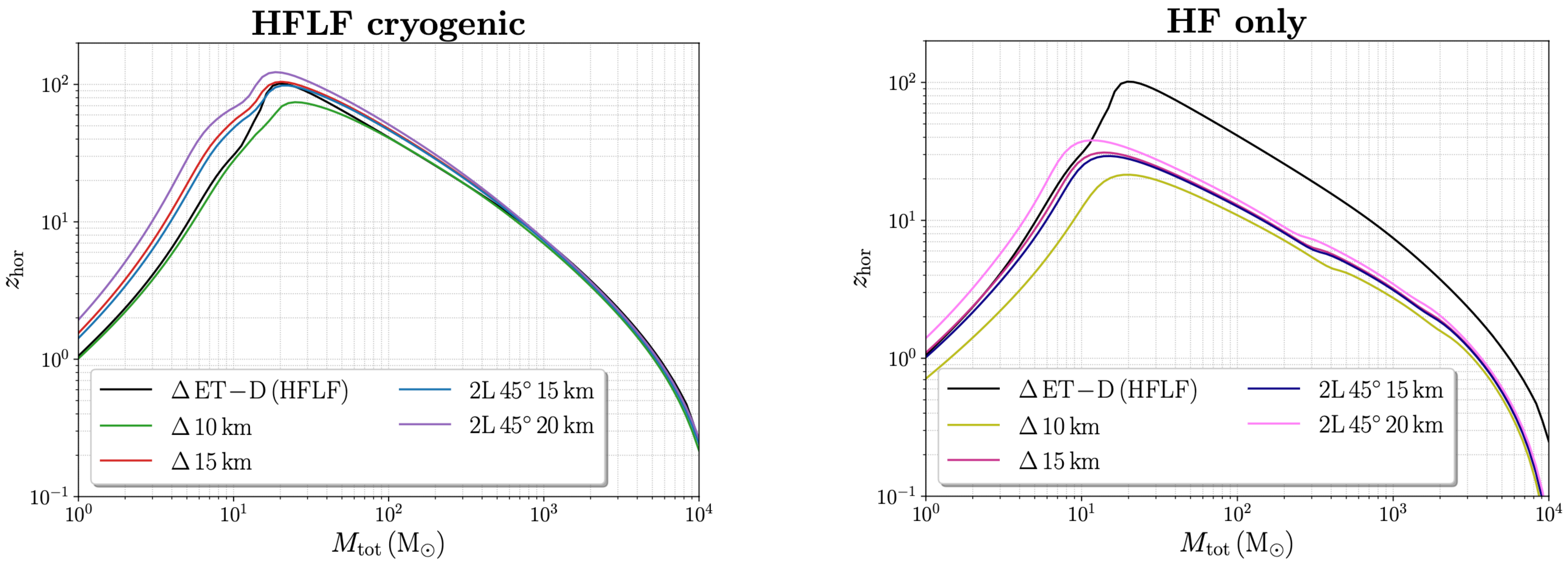

Conclusions Part III

- The remarkable capabilities of next generation GW detectors will allow us to **probe compact binary mergers at cosmological distances**

- The existence of **wide field** X-ray and γ-ray monitors in the next decades will be **crucial,** in order to localize the EM counterpart and possibly identify the host galaxy with ground-based telescopes

- **γ-ray telescopes** are ideal to detect sources up to cosmological distances, while **WFX-ray instruments** are optimal for off-axis and sub-luminous events in the local Universe

- It is necessary to define an **optimal strategy to select GW events, based on the estimation of the GW parameters,** for which the detection of EM signal is higher

- The developed methodology for the estimation of GW+EM detection is **highly versatile** $\Rightarrow$ applicable to different combinations of instruments and for different models of emission

Conclusions

- With almost 20 years of activity, the **Swift database represents a precious source** of information to better investigate the physical nature of GRBs

- The study of the **X-ray steep decay** and the associated spectral evolution **leads to useful hints** about the prompt emission physics

- A systematic **multi-band** time-resolved **spectral analysis of the X-ray plateau** brings a step further in the interpretation of its origin

- A comprehensive data-based understanding of the prompt and afterglow features of GRB is **essential to forecast the scientific outcome** of future γ-ray and X-ray missions

- It is an urgent priority to define the **perspectives of multi-messenger observations with 3G GW detectors and future high-energy telescopes** to identify the best instrumental technical design, the most effective observational plans and to evaluate the scientific potential to unveil the physics of GRBs

Thanks!

Backup slides

Ongoing work and future prospects

I currently work at the **Swift Mission Operation Center** (PennState University), giving my contribution for the preparatory phase for the next GW observing run 04:

- Monitoring and development of the real-time pipeline GUANO for the **search of Swift-BAT sub-threshold events**

- Optimization of the **tiling strategy of XRT/UVOT** for the search of the EM counterpart of BNS mergers

BAT coded mask

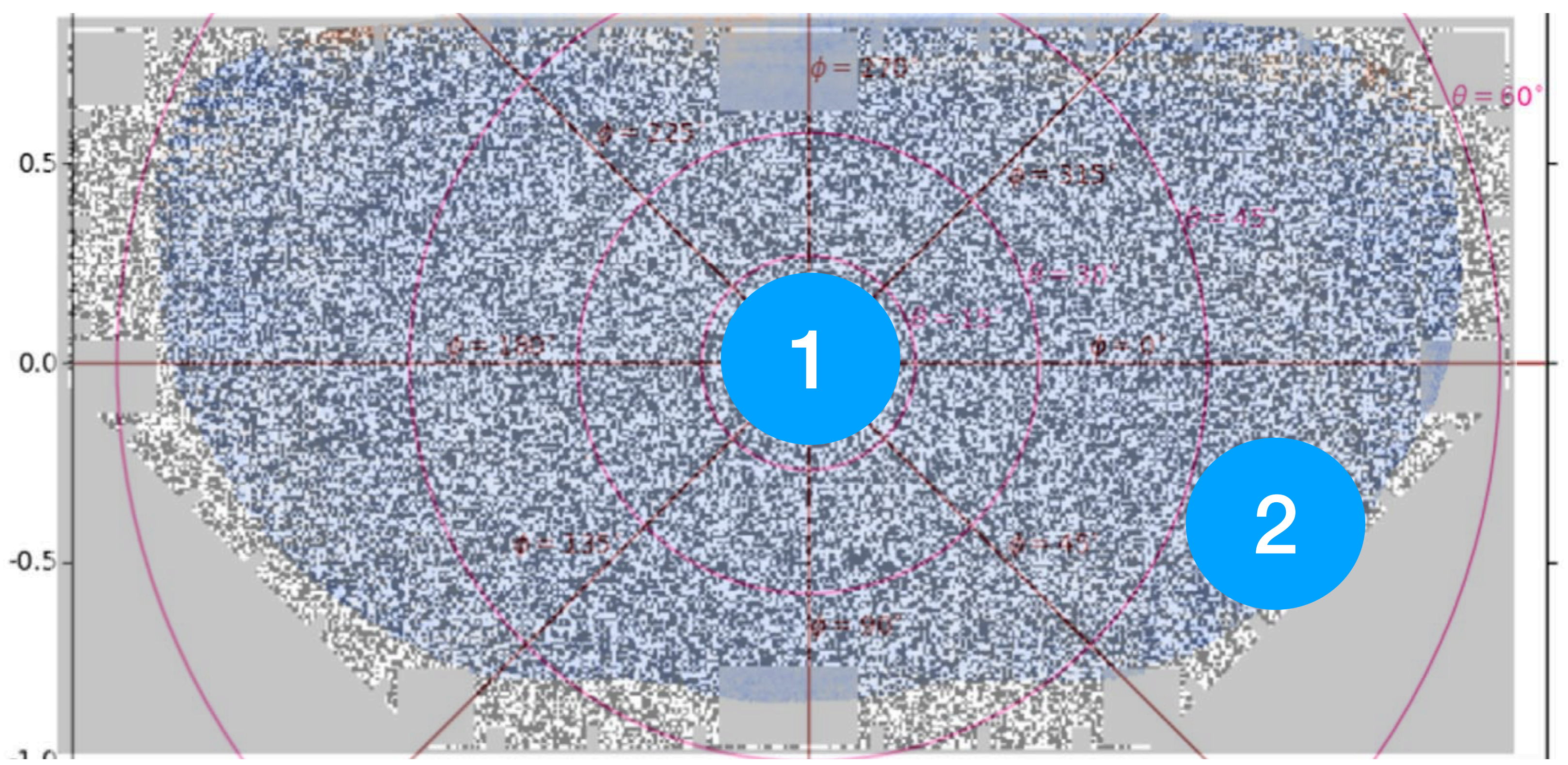

Some GRBs potentially detectable by BAT are missed because, e.g.:

- occurring close to the edge of the coded mask
- Occurring during slew
- Located out of the FOV

We can recover them, with a deeper low-latency analysis

The efficiency of the trigger algorithm degrades as we move from the center of the FoV

1 $P(det|F > F_{th}) = 100\%$

2 $P(det|F > F_{th}) < 100\%$

Application to the multi-messenger science case:

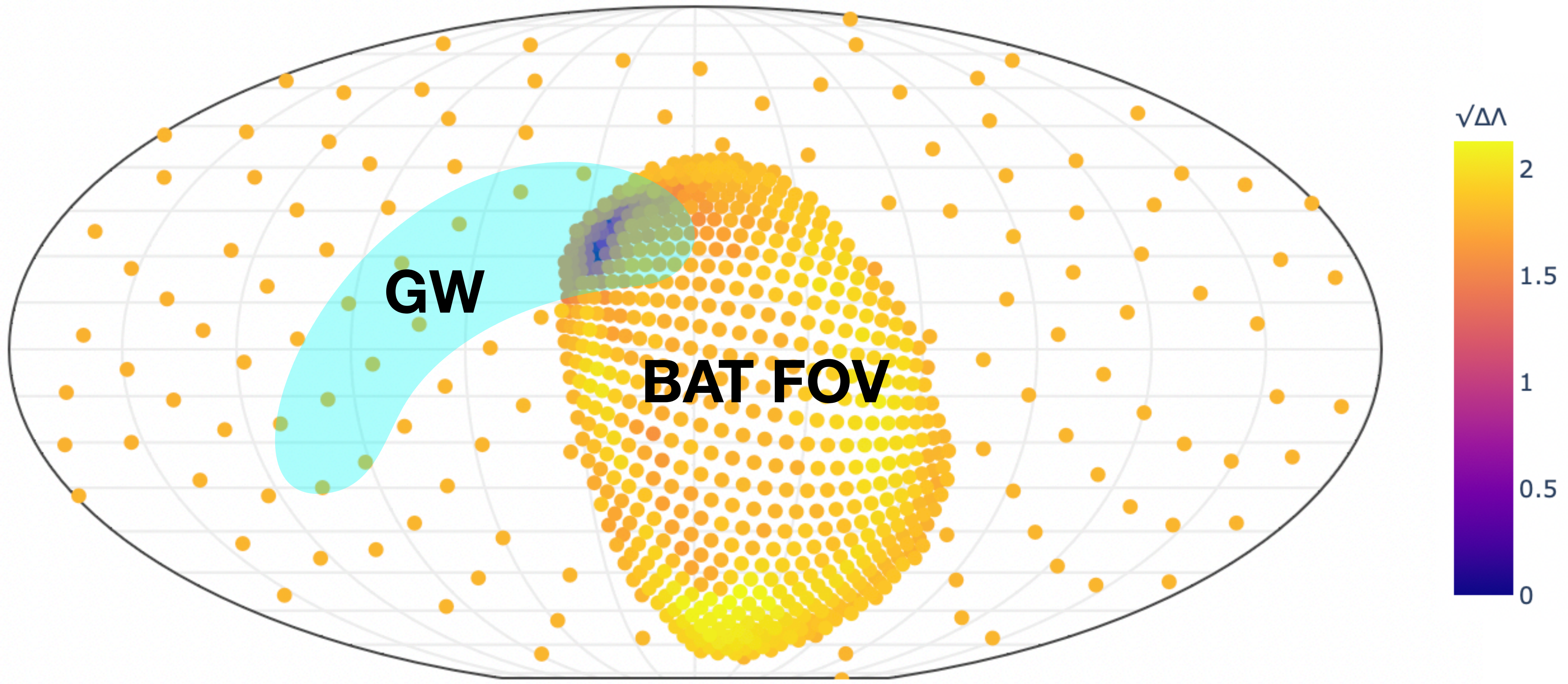

1. GW trigger
2. Swift-BAT does not trigger
3. The GUANO analysis reveals a significant event, **providing arcmin localization**
4. EM follow up

Gamma-ray Urgent Archiver for Novel Opportunities (GUANO)

Flowchart

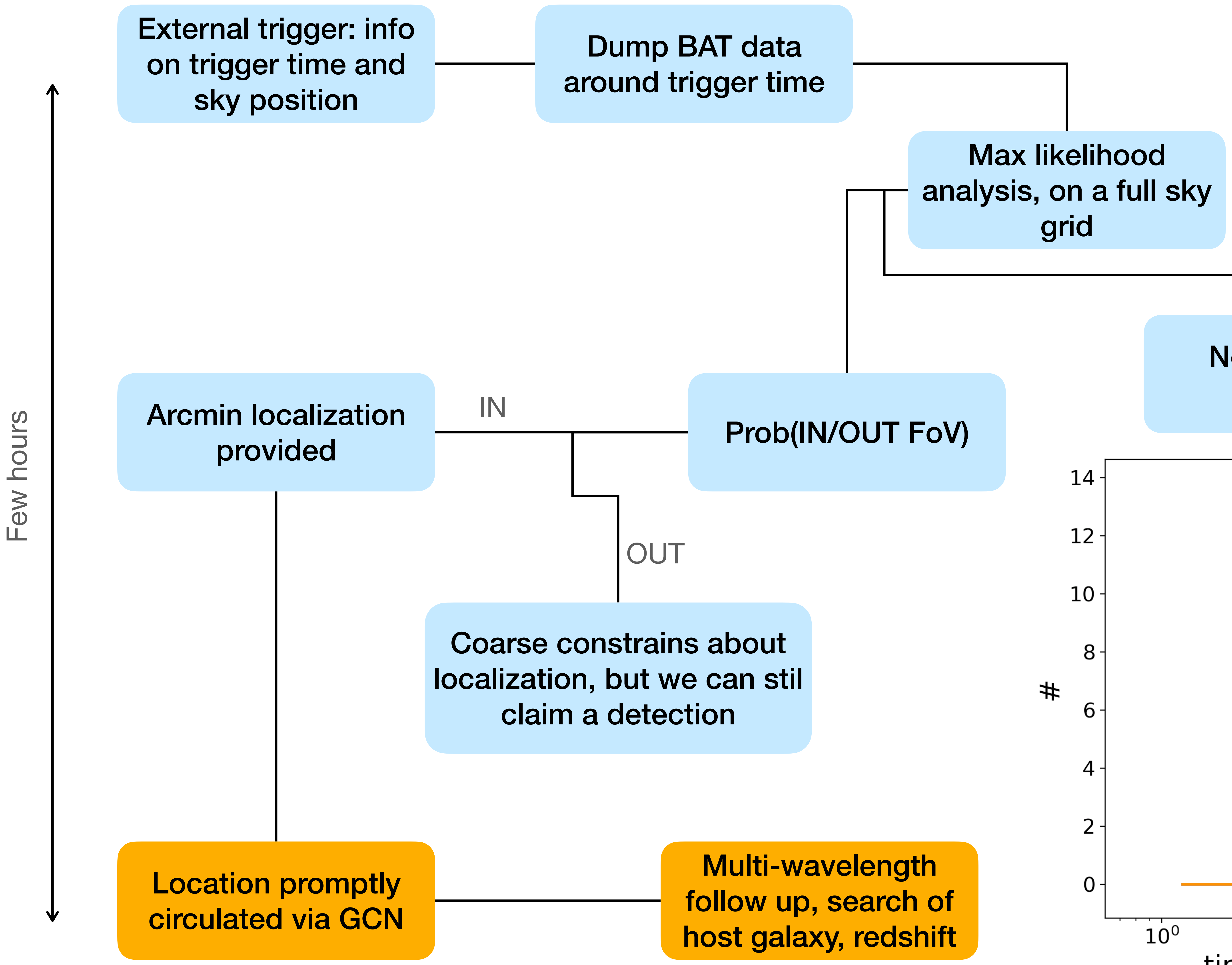

Successfully operative in O3, both for above- and sub threshold events

Ready to run in low-latency also during O4

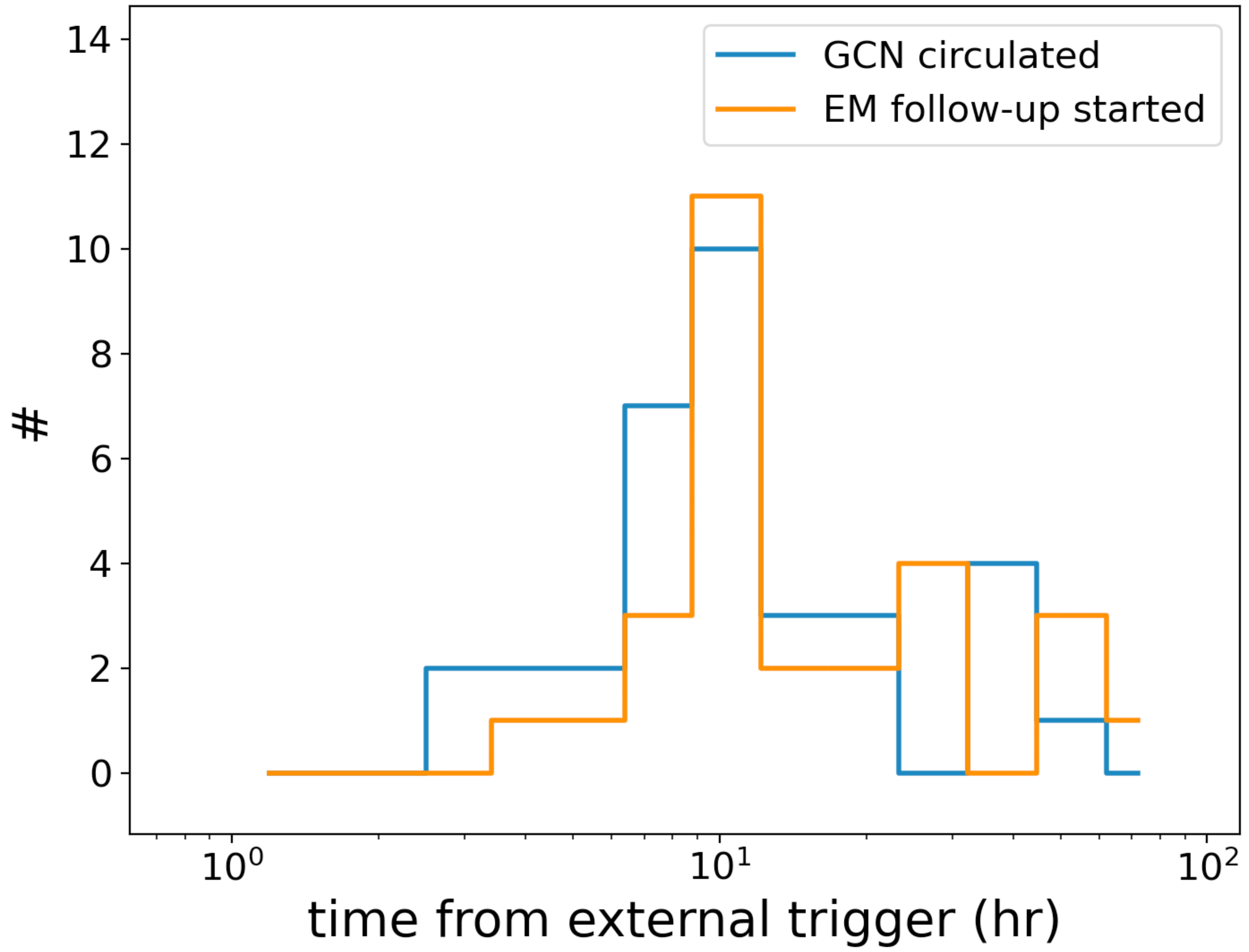

Ingested external triggers:

1. Fermi/GBM, Integral, Calet, GECAM
2. **GWs**
3. IceCube
4. HAWC
5. FRBs

Success rate:

- more than 100 GRBs recovered with GUANO so far
- 32 with arcmin position (24 long + 8 short)
- In 14 of them the afterglow emission was detected (1/2 of which are short)

The sample of GRBs with X-ray plateau

Incidence of plateau in short and long GRBs

P/T	Z/T	$\frac{P \cap Z}{Z}$	$\frac{P \cap Z}{P}$	$\frac{P \cap Z}{T}$	S/T	$\frac{S \cap Z}{Z}$	$\frac{S \cap P}{P}$	$\frac{S \cap P \cap Z}{P \cap Z}$
32.3%	24.9%	47.4%	36.5%	11.8%	9%	4.3%	3.3%	2.6%

$\frac{S \cap Z}{S}$	$\frac{S \cap P}{S}$	$\frac{S \cap P \cap Z}{S \cap Z}$	$\frac{S \cap P \cap Z}{S \cap P}$
11.9%	11.8%	60.4%	61.0%

$\frac{L \cap Z}{L}$	$\frac{L \cap P}{L}$	$\frac{L \cap P \cap Z}{L \cap Z}$	$\frac{L \cap P \cap Z}{L \cap P}$
26.2%	34.3%	48.2%	36.8%

T=all GRBs

P= GRBs with X-ray plateau

S=short GRBs

L=long GRBs

Z= GRBs with measured redshift

Presence of X-ray plateau determined by the results of the Swift automatic analysis (light curve fitted with a series of power laws)

Redshift distribution: no evidence of dependence of X-ray plateau from the redshift

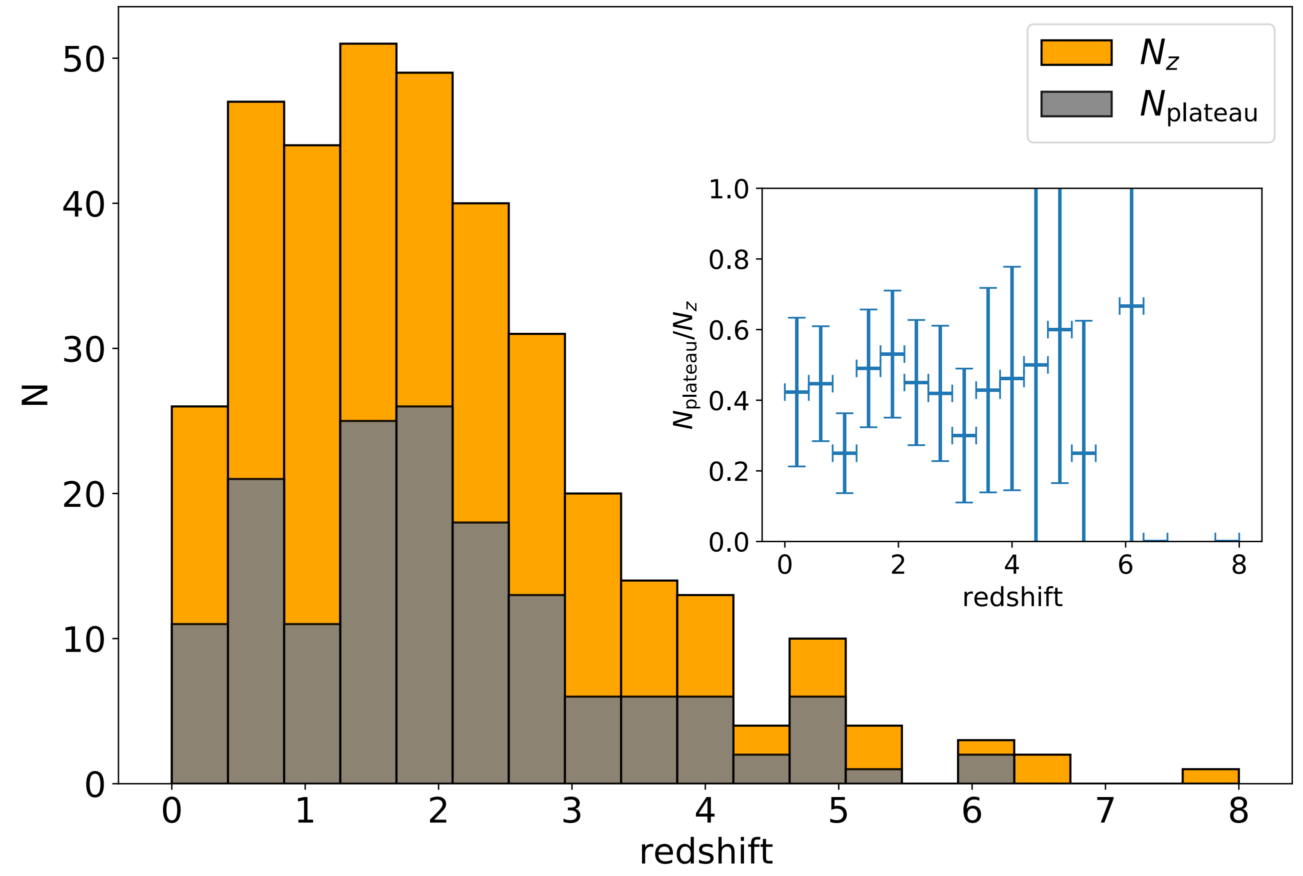

We verified the consistency with the L_p-t_p anti-correlation, previously found in literature

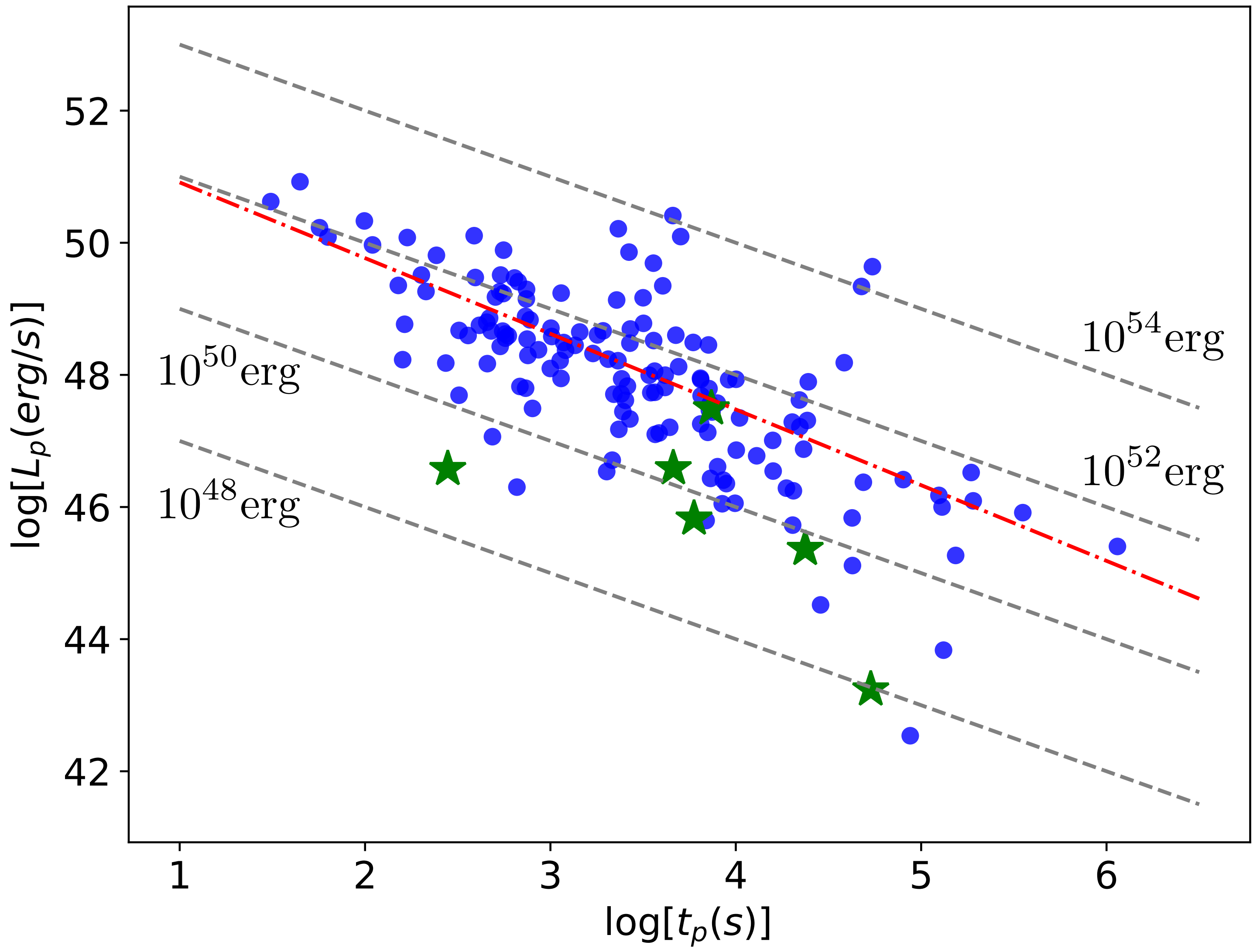

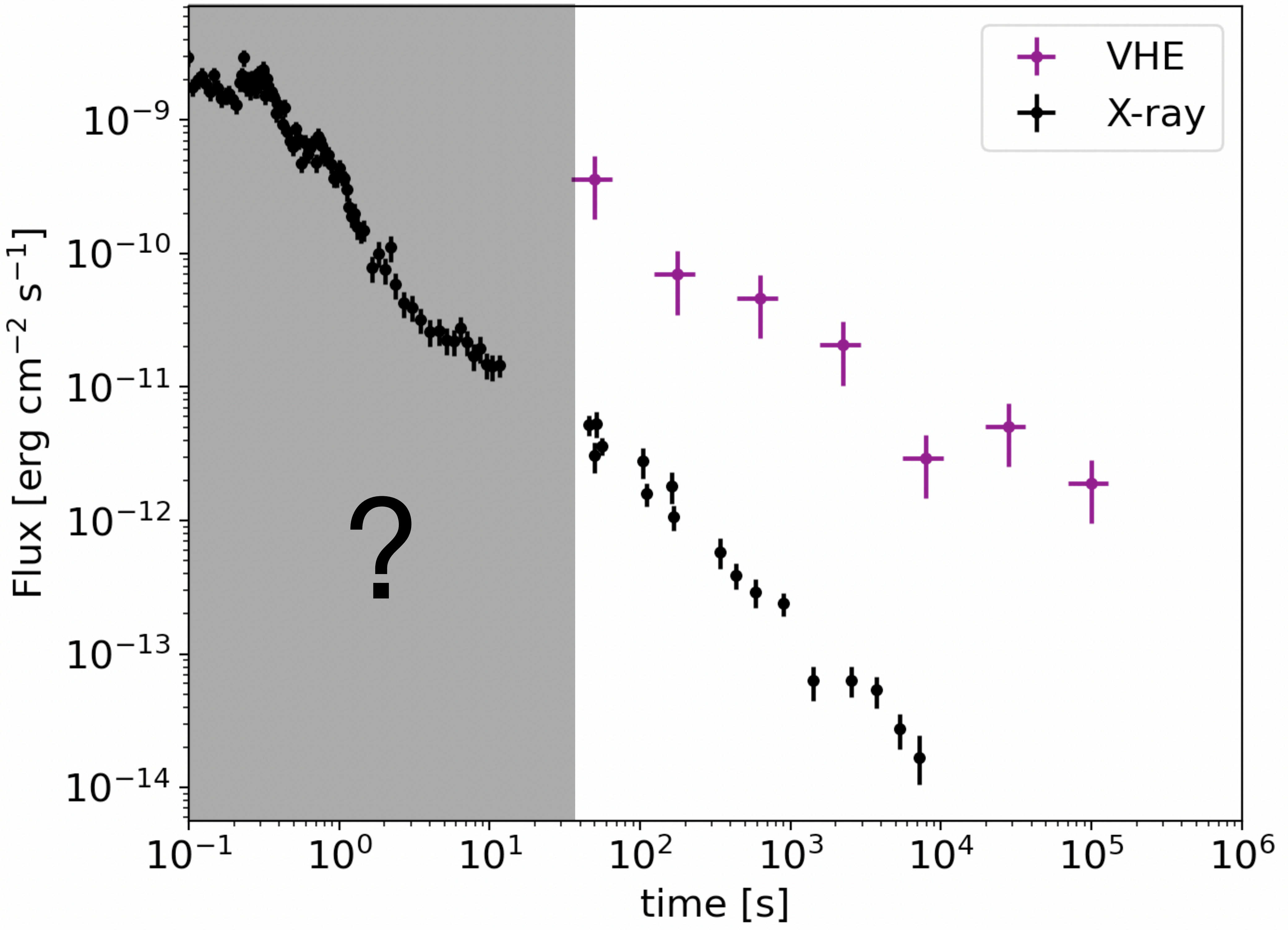

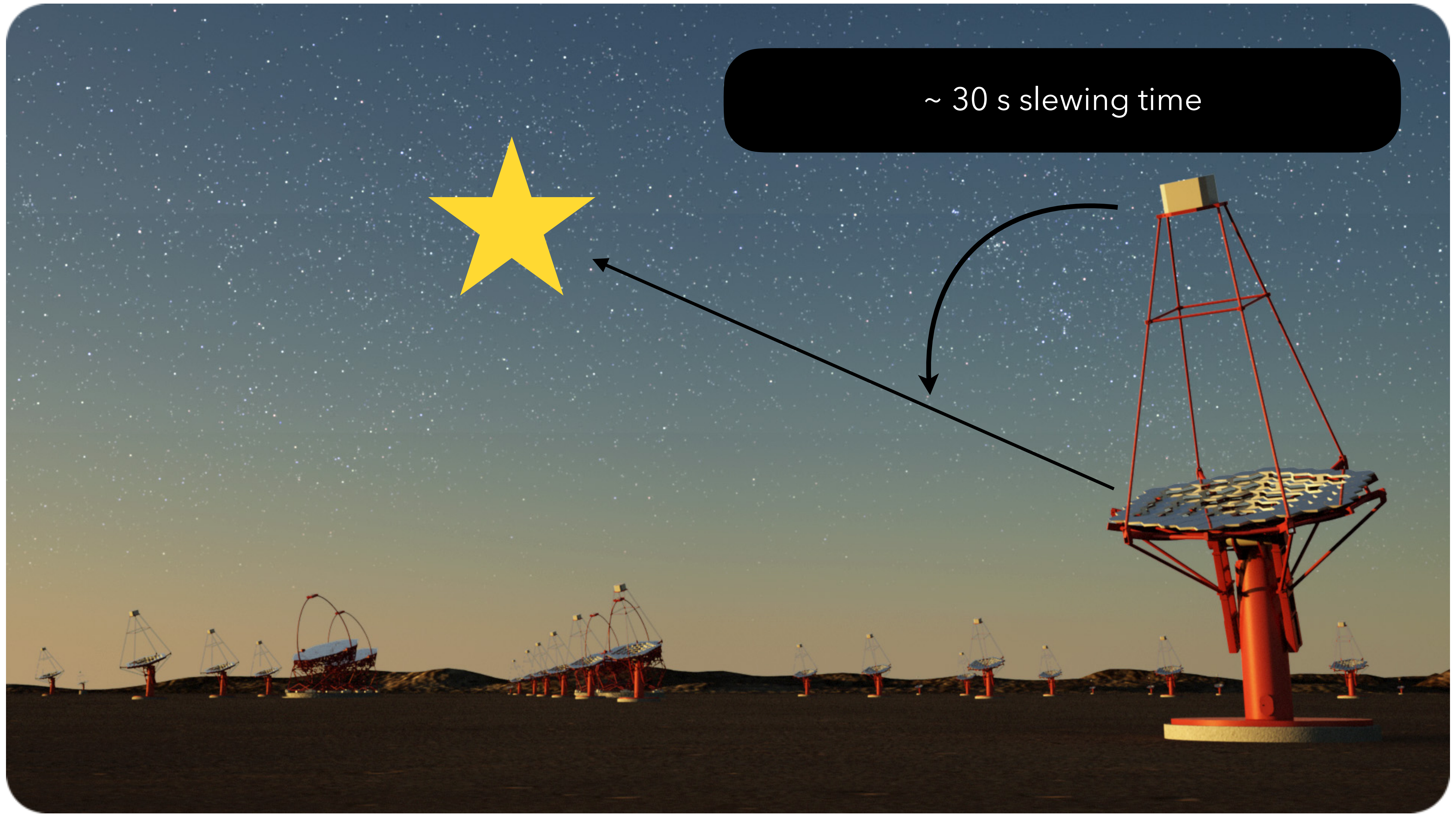

MAGIC and HESS detected VHE during GRB afterglows → **what about the prompt emission?**

During the activity of 3G GW detectors, **CTA** should be operative as well

Pre-merger sky localisation and VHE from sGRBs

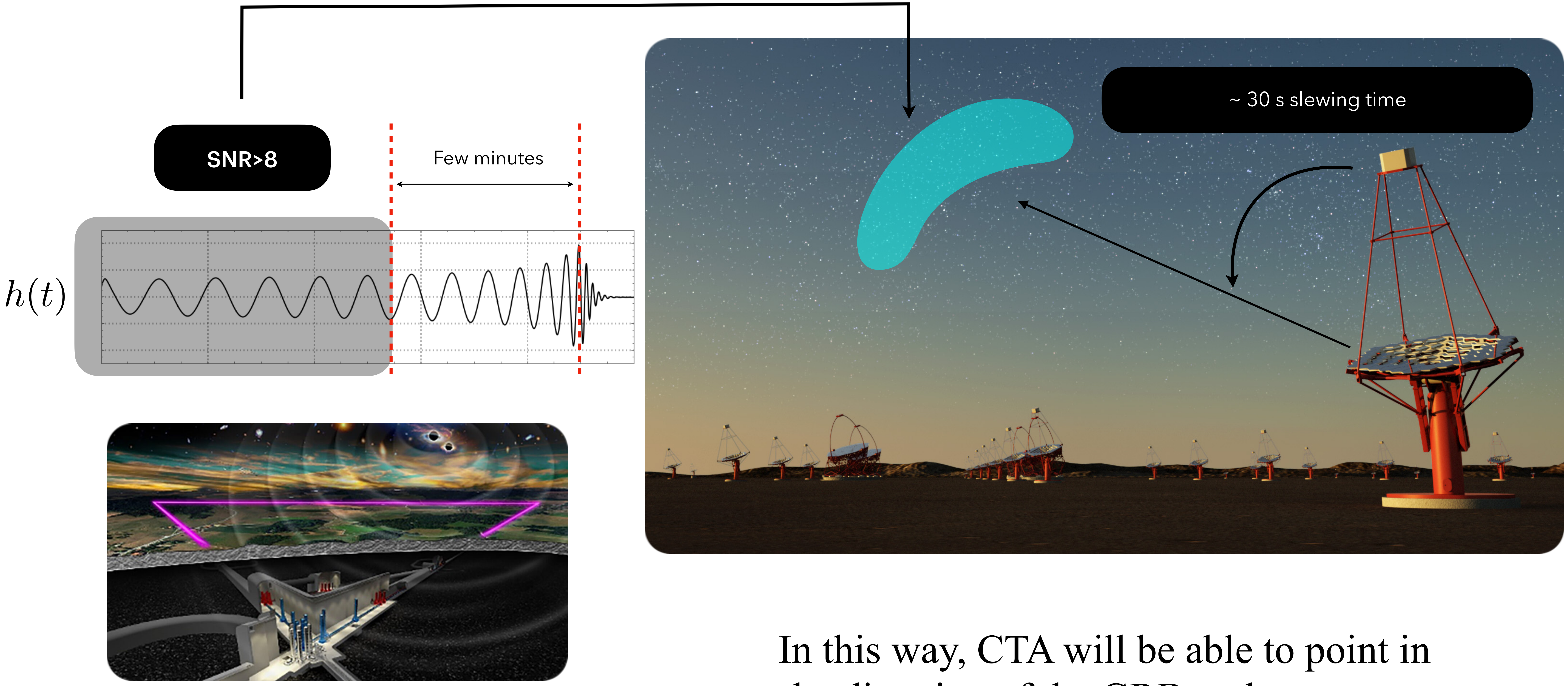

In this way, CTA will be able to point in the direction of the GRB at the moment of the merger, allowing to **detect possible VHE emission during the prompt phase**

Samuele Ronchini, Gran Sasso Science Institute
PhD Defense

The role of sensitive X-ray instruments

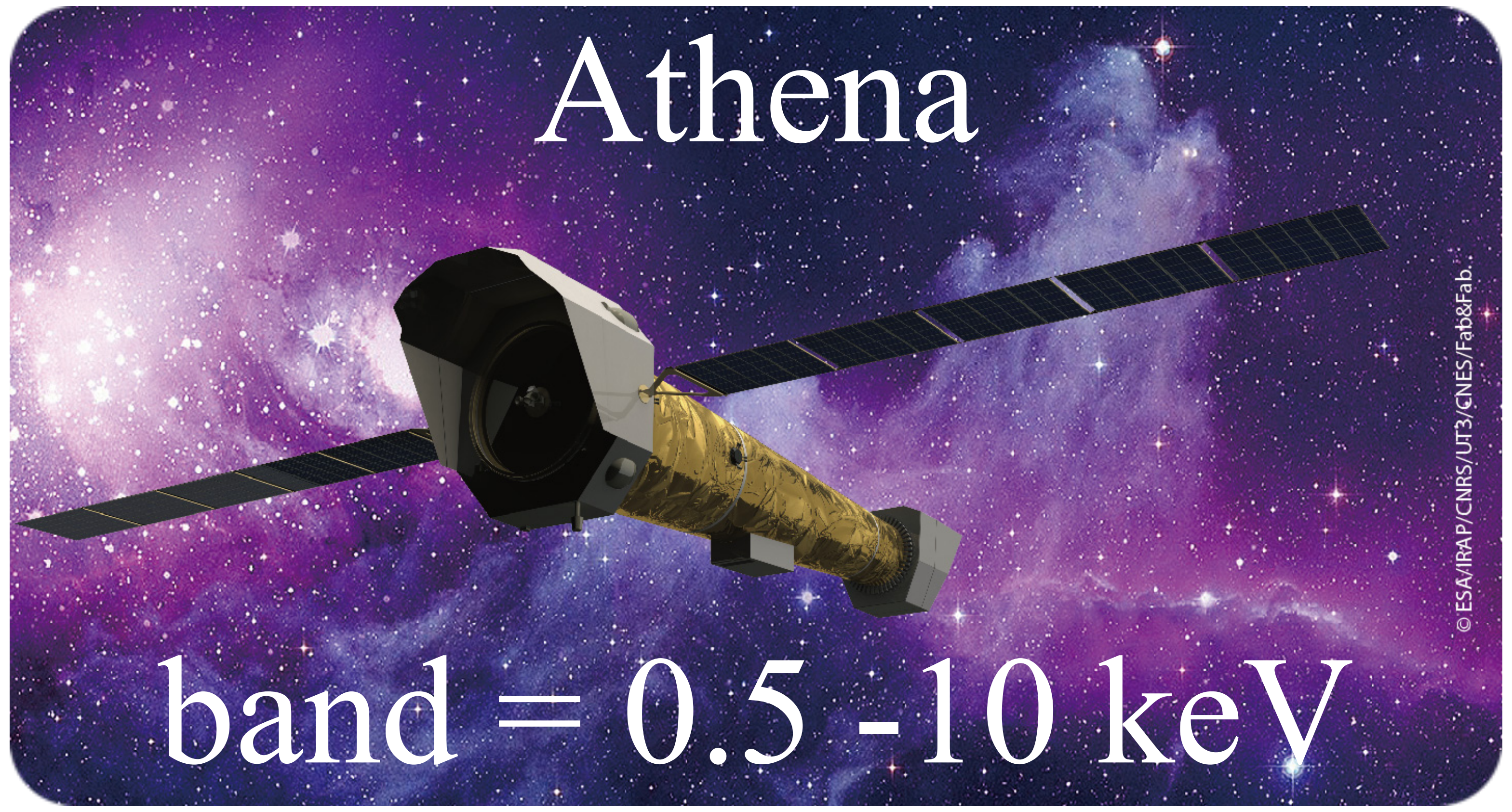

1. **X-IFU**: needs arcmin localisation, provided by WFX-ray telescopes

The **totality** of sources identified with WFX-ray monitors can be detected by X-IFU

2. **WFI:** can carry out a **mosaic of a sky region of ~10 deg²** localisation provided by GW detectors

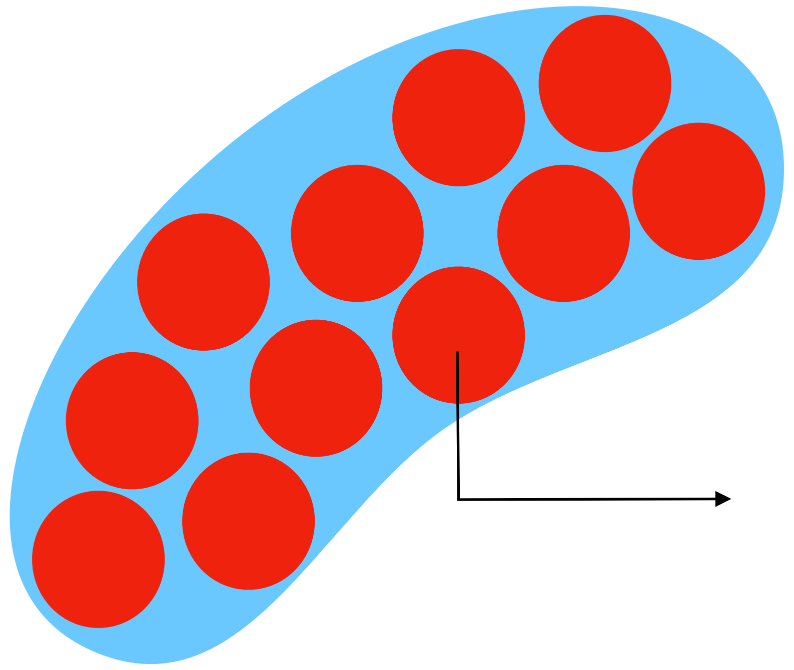

For ET+2CE

~5 joint detections per year, excluding cases with ϑ_v**>50°**

~15 joint detections per year, excluding cases with ϑ_v**>30°**

The role of sensitive X-ray instruments

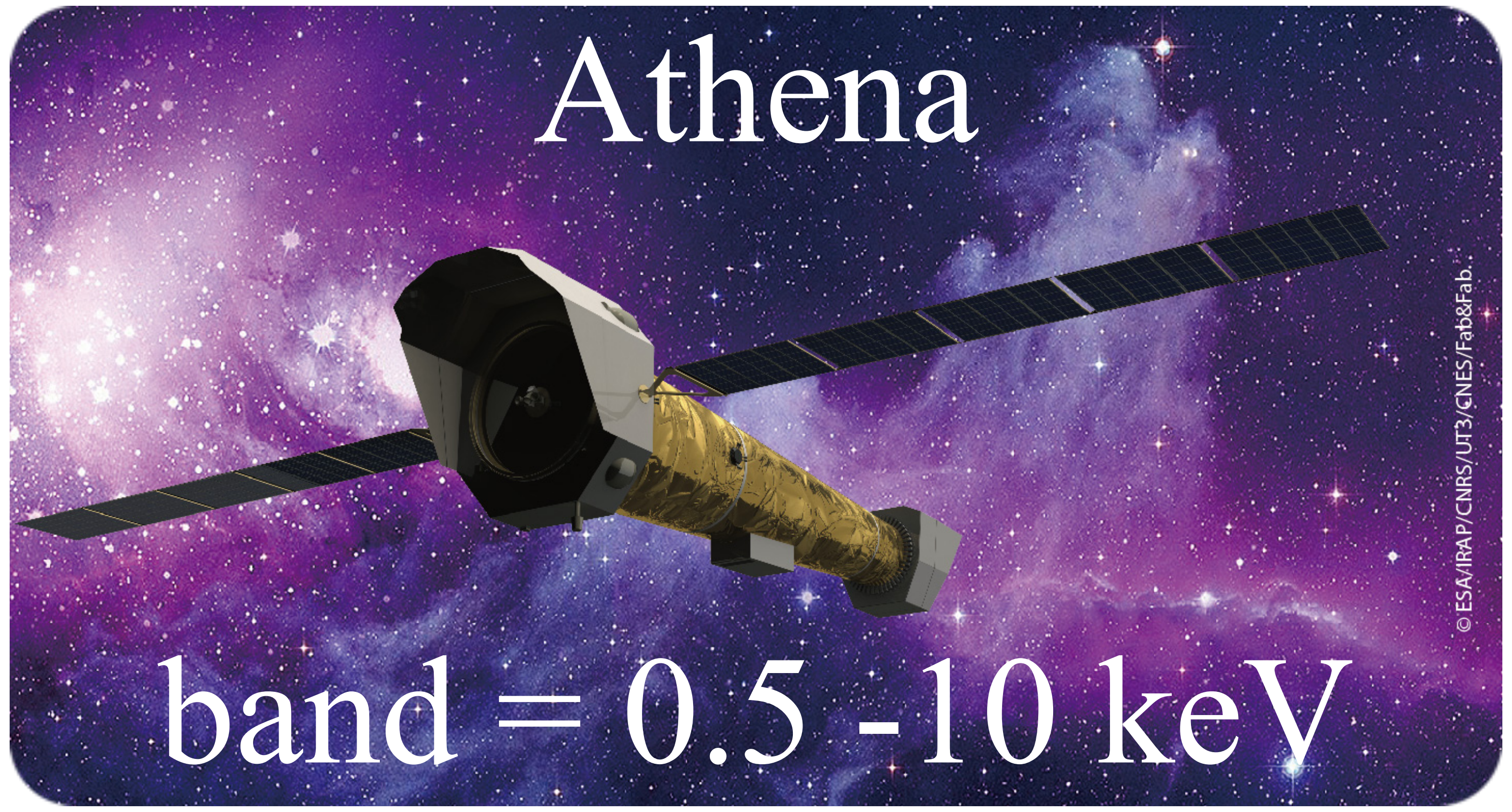

Piro et al. 2021

Unprecedented sensitivity in the soft X-rays

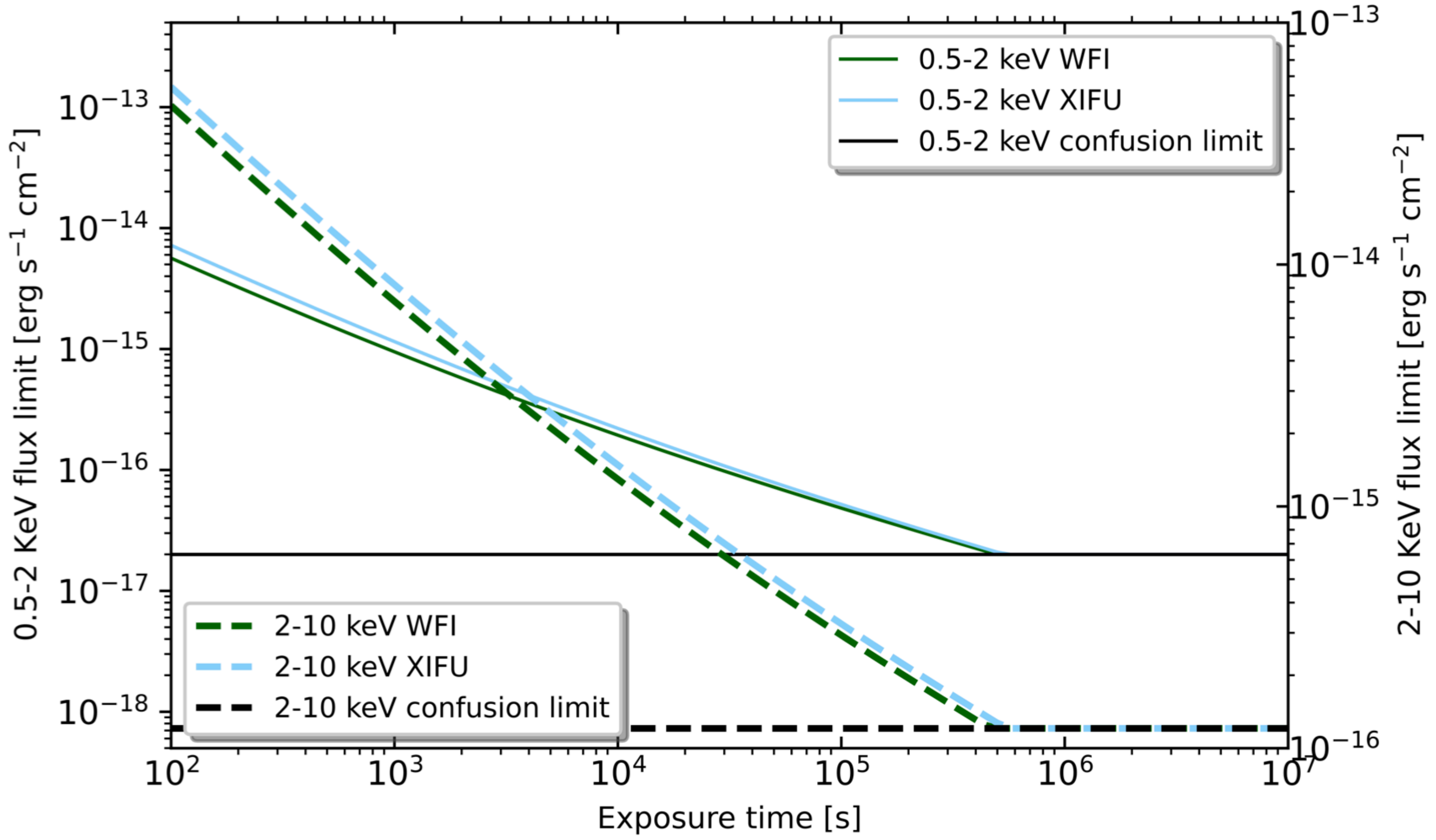

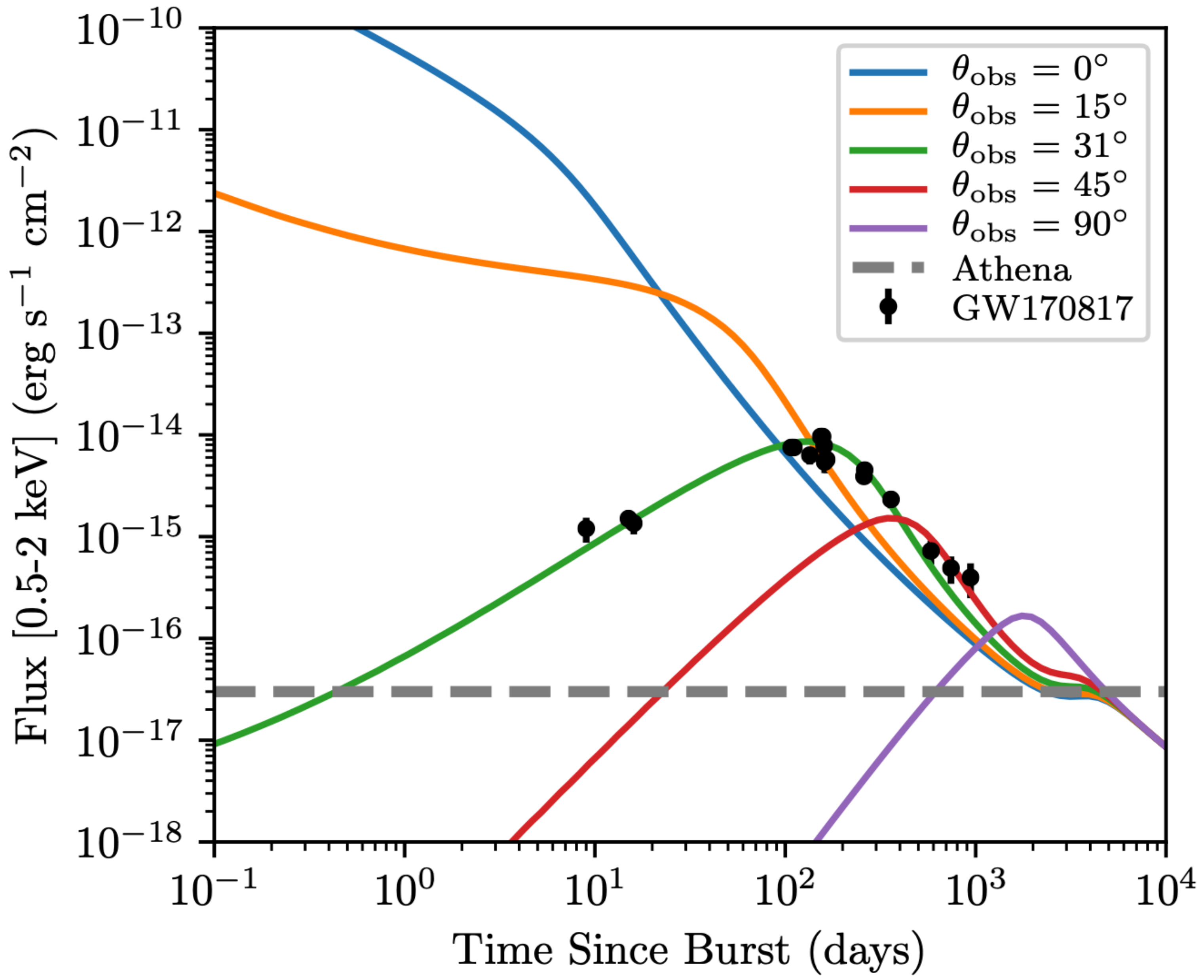

GW170817-like events are detectable:

- Months/years after the merger
- Up to large inclination angles

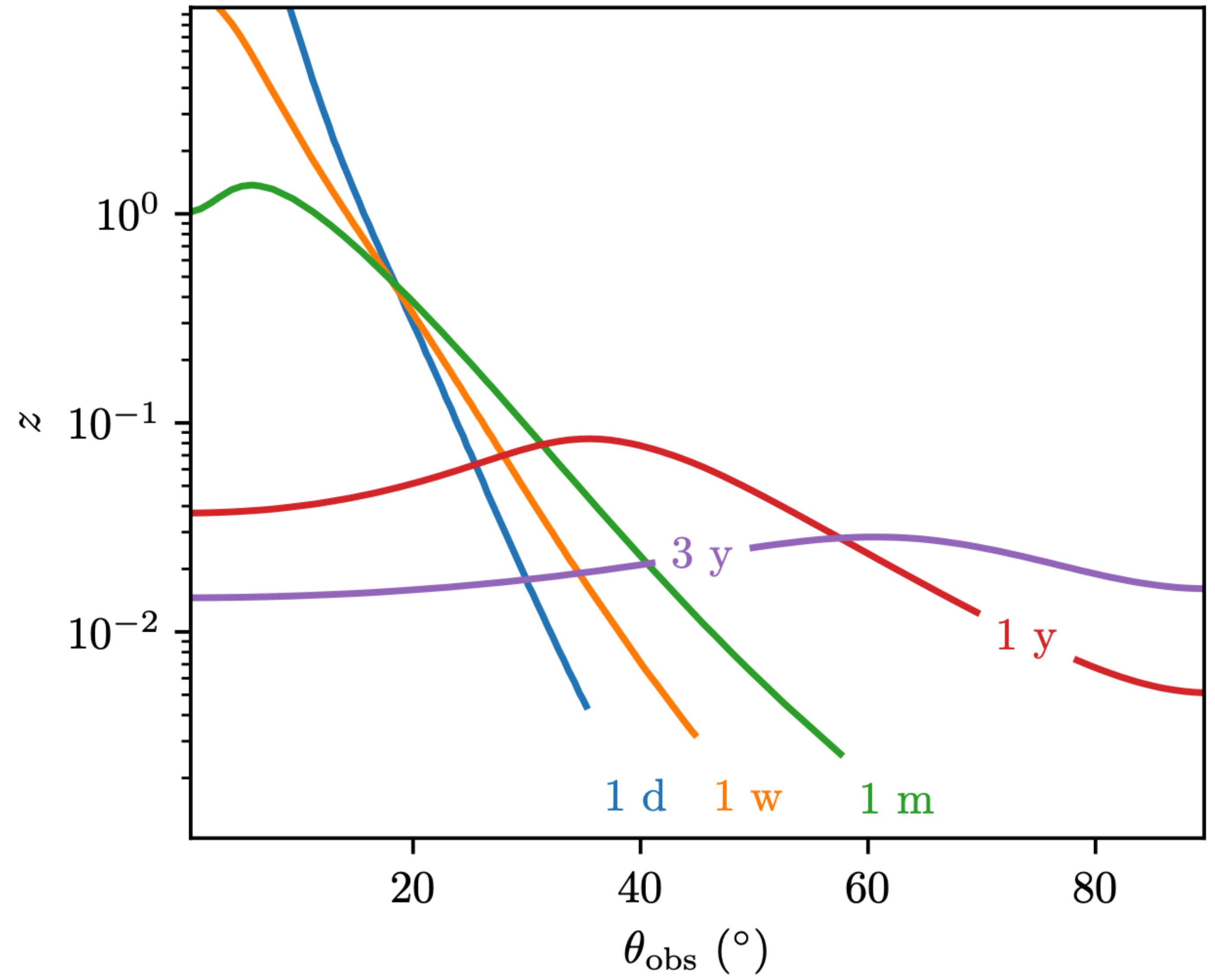

Transversal section of the jet

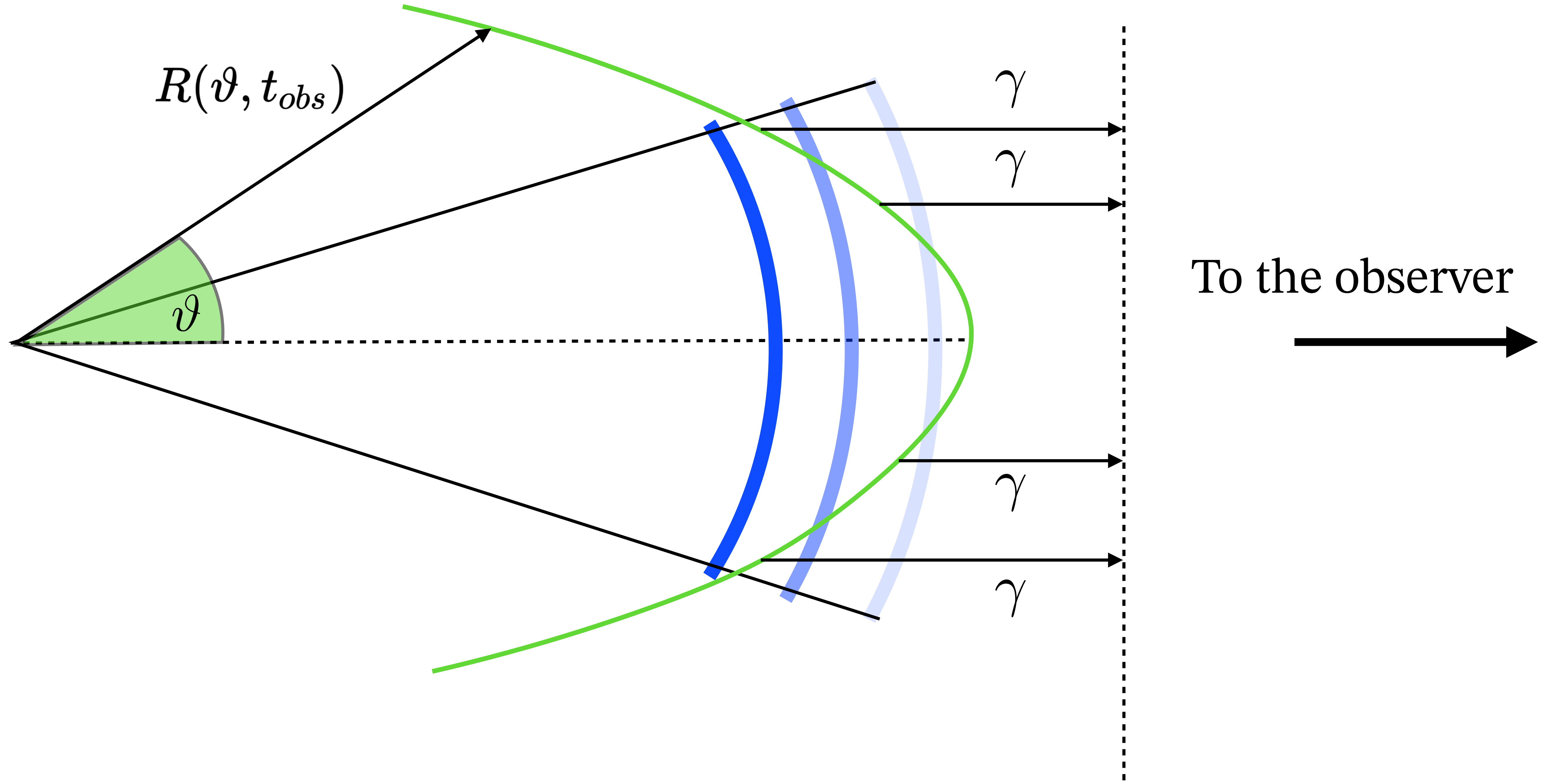

Conservation of entropy

$$\langle\gamma\rangle^3 V' = \text{const}$$

For a synchrotron spectrum

$$\nu_p \propto \langle\gamma\rangle^2 B$$

Prescription for B evolution

$$B = B_0 \left(\frac{R}{R_0}\right)^{-\lambda}$$

Fermi Telescope: GBM + LAT

All sky monitor
Wide spectral coverage:
GBM—> 8 keV - 40 MeV
LAT—> 20 MeV - 300 GeV

More clear insights about the spectral properties of the prompt emission

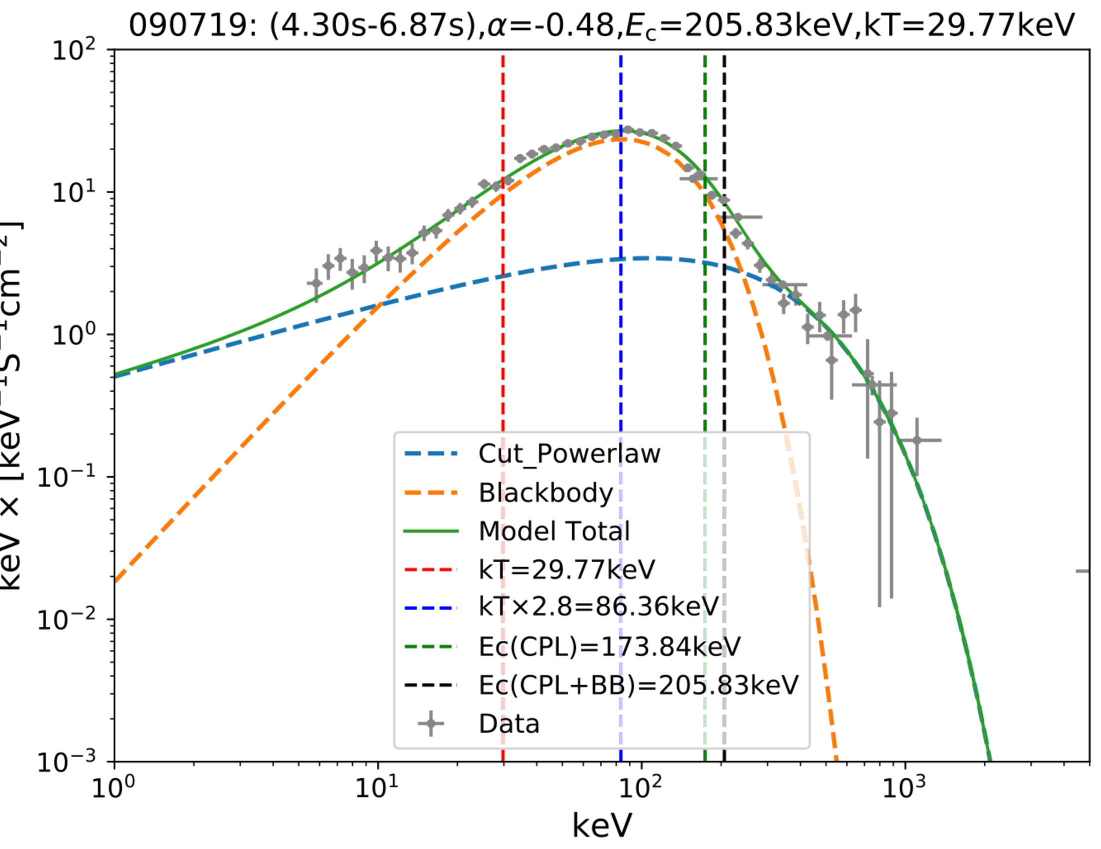

Li 2019

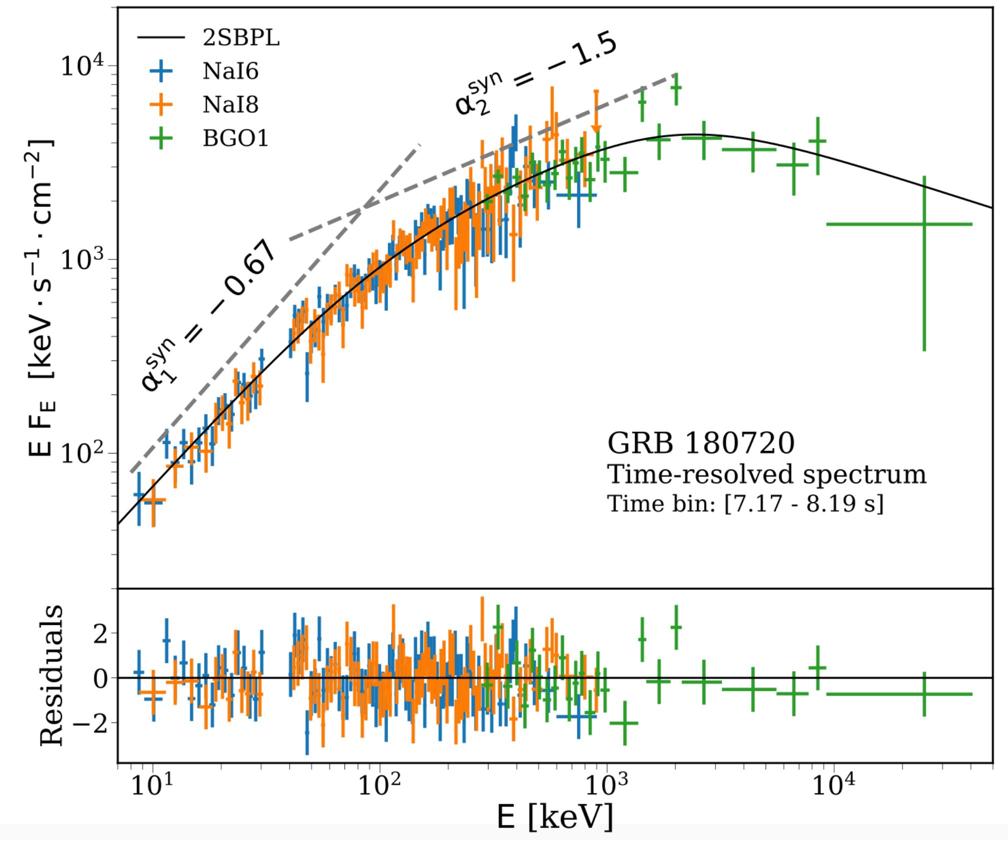

Ravasio 2019

Imaging Atmospheric Cherenkov Telescopes

MAGIC: 190114C

H.E.S.S. : 190829A

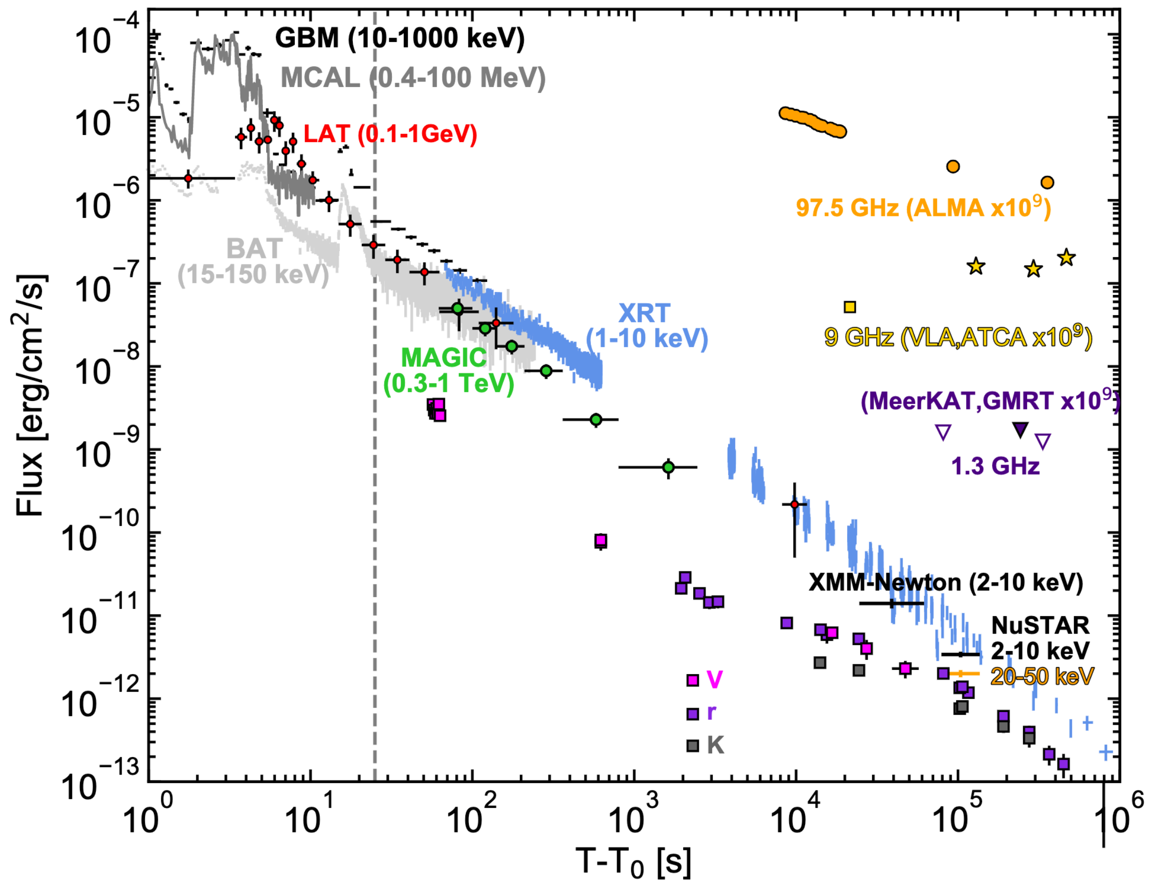

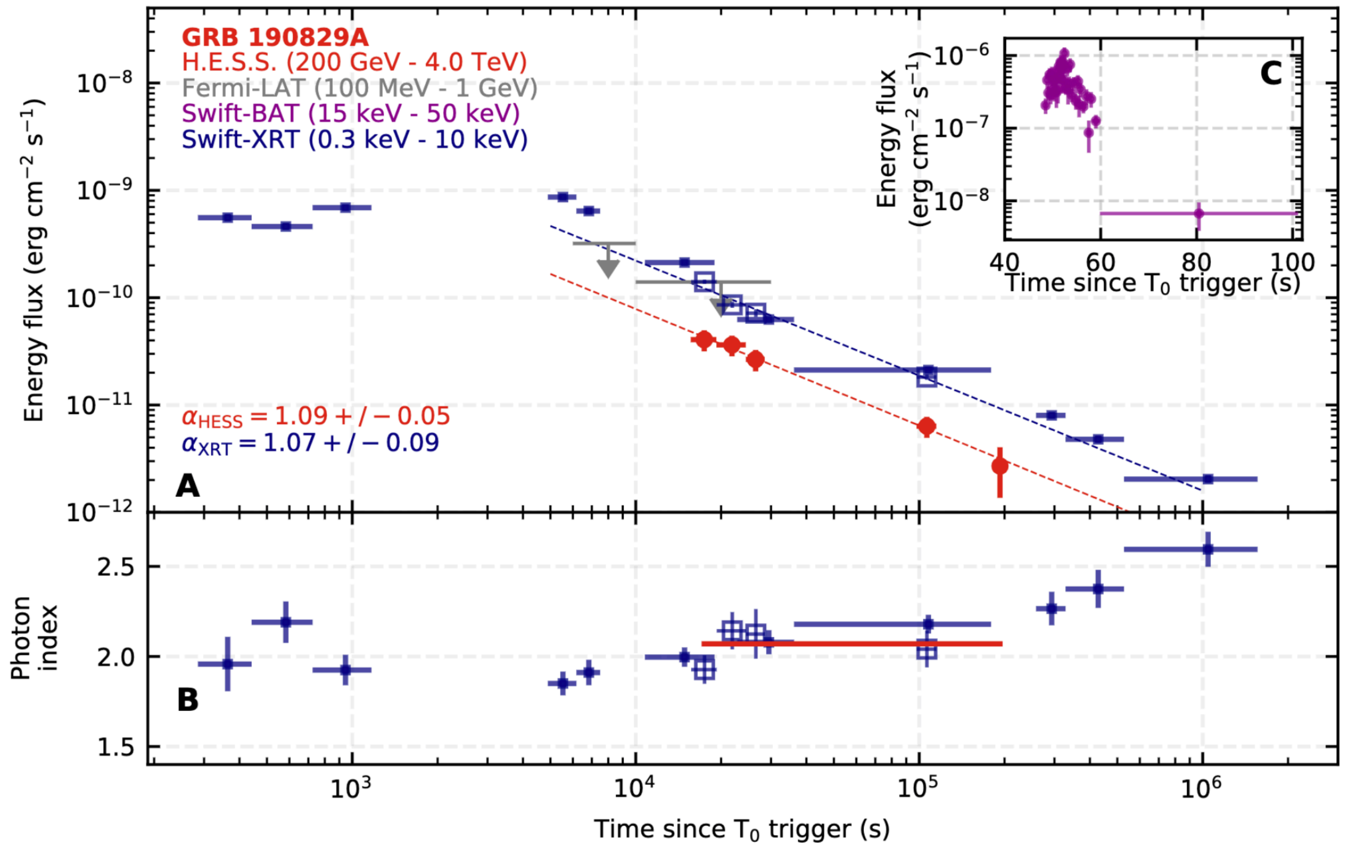

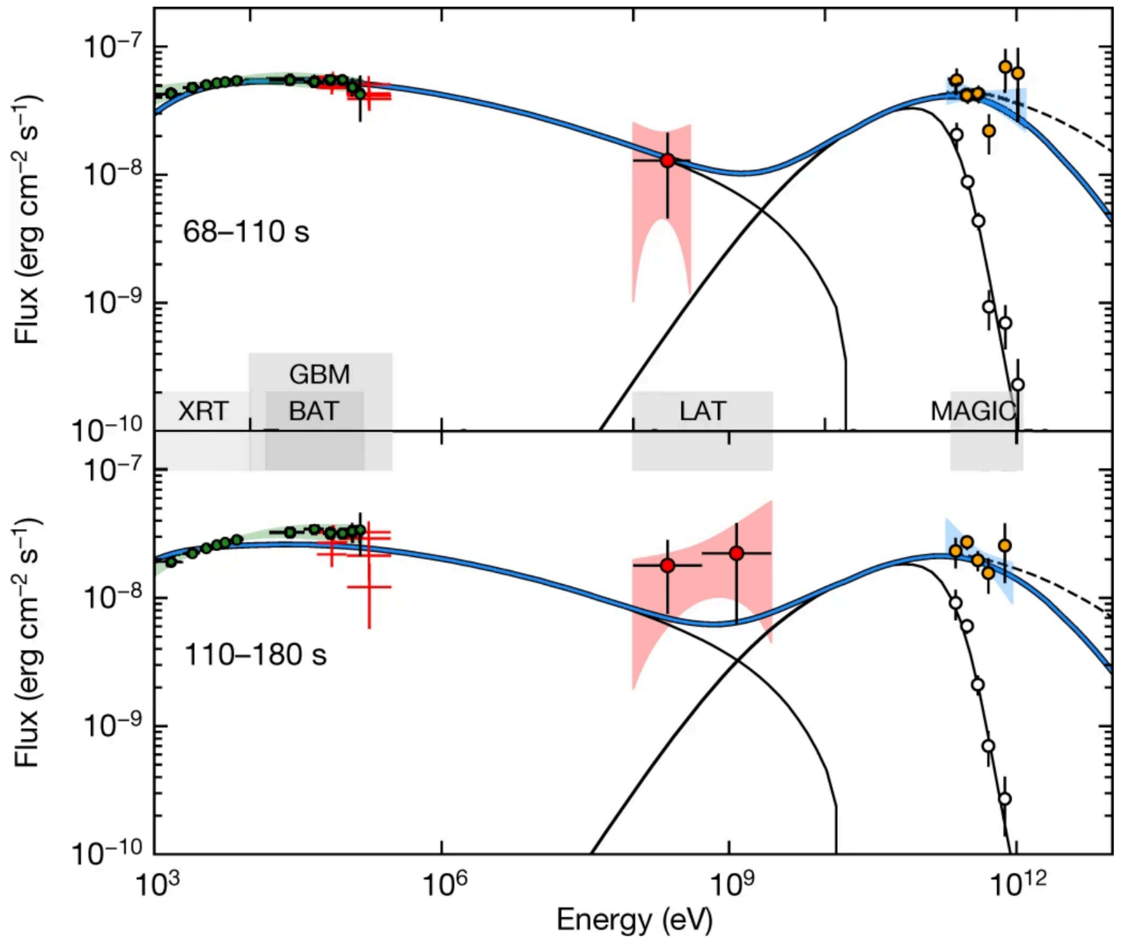

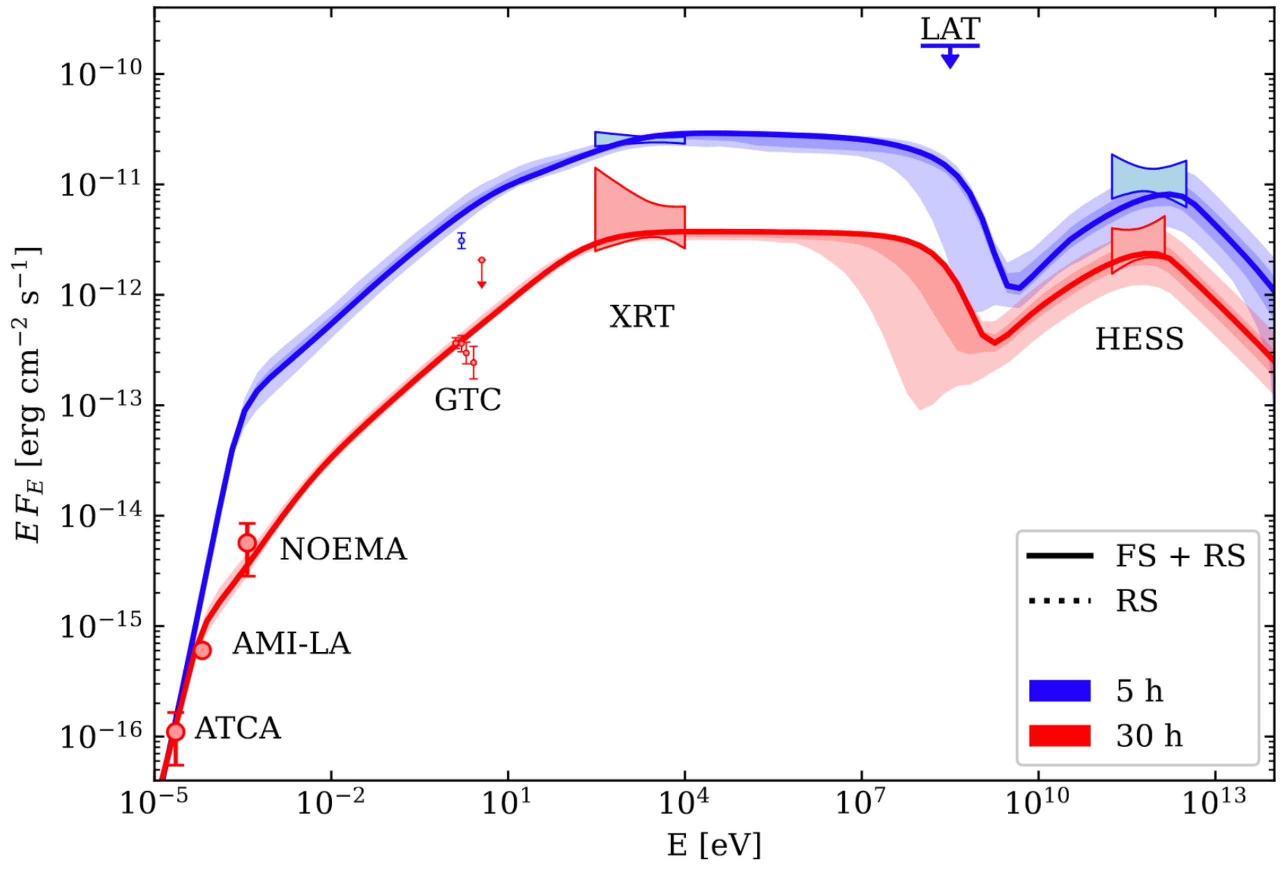

Results: Sample 1

The temporal evolution of X-ray and optical flux and break frequency is fitted with a power law

$$\nu_b \propto t^{-s}$$

	s<0	s=0	s>0
# cases	3	5	11

We find:

1. The **standard FS scenario**, even assuming time-dependent micro-physical parameters, **cannot explain the X-ray/optical evolution**

2. In the **energy injection scenario in agreement**

3. **The structured jet scenario**, as well, **is able to explain the observed spectral evolution**, assuming different possible ISM density profiles

Energy injection favored? Not necessarily

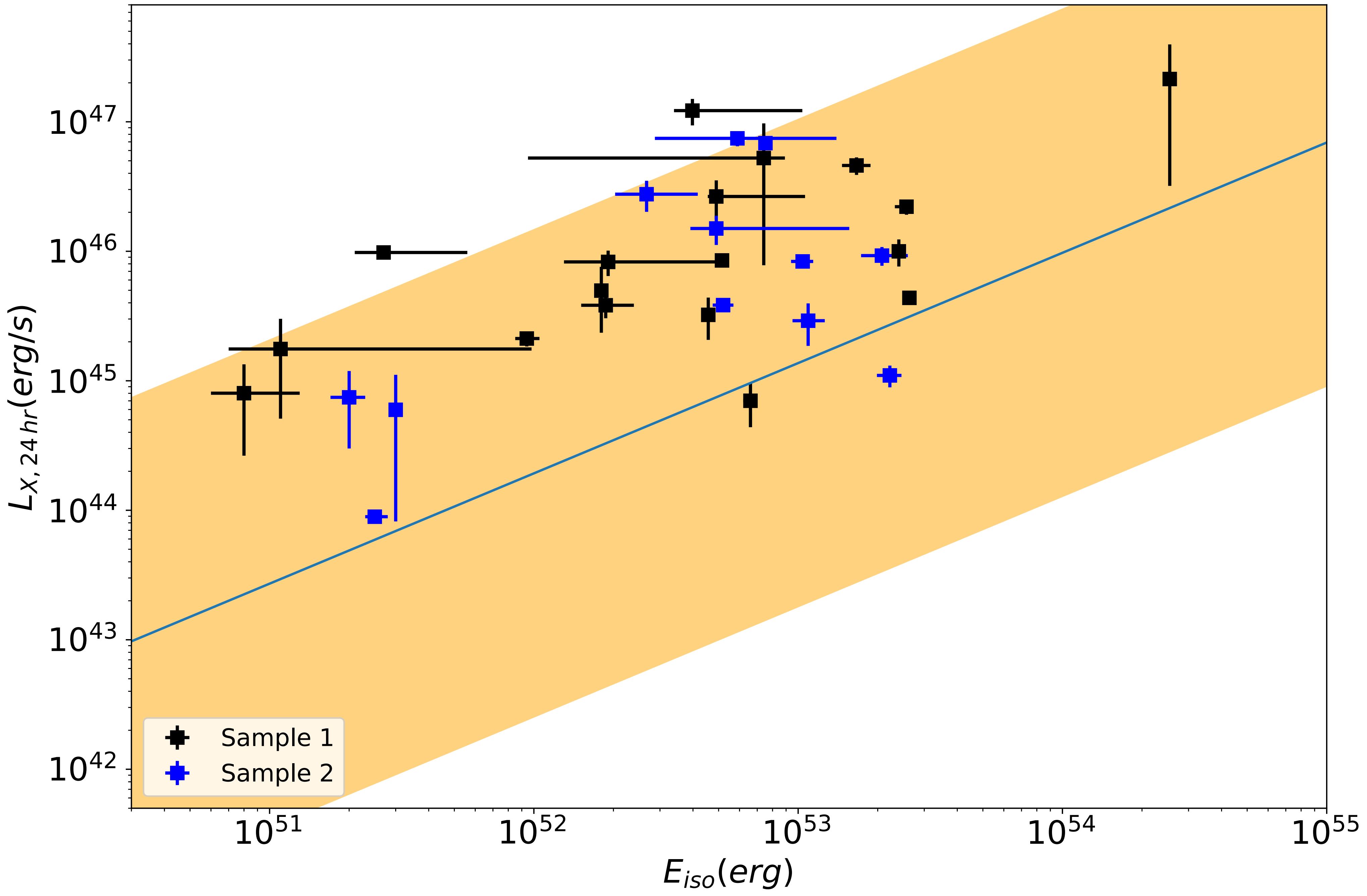

Why we need joint GW+EM detections?

Info from GWs:

- masses of the system
- inclination of the orbital plane
- nature of the remnant

- luminosity distance

Relativistic astrophysics and fundamental physics

- Who are the progenitors of short GRBs
- How the jet properties depend on the central engine (BH vs NS)
- EoS of NS

- Cosmological studies
- Hubble diagram
- Tests of GR

Info from EM signals:

- energetic and dynamical properties of the outflow (jet+kilonova ejecta)

- redshift

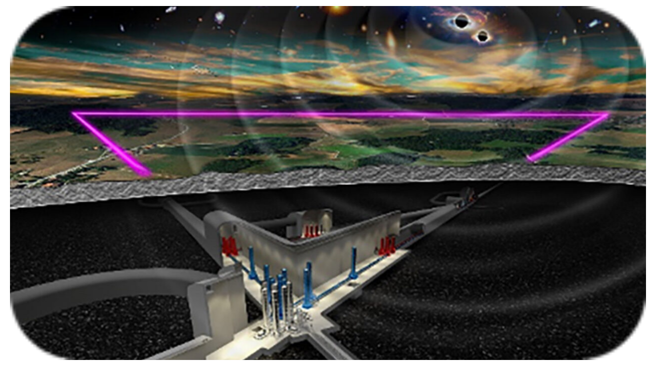

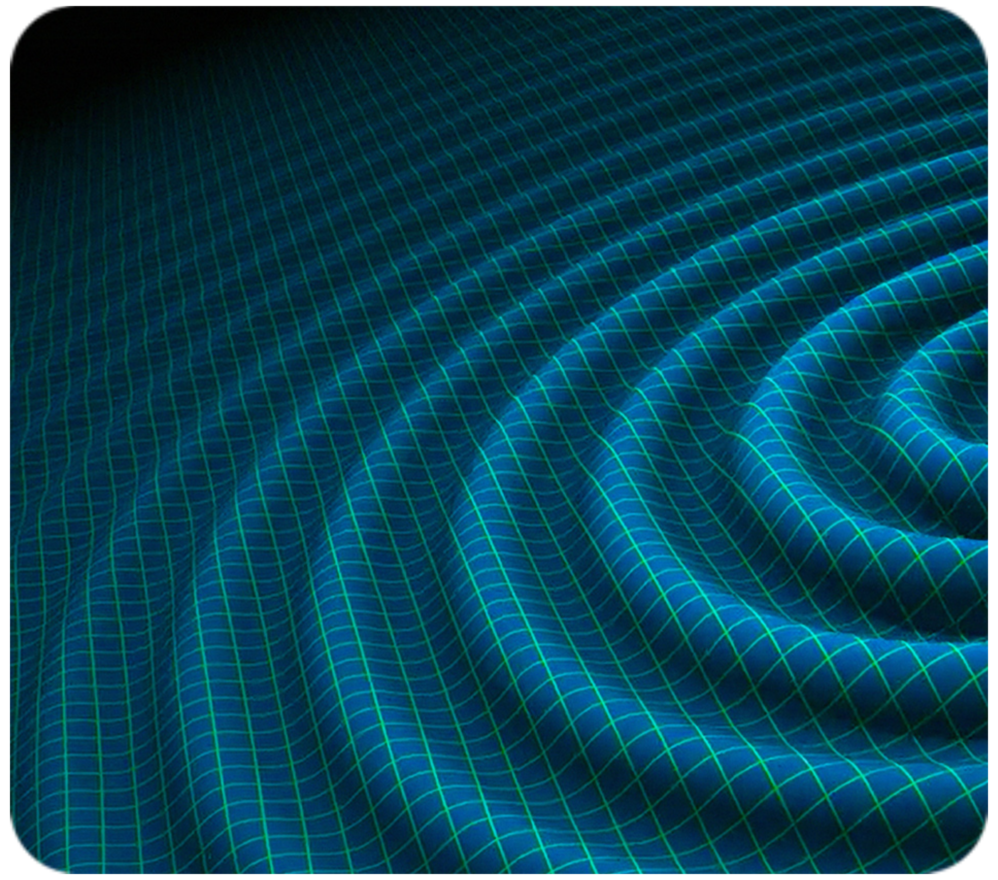

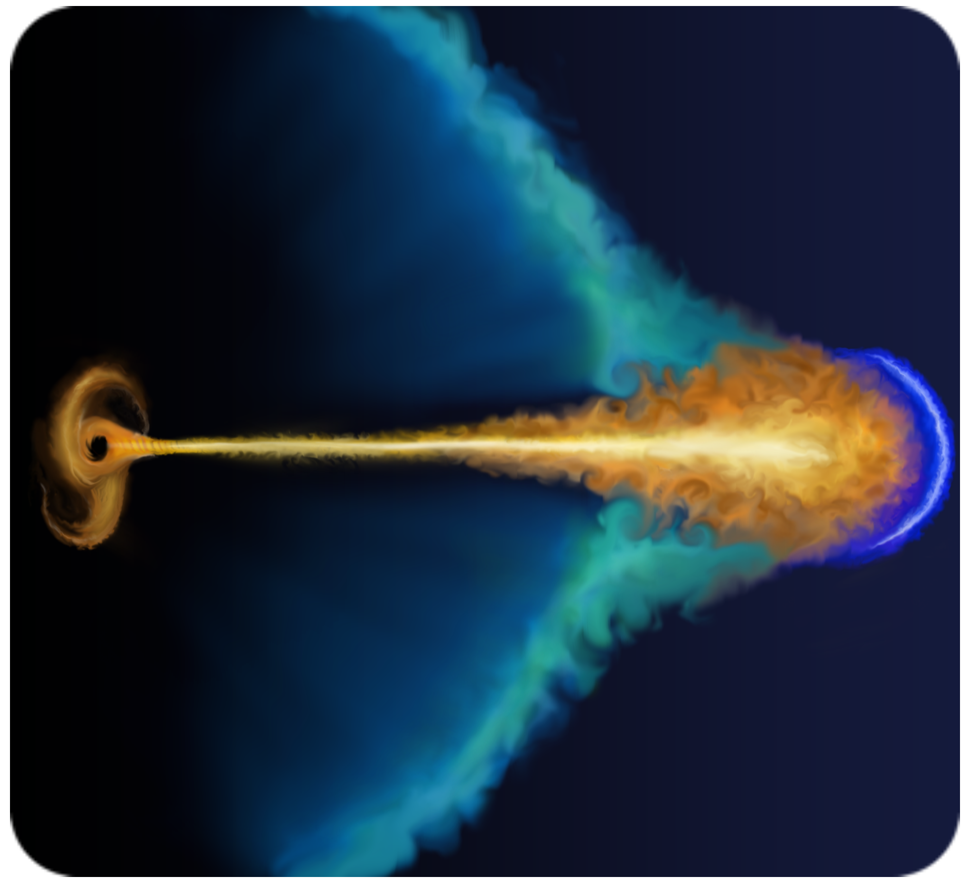

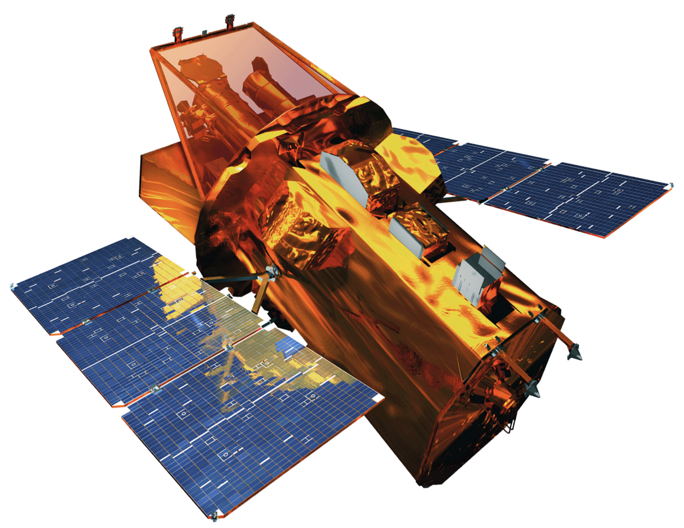

The multi-messenger revolution

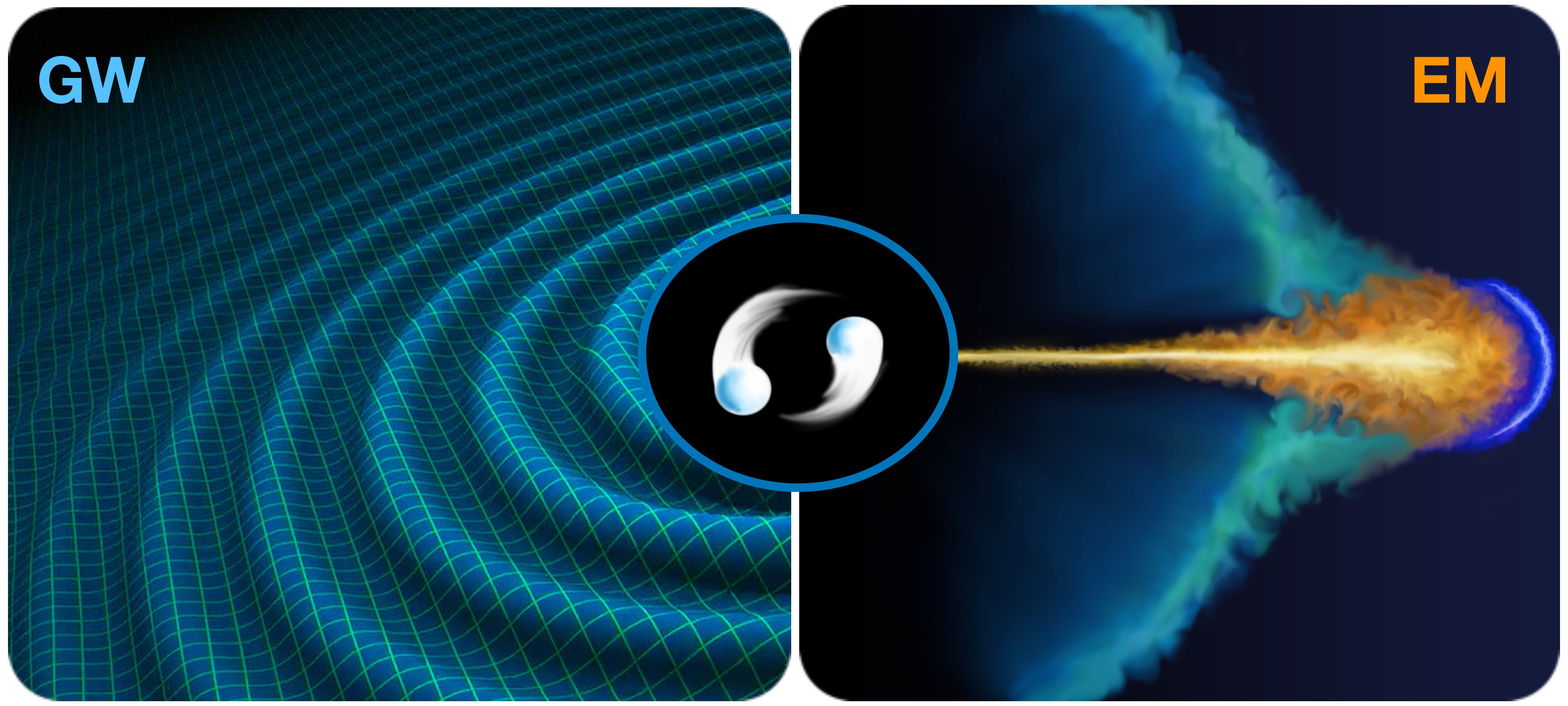

- Compact Binary Coalescences (CBCs) are GW emitters
- The central remnant of the merger can potentially launch a relativistic jet
- If at least one NS is involved, an EM signal is expected
- NS-BH and NS-NS mergers produce a variety of ejecta—> dynamical, disk winds, polar
- The radioactive decay of heavy elements powers the kilonova (KN) emission (Li & Paczynski 1998)
- On time scales of days-week, emission in UV/optical/IR

The **first smoking gun** of BNS merger / sGRB / KN association: GW170817, GRB 170817A and AT2017gfo

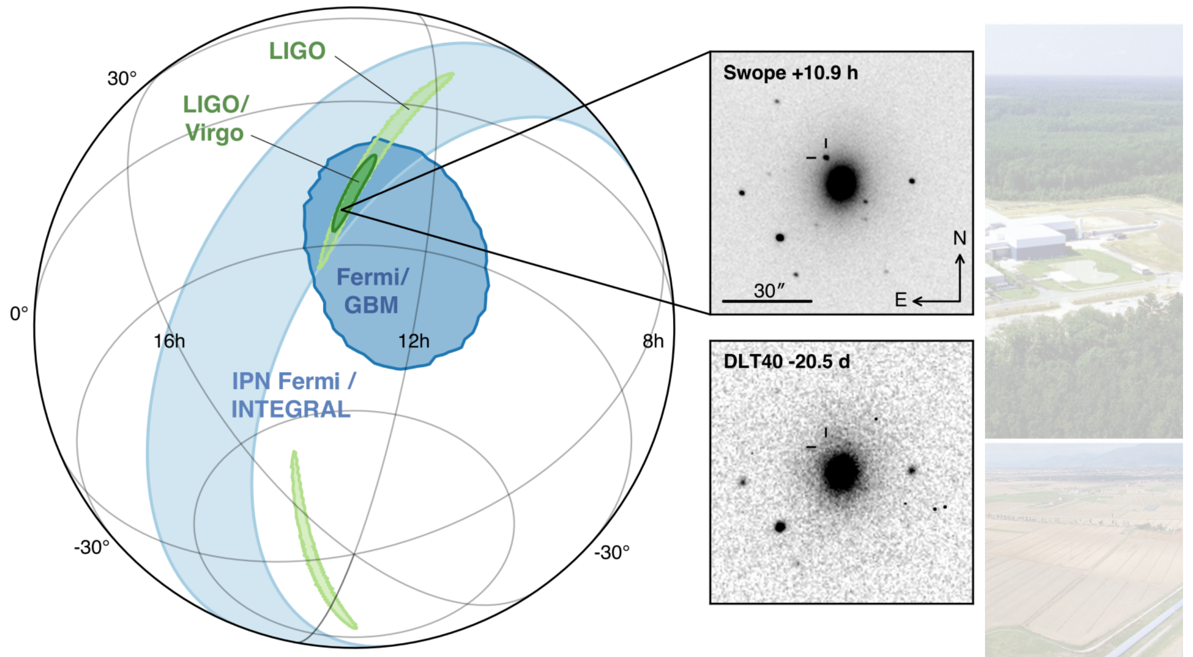

e.g. Abbott+ 2017, Goldstein+ 2017, Pian+ 2017, Smartt+ 2017, Villar + 2017, D'Avanzo+ 2018, Ghirlanda+ 2019

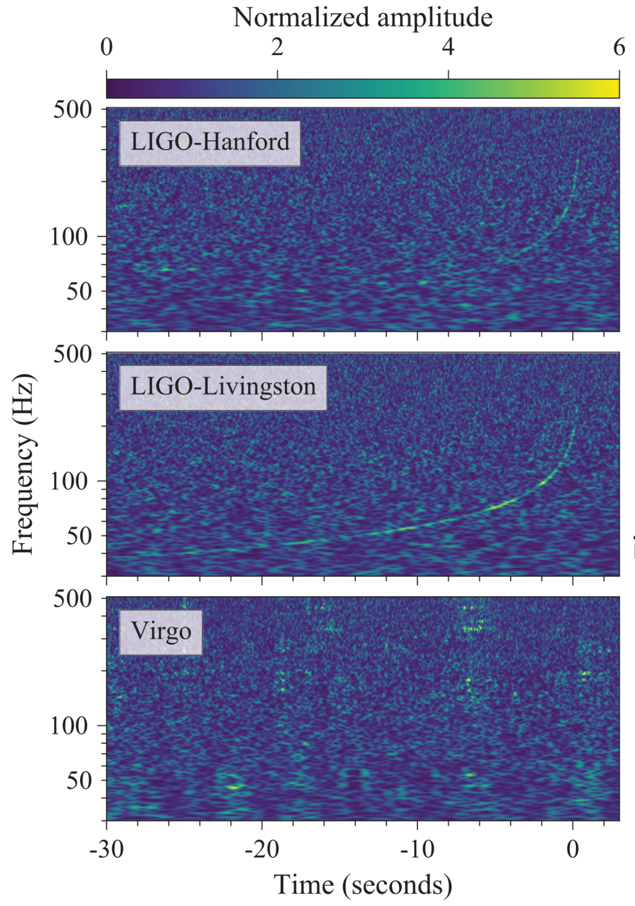

KN spectra

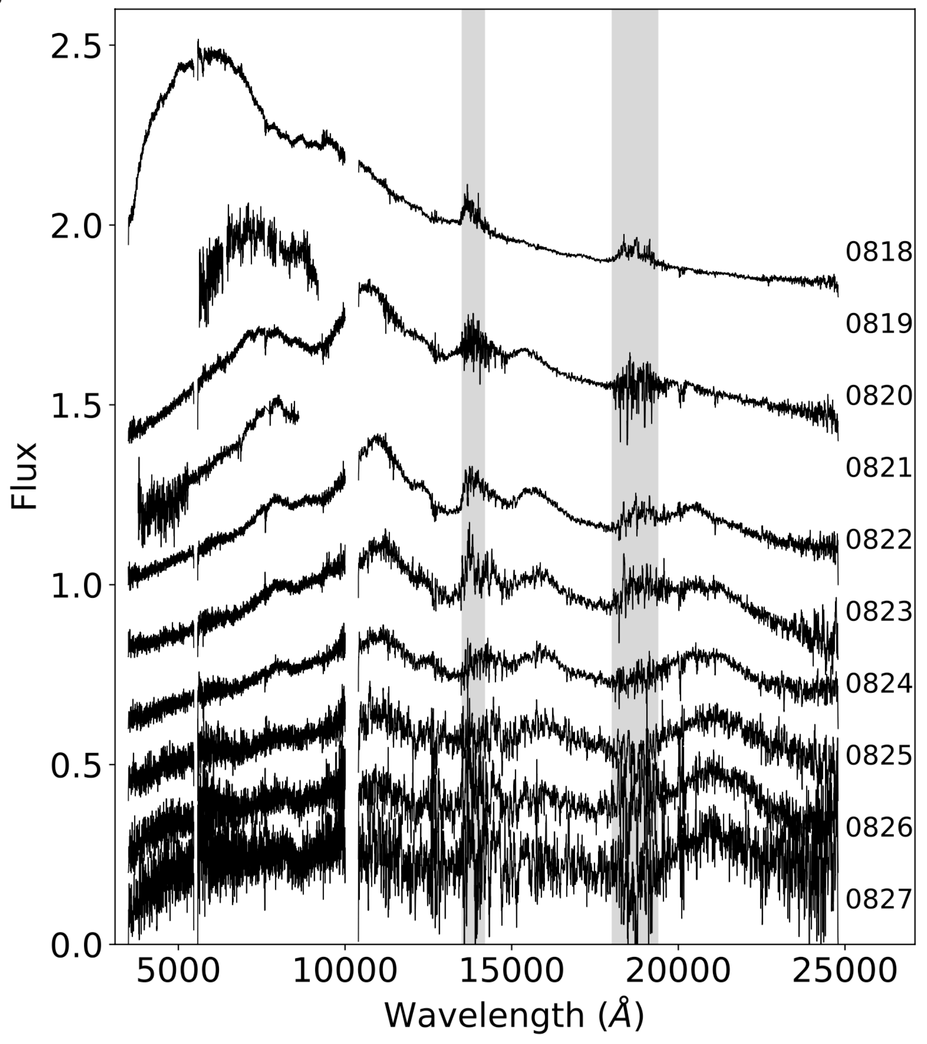

KN light curve

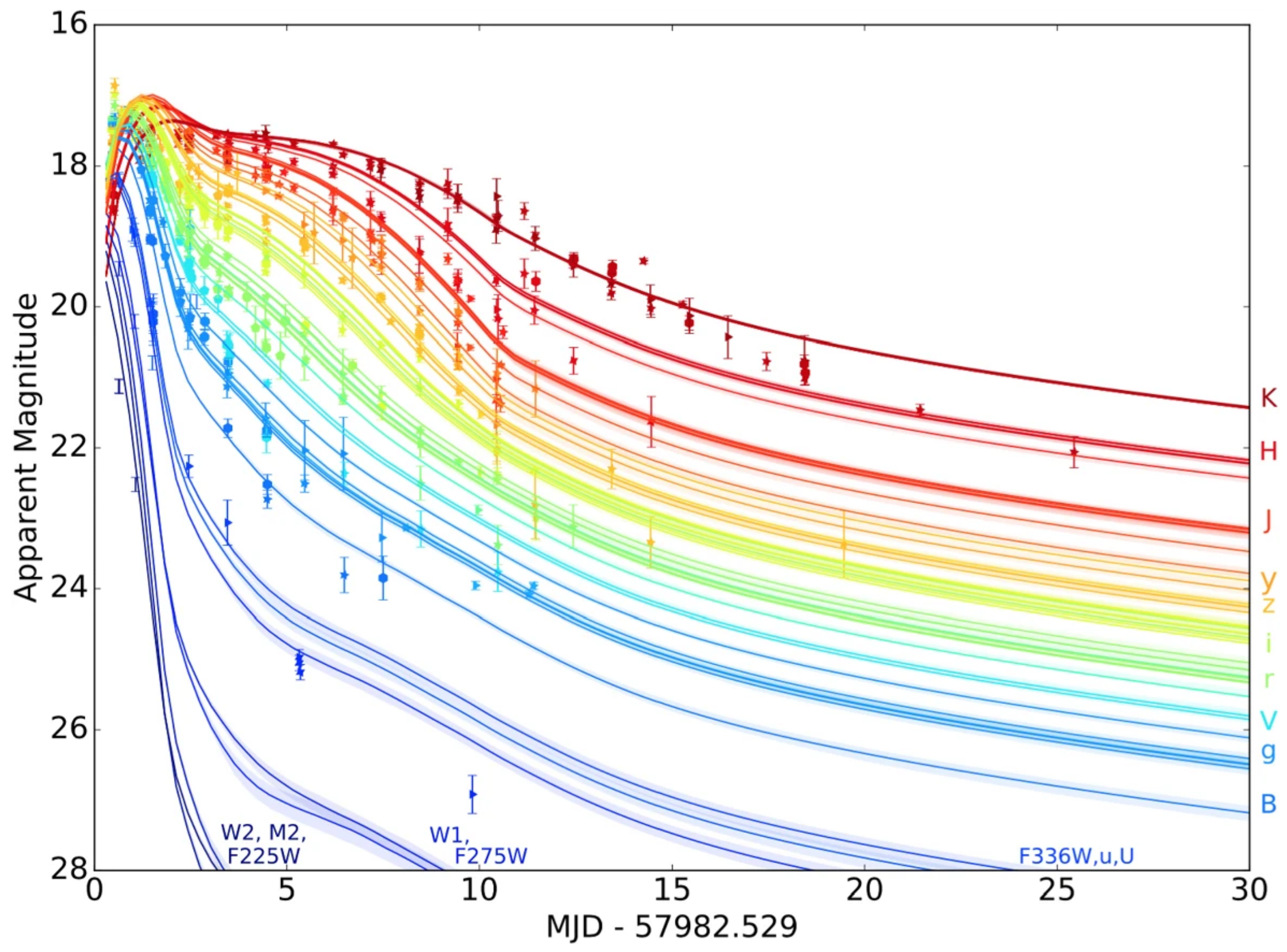

Radio to X-ray afterglow